The University Of Sheffield.

Characterisation of Amino Acid Transport Processes in Chinese Hamster Ovary (CHO) Cells

Darren Geoghegan

A thesis submitted in partial fulfilment of the requirements for the degree of
Doctor of Philosophy

The University of Sheffield
Faculty of Engineering
Department of Chemical and Biological Engineering

September 2015

This electronic version of the thesis has been edited to remove commercially sensitive information. The results, discussions and conclusions presented herein are identical to those in the printed version. The final, awarded and examined version is available for consultation via the University Library.

Acknowledgements

First and foremost, I would like to thank Professor David James for giving me the opportunity to undertake a PhD in his research group. Your continual guidance, availability, and enthusiasm for this project have been invaluable. This research would not have been possible without the financial support of the EPSRC and MedImmune, for which I am extremely grateful. A huge thank you must also go to my industrial supervisors, Dr Diane Hatton and Dr Tarik Senussi, for their input, feedback, and support throughout this project. I would like to give Diane an additional thank you for taking the time to read through a draft copy of this thesis.

To all the DCJ lab members, past and present, I cannot think of a better bunch of guys with whom to share the highs and lows of completing a PhD. Thank you for providing a supportive and enjoyable environment to work in. I intentionally omit names to save myself the embarrassment of accidently forgetting someone, however a special thank you must go to Dave Wengraf for all the technical support he provides the lab. Dave, you truly keep the lab moving.

I thank MedImmune for access to their cell lines and other materials used to complete this project, including access to equipment. I would like to give Dr Chris Sellick particular thanks for performing the quantification of amino acids. To all members of the Cell Culture and Fermentation Sciences team at Cambridge, thank you for always making me feel welcome.

Finally, I never would have got to this stage without the support from all my friends and family who never stopped believing in me. Kathleen, my transatlantic flatmate, thanks for all the laughter, baking, Netflix, wine, and terrible movie choices. To my parents, thank you for teaching me the value of hard work, a value which has got me to where I am today. Lastly, Tom, thank you for your patience, understanding, and support over the last four years.

Abstract

Amino acid transport is controlled by a system of transporter proteins whose function remains poorly defined in CHO cells. In this thesis, the relationship between amino acid transporter activity and culture performance parameters was investigated and used as a basis to explore new opportunities for improving cell line productivity. Transcriptomic analysis of transporter expression was first performed in two non-producing CHO cell lines and one antibody-producing CHO cell line during fed-batch cultures. Seven transporters were highly expressed across the three cell lines (ASCT1, CAT-1, GLAST, LAT1, SNAT2, xCT and y^+LAT2). For all cell lines, the cystine-glutamate xCT transporter was significantly upregulated at stationary phase and formed part of a larger adaptive response to support the cellular availability of glutathione. The antibody-producing cell line also upregulated ASCT1 and LAT1 transporter expression during stationary phase, which allowed the cells to maintain a high consumption rate of amino acids abundant in the antibody. Cells were next treated with inhibitors that block amino acid transport through individual or groups of transporters. Inhibition results confirmed that xCT transport activity is a key determinant of culture viability in all cell lines, and along with LAT1, also supports specific productivity during late-stage culture in the antibody-producing cell line. A directed evolution strategy was subsequently developed to increase xCT transport capability in the host. Evolved host cells demonstrated an increased capacity for GSH synthesis, increased resistance to a ROS insult, and a heritable improvement in cell growth but were not able to outperform the unevolved host in the transient production of an IgG. Finally, a mechanistic model to describe essential amino acid transport processes in CHO cells was constructed from transcriptomic and inhibitor data. This model can be used to direct future optimisation of amino acid concentrations in culture media to maximise cell growth and antibody production.

Contents

List of Figures 1
List of Tables 5
Amino Acid Abbreviations 7
Acronyms and Abbreviations 8

Chapter 1: Manufacturing Recombinant Therapeutic Monoclonal Antibodies ... 9
1.1 Biologics Market 9
1.2 Expression Systems 9
1.3 Chinese Hamster Ovary (CHO) Expression System 11
1.4 Manufacturing Antibodies 11
1.5 Upstream Process Development 11
1.5.1 Cell Line Development (CLD) 11
1.5.2 Cell Culture Process Development 13
1.6 Summary 14

Chapter 2: Amino Acid Metabolism and Transport 15
2.1 Mammalian Cell Metabolism 15
2.1.1 Aerobic Glycolysis and Glutaminolysis Support Cell Proliferation 17
2.1.2 Stationary Phase is Associated With Oxidative Metabolism and PPP Activity 19
2.1.3 CHO Cell Metabolism is Cell Line Dependent 19
2.2 Amino Acids and Signaling Pathways 21
2.2.1 Leucine and Glutamine Stimulate mTORC1 Signaling 21
2.2.2 Amino Acid Response (AAR) Pathway 22
2.3 Mammalian Amino Acid Transporters 22
2.4 Amino Acid Transporters in Cancer 30
2.5 Amino Acid Transporters as Potential Cell Engineering Targets 32
2.6 Summary 33
2.7 Thesis Overview 34

Chapter 3: Materials and Methods 36
3.1 Cell Lines and Culture 36
3.1.1 Cell lines 36

3.1.2 Routine Sub-Culture 36
3.1.3 Cell Growth Parameters 36
3.1.3.1 Cell Specific Growth Rate 37
3.1.3.2 Integral of Viable Cell Density 37
3.1.3.3 Generation Number 37
3.2 Extracellular Amino Acid Analysis 37
3.3 Antibody Quantification 38

Chapter 4: Amino Acid Transporter Gene Expression Analysis in CHO Cells Using RNA-Sequencing 39
4.1 Introduction 39
4.2 Materials and Methods 43
4.2.1 Cell Culture 43
4.2.2 Sample Collection 43
4.2.3 RNA Extraction 43
4.2.4 RNA Assessment 44
4.2.5 Library Preparation and Sequencing 44
4.2.6 Read Mapping and Transcriptome Assembly 44
4.3 Results 45
4.3.1 Growth Profiles and RNA-Sequencing Sample Selection 45
4.3.2 Transcriptome Data Sets 46
4.3.3 Amino Acid Transporter Expression Analysis 47
4.3.3.1 Proteinogenic Transporter Expression at Exponential Growth Phase 49
4.3.3.2 Proteinogenic Transporter Expression at Stationary Growth Phase 51
4.3.3.3 Expression of Genes Involved in Regulating Cellular GSH Levels 55
4.3.3.4 Expression of Target Genes of the AAR Pathway 57
4.3.3.5 Expression of Non-Proteinogenic Transporters 58
4.3.4 Amino Acid Transport Rate Analysis 59
4.3.5 Amino Acid Analysis of Two Additional IgG-Producing Cell Lines 63
4.4 Discussion 67
4.4.1 LAT1, ASCT1 and SNAT2 Transport Neutral Amino Acids 67
4.4.2 GLAST, CAT-1 and y^+LAT2 Transport Charged Amino Acids 69

4.4.3 ASCT1, LAT1 and xCT Are Potential Markers for Antibody Production 70
4.4.4 Increased xCT Expression During Stationary Growth Forms Part of An Adaptive Response That Supports Cellular Availability of GSH 71
4.4.5 Changes in ASCT1, LAT1 and xCT Expression Could be an Adaptive Response to Support Antibody Production 72
4.4.6 Summary 74

Chapter 5: Inhibition of Amino Acid Transport and its Effects on Cell Growth and Antibody Production 76
5.1 Introduction 76
5.2 Materials and Methods 77
5.2.1 Inhibitor Treatment at Exponential Growth 77
5.2.2 Inhibitor Treatment at Stationary Growth 78
5.2.3 Analysis of Factorial Experimental Data 78
5.3 Results 79
5.3.1 System L Transport Inhibition 82
5.3.2 System A Transport Inhibition 87
5.3.3 System X_C^- Transport Inhibition 92
5.3.4 System ASC Transport Inhibition 98
5.3.5 GlyT1 Transport Inhibition 104
5.3.6 Multi-Transporter Inhibition in T127 Cells During Exponential Growth 109
5.3.6.1 Multi-Transporter Inhibition and Growth Rate 111
5.3.6.2 Multi-Transporter Inhibition and Culture Viability 112
5.3.6.3 Multi-Transporter Inhibition and Specific Productivity 112
5.4 Discussion 113
5.4.1 System L Inhibition Blocks Essential Amino Acid Uptake, Suppresses Cell Growth and Inhibits Antibody Production 113
5.4.2 Dependence Upon System A and ASC Transport for Cell Growth Differs Between Cell Lines 114
5.4.3 The xCT Transporter Supports Cell Viability in all Cell Lines and Antibody Production During Late-Stage Culture 116
5.4.4 The GlyT1 Transporter Supports Antibody Production During Late-Stage Culture 117

5.4.5 Conclusions and Future Perspectives 117

Chapter 6: Evolving Resistance to Amino Acid Transport Inhibition for Improved Cell Line Performance 119

6.1 Introduction 119

6.2 Materials and Methods 122

6.2.1 Transient Transfection 122

6.2.1.1 Expression Vectors 122

6.2.1.2 Lipofection 122

6.2.2 Flow Cytometry 123

6.2.3 Cellular Glutathione Quantification 124

6.2.4 Inhibitor Treatment 124

6.2.5 Batch Overgrow Shake Flask Cultures 124

6.2.6 Fed-Batch Overgrow Shake Flask Cultures 125

6.3 Results 125

6.3.1 Creation of a SAS-Resistant CAT-S Cell Line (CAT-R-S700) 125

6.3.1.1 Growth Profile of the CAT-R-S700 Cell Line 126

6.3.1.2 Intracellular Glutathione Content and Cell Line Responses to Reactive Oxygen Species Exposure 129

6.3.1.3 Heritability of the CAT-R-S700 Phenotype 130

6.3.2 Creation of a GPNA-Resistant CAT-S Cell Line (CAT-R-G200) 132

6.3.2.1 Growth Profile of the CAT-R-G200 Cell Line 134

6.3.2.2 Heritability of the CAT-R-G200 Phenotype 136

6.3.3 Transfection Efficiency and Transient Production of a Recombinant IgG Antibody in Parental and Resistant Cell Lines 137

6.3.4 Creation of SAS-Resistant T127 Cell Lines 139

6.3.4.1 Growth and Antibody Production Characteristics for Non-Evolved and Resistant T127 Cell Lines 140

6.4 Discussion 144

Chapter 7: Rational Design of Culture Media From an Understanding of Amino Acid Transport Mechanisms 149

7.1 Introduction 149

7.2 Materials and Methods 150

7.2.1 Generation of Amino Acid Transport Profile Data 150

7.2.1.1 CAT-S Transport Profiles 151
7.2.1.2 GS-Null Transport Profiles 151
7.2.1.3 T127 Transport Profiles 151
7.2.3 Statistical Analysis 151
7.3 Results 151
7.3.1 Essential Amino Acid Correlations 155
7.3.2 Non-Essential Amino Acid Correlations 159
7.4 Discussion 160

Chapter 8: Conclusions and Future Work 163
8.1 Conclusion 163
8.1.1 Characterisation of Amino Acid Transport Processes 163
8.1.2 Improving Cell Growth and Productivity 165
8.2 Future Work 166

Appendix A 168
Appendix B 183
Appendix C 189

References 194

List of Figures

Figure 2.1 Central metabolism in mammalian cells..... 16
Figure 2.2 Comparison of flux through CHO central metabolic pathways at exponential growth and stationary phase..... 20
Figure 2.3 Amino acid transporters are functionally coupled to metabolic and signaling pathways that promote cell proliferation..... 32

Figure 4.1 Production characteristics of CAT-S, GS-Null, and T127 cells grown in a 14-day fed-batch operation 46
Figure 4.2 Differential expression of amino acid transporter genes between CAT- S, GS-Null, and T127 cells at exponential growth phase..... 50
Figure 4.3 Differential expression of amino acid transporter genes within culture... 52
Figure 4.4 Differential expression of amino acid transporter genes between CAT- S, GS-Null, and T127 cells at stationary growth phase..... 53
Figure 4.5 Comparison of proteinogenic amino acid transporter expression in CAT-S, GS-Null, and T127 cells at exponential and stationary growth phase 55
Figure 4.6 Comparison of specific amino acid transport rates throughout culture for CAT-S, GS-Null, and T127 cells 60
Figure 4.7 Production characteristics of T29, T48, and T127 cells grown in a 14- day fed-batch operation..... 64
Figure 4.8 Comparison of specific amino acid transport rates throughout culture for T29, T48, and T127 cells 65

Figure 5.1 Inhibitors used to block amino acid transporter activity at exponential and stationary growth phases of batch cultures. 81
Figure 5.2 The effect of BCH treatment on cell proliferation during exponential growth phase..... 83
Figure 5.3 The effect of BCH treatment on culture viability and amino transport rates during exponential growth phase 84
Figure 5.4 The effect of BCH treatment on antibody production during exponential growth phase 85
Figure 5.5 The effect of BCH treatment on CAT-S and T127 cells at stationary phase of batch culture 87

Figure 5.6 The effect of MeAIB treatment on cell proliferation during exponential growth phase 88
Figure 5.7 The effect of MeAIB treatment on culture viability and amino transport rates during exponential growth phase 89
Figure 5.8 The effect of MeAIB treatment on antibody production during exponential growth phase 91
Figure 5.9 The effect of MeAIB treatment on CAT-S, GS-Null, and T127 cells at stationary phase of batch culture 92
Figure 5.10 The effect of SAS treatment on cell proliferation during exponential growth phase 94
Figure 5.11 The effect of SAS treatment on culture viability and amino transport rates during exponential growth phase 95
Figure 5.12 The effect of SAS treatment on antibody production during exponential growth phase 97
Figure 5.13 The effect of SAS treatment on CAT-S, GS-Null, and T127 cells at stationary phase of batch culture 98
Figure 5.14 The effect of GPNA treatment on cell proliferation during exponential growth phase 100
Figure 5.15 The effect of GPNA treatment on culture viability and amino transport rates during exponential growth phase 101
Figure 5.16 The effect of GPNA treatment on antibody production during exponential growth phase 103
Figure 5.17 The effect of GPNA treatment on CAT-S, GS-Null, and T127 cells at stationary phase of batch culture 104
Figure 5.18 The effect of ALX 5407 HCl treatment on CAT-S, GS-Null, and T127 cells during exponential growth phase 106
Figure 5.19 The effect of ALX 5407 HCl treatment on CAT-S, GS-Null, and T127 cells at stationary phase of batch culture 108
Figure 5.20 The effect of multi-transporter inhibition on T127 cells during exponential growth phase 110

Figure 6.1 Gated population of viable cells 123
Figure 6.2 Example daughter plot for GFP expression 124
Figure 6.3 Creation of a SAS-resistant CAT-S cell line 126

Figure 6.4 Batch and fed-batch culture growth curves for parental, CAT-CTRL and CAT-R-S700 cells 128
Figure 6.5 Glutathione content and effect of H_2O_2 treatment on parental and CAT- R-S700 cells during exponential growth phase 130
Figure 6.6 Heritability of the CAT-R-S700 phenotype 131
Figure 6.7 Creation of the GPNA-resistant CAT-S cell line 133
Figure 6.8 Batch and fed-batch culture growth curves for parental, CAT-CTRL and CAT-R-G200 cells 135
Figure 6.9 Heritability of the CAT-R-G200 phenotype 136
Figure 6.10 Growth characteristics of parental and resistant CAT-S cells transiently expressing GFP and an IgG monoclonal antibody 138
Figure 6.11 Transient production of an IgG monoclonal antibody in parental and resistant CAT-S cells 139
Figure 6.12 Creation of SAS-resistant T127 cell lines 140
Figure 6.13 Batch culture growth curves for non-evolved T127, T127-CTRL, T127-R-S500 and T127-R-S700 cells 142
Figure 6.14 Comparison of growth and production characteristics for non-evolved T127, T127-CTRL, T127-R-S500 and T127-R-S700 cells as assessed in batch cultures 143

Figure 7.1 Relationships between total specific amino acid transport rates and growth rates in CAT-S, GS-Null and T127 cells 152
Figure 7.2 Correlations between the 20 proteinogenic amino acids in CAT-S, GS- Null and T127 cells 154
Figure 7.3 Proposed mechanistic model of essential amino acid transport in CAT- S, GS-Null and T127 cells 156

Figure A1 Extracellular amino acid concentrations for CAT-S, GS-Null, and T127 cells throughout culture 181

Figure B1 Half-normal probability plot of absolute effects for growth response 184
Figure B2 Normal probability plot of residuals for growth rate 184
Figure B3 Half-normal probability plot of absolute effects for culture viability 185
Figure B4 Normal probability plot of residuals for culture viability 185
Figure B5 Interactions between systems ASC, L, and X_C^- for culture viability 186

Figure B6 Half-normal probability plot of absolute effects for specific productivity 187
Figure B7 Normal probability plot of residuals for specific productivity..... 188

Figure C1 Relationships between transport rates of individual amino acids and growth rates in CAT-S, GS-Null and T127 cells 189

List of Tables

Table 1.1 Expression systems commonly used to express recombinant proteins 10

Table 2.1 Mammalian amino acid transporters and their transport properties 24

Table 4.1 Proteinogenic amino acid transporters with medium or high expression at exponential and stationary growth phase 48
Table 4.2 Differential expression of enzymes involved in regulating cellular GSH levels in response to transition from exponential to stationary growth phase of culture 56
Table 4.3 Differential expression of genes regulated by the AAR pathway in response to transition from exponential to stationary growth phase of culture 57
Table 4.4 Non-proteinogenic amino acid transporters with medium or high expression at exponential and stationary growth phase 58
Table 4.5 Total specific amino acid transport rates throughout culture for CAT- S, GS-Null, and T127 cells 61
Table 4.6 Total specific amino acid transport rates throughout culture for T29, T48, and T127 cells 66
Table 4.7 Amino acid composition of a mammalian cell and an IgG antibody 74

Table 5.1 Summary of growth and production characteristics of five CHO cell lines as assessed in 14-day fed-batch operations 80

Table 7.1 Specific transport rates of amino acids in CAT-S, GS-Null and T127 cells grown under control conditions 158

Table A1 CHO amino acid transporters identified in genome, transcriptome, and proteome studies 168
Table A2 Transcript abundance of CAT-S amino acid transporter genes at exponential and stationary growth phase of culture 171
Table A3 Transcript abundance of GS-Null amino acid transporter genes at exponential and stationary growth phase of culture 174
Table A4 Transcript abundance of T127 amino acid transporter genes at exponential and stationary growth phase of culture 177

Table A5 FPKM boundaries for low, medium, and high gene expression in CAT-S, GS-Null, and T127 cells at exponential and stationary growth phase..... 180

Table B1 Design matrix for the two-level factorial experiment showing factor interactions, response variable data, and calculated effects..... 183

Table C1 Spearman's rank correlation coefficient values for CAT-S cells..... 192
Table C2 Spearman's rank correlation coefficient values for GS-Null cells..... 192
Table C3 Spearman's rank correlation coefficient values for T127 cells..... 193

Amino Acid Abbreviations

Amino acid	Three-letter code	One-letter code
Alanine	Ala	A
Arginine	Arg	R
Asparagine	Asn	N
Aspartate	Asp	D
Cysteine	Cys	C
Cystine	Cys2	C-C
Glutamate	Glu	E
Glutamine	Gln	Q
Glycine	Gly	G
Histidine	His	H
Isoleucine	Ile	I
Leucine	Leu	L
Lysine	Lys	K
Methionine	Met	M
Phenylalanine	Phe	F
Proline	Pro	P
Serine	Ser	S
Threonine	Thr	T
Tryptophan	Trp	W
Tyrosine	Tyr	Y
Valine	Val	V

Acronyms and Abbreviations

AAA	Aromatic amino acids
AAR	Amino acid response
ATP	Adenosine triphosphate
BCAA	Branched-chain amino acids
BCH	2-amino-2-norbornanecarboxylic acid
CHO	Chinese hamster ovary
DMSO	Dimethyl sulfoxide
DoE	Design of experiments
FPKM	Fragments per kilobase of transcript per million fragments mapped
GFP	Green fluorescent protein
GPNA	L-γ-glutamyl-p-nitroanilide
GS	Glutamine synthetase
GSH	Reduced glutathione
GSSG	Oxidised glutathione
IgG	Immunoglobulin G
MeAIB	α-(methylamino)isobutyric acid
MFA	Metabolic flux analysis
mTORC1	Mammalian target of rapamycin (mTOR) complex 1
NADPH	Nicotinamide adenine dinucleotide phosphate
PPP	Pentose phosphate pathway
ROS	Reactive oxygen species
SAS	Sulfasalazine
SLC	Solute carrier
TCA	Tricarboxylic acid

Chapter 1

Manufacturing Recombinant Therapeutic Monoclonal Antibodies

This chapter provides an overview of the manufacturing of monoclonal antibodies in CHO cells with a focus on upstream process development. Industrial drivers are discussed such as high product titres, product quality attributes and speed to market, and how this has influenced the development of current industrial manufacturing processes.

1.1 Biologics Market

Recombinant therapeutic proteins are a class of biologics that are produced using recombinant DNA technology. Products within this group include blood factors, cytokines, fusion proteins, growth factors, hormones, monoclonal antibodies (mAbs), therapeutic enzymes, and vaccines (Aggarwal, 2014). Of these, mAbs dominate the biologics market, accounting for around 38.7% of total sales in 2012 (Aggarwal, 2014) and for six of the top ten selling biologics in 2013 (Walsh, 2014). Nearly all marketed mAbs are treatments for cancers and autoimmune diseases such as Crohn's disease, psoriasis, rheumatoid arthritis and ulcerative colitis, all of which are chronic conditions that typically require high treatment doses (≥100 mg; Jain and Kumar, 2008). The development of cost-effective manufacturing processes that yield high mAb titres is therefore a major industrial challenge to meet current and future patient demands (Kelley et al., 2001; Shukla and Thomas, 2010).

1.2 Expression Systems

A variety of cell-based systems exist that can be used to express recombinant proteins, including *Escherichia coli*, yeast cells, insect cells, and mammalian cells (Table 1.1). The choice of expression system is largely dictated by any post-translational

modification (PTM) requirements the protein may have for folding, assembly and *in vivo* activity in patients. All therapeutic mAbs are of the IgG (immunoglobulin G) isotype (Walsh, 2014), which are composed of two heavy and two light polypeptide chains that are assembled into a Y-shaped monomer (Schroeder and Cavacini, 2010). Correct assembly requires disulphide bond formation between polypeptide chains, while glycosylation affects the stability, function, half-life and immunogenicity of mAbs in patients (Schroeder and Cavacini, 2010; Walsh and Jefferis, 2006). These two PTM requirements necessitate the use of a mammalian expression system, as *E. coli* are unable to glycosylate and generate inclusion bodies, while lower eukaryotes such as yeast and insect cells can produce incorrect glycosylation patterns (reviewed in Demain and Vaishnav, 2009). Around 56% of all recombinant therapeutic proteins approved between 1982 and 2014 are manufactured using a mammalian expression system, of which approximately 63% are produced using Chinese hamster ovary (CHO) systems (Walsh, 2014).

Table 1.1 Expression systems commonly used to express recombinant proteins

Expression systems
Prokaryotic
Escherichia coli
Yeast
Saccharomyces cerevisiae
Pichia pastoris
Mammalian
Chinese hamster ovary (CHO)
Baby hamster kidney (BHK)
Mouse myeloma (NS0)
Mouse B cell hybridoma (SP2/0)
Human embryonic kidney (HEK-293)
Human retinoblast (PER.C6)
Insect
Drosophila melanogaster (S2)
Spodoptera frugiperda (SF9 and SF21)

1.3 Chinese Hamster Ovary (CHO) Expression System

The CHO cell line (CHO-K1) was first isolated in 1958 from a population of immortalised ovarian fibroblasts taken from a Chinese hamster (*Cricetulus griseus*; Puck et al., 1958). Mutagenesis of the CHO-K1 cell line over subsequent years resulted in the creation of cell line variants (DG44 and DXB11) that are currently in use within the biotechnology industry (Wurm and Hacker, 2011). CHO cell lines offer a number of industrial advantages, in addition to their ability to glycosylate, that have made them a popular expression system. They can be easily genetically manipulated, adapted into scalable single cell suspension cultures, and adapted to grow in serum-free chemically defined media (Jayapal et al., 2007). The first CHO recombinant product, tissue plasminogen activator (tPA), was marketed by Genentech in 1987 (Activase®) and manufactured using suspension-adapted cells cultured in bioreactors (De Jesus and Wurm, 2011). Since 1987, the establishment of productive and efficient CHO cell manufacturing processes that have a proven track record with regulatory authorities has helped secure CHO cells as the dominant mammalian expression system.

1.4 Manufacturing Antibodies

A typical manufacturing process begins with the culture of recombinant CHO cell lines in stirred-tank bioreactors for antibody production. At the end of the production process the culture is harvested, centrifuged and filtered to remove cells and cell debris (Shukla and Thomas, 2010). Purification of the antibody is achieved through a series of capture (protein A) and polishing (anion/cation exchange) chromatography steps that remove impurities such as host cell proteins and DNA (Shukla and Thomas, 2010). Platform approaches to manufacturing have helped develop processes that are efficient (reduced costs and fast), reproducible, well characterised, and adaptable to new products (Shukla and Thomas, 2010). Specifically, developments to upstream processing have resulted in cell cultures capable of achieving antibody yields of up to 5 g/L (De Jesus and Wurm, 2011) with multiple grams per litre titres also being reported (Jiang et al., 2012).

1.5 Upstream Process Development

1.5.1 Cell Line Development (CLD)

The construction of a recombinant CHO cell line with a high specific antibody production rate (pg/cell/day) is the first step in the development of a productive cell

culture process. Specific productivities (Q_P) are reported to be in the range of 50–60 pg/cell/day (De Jesus and Wurm, 2011). These values have largely been achieved through the development of improved expression vectors and screening platforms to select for rare cells with a high Q_P.

Expression vectors are DNA molecules encoding genes for both the heavy and light antibody chains in addition to a selection marker for positive transfectants. To maximise specific productivity the coding sequences are optimised for expression (e.g. codon optimisation and removal of cryptic splice sites). Additionally the vector backbone contains elements that enhance transcription, translation and secretion such as viral promoters (e.g. CMV), poly(A) tails, Kozak sequences and signal peptides (reviewed in Birch and Racher, 2006). The two leading platform vector systems for recombinant gene expression in CHO cells are the dihydrofolate reductase (DHFR) and Lonza's proprietary glutamine synthetase (GS) selection systems. The DHFR system introduces a functional copy of the DHFR gene into DHFR-deficient CHO-K1 variants (DG44 and DXB11). Transfectants are selected by growth in glycine, hypoxanthine and thymidine free media (GHT^-), and the DHFR inhibitor methotrexate (MTX) is used to increase expression of both DHFR and the recombinant gene over multiple amplification rounds (Jayapal et al., 2007). The GS system introduces a recombinant GS gene and transfectants are grown in glutamine free media. Methionine sulfoximine (MSX) is used to inhibit endogenous CHO GS and to select for high producers in a single amplification round. The GS system is preferentially used as the single amplification round can reduce the cell line development period to ~3 months compared to ~6 months with the DHFR system (Barnes et al., 2000).

Transfected CHO cells typically demonstrate significant variation in recombinant antibody expression. Cells exhibiting a high Q_p are rare and must be selected for. Automated high-throughput screening platforms such as fluorescence-activated cell sorting (FACS) and ClonePix can help screen 100-1000s of individual cells (reviewed in De Jesus and Wurm, 2011). In addition to a high Q_p, selected cells must have a growth rate suitable to meet large-scale production process times, and produce antibodies with the correct quality attributes (e.g. glycosylation profile) to ensure they are safe and efficacious in patients. Regulatory authorities require the cell line to be clonal, and stability testing is performed to ensure that clonal cell growth, Q_p and product quality is heritable over multiple generations (typically 60–80).

1.5.2 Cell Culture Process Development

Despite improvements to expression vectors, specific productivities have not changed significantly over the last 25 years and a biological limit of 100 pg/cell/day has been put forward (De Jesus and Wurm, 2011). Improvements in antibody titres have instead been reached mostly by the development of scalable fed-batch stirred-tank bioreactor processes, capable of achieving very high cell densities. A fed-batch process involves an initial growth period with a basal medium followed by the addition of a concentrated feed medium at set intervals throughout the culture (Whitford, 2006; Jiang et al., 2012). As the majority of antibody synthesis is uncoupled from cell growth, a fed-batch process must be designed to rapidly generate high cell densities that can be maintained for extended periods at high viabilities.

The design of a fed-batch process typically involves optimisation of either (or both) the basal and feed media composition, as well as process control parameters such as temperature, pH, dissolved oxygen, and feeding schedule. Design of experiments (DoE) is a statistical method frequently used in media development to identify optimal concentrations of media components for improved cell line productivity (reviewed in Chapter 7; Section 7.1). The feed primarily replenishes depleted nutrients, particularly amino acids, however it can also contain other components to extend culture longevity (e.g. antioxidants), or increase specific productivity (e.g. butyrate) late in culture (reviewed in Whitford, 2006). For optimisation of process control, temperature reduction during late culture is widely used to extend the stationary phase and boost specific IgG productivity (Sou et al., 2015). Although this can have a negative effect on IgG glycosylation (Sou et al., 2015), which must be characterised to ensure product safety and efficacy is unaffected. Jiang et al. (2012) demonstrated that DoE could be used to optimise the basal medium, feed medium, and process control (temperature shift, feeding schedule and seeding density) in a single workflow. This integrated approach to fed-batch design resulted in faster growth rates and cell densities in excess of 25 million cells/mL for an antibody-producing CHO cell line. More recently the development of scaled-down micro bioreactors such as the ambr™ (TAP Biosystems, UK) have been widely adopted by the industry to speed up cell line selection, fed-batch process optimisation, and process characterisation. The ambr™ system comprises of 24 or 48 parallel disposable vessels of 10-15 mL working volumes in which agitation, temperature, pH, DO, and automated sampling and feeding can be controlled with each vessel. Importantly, the system has been demonstrated to be capable of simulating cell

culture performances in traditional stirred-tank bioreactors up to 200 L with a high level of reproducibility (Rameez et al., 2014).

1.6 Summary

CHO cells are the dominant expression system in the biotechnology industry as they can deliver on the major industrial drivers such as production of high product titres, required quality attributes, speed to market, and are compatible with cost-effective manufacturing processes. The introduction of high-throughput technology for screening cell lines and the development of fed-batch cell culture processes has helped to significantly improve product titres since the approval of Activase® in 1987. However, it is considered that antibody titres can be improved further by further increasing cell densities and maintaining them for longer (De Jesus and Wurm, 2011). To help with this, a significant level of research has been directed at trying to further understand CHO cell metabolism. The aim being to identify cell line engineering targets, or rational methods of optimising feed compositions and feeding regimes to improve cell growth and productivity. Much of this research has focused on understanding and altering flux rates through central metabolic pathways involved in glucose, glutamine, lactate and ammonia metabolism (discussed further in Chapter 2). Yet, the intracellular availability of nutrients is controlled by systems of membrane transporter proteins, whose function remains largely unknown in CHO cells. Chapter 2 explores how further investigation of CHO amino acid transport is of importance to upstream process development and sets the context for the work in this thesis.

Chapter 2

Amino Acid Metabolism and Transport

This chapter reviews amino acid metabolism and transport to help contextualise the subsequent work within this thesis. An overview of how biomass synthesis in transformed cell lines is supported by amino acids is first provided. The chapter then reviews mammalian amino acid transporters and how their activity is functionally coupled to metabolic and signaling pathways critical to cell growth. A short discussion on the potential of amino acid transporters as cell engineering targets is then given. Finally, the aims and objectives of this thesis are discussed, including a brief synopsis for each of the subsequent results chapters.

2.1 Mammalian Cell Metabolism

Cultured cells import small nutrients (e.g. amino acids, glucose, and fatty acids) from their extracellular environment to build the macromolecules (e.g. nucleic acids, proteins, and lipids) required for cell division. Many anabolic processes are supported by ATP and enzyme cofactors such as NADPH, which must be regenerated through the metabolism of assimilated nutrients (Lunt and Vander Heiden, 2011). For example, synthesis of the fatty acid palmitate requires 7 molecules of ATP and 14 molecules of NADPH in addition to 16 carbons (Vander Heiden et al., 2009). Three metabolic pathways can meet the majority of anabolic demands: glycolysis, the tricarboxylic acid (TCA) cycle, and the pentose phosphate pathway (PPP) (Figure 2.1).

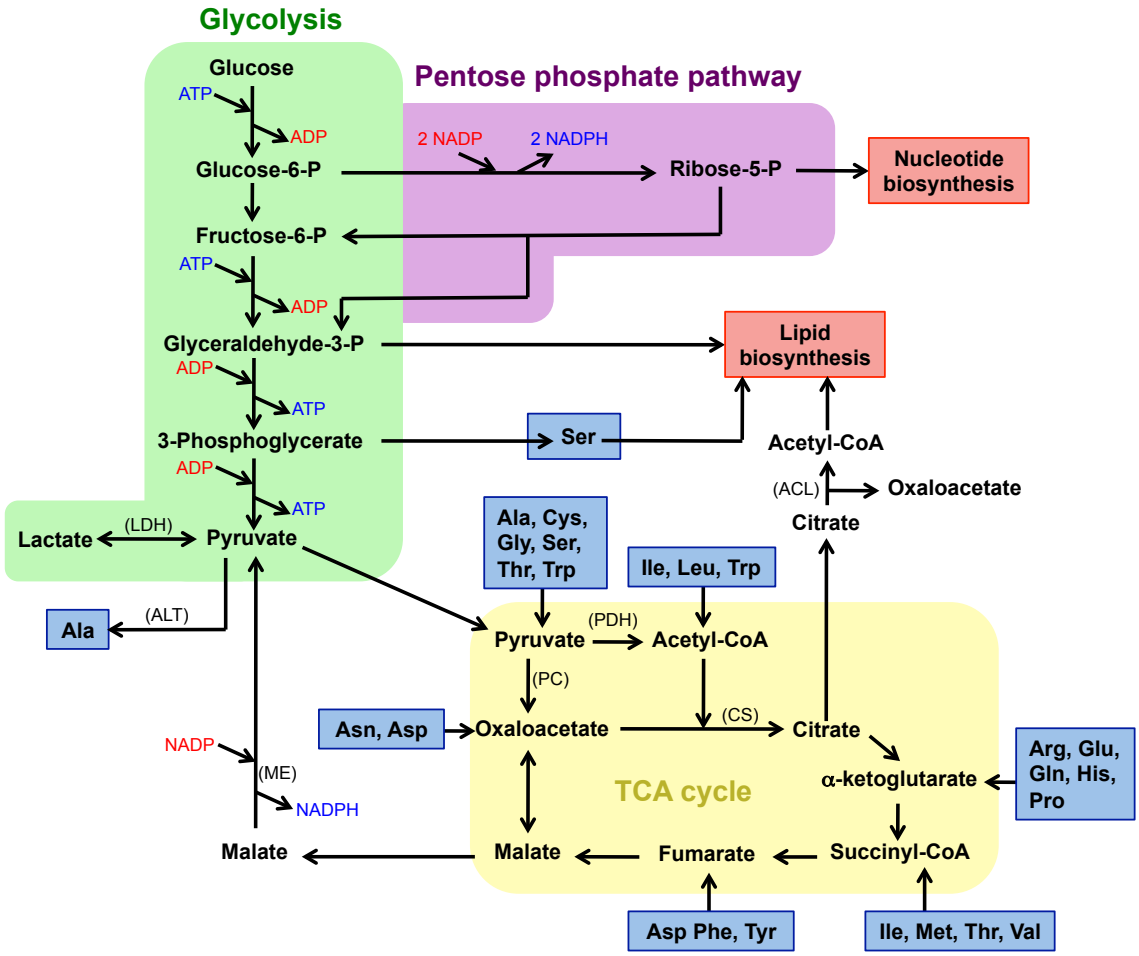

Figure 2.1 Central metabolism in mammalian cells. Amino acids and glucose are directed through glycolysis, the PPP, and the TCA cycle to support ATP and biomass production. Pathways have been simplified to demonstrate the important fluxes described in the main text as well as the interconnectivity of the three pathways. Key metabolic enzymes are provided in parentheses. ***ACL***, ATP citrate lyase; ***ALT***, Alanine transaminase; ***CS***, Citrate synthase; ***LDH***, Lactate dehydrogenase; ***ME***, Malic enzyme; ***PC***, Pyruvate carboxylase; ***PDH***, Pyruvate dehydrogenase.

Glucose is the primary carbon source consumed by mammalian cells (Lunt and Vander Heiden, 2011). Glucose is first metabolised through glycolysis to generate pyruvate and 2 net molecules of ATP (Berg et al., 2007). Subsequent decarboxylation and oxidation of pyruvate to acetyl-CoA by pyruvate dehydrogenase (PDH) allows it to enter the mitochondrial TCA cycle as citrate by condensing with oxaloacetate. As citrate moves through the TCA cycle it undergoes both decarboxylation and oxidation reactions with released electrons being donated to the electron transport chain. This metabolism, known as oxidative phosphorylation, allows the cell to generate a further

28 molecules of ATP per molecule of glucose (Berg et al., 2007). Under hypoxic conditions this process is inhibited and pyruvate must instead be converted to lactate and secreted from the cell, a process known as anaerobic glycolysis. Mammalian cells can redirect glycolytic intermediates to support the biosynthesis of nucleotides, amino acids, and lipids (Lunt and Vander Heiden, 2011). TCA cycle intermediates can also exit the mitochondria, a process known as cataplerosis, and be used for amino acid or lipid synthesis (Figure 2.1).

Amino acids are required by mammalian cells for protein synthesis and as a source of nitrogen, primarily for nucleotide synthesis. However, removal of the amine group leaves a carbon skeleton that can also be used to support biosynthesis processes, replace TCA cycle intermediates lost through cataplerotic reactions (anaplerosis), or be used as an energy source (Berg et al., 2007) (Figure 2.1). Glutamine is the highest consumed amino acid by mammalian cells and provides a second major carbon source (Lunt and Vander Heiden, 2011).

2.1.1 Aerobic Glycolysis and Glutaminolysis Support Cell Proliferation

Antibody-producing CHO cells growing in a fed-batch process transition through three growth phases: exponential, stationary, and decline. Exponential growth is characterised by rapid cell division and minimal antibody production. During the stationary phase cells cease division but remain viable and maximise their antibody production. Significant cell death towards the end of culture causes the decline phase. CHO cells exhibit high consumption rates for glucose and glutamine together with high secretion rates of alanine, ammonia, and lactate during exponential growth (Altamirano et al., 2004). Ammonia and lactate are toxic to cell growth and antibody production. The metabolism of glucose to lactate proceeds even in the presence of oxygen, a metabolic characteristic of cancer cells termed Warburg metabolism or aerobic glycolysis (Warburg, 1956).

An increasing number of studies have used metabolic flux analysis (MFA) to better understand the altered metabolism of cultured mammalian cells. MFA uses mathematical models of simplified metabolic networks in combination with experimentally measured transport rates of culture metabolites to estimate the flux through intracellular pathways (technique reviewed by Quek et al., 2010). Replacing nutrients such as glucose with ^{13}C tracers and then measuring their distribution within metabolites have significantly improved MFA estimates (^{13}C-MFA)(Ahn and Antoniewicz, 2012).

Aerobic glycolysis was investigated in a human glioblastoma cell line using ^{13}C-labeled glucose and glutamine (DeBerardinis et al., 2007). Over 90% of glucose was metabolised to lactate and alanine through glycolysis. However, TCA cycle activity was detected with pyruvate entering only as acetyl-CoA and citrate being exported for fatty acid synthesis. Glutamine was found to act as an anaplerotic substrate, replacing lost oxaloacetate. The study also found that 60% of glutamine was converted to lactate (glutaminolysis) via efflux of malate from the TCA cycle, generating NADPH. It has been hypothesised that high rates of aerobic glycolysis and glutaminolysis in cancer cells supports cell proliferation by sustaining a rapid supply of ATP, NADPH, and biosynthetic precursors for biomass synthesis (Vander Heiden et al., 2009).

^{13}C-MFA studies with CHO cells provide evidence that the TCA cycle functions in a similar manner to glioblastoma cells during exponential growth phase (Ahn and Antoniewicz, 2011; Dean and Reddy, 2013; Templeton et al., 2013). Feeding ^{13}C-labelled glucose to a non-producing adherent CHO-K1 cell line, Ahn and Antoniewicz (2011) found the majority of pyruvate produced by glycolysis metabolism was secreted as lactate. Most of the remaining pyruvate entered the TCA cycle as acetyl-CoA via PDH. Flux through the malic enzyme (ME) represented a significant cataplerotic reaction but negligible citrate export was observed. TCA cycle replenishment was mediated by pyruvate and glutamine through the anaplerosis reactions catalysed by pyruvate carboxylase (PC) and glutamate dehydrogenase (GDH) respectively. Templeton et al. (2013) found significant cataplerotic flux through ATP citrate lyase (ACL) in addition to ME in an antibody-producing CHO cell line. Pyruvate flux through PC helped replace oxaloacetate, however a parallel study found glutamine and asparagine also significantly contributed to TCA cycle replenishment (Dean and Reddy, 2013). Furthermore, 25% of secreted lactate was derived from glutamine but none from asparagine. However, asparagine majorly contributed to the production of the fatty acid palmitate whereas minimal glutamine carbon was detected in this macromolecule. In support of the importance of asparagine and glutamine consumption to exponential growth, Sellick et al. (2011) found that depletion of asparagine, aspartate and glutamate coincided with the end of exponential growth for an antibody-producing GS-CHO cell line. Feeding back these amino acids in addition to pyruvate extended exponential growth and increased antibody titre by 75%.

2.1.2 Stationary Phase is Associated With Oxidative Metabolism and PPP Activity

Transition into stationary phase has been found to coincide with lactate uptake, a drop in cataplerosis and anaplerosis rates, and an increased flux of pyruvate towards acetyl-CoA, which collectively indicate a shift in TCA cycle function towards oxidative metabolism (Ahn and Antoniewicz, 2011; Dean and Reddy, 2013; Templeton et al., 2013). Zagari et al. (2013) found lactate consumption during stationary phase correlated with increased mitochondrial membrane potential and oxygen consumption, two key indicators of oxidative metabolism.

Stationary phase has also been found to coincide with increase flux through the PPP whose activity is minimal during exponential growth phase (Ahn and Antoniewicz, 2011; Templeton et al., 2013). Sengupta et al. (2011) found nearly all ^{13}C-glucose was metabolised to pyruvate via the PPP before entering the TCA cycle for an antibody-producing GS-CHO cell line at stationary phase. Increased activity of the PPP cannot be due to an increased requirement of ribose-5-phosphate for nucleotide synthesis as all the glucose was cycled back to glycolysis. Increased flux through the PPP is therefore likely to promote NADPH production (Figure 2.1). In addition to supporting anabolic reactions, NADPH is required by glutathione reductase for catalysing the reduction of oxidised glutathione (GSSG) back to glutathione (GSH). GSH – a tripeptide (glutamate, cysteine, and glycine) – is a major cellular antioxidant that helps remove reactive oxygen species (ROS). Sengupta et al. (2011) hypothesised that high NADPH production may help to protect the cell from oxidative stress since minimal cellular biomass production takes place at stationary phase. In support of this Templeton et al. (2013) found that both the GSH/GSSG and NADPH/NADP$^+$ ratios decreased as cells transition into late exponential growth and stationary phases. However, this also indicates that increased flux through the PPP is still not enough to maintain NADPH at levels equivalent to early exponential growth phase and to fully regenerate GSH.

2.1.3 CHO Cell Metabolism is Cell Line Dependent

The above studies demonstrate that transition from exponential to stationary growth phase is accompanied by a significant shift in CHO cell metabolism. Figure 2.2 summarises how fluxes through glycolysis, the TCA cycle, and the PPP are redirected to support the biomass objectives of both growth phases.

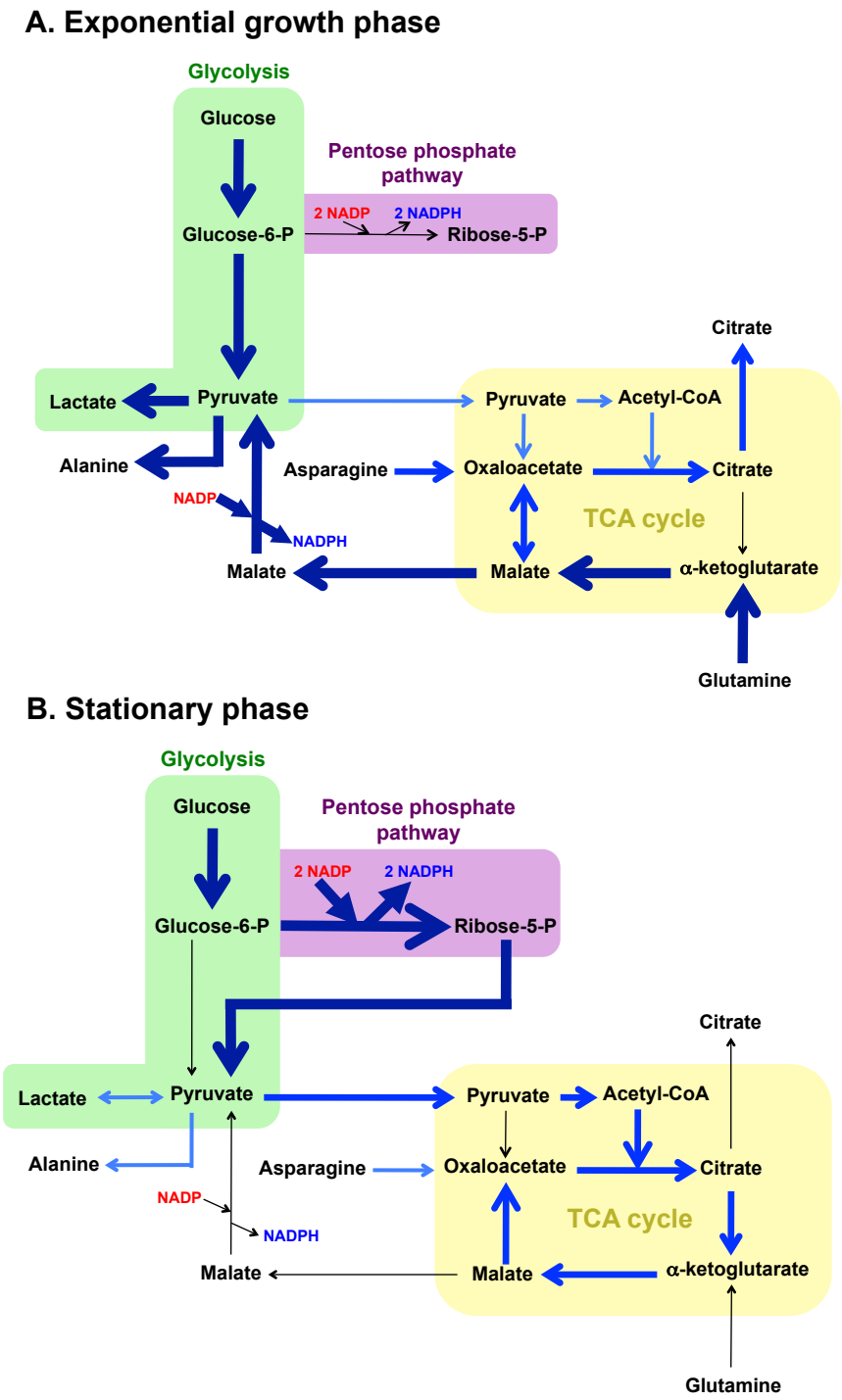

Figure 2.2 Comparison of flux through CHO central metabolic pathways at exponential growth and stationary phase. (**A.**) Aerobic glycolysis and glutaminolysis support biomass production during exponential growth phase. (**B.**) Increased oxidative metabolism and flux through the PPP takes place during stationary phase. Arrow weight indicates the magnitude of flux through a pathway with thick arrows representing high flux rates.

Cell metabolism can however also be very heterogeneous within a cell line. Zagari et al. (2013) found lactate metabolism to differ between a parental CHO-S cell line and a subclone. The parental cell line exhibited a shift to lactate consumption at stationary phase while the subclone continued to be a lactate producer. Furthermore, changing the media composition was shown to shift lactate metabolism in both cell lines. Such a cell-media interaction is in agreement with a study by Dietmair et al. (2012a), which showed that growing a single cell line in three different commercial media resulted in three distinct growth profiles, each with their own unique metabolic profile. Luo et al. (2011) found that changing just the copper concentration in media could significantly alter CHO cell metabolism, demonstrating that cell-media interactions are not just dependent on the nutrient composition of the media.

2.2 Amino Acids and Signaling Pathways

Availability of intracellular amino acids also plays an essential role in regulating global protein synthesis. Amino acid sufficiency stimulates the mammalian target of rapamycin (mTOR) complex 1 (mTORC1) signaling pathway whose activation promotes cell growth (Kim and Guan, 2011; Wullschleger et al., 2006). Amino acid depletion however stimulates the amino acid response (AAR) signaling pathway whose activation inhibits growth (Kilberg et al., 2009).

2.2.1 Leucine and Glutamine Stimulate mTORC1 Signaling

mTOR is a serine-threonine protein kinase that associates with several secondary proteins to form mTORC1 whose structure, upstream regulators, and downstream targets have been extensively reviewed (Kim and Guan, 2011; Wullschleger et al., 2006). Activation of mTORC1 promotes ribosome biogenesis in addition to global protein synthesis while also inhibiting autophagy. Leucine is a potent activator of mTORC1 mediated phosphorylation of both the 70 kDa ribosomal protein S6 kinase (S6K) and the eukaryotic translation initiation factor 4E (eIF4E) binding protein (4E-BP1) (Christie et al., 2002; Hara et al., 1998). Phosphorylation of both S6K and 4E-BP1 activates cellular mechanisms that mediate an increase in protein translation (Wullschleger et al., 2006). Increasing intracellular leucine by 7% in *Xenopus laevis* oocytes was shown to induce a 50% maximal increase in S6K phosphorylation, suggesting a highly sensitive leucine sensing mechanism (Christie et al., 2002). More recently, glutamine has been shown to activate mTORC1 signaling but through a

mechanism distinct from leucine (Jewell et al., 2015). Constitutive expression of human mTOR in CHO cells was shown to increase growth rate, maximal cell density, cell size, total protein content, specific antibody productivity, and culture viability (Dreesen and Fussenegger, 2011). Furthermore, mTOR expression minimised the negative impact that oxygen and nutrient depletion stress conditions had on process productivity.

2.2.2 Amino Acid Response (AAR) Pathway

Depletion of intracellular amino acid levels reduces mTORC1 activity and stimulates autophagy (Kim and Guan, 2011) but also activates the AAR pathway, which acts to decrease global protein synthesis. Kilberg et al. (2009) provide a detailed review of AAR signaling. In brief, a decrease in any amino acid leads to an increase of uncharged tRNA molecules. Their accumulation permits the binding of the general control non-depressible 2 (GCN2) protein kinase, which subsequently phosphorylates the translation initiation factor eIF2α. This inhibits global protein synthesis, but permits an increase in translation of a small subset of genes that includes activating transcription factor 4 (ATF4). ATF4 increases transcription of a number of genes that contain amino acid response elements (AARE), which include a number involved in amino acid transport (xCT/SLC7A11; SNAT2/SLC38A2; CAT-1/SLC7A1) and amino acid biosynthesis (ASNS, asparagine synthetase). Mammalian cells therefore use a combination of autophagy and transport to restore intracellular amino acid levels during nutrient starvation stress.

2.3 Mammalian Amino Acid transporters

Membrane transporters control the movement of amino acids across mammalian cell membranes. These are large proteins containing multi transmembrane domains that create a hydrophilic passage spanning the phospholipid bilayer. Early research on mammalian amino acid transport identified distinct transport systems defined by characteristics such as substrate specificity, ion dependency, transport mechanisms, and sensitivity to substrate analogs (Christensen et al., 1967; Oxender and Christensen, 1963). Many of the individual transporters belonging to these systems were subsequently identified and named during the 90s using molecular cloning and functional characterisation in *X. laevis* oocytes. Amino acid transporters are now grouped into 9 solute carrier (SLC) families based upon amino acid sequence homology to other family members (Bodoy et al., 2013; Fotiadis et al., 2013; Hediger et al., 2004;

Kanai et al., 2013; Pramod et al., 2013; Schiöth et al., 2013; Smith et al., 2013). Genes are named using the SLC symbol, followed by a number to indicate the family it belongs to, then the letter A and a second number to indicate an individual transporter (Hediger et al., 2004). Both the traditional and SLC naming systems are however commonly used within the literature.

To date, 61 mammalian genes encoding proteins with amino acid transport activity at the plasma membrane have been identified (see Table 2.1). These genes can be grouped into four categories: 43 proteinogenic amino acid transporters (those that transport the 20 proteinogenic amino acids), 9 orphan transporters (those with an unknown amino acid transport function), 4 di/tripeptide transporters (those that transport a range of di/tripeptides), and 5 other amino acid transporters (those that transport molecules with an amino acid like structure such as taurine and GABA).

Table 2.1 demonstrates that individual proteinogenic amino acid transporters facilitate the movement of multiple amino acids. Neutral amino acids are mostly transported through transporters belonging to systems A, ASC, B^0, $B^{0,+}$, Gly, L and N. Anionic transport is predominately through systems X_{AG}^- and X_C^-, and cationic transport is predominately through systems y^+ and y^+L. The two proteins belonging to SLC3 have no transport function but multiple SLC7 family transporters must form disulphide bridges with a SLC3 protein for cell surface expression.

Table 2.1 Mammalian amino acid transporters and their transport properties

Gene name (SLC ID)	Protein name	Associated transport system	Amino acid substrates*	Transport mechanism	Ion dependency	References
Proteinogenic amino acid transporters:						
SLC1A1	EAAC1, EAAT3	X^-_{AG}	D, E	S	Na^+, H^+ (S) | K^+ (A)	Kanai et al., 2013
SLC1A2	GLT-1, EAAT2	X^-_{AG}	D, E	S	Na^+, H^+ (S) | K^+ (A)	Kanai et al., 2013
SLC1A3	GLAST, EAAT1	X^-_{AG}	D, E	S	Na^+, H^+ (S) | K^+ (A)	Kanai et al., 2013
SLC1A4	ASCT1, SATT	ASC	A, S, C, T, (V)	A	Na^+	Arriza et al., 1993; Kanai et al., 2013
SLC1A5	ASCT2, AAAT	ASC	A, S, C, T, Q, N, (M, L, G, V, E)	A	Na^+	Kanai et al., 2013; Utsunomiya-Tate et al., 1996
SLC1A6	EATT4	X^-_{AG}	D, E	S	Na^+, H^+ (S) | K^+ (A)	Kanai et al., 2013
SLC1A7	EATT5	X^-_{AG}	D, E	S	Na^+, H^+ (S) | K^+ (A)	Kanai et al., 2013
SLC3A1	rBAT	Heterodimerizes with SLC7A9				Fotiadis et al., 2013
SLC3A2	4F2hc	Heterodimerizes with SLC7 members				Fotiadis et al., 2013
SLC6A5	GlyT2		G	S	Na^+, Cl^-	Pramod et al., 2013
SLC6A7	PROT		P	S	Na^+, Cl^-	Pramod et al., 2013
SLC6A9	GlyT1		G	S	Na^+, Cl^-	Pramod et al., 2013

Gene name (SLC ID)	Protein name	Associated transport system	Amino acid substrates*	Transport mechanism	Ion dependency	References
SLC6A14	$ATB^{0,+}$	$B^{0,+}$, beta-alanine carrier system	All AA except: D, E	S	Na^+, Cl^-	Pramod et al., 2013; Ugawa et al., 2001
SLC6A15	B0AT2	B^0	L, I, V, M, P (A, Q, F)	S	Na^+	Bröer et al., 2006; Pramod et al., 2013
SLC6A17	XT1, NTT4		P, L, M, (C, A, Q, S)	S	Na^+	Pramod et al., 2013; Zaia and Reimer, 2009
SLC6A18	B0AT3, XT2	Gly	L, I, V, M, A, G, S, C	S	Na^+, Cl^-	Pramod et al., 2013; Singer et al., 2009
SLC6A19	B0AT1, HND	B^0	L, I, V, M	S	Na^+	Böhmer et al., 2005; Pramod et al., 2013
SLC6A20	XT3, Xtrp3	IMINO	P	S	Na^+, Cl^-	Pramod et al., 2013
SLC7A1	CAT-1, ATRC1	y^+	R, K, H, O	U	-	Closs et al., 2006; Fotiadis et al., 2013
SLC7A2	CAT-2	y^+	R, K, O	U	-	Closs et al., 2006; Fotiadis et al., 2013
SLC7A3	CAT-3, ATRC3	y^+	R, K, O	U	-	Fotiadis et al., 2013; Vekony et al., 2001
SLC7A5/SLC3A2	LAT1/4F2hc	L	L, I, F, M, Y, H, W, V, (Q)	A	-	Kanai et al., 1998; Yanagida et al., 2001
SLC7A6/SLC3A2	y^+LAT2/4F2hc	y^+L	R, K, H, O, Q, L, M	A (CAA out & NAA in)	Na^+ (S with NAA)	Bröer et al., 2000; Fotiadis et al., 2013
SLC7A7/SLC3A2	y^+LAT1/4F2hc	y^+L	R, K, H, O, Q, L, M	A (CAA out & NAA in)	Na^+ (S with NAA)	Kanai et al., 2000; Torrents et al., 1998
SLC7A8/SLC3A2	LAT2/4F2hc	L	L, I, F, M, Y, H, W, V, G, A, S, T, C, N, (Q)	A	-	Pineda et al., 1999; Segawa et al., 1999

Gene name (SLC ID)	Protein name	Associated transport system	Amino acid substrates*	Transport mechanism	Ion dependency	References
SLC7A9/SLC3A1	$b^{0,+}$AT/rBAT	$b^{0,+}$	R, K, H, L, F, C-C	A (NAA out & CAA in)	-	Chillarón et al., 1996
SLC7A10/SLC3A2	Asc-1/4F2hc	asc	A, C, G, S, T	A	-	Fukasawa et al., 2000; Nakauchi et al., 2000
SLC7A11/SLC3A2	xCT/4F2hc	X^-_C	E, C-C	A (E out & C-C in)	-	Sato et al., 1999
SLC7A12	Asc-2	asc	A, C, G, S, T	U	-	Chairoungdua et al., 2001
SLC7A13	AGT-1, XAT2		D, E	A	-	Matsuo et al., 2002
SLC7A15	ArpAT		Y, W, F, A, S, Q	A	-	Fernández et al., 2005
SLC16A10	TAT1, MCT10	T	F, W, Y	U	-	Kim et al., 2001
SLC36A1	PAT1	PAT	A, G, P	S	H^+	Schiöth et al., 2013
SLC36A2	PAT2	PAT	A, G, P	S	H^+	Schiöth et al., 2013
SLC36A4	PAT4		P, W	S	H^+	Schiöth et al., 2013
SLC38A1	SNAT1	A	Q, N, H, A, M, S	S	Na^+	Schiöth et al., 2013

Gene name (SLC ID)	Protein name	Associated transport system	Amino acid substrates*	Transport mechanism	Ion dependency	References
SLC38A2	SNAT2	A	Q, N, H, A, M, S, C, P, G	S	Na^+	Schiöth et al., 2013
SLC38A3	SNAT3	N	Q, N, H, A	S	Na^+ (S) | H^+ (A)	Schiöth et al., 2013
SLC38A4	SNAT4	A	N, A, S, C, G, T	S	Na^+	Schiöth et al., 2013
SLC38A5	SNAT5	N	Q, N, H, A, G, S	S	Na^+ (S) | H^+ (A)	Schiöth et al., 2013
SLC38A7	SNAT7	A/N	Q, N, H, A, S	unknown	unknown	Schiöth et al., 2013
SLC43A1	LAT3	L	L, I, V, F, M	U	-	Babu et al., 2003
SLC43A2	LAT4	L	L, I, V, F, M	U	-	Bodoy et al., 2005
Orphan transporters:						
SLC7A4	CAT-4		-			Fotiadis et al., 2013
SLC7A14			-			Fotiadis et al., 2013
SLC36A3	PAT3		-			Schiöth et al., 2013

Gene name (SLC ID)	Protein name	Associated transport system	Amino acid substrates*	Transport mechanism	Ion dependency	References
SLC38A6	SNAT6		-			Schiöth et al., 2013
SLC38A8			-			Schiöth et al., 2013
SLC38A9			-			Schiöth et al., 2013
SLC38A10			-			Schiöth et al., 2013
SLC38A11			-			Schiöth et al., 2013
SLC43A3	EEG1		-			Bodoy et al., 2013
Di/Tripeptide transporters:						
SLC15A1	PepT1		di- and tripeptides	S	H^+	Smith et al., 2013
SLC15A2	PepT2		di- and tripeptides	S	H^+	Smith et al., 2013
SLC15A3	PhT2		di- and tripeptides	S	H^+	Smith et al., 2013
SLC15A4	PhT1		di- and tripeptides	S	H^+	Smith et al., 2013
Other amino acid transporters:						
SLC6A1	GAT1		GABA			Pramod et al., 2013
SLC6A6	TauT	b	Taurine			Pramod et al., 2013

Gene name (SLC ID)	Protein name	Associated transport system	Amino acid substrates*	Transport mechanism	Ion dependency	References
SLC6A11	GAT-B, GAT-3		GABA			Pramod et al., 2013
SLC6A12	BGT1		GABA, Betaine			Pramod et al., 2013
SLC6A13	GAT2		GABA			Pramod et al., 2013

Amino acids are given by their one-letter codes. *****Substrates with a low transport affinity are given in parentheses. ***AA***, amino acids; ***CAA***, cationic amino acids; ***NAA***, neutral amino acids; ***O***, ornithine; ***C-C***, cystine; ***A***, antiport; ***S***, symport; ***U***, uniport. Protein names and associated transport systems represent the traditional naming system for amino acid transporters.

2.4 Amino Acid Transporters in Cancer

Cancer cell lines support their increased demand for nutrients by upregulating the expression of nutrient transporters (Ganapathy et al., 2009). Amino acid transporters reported to be upregulated in many cancer cell lines include four neutral transporters: ASCT2 (SLC1A5), LAT1/4F2hc (SLC7A5/SLC3A2), SNAT5 (SLC38A5), and $ATB^{0,+}$ (SLC6A14), plus the anionic transporter xCT/4F2hc (SLC7A11/SLC3A2) (Fuchs and Bode, 2004; Ganapathy et al., 2009; Karunakaran et al., 2011).

A detailed review of neutral amino acid transport in cancer concluded that the majority of cancers preferentially increase their expression of ASCT2 and LAT1 over other neutral amino acid transporters, though $ATB^{0,+}$ expression was not considered in this analysis (Fuchs and Bode, 2004). ASCT2 is a Na^+-dependent obligatory amino acid antiporter that transports a broad range of small neutral amino acids (Utsunomiya-Tate et al., 1996). Because of its high affinity for glutamine (Table 2.1), upregulation of ASCT2 expression has been hypothesised to support mitochondrial glutaminolysis during cell proliferation (Wise and Thompson, 2010). LAT1 is a Na^+-independent obligatory amino acid antiporter that transports neutral amino acids with large, branched or aromatic side-chains, which includes the mTORC1 activating leucine (Kanai et al., 1998; Mastroberardino et al., 1998). In contrast to ASCT2 and LAT1, $ATB^{0,+}$ can transport all neutral and cationic amino acids but not aspartate and glutamate (Karunakaran et al., 2011). The transport of 18 amino acids through a single transporter may however not be beneficial to a proliferating cell as important amino acids such as glutamine and leucine will compete with each other for cell entry.

Nicklin et al. (2009) identified a two-step transport mechanism in HeLa cells by which ASCT2 and LAT1 are functionally coupled to regulate mTORC1 activation. Glutamine is first transported into the cell through ASCT2 and then serves as an efflux substrate through LAT1 for leucine uptake, which subsequently activates mTORC1. The transport of glutamine was found to be rate limiting for mTORC1 activation. This is consistent with the finding that LAT1 has an intracellular affinity for amino acids that is around 100-fold lower than on the extracellular side (Meier et al., 2002), meaning a high intracellular concentration of glutamine is first required to stimulate leucine influx. Interestingly, MCF7 cells have a high basal intracellular concentration of glutamine and are therefore not dependent on glutamine influx through ASCT2 for leucine uptake and mTORC1 activation (Nicklin et al., 2009). This study demonstrates the existence of functional relationships between transporters and how metabolic processes can regulate

transport activity. This could have some important implications for recombinant CHO cells using the glutamine synthetase system when compared to the parental host cells.

Mammalian cells require the activity of uniporters to net accumulate amino acids. In the transport mechanism described above, ASCT2 and LAT1 antiporter activity function together to modify the relative composition of the existing intracellular pool in favor of leucine. Boer (2002) proposed that intracellular glutamine accumulated through uniport transporters from systems A and N may act as an efflux substrate for antiporters belonging to systems ASC and L. In support of this model, coexpression of the system A uniporter SNAT2 (SLC38A2) with LAT1 enhanced leucine uptake in *X. laevis* oocytes (Baird et al., 2009). The expression of the system N SNAT5 in some cancer cell lines (Fuchs & Bode, 2004; Wise et al., 2008) may therefore be supporting antiporter function in addition to glutamine uptake. The efflux of alanine (a ASCT2 substrate) as a waste product during cell proliferation may however be enabling ASCT2 to effectively act as a uniporter and accumulate glutamine in place of a system A or N transporter.

Just one transporter mediates system X_C^- activity – the xCT antiporter. xCT provides the primary import route for cystine (oxidative product of two cysteine molecules) in exchange for exporting intracellular glutamate (Fotiadis et al., 2013; Sato et al., 1999). Cysteine is oxidised to cystine in culture medium and the xCT transporter is commonly expressed in cultured cell lines to support its uptake (Ganapathy et al., 2009). Within the cell, cystine is reduced back to cysteine and can be directed towards the biosynthesis of GSH. Incorporation of cysteine into GSH is the rate-limiting step in its synthesis (Griffith, 1999). The relationship between system X_C^- activity and GSH synthesis has been examined (Chung et al., 2005; Shih et al., 2006). System X_C^- inhibition in human glioma cell lines exhibiting high expression of xCT resulted in rapid depletion of total intracellular GSH and caspase-mediated apoptotic cell death (Chung et al., 2005). Whereas ectopic overexpression of xCT was shown to increase GSH content and offer increased protection from oxidative stress conditions in neuronal rat cells (Shih et al., 2006). Activity of high-affinity glutamate uniporters belonging to system X_{AG}^- can support GSH synthesis by accumulating intracellular glutamate, which is subsequently exported through xCT for cystine import (Lewerenz et al., 2006). This is an example of the functional coupling between uniporters and antiporters as proposed by Boer (2002).

Figure 2.3 summarises the transport activities of the transporters described above and how they function to support the metabolic and signaling pathways that promote cell proliferation.

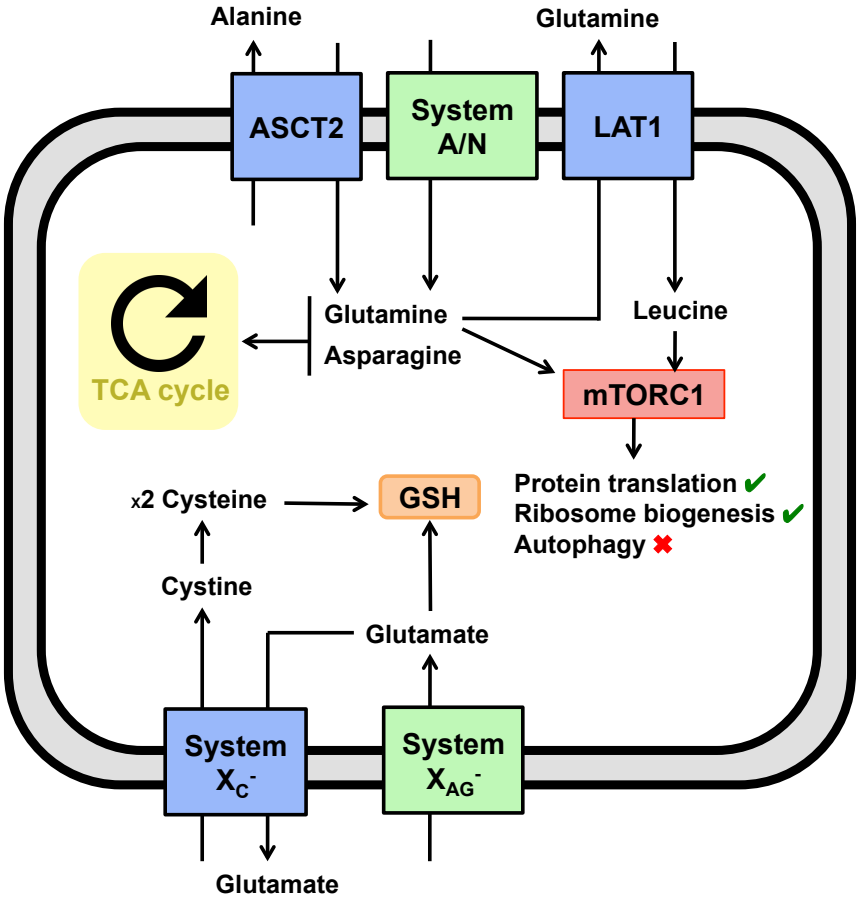

Figure 2.3 Amino acid transporters are functionally coupled to metabolic and signaling pathways that promote cell proliferation.

2.5 Amino Acid Transporters as Potential Cell Engineering Targets

Metabolic engineering can significantly improve the productivity of mammalian cell lines. Most strategies have targeted genes involved in pyruvate metabolism with the aim of decreasing lactate accumulation during culture. For example, overexpression of pyruvate carboxylase (PC) in BHK-21 or CHO cells has been shown to significantly decrease lactate production, improve culture viability, increase product titres, and elevate the ATP content of cells by increasing carbon flux into the TCA cycle (Fogolin et al., 2004; Irani et al., 1999; Kim and Lee, 2007). An alternative engineering strategy has been to knock down gene expression. Zhou et al. (2011) stably expressed small inhibitory RNAs (siRNA) against lactate dehydrogenase (LDH) and three pyruvate dehydrogenase (PDH) kinases (PDHK) whose function is to phosphorylate PDH, which

inhibits PDH activity. Simultaneously reducing LDH and PDHK expression decreased lactate levels and increased antibody production in CHO cells.

Amino acid transporters represent a novel metabolic engineering target because their substrates often feed into several cellular processes that promote growth (Figure 2.3). Similar to overexpression of mTOR discussed above (section 2.2.1), increased expression of amino acid transporters have the potential to simultaneously improve growth, viability, and productivity. A limited number of studies have attempted to engineer mammalian metabolism by targeting transporters. Paredes et al. (1999) used siRNA against GLUT1 (SLC2A1), a high-affinity glucose transporter, to reduce glucose consumption. Wlaschin and Hu (2007) demonstrated that stable expression of GLUT5 (SLC2A5), a fructose-specific transporter, could improve cell growth and reduce lactate production when the main carbon source was switched to fructose. Recently, Tabuchi et al. (2010) demonstrated that overexpression of TauT (SLC6A6), a taurine transporter, can increase culture viability and productivity. TauT helps osmoregulates cells by transporting taurine (Pramod et al., 2013). However, TauT overxpression stimulated increased glutamine consumption and an upregulation of genes involved in GSH metabolism compared to the parental cell line (Tabuchi et al., 2010).

2.6 Summary

The growth of transformed cell lines including CHO cells is supported by amino acids. They can be used directly for macromolecule synthesis (proteins and nucleic acids) and protection against oxidative stress (GSH production), however removal of the amine group leaves a carbon skeleton that can be used for biomass synthesis or anaplerosis of the TCA cycle to support ATP and NADPH production. Amino acids also have a critical role in signaling to pathways that regulate global protein synthesis (mTORC1 and AAR). Cancer cells, as examples of transformed cell lines, support proliferation at high cell densities by upregulating the expression of certain amino acid transporters. These proteins are unique in that they interface with both the extra- and intracellular environment, coupling amino acid influx to metabolic and signaling pathways that promote cell growth. Amino acid transporters therefore represent an attractive group of proteins to investigate further in CHO cells as an understanding of their activity could support media design or open up new cell engineering strategies to improve biomass synthesis. Preliminary evidence in the literature suggests that manipulating amino acid transporter expression in CHO cells can improve productivity.

2.7 Thesis Overview

CHO cells meet the major industrial manufacturing requirements for bringing a recombinant therapeutic mAb to market, securing them as the dominant mammalian expression system. However, the biotechnology industry is continually looking at ways to reduce process development timelines and further increase mAb titres to meet current and future patient demands. A significant level of research has been directed towards understanding CHO cell metabolism, including amino acids, with the aim of identifying cell line engineering targets or rational methods of optimising media compositions to improve cell line productivity. Yet, the intracellular availability of amino acids is controlled by a system of transporter proteins whose function remains largely unknown in CHO cells. The first aim of this thesis is to address this knowledge gap by characterising amino acid transport processes in CHO cells and to understand how they might support culture performance (Chapters 4 & 5). The second aim is to use this knowledge as a basis for exploring ways to improve cell growth and antibody production. Both a cell engineering strategy (Chapter 6) and media design strategy (Chapter 7) is explored.

The first objective in characterising amino acid transport processes was to understand how transporter expression correlates with growth rate, cell viability, and IgG antibody titre. In Chapter 4, Illumina next-generation sequencing was used to measure the expression of amino acid transporter genes in a parental host and two recombinant cell lines throughout a fed-batch process. The data was analysed to identify key transporters and investigate expression differences between the three cell lines at exponential and stationary growth phases. The results indicated that GLAST (SLC1A3, system X^-_{AG}) expression acted as a marker for GS expression, while ASCT1 (SLC1A4, system ASC), LAT1 (SLC7A5, system L), and xCT (SLC7A11, system X_C^-) expression acted as potential markers for production of a recombinant IgG antibody. Furthermore, the xCT transporter was significantly upregulated in all cell lines at stationary phase and formed part of a larger adaptive response to support cellular availability of GSH. Despite xCT upregulation, cystine influx is identified as a bottleneck in GSH synthesis.

Chapter 5 builds upon Chapter 4 by disrupting the activity of amino acid transporters and evaluating the impact this has on culture performance parameters. Cells were treated with inhibitors that block amino acid movement through specific transporter(s). The results confirmed that LAT1 and xCT transport activity supports recombinant antibody production, while xCT transport was also confirmed as a key determinant of culture viability throughout culture for all cell lines. The glycine

transporter GlyT1 (SLC6A9) was also found to support antibody production during late culture. Inhibition of branched-chain and aromatic amino acid transport was found to inhibit cell growth in all cell lines. For non-essential amino acids, the primary entry route for glutamine in parental CHO cells is through system ASC transporters, inhibition of which results in cell death. In contrast, recombinant GS cells were found to be highly dependent on SNAT2 (SLC38A2, system A) activity for cell growth.

In Chapter 6, a directed evolution method was established to isolate sub-populations of the parental host and an antibody-producing cell line resistant to xCT transport inhibition. It was hypothesised that these cells would have increased xCT transport activity and provide the cells with a greater capacity for cystine import to support GSH and antibody synthesis. The evolved host demonstrated increased rates of GSH synthesis, a better ability to deal with an oxidative stress insult, and a heritable improvement in cell growth compared to the non-evolved host. Results regarding specific productivity with the evolved antibody-producing cell line were inconclusive and require further investigation. A sub-population of host cells resistant to system ASC inhibition was also isolated. Neither these cells, nor the host cells with evolved resistance to xCT inhibition were able to outperform the non-evolved parental host in the transient production of a recombinant IgG antibody. The work in this chapter demonstrates that it is possible to isolate cell lines with desirable characteristics for biomanufacturing through manipulation of amino acid transport processes. It however also requires further chracterisation work, which is discussed.

Chapter 7 explores how knowledge of CHO transport processes can be used to rationally direct the optimisation of amino acid concentrations in basal and feed media. In this chapter a mechanistic model for essential amino acid transport is constructed from data generated in Chapters 4 and 5. This model, validated with a subset of data from Chapter 5, demonstrates a hypothetical approach to controlling amino acid consumption rates through modulation of extracellular concentrations. A discussion is provided on how this can then be exploited to maximise the changing biomass objectives throughout cell culture.

Chapter 3

Materials and Methods

This chapter describes general experimental techniques used throughout the subsequent results chapters. Experiments requiring specialised techniques are described in the relevant results chapters.

3.1 Cell Lines and Culture

3.1.1 Cell Lines

MedImmune kindly provided their proprietary suspension-adapted parental CHO host cell line (CAT-S) and four stable recombinant cell lines (GS-Null, T29, T48 and T127). The GS-Null cell line was transfected with an empty glutamine synthetase (GS) vector. The T29, T48 and T127 cell lines were transfected with a vector containing genes for GS, and the heavy and light chains of a human IgG monoclonal antibody (mAb-109).

3.1.2 Routine Sub-Culture

All cell lines were sub-cultured every 3–4 days at a seeding density of 2×10^5 cells.mL^{-1} in 25 mL of CD-CHO medium (Life Technologies, Paisley, UK) in 125 mL vented Erlenmeyer flasks (Corning, Surrey, UK) shaking at 140 rpm in 37^{o}C and 5% CO_2 air (Infors UK, Reigate, UK). CAT-S and recombinant cells were supplemented with 8 mM L-glutamine (Life Technologies) and 50 μM L-methionine sulfoximine (Sigma-Aldrich, Dorset, UK) respectively. Routine assessment of cell concentration and viability was performed by automated trypan blue exclusion using a Vi-CELL Cell Viability Analyzer (Beckham Coulter, High Wycombe, UK).

3.1.3 Cell Growth Parameters

Three parameters were used to describe cell growth: i) Growth rate (μ), ii) Integral of viable cell density (IVCD), and iii) Generation number (GN).

3.1.3.1 Cell Specific Growth Rate

The cell specific growth rate (μ) represents the rate of cell biomass accumulation and was calculated with equation 2.1:

$$\mu\ (\mathrm{hr}^{-1}) = \ln\left(\frac{\mathrm{VCD}_2}{\mathrm{VCD}_1}\right) * \frac{1}{(\mathrm{t}_2 - \mathrm{t}_1)}$$

Where, VCD_1 and VCD_2 is the viable cell density ($x10^6$ cells.mL^{-1}) at the first and second time point t (hr^{-1}) respectively.

3.1.3.2 Integral of Viable Cell Density

The integral of viable cell density (IVCD) is the area under the growth curve. It quantifies the number of working cell hours per unit volume of culture and was used to calculate specific transport rates of amino acids (section 3.2) and antibody production (section 3.3). IVCD was calculated with equation 2.2:

$$\mathrm{IVCD}\ (10^6 \mathrm{cell.hr.mL}^{-1}) = \left(\frac{\mathrm{VCD}_2 + \mathrm{VCD}_1}{2}\right) * (\mathrm{t}_2 - \mathrm{t}_1)$$

3.1.3.3 Generation Number

The generation number (GN) is a measure of cell age and was calculated with equation 2.3:

$$\mathrm{GN} = \ln\left(\frac{\mathrm{VCD}_2}{\mathrm{VCD}_1}\right) * \frac{1}{\ln(2)}$$

3.2 Extracellular Amino Acid Analysis

Culture samples were centrifuged at 200g for 5 min. The supernatant was removed and frozen at -80°C until analysis. Quantification of amino acids was performed at MedImmune by Dr Chris Sellick using the Waters Acquity UPLC® Amino Acid Analysis (AAA) Solution (Waters, Hertfordshire, UK). Specific amino acid transport rates were calculated with equation 2.4:

$$\text{Specific amino acid transport rate } (\text{nmol}.10^6\text{cell}^{-1}.\text{hr}^{-1}) = \frac{AA_2 - AA_1}{IVCD_2 - IVCD_1}$$

Where, AA_1 and AA_2 is the amino acid concentration (nmol.mL^{-1}) at the first and second time point respectively.

3.3 Antibody Quantification

Culture samples were centrifuged at 200g for 5 min. The supernatant was removed and frozen at -80^{o}C until analysis. Quantification of antibody was performed using either a FastELYSA Human Immunoglobulin G Quantification Kit (RD Biotech, Besançon, France), or at MedImmune by Dr Chris Sellick using either an in-house Protein A chromatography method or the Octet® System (Pall Life Sciences, Portsmouth, UK). Specific monoclonal antibody productivity (Q_{mAb}) rates were calculated with equation 2.5:

$$Q_{mAb}\ (\text{mg mAb}.10^6\text{cell}^{-1}.\text{hr}^{-1}) = \frac{mAb_2 - mAb_1}{IVCD_2 - IVCD_1}$$

Where, mAb_1 and mAb_2 is the IgG antibody concentration (mg.mL^{-1}) at the first and second time point respectively.

Chapter 4

Amino Acid Transporter Gene Expression Analysis in CHO Cells Using RNA-Sequencing

This chapter characterises the expression of amino acid transporter genes in a parental CHO host and two recombinant cell lines throughout a fed-batch process. Illumina next-generation sequencing data in combination with measured amino acid transport rates were analysed to identify seven key CHO transporters required to support culture performance. The expression of three transporters: SLC1A4, SLC7A5, and SLC7A11, correlated well with productivity and warrant further investigation as potential targets for cell engineering strategies to improve cell line productivity.

4.1 Introduction

As discussed in Chapters 1 and 2, amino acids support the growth of mammalian cells in a plethora of ways and optimisation of their concentrations in culture medium has helped to significantly improve cell line productivity in fed-batch processes. However, intracellular availability of amino acids is controlled by a system of membrane transport proteins whose function remains largely unknown in CHO cells. Understanding how the expression and activity of these transporters correlates with critical culture performance parameters such as growth rate, cell viability, and product titre could help identify potential bottlenecks in amino acid transport and/or offer new opportunities for improving cell line productivity.

The identity of amino acid transporters in CHO cells is just emerging. Early research found transport systems for neutral amino acids (A, ASC, and L), cationic amino acids (y^+), and anionic amino acids (X_{AG}^- and X_C^-) in CHO cells (Ash et al., 1993; Bass et al., 1981; Igo and Ash, 1998; Rotoli et al., 1989; Shotwell et al., 1981). But it was not until the development of CHO-specific DNA microarrays (Melville et al., 2011; Wlaschin et al., 2005) that expression of individual transporters began to be identified in industrial cell lines (Birzele et al., 2010; Clarke et al., 2011; Doolan et al.,

2010; Shen et al., 2010). However, only a fraction of all mammalian transporters were found using microarrays due to incomplete coverage of the CHO transcriptome. Subsequent studies using next-generation sequencing (NGS) platforms expanded transcriptome coverage and identified the expression of additional CHO amino acid transporters (Becker et al., 2011; Birzele et al., 2010). Recent CHO genome sequencing projects have now predicted the existence of almost all amino acid transporter genes (Lewis et al., 2013; Xu et al., 2011) and has been used to help identify further transporters at both the transcriptomic (Kyriakopoulos et al., 2013) and proteomic level (Baycin-Hizal et al., 2012). To date, of the 61 mammalian genes known to encode proteins with amino acid transport activity at the plasma membrane, 56 have been identified in the CHO genome and 46 have been found expressed at either the transcriptomic or proteomic level. A full list can be found in Appendix Table A1. Of the amino acid transporters reported to be upregulated in cancer cell lines (see Chapter 2; Section 2.4), all but $ATB^{0,+}$ (SLC6A14) have had their expression identified in CHO cells.

Comparative CHO transcriptomic studies have also been used to help identify genes whose expression are associated with desirable cellular biomanufacturing characteristics such as Q_p (Harreither et al., 2005) or high growth rate (Doolan et al., 2010), and to understand the biological mechanisms by which process control strategies such as temperature shift (Kantardjieff et al. 2010) and the inclusion of media components such as copper (Yuk et al., 2014) or sodium butyrate (Yee et al., 2008; Kantardjieff et al. 2010) can enhance cell line productivity. In these studies, the authors analyse the transcriptional response to a treatment compared to control conditions to identify differentially expressed genes (upregulated or downregulated) that are then mapped back to biological pathways. Such studies have helped to identify genes, cellular pathways or processes that are amenable to engineering approaches to increase cell line productivity. For example, Doolan et al. (2010) investigated differences in the transcriptome and proteome of four CHO cells with either a fast or slow growth rate. The authors identified 21 genes associated with a high cell proliferation rate phenotype, 5 of which were investigated further by manipulating their expression with siRNA or overexpression. Interestingly, overexpression of valosin-containing protein (VCP), a gene not obviously identified as having a growth-related function, could increase cell densities by 2.1-fold. The authors concluded that transcriptomic approaches in CHO cells offer a non-hypothesis-limited approach to cell engineering strategies. Other studies have also used transcript profiling to focus on specific cellular pathways. Wong

et al. (2006a) used a CHO-specific DNA microarray to compare the transcriptomes of a CHO cell line producing a recombinant human interferon gamma (IFN-γ) at different growth phases of batch and fed-batch cultures. The authors focused their analysis on apoptosis-related genes and identified 2 anti-apoptotic genes (*Fadd* and *Faim*) and 2 pro-apoptotic genes (*Alg-2* and *Requiem*) that were overexpressed and knocked down respectively in a subsequent cell line engineering study (Wong et al., 2006b). All four approaches were able to delay the onset of apoptosis in batch and fed-batch cultures, which increased IFN-γ titres up to 2.5-fold due to extended periods of high culture viabilities. Kyriakopoulos et al. (2013) is the only transcriptomic study to purposely investigate amino acid transporter expression in CHO cells. By performing qRT-PCR, they identified the expression of 22 amino acid transporter genes in three CHO cell lines grown in batch culture: a non-producer expressing the glutamine synthetase vector, and two antibody-producing cell lines differing in their specific productivity. Of this subset, 21 were proteinogenic amino acid transporters, all of which were upregulated at stationary phase for all cell lines with the largest change observed for the SLC7A11 (xCT, system X_C^-) transporter (up to 16-fold). As discussed in Chapter 2, GSH synthesis is critically dependent upon xCT activity for cystine uptake (Chung et al., 2005; Shih et al., 2006). In addition to SLC7A11, Kyriakopoulos et al. (2013) found transporters for glycine and glutamate, also required for GSH synthesis, to be significantly upregulated for all cell lines at stationary phase. This is suggestive that CHO cells, independent of recombinant protein production, may be modifying their transporter expression at stationary phase to support GSH synthesis.

Kyriakopoulos et al. (2013) focused their data analysis on significant fold-changes in expression and did not take into account transcript abundance. However, a reanalysis of their data revealed some interesting biological conclusions that were missed by the authors. For example, similar to observations in cancer cell lines, there was high expression of SLC7A5 (LAT1, system L), SLC7A11, and their heterodimeric partner SLC3A2 (4F2hc) for all three cell lines. But unlike cancer cells, expression of SLC1A5 (ASCT2, system ASC) was low and SLC38A2 (SNAT2, system A) was very high, suggesting a difference in transport mechanism of small neutral amino acids such as asparagine and serine in CHO cells. There was also equally high expression of the aspartate/glutamate SLC1A3 (GLAST, system X_{AG}^-) transporter, indicating a possible adaptation of cells expressing glutamine synthetase to glutamine free media. The parental host cell line was not analysed however, which could have confirmed this. A comparison of gene expression between the three cell lines found SLC43A1 (LAT4,

system L) and SLC1A2 (GLT-1, system X_{AG}^-) to be significantly upregulated at all time points in culture for antibody-producing cells. The authors suggested that these two transporters could be used as possible biomarkers for productivity. However, the biological significance of these markers is unclear. For example, transcript abundance of SLC1A2 was just a fraction of the abundance of SLC1A3 and both transporters share identical transport kinetics (Danbolt, 2001), suggesting the biological function of GLT-1 is insignificant. A similar comparison can be made with LAT4 and LAT1.

In this chapter, a proprietary parental CHO host cell line (CAT-S) and two recombinant cell lines transfected with either an empty glutamine synthetase (GS) vector (GS-Null) or a human IgG mAb (T127) were grown in a fed-batch process. Illumina next-generation sequencing was used to sequence the transcriptome of the three cell lines at exponential and stationary growth phases. Data on amino acid transporter expression were extracted from the data sets to identify key transporters and investigate possible expression differences between the three cell lines throughout culture. Seven transporters were highly expressed in all three cell lines which collectively account for the transport of all 20 proteinogenic amino acids: SLC1A4 (ASCT1, system ASC), SLC7A1 (CAT-1, system y^+), SLC1A3, SLC7A5, SLC38A2, SLC7A11, and y^+LAT2 (SLC7A6, system y^+L). Of these, SLC1A3 expression acted as a marker for glutamine synthetase expression. While SLC1A4, SLC7A5, and SLC7A11 were identified as potential markers for antibody production in the T127 cell line. Similar to observations reported by Kyriakopoulos et al. (2013), SLC7A11 expression was significantly upregulated at stationary phase in all cell lines. This was found to form part of a larger adaptive response to support cellular availability of GSH. However, measurements of cystine transport rates indicate that despite the upregulation of SLC7A11, cystine transport represents a bottleneck. Together these data demonstrated that ASCT1, LAT1, and xCT warrant further investigation as potential targets for cell engineering or selection strategies to improve cell line productivity.

4.2 Materials and Methods

This section describes the materials and methods used for RNA sample preparation, sequencing, and transcriptome assembly only. The reader is referred to Chapter 3 for details on all other experimental techniques performed in this chapter.

4.2.1 Cell Culture

Fed-batch cultures were performed in parallel duplicate 1-L DASGIP® benchtop stirred-tank bioreactors (Eppendorf, Stevenage, UK). Bioreactors were inoculated at approximately 5 x 10^5 viable cells.mL^{-1} in 800 mL of CD-CHO medium (Life Technologies, Paisley, UK). The bioreactor environment was controlled using DASGIP Control 4.0 software (Eppendorf, Stevenage, UK) with the following set points: agitation 175 rpm; temperature 36.5^oC; dissolved oxygen (DO) 50%; pH range 6.8 ± 0.1. Temperature was controlled using a heater blanket; DO by sparging with a blend of air and oxygen; pH using CO_2 or 1 M $NaHCO_3$. Cultures were maintained for 14 days by feeding 10% of the initial culture volume of a proprietary chemically defined nutrient feed every 48 hr from day 2 onwards. Glucose was measured daily offline using a NOVA 100 Bioprofile Analyzer (Nova Biomedical, Cheshire, UK) and maintained at 8 g.L^{-1} using a separate feed. CAT-S cells were supplemented with 8 mM L-glutamine (Life Technologies) at day 0.

4.2.2 Sample Collection

Duplicate samples of 5 x 10^6 viable cells were collected daily from each bioreactor. Samples were centrifuged at 300g for 5 min, washed once in room temperature PBS, and recentrifuged to remove the supernatant. Cell pellets were snap frozen on dry ice before storing at -80^oC until RNA extraction.

4.2.3 RNA Extraction

Total RNA was extracted from samples using the RNeasy® Mini Kit (QIAGEN, Manchester, UK). In brief, samples were lysed and homogenised in the presence of guanidine salt buffers and passed through a silica membrane within a spin column. The membrane selectively binds RNA molecules longer than 200 nucleotides, which enriched the extracted samples for mRNA molecules. An on-column DNase I digestion using the RNase-Free DNase Set (QIAGEN, Manchester, UK) was performed to remove contaminating genomic DNA.

4.2.4 RNA Assessment

RNA integrity was assessed using a 2100 Bioanalyzer (Agilent Technologies, Cheshire, UK). This is an automated microfluidic device that offers a standardised method of assessing RNA integrity (reviewed in Schroeder et al., 2006). The device separates RNA samples according to their molecular weight and examines multiple features associated with 28S and 18S ribosomal RNA (rRNA) peaks, which then get analysed by an algorithm to generate a RNA Integrity Number (RIN). RIN is graded on a scale of 1 (totally degraded RNA) to 10 (intact). All samples had a RIN > 9.

RNA purity was assessed using a NanoDrop 2000 Spectrophotometer (Thermo Scientific, Loughborough, UK). The ratio of absorbance at 260 nm and 280 nm ($A_{260/280}$), and at 260 nm and 230 nm ($A_{260/230}$) was used to check for carry-over of guanidine salts or other contaminants from the RNA extraction step. All samples were free of contaminants.

4.2.5 Library Preparation and Sequencing

Library preparation and sequencing was outsourced to The Genome Analysis Centre (Norwich, UK). Indexed cDNA libraries were constructed using the TruSeq® RNA Sample Prep Kit (Illumina, Little Chesterford, UK). In brief, poly(A) containing mRNA molecules were extracted from total RNA using poly(T) oligo-attached magnetic beads through two rounds of selection. During the second poly(A) purification round, the RNA was fragmented to help minimise secondary structure formations (Zeng and Mortazavi, 2012). First strand cDNA synthesis was performed on the fragmented RNA molecules using reverse transcriptase and random primers. Following second strand synthesis, 3' and 5' overhangs were removed, and a single A nucleotide was added to the 3' end for subsequent adaptor ligation. Index adaptor oligos were then ligated to both ends of the cDNA and fragments were amplified by PCR to create the final cDNA libraries.

Indexed cDNA libraries were sequenced using the Illumina HiSeq 2000 System (Illumina, Little Chesterford, UK). 12 libraries were loaded over 4 flow cell lanes (3 libraries per lane) and sequenced using 100 bp paired-end reads. Across the 12 libraries 66,085,235 ± 3,954,267 (mean ± SD; n = 12) sequence reads were obtained.

4.2.6 Read Mapping and Transcriptome Assembly

Read mapping and transcriptome assembly was outsourced to The Genome Analysis Centre (Norwich, UK) and performed using the Tuxedo analysis package (Trapnell et

al., 2012). In brief, sequence reads were first mapped to the Bioprocessing Research Industry Club (BRIC) sequenced reference CHO-K1 (ECACC catalogue number 85051005) genome with TopHat. Mapped reads were then provided to Cufflinks to assemble transcripts and estimate their abundance. Transcript abundance within each library was normalised by transcript length and the total number of sequence reads obtained to generate FPKM (fragments per kilobase of transcript per million fragments mapped) values (reviewed in Trapnell et al., 2012). Cuffdiff was subsequently used to compare experimental conditions to identify differentially expressed genes. This analysis package tested the observed log2 fold change in gene expression against the null hypothesis of no change (Trapnell et al., 2012). Significance was determined by assessing the false discovery rate (FDR) adjusted *P*-values (*Q*-values), which was used to reduce the number of false-positives.

4.3 Results

4.3.1 Growth Profiles and RNA-Sequencing Sample Selection

The parental host cell line (CAT-S), a stable transfectant pool expressing the empty glutamine synthetase vector (GS-Null) and a non-clonal cell line expressing an IgG antibody (T127) were grown in fed-batch operations. Growth profiles of the CAT-S, GS-Null, and T127 cell lines are shown in Figure 4.1. The three cell lines were grown in parallel duplicate fed-batch operations but the T127 cell line failed to grow in the second bioreactor. Both CAT-S and T127 cells had an extended exponential growth period and reached stationary phase on day 8 compared to day 6 for the GS-Null cell line. During stationary phase CAT-S and T127 cells diverged in growth with the latter able to maintain higher culture viability until day 14.

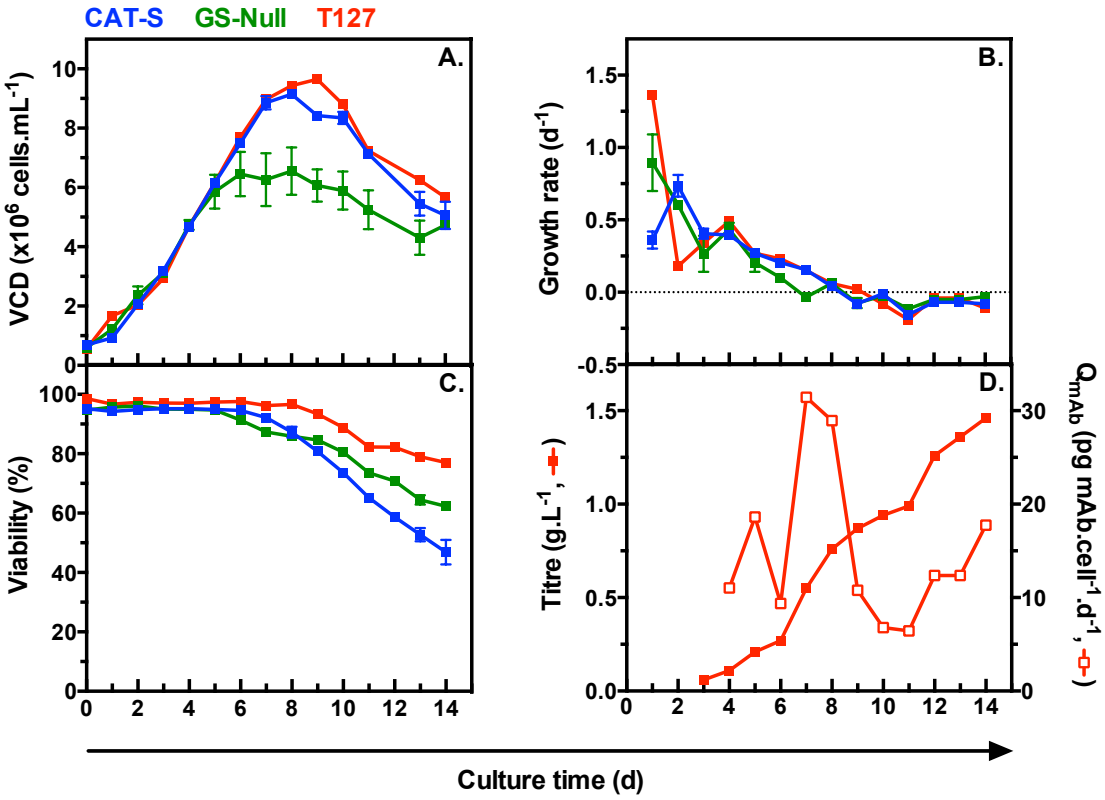

Figure 4.1 Production characteristics of CAT-S, GS-Null, and T127 cells grown in a 14-day fed-batch operation. CAT-S (blue) and GS-Null (green) cells were grown in parallel duplicate 1-L bioreactors (mean ± SEM, n = 2). T127 (red) cells were grown in a single bioreactor. (**A.**) Viable cell density (VCD). (**B.**) Daily growth rates. (**C.**) Culture viability. (**D.**) IgG titre and specific productivity (Q_{mAb}) across the culture period for T127 cells only.

Duplicate samples were taken from a single representative bioreactor at days 4 (mid-exponential) and 8 (stationary) for each cell line and used for RNA-sequencing. The growth rate (d^{-1}) at day 4 was approximately equivalent for the three cell lines (0.44 ± 0.03; mean ± SEM) and cell specific productivity for the T127 cell line was 11.0 pg mAb.cell^{-1}.d^{-1}. At day 8 all cell lines had culture viabilities greater than 80% and the growth rate became negligible (0.05 ± 0.01; mean ± SEM) but cell specific productivity increased approximately 3-fold to 28.9 pg mAb.cell^{-1}.d^{-1}.

4.3.2 Transcriptome Data Sets

The mRNA species from the 12 samples described above was sequenced by synthesis using the Illumina HiSeq 2000 System. From each sample, 66 ± 4 million 100-bp reads (mean ± SD) was obtained and mapped to the Bioprocessing Research Industry Club

(BRIC) sequenced reference CHO-K1 genome (see 4.2 Materials and Methods). Gene expression levels are reported as normalised FPKM values, enabling direct comparisons of expression within and between biological samples.

4.3.3 Amino Acid Transporter Expression Analysis

The transcriptome data sets were mined to obtain average FPKM values for all amino acid transporters for each cell line at both exponential and stationary growth phases (Appendix Table A2–4). Of the 61 known mammalian transporters, 17 were missing from the transcriptome data sets. The remaining 44 transporters were grouped by their FPKM values into low, medium, and high expression. Expression boundaries were determined by dividing the FPKM values for all genes in each transcriptome data set into quartiles (Appendix Table A5) (method adapted from Toung et al., 2011). Proteinogenic transporters were then filtered for those whose expression is either medium or high (top 75% percentile) relative to the global transcriptome (Table 4.1). Applying a FPKM cut-off risks missing biologically important transporters with low expression. However, the transporters identified in Table 4.1 can account for the transport of all 20 amino acids. Furthermore, many of these transporters have high substrate affinities and some have biological significance in cancer cell lines (see Chapter 2).

Table 4.1 Proteinogenic amino acid transporters with medium or high expression at exponential and stationary growth phase

		FPKM					
		Exponential			Stationary		
SLC ID	Protein name	CAT-S	GS-Null	T127	CAT-S	GS-Null	T127
Transporters of small neutral amino acids (broad specificity):							
SLC38A2	SNAT2	89.87	127.22	93.19	107.48	149.09	129.40
SLC1A4	ASCT1, SATT	39.08	39.76	76.81	70.68	80.95	243.63
SLC38A7	SNAT7	19.29	20.14	19.62	22.08	16.74	22.06
SLC38A4	SNAT4	3.38[a]	5.01	7.68	5.92	8.40	7.57
Transporters of small neutral amino acids (narrow specificity):							
SLC36A4	PAT4	14.06	17.43	10.89	19.67	23.72	19.91
SLC6A9	GlyT1	4.65	10.31	7.07	8.40	12.25	13.14
SLC36A1	PAT1	7.57	9.53	5.70	9.97	12.40	10.30
Transporters of branch-chained and aromatic amino acids:							
SLC7A5	LAT1	58.57	81.76	30.85	77.31	82.27	91.26
SLC43A2	LAT4	28.42	18.41	18.87	26.07	14.62	19.74
SLC6A15	B0AT2, v7-3, NTT7-3	21.29	27.38	16.66	28.16	31.66	20.06
SLC7A15	ArpAT	11.64	9.65	12.76	12.54	12.31	14.12
Transporters of cationic amino acids:							
SLC7A1	CAT-1, ATRC1	23.07	25.71	26.09	24.65	26.00	28.31
SLC7A6	y+LAT2	23.98	23.54	23.25	23.86	21.69	20.53
SLC7A7	y+LAT1	7.88	12.05	11.77	9.48	12.73	13.70
Transporters of anionic amino acids:							
SLC1A3	GLAST, EAAT1	26.91	46.64	39.35	32.74	50.99	59.95
SLC7A11	xCT	2.89[a]	9.45	5.99	15.36	22.58	49.86
SLC1A2	GLT-1, EAAT2	0.99[a]	2.25[a]	0.90[a]	2.22[a]	4.01	2.55[a]
Heterodimeric/heavy subunit partner:							
SLC3A2	4F2hc	113.23	136.64	161.58	128.09	138.43	215.08

All FPKM values are the average of two independently sequenced samples. [a]Indicates that expression was in the bottom 25th percentile at the given time point but has been included in the table for comparison purposes.

4.3.3.1 Proteinogenic Transporter Expression at Exponential Growth Phase

The 18 transporters in Table 4.1 were first examined to identify transporters with a high expression during exponential growth and to detect possible expression differences between the three cell lines at this point in culture.

When ranked in order of increasing expression, four transporters were found to be highly expressed in all three cell lines: SLC3A2 (4F2hc, heavy subunit partner of multiple SLC7 family transporters), SLC38A2 (SNAT2, system A), SLC1A4 (ASCT1, system ASC), and SLC7A5 (LAT1, system L). Both SNAT2 and ASCT1 transport small non-essential neutral amino acids such as alanine, asparagine, glutamine, and serine. Whereas LAT1 transports both branched-chained and aromatic essential amino acids such as leucine and phenylalanine respectively (see Chapter 2; Table 2.1). For the two cell lines expressing glutamine synthetase (GS-Null and T127), SLC1A3 (GLAST, system X_{AG}^-) – a glutamate and aspartate transporter, was also highly expressed. Moderate expression of SLC7A1 (CAT-1, system y^+) and SLC7A6 (y^+LAT2, system y^+L) in all three cell lines suggests that these transporters facilitate the transport of arginine and lysine (the cationic amino acids).

Differences between the three cell lines were investigated by identifying transporters differentially expressed with a statistical significance of Q-value < 0.05 (Figure 4.2). The effect of recombinant glutamine synthetase on transporter expression was first explored by comparing the CAT-S and GS-Null cell lines (Figure 4.2 A). Both SLC7A11 (xCT, system X_C^-) – a cystine and glutamate transporter, and SLC6A9 (GlyT1) – a glycine transporter, were found to be significantly upregulated by over 2-fold (log2 value of 1.0) in GS-Null cells. The SLC1A3 transporter was also found to be significantly upregulated but just short of a 2-fold increase.

The effect of antibody expression on transporter expression was then explored by comparing the CAT-S and T127 cell lines (Figure 4.2 B). As with GS-Null cells, SLC7A11 was again found to be significantly upregulated by over 2-fold in T127 cells. Both SLC1A3 and SLC6A9 were also again significantly upregulated but the magnitude of increase was lower in the antibody producing cells compared to GS-Null cells. Differences in expression unique to antibody producing cells were found with two transporters described above as having high FPKM values in all three cell lines: SLC1A4 and SLC7A5. The SLC1A4 transporter was found to be significantly upregulated by over 2-fold, while the SLC7A5 transporter was found to be significantly downregulated by approximately 2-fold in T127 cells. Interestingly, SLC43A2 (LAT4) – a second system L transporter with similar selectivity for branched-chain amino acids,

was also found to be significantly downregulated in T127 cells during exponential growth. Lastly, SLC38A4 (SNAT4) – a second system A transporter with similar amino acid selectivity and transport kinetics to SNAT2, was found to be significantly upregulated by 2-fold in T127 cells. However, SLC38A4 has a very low FPKM value compared to SLC38A2 suggesting that despite the large change in expression, this transporter makes a small contribution to the movement of small non-essential neutral amino acids in T127 cells during exponential growth.

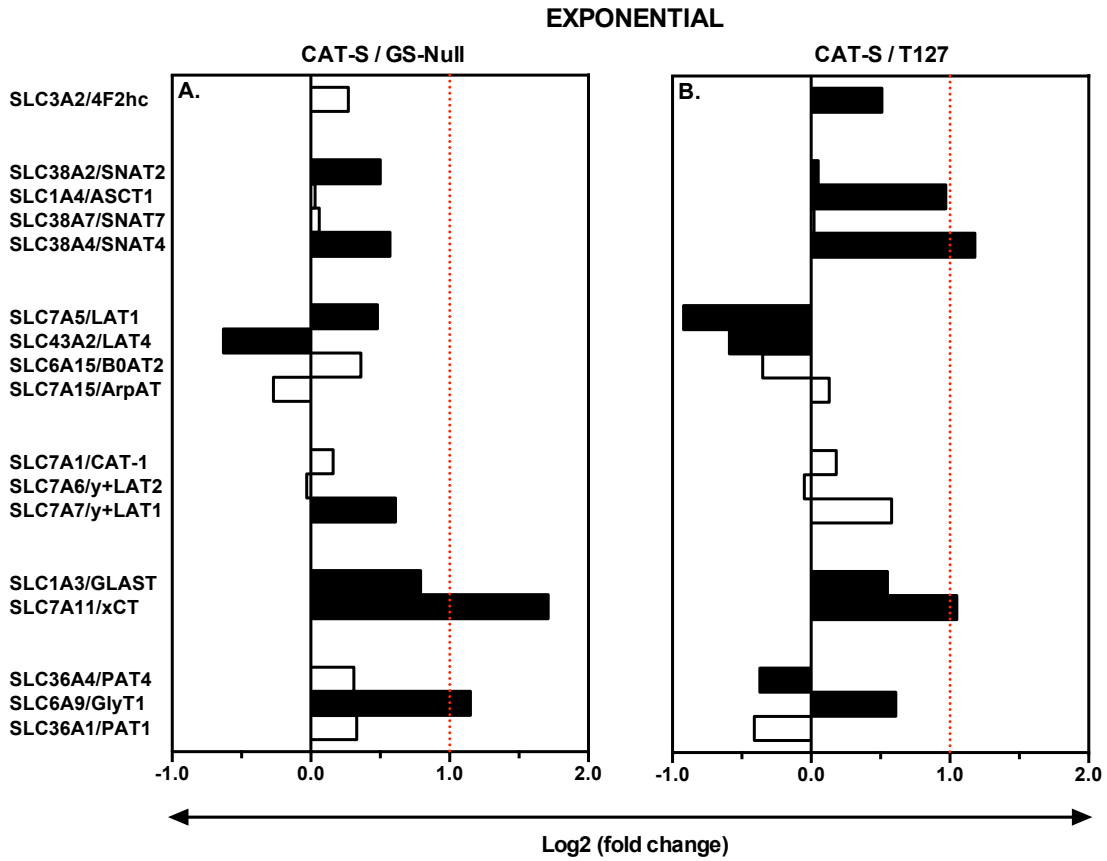

Figure 4.2 Differential expression of amino acid transporter genes between CAT-S, GS-Null, and T127 cells at exponential growth phase. (**A.**) Comparison of CAT-S and GS-Null cells. (**B.**) Comparison of CAT-S and T127 cells. Average (n = 2) log2 fold change in gene expression was provided by Cuffdiff (see 4.2 Materials and Methods). Closed bars represent significant changes in expression (Q-value < 0.05). Broken red line at 1.0 indicates a 2-fold change in expression.

4.3.3.2 Proteinogenic Transporter Expression at Stationary Growth Phase

Stationary growth phase is characterised by the arrest of cell proliferation and maintenance of high cell viability. For antibody producing cells it is also associated with an increase in antibody production compared to exponential growth. Expression of the 18 transporters from Table 4.1 was examined to identify any significant differences in gene expression that may support these changes in biomass objectives. Two comparisons were performed: within culture for a given cell line (Figure 4.3) and between cell lines at stationary phase (Figure 4.4), the latter identical to the previous analysis for exponential growth.

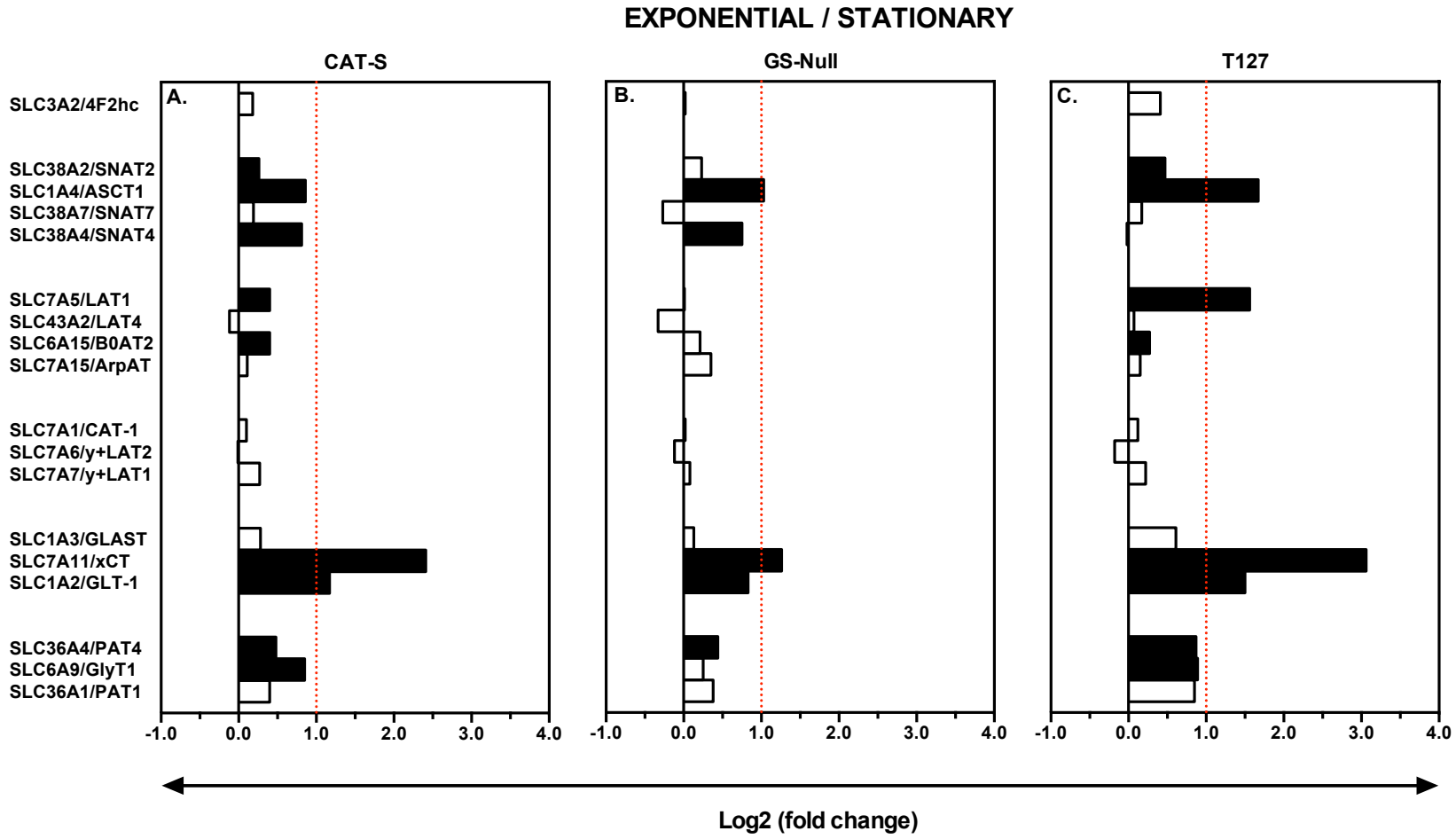

Figure 4.3 Differential expression of amino acid transporter genes within culture. (**A.**) CAT-S, (**B.**) GS-Null, and (**C.**) T127 cells had their expression compared at exponential and stationary growth phase. Average (n = 2) log2 fold change in gene expression was provided by Cuffdiff. Closed bars represent significant changes in expression (*Q*-value < 0.05). Broken red line at 1.0 indicates a 2-fold change in expression.

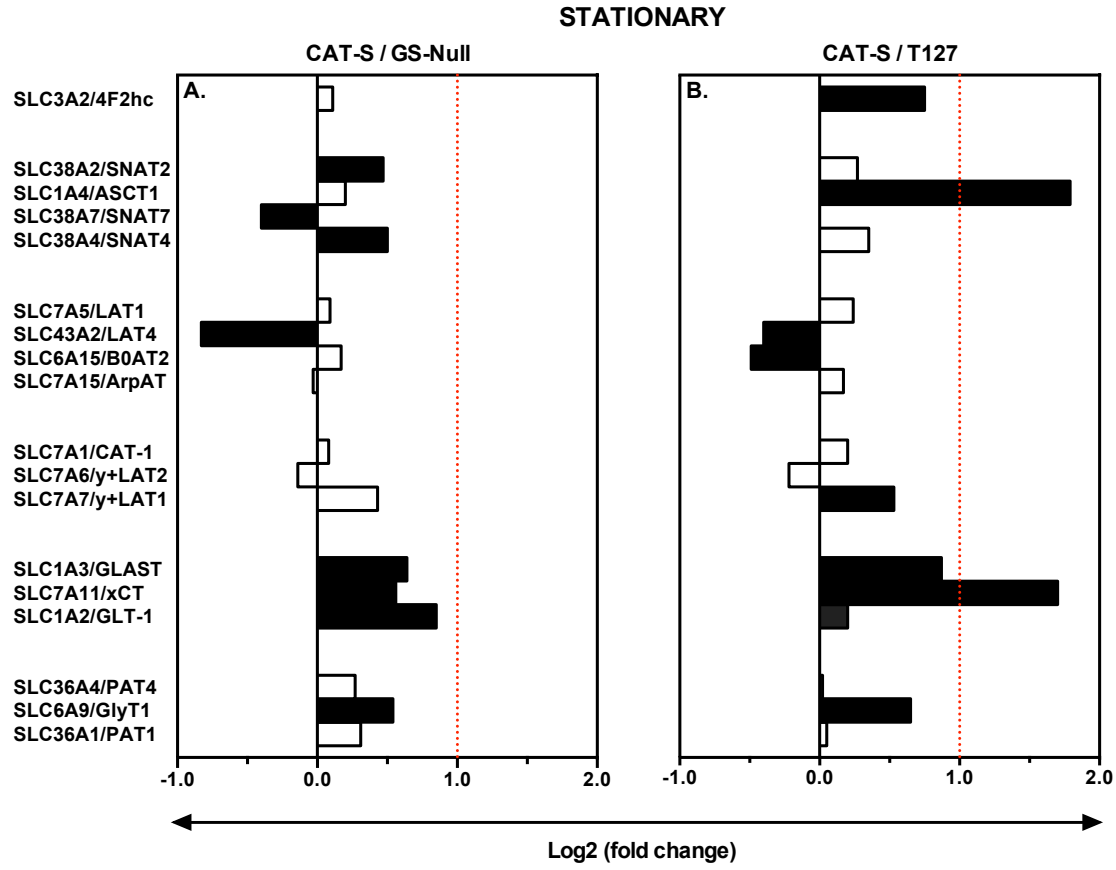

Figure 4.4 Differential expression of amino acid transporter genes between CAT-S, GS-Null, and T127 cells at stationary growth phase. (**A.**) Comparison of CAT-S and GS-Null cells. (**B.**) Comparison of CAT-S and T127 cells. Average (n = 2) log2 fold change in gene expression was provided by Cuffdiff (see 4.2 Materials and Methods). Closed bars represent significant changes in expression (*Q*-value < 0.05). Broken red line at 1.0 indicates a 2-fold change in expression.

Transition into stationary growth phase was associated with a significant upregulation of SLC7A11 in all three cell lines (Figure 4.3). The magnitude of increase was largest in the T127 cells (8-fold) such that its expression is now 3-fold higher than the host cell line and one of the most abundantly expressed transporters in T127 cells (Figure 4.4 B and Table 4.1). Expression of SLC7A11 is associated with GSH synthesis and resistance to ROS (Chung et al., 2005; Shih et al., 2006). Interestingly, CAT-S and T127 cells, which demonstrated the largest upregulation of SLC7A11, also demonstrate a large significant upregulation of the glutamate and glycine transporters SLC1A2 (GLT-1, system X_{AG}^-) and SLC6A9 respectively (Figure 4.3). The same observation was made by Kyriakopoulos et al. (2013). Increased expression of SLC7A11 was found to correlate with increased cell viability in T127 cells compared to the host and GS-Null

cell line (Figure 4.1 C). In addition to SLC7A11 the SLC1A4 transporter was also found to be significantly upregulated in all three cell lines (Figure 4.3). SLC1A4 expression is now the most abundant transporter in T127 cells with an expression 3-fold higher than the host cell line (Figure 4.4 B and Table 4.1). A change unique to the antibody expressing cell line is the significant upregulation (3-fold) of the SLC7A5 transporter. Whilst found to be downregulated compared to the host and GS-Null cell lines during exponential growth, the transporter is now expressed equivalently across the three cell lines (Figure 4.4).

Ranking the 18 transporters in order of increasing expression again shows that SLC3A2 and SLC38A2 remain amongst the most abundant transporters during stationary growth in all cell lines with no considerable change in expression from exponential growth (Table 4.1 and Figure 4.3). SLC1A3 expression also remains high in the two glutamine synthetase expressing cell lines (GS-Null and T127), whereas SLC7A1 and SLC7A6 remain moderately expressed in all cell lines and do not change throughout culture.

Figure 4.5 provides a graphical summary of proteinogenic amino acid transporter expression differences between cell lines and within culture.

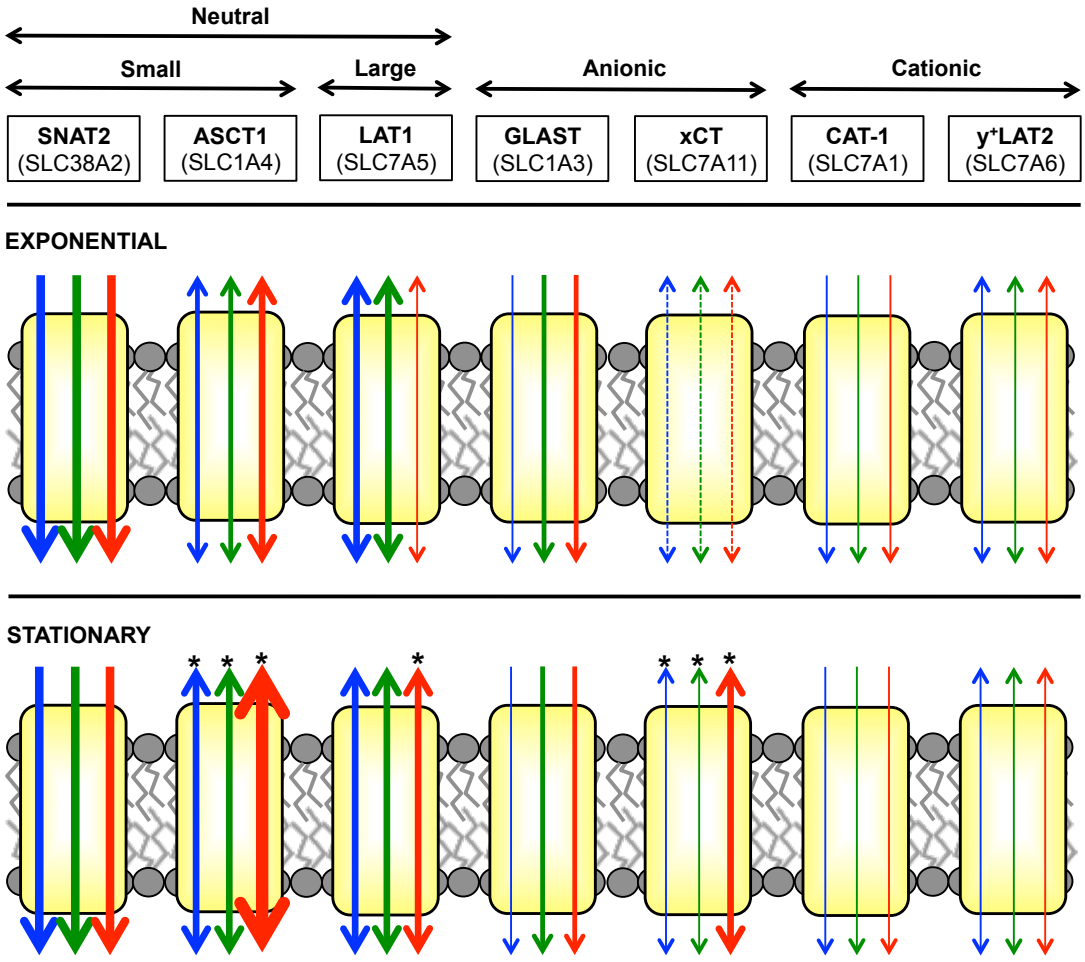

Figure 4.5 Comparison of proteinogenic amino acid transporter expression in CAT-S, GS-Null, and T127 cells at exponential and stationary growth phase. Arrow thickness is weighted to represent relative differences in abundance (FPKM values) with the broken arrow indicating low expression. Blue, green, and red arrows represent CAT-S, GS-Null, and T127 cell lines respectively. Single and double arrows signify uniport and antiport transport respectively. An asterisk denotes a significant upregulation of transporter expression by 2-fold at stationary phase compared to exponential phase (Q-value < 0.05).

4.3.3.3 Expression of Genes Involved in Regulating Cellular GSH Levels

To investigate if increased SLC7A11 expression at stationary phase is part of an adaptive response to support GSH synthesis, the expression of enzymes involved in regulating cellular GSH levels was examined in the three cell lines (Table 4.2). *De novo* synthesis of GSH is mediated by the sequential action of γ-glutamylcysteine synthetase (heterodimer of GCLM and GCLC) and GSH synthetase (GSS) (Griffith, 1999). The

intermediate of these reactions, L-γ-glutamyl-L-cysteine, can be degraded by γ-glutamylcyclotransferase (GGCT), which limits GSH synthesis via GSS (Griffith, 1999). Finally, glutathione reductase (GSR) activity increases cellular availability of GSH by catalysing the reduction of GSSG back to GSH (discussed in Chapter 2). Both the recombinant glutamine synthetase expressing cell lines exhibited a significant downregulation (~2-fold) of GGCT. The T127 cell line also exhibited a significant upregulation (~1.5-fold) of GSR. In contrast, the CAT-S cells showed a significant upregulation of GCLM but the fold-change was relatively small. In summary, T127 and GS-Null cells modulate the expression of three and two genes respectively to increase GSH availability, while CAT-S cells modulate a single gene. The total number of changes correlates well with observed culture viabilities during late culture: T127 > GS-Null > CAT-S (Figure 4.1 C).

Table 4.2 Differential expression of enzymes involved in regulating cellular GSH levels in response to transition from exponential to stationary growth phase of culture

		Log2 (fold change)		
Gene symbol	**Gene name**	**CAT-S**	**GS-Null**	**T127**
Genes that promote cellular GSH levels:				
SLC3A2	Solute carrier family 3 (amino acid transporter heavy chain), member 2; 4F2hc	0.18	0.02	0.41
SLC7A11*	Solute carrier family 7 (anionic amino acid transporter light chain, xc- system), member 11	**2.41**	**1.26**	**3.06**
GSR*	Glutathione reductase	0.04	-0.04	**0.72**
GCLM	Glutamate-cysteine ligase, modifier subunit	**0.39**	0.07	0.15
GCLC	Glutamate-cysteine ligase, catalytic subunit	-0.09	-0.03	0.14
GSS	Glutathione synthetase	-0.34	-0.31	0.16
Genes that limit cellular GSH levels:				
GGCT	Gamma-glutamyl cyclotransferase	-0.26	**-0.87**	**-0.97**

Average (n = 2) log2 fold change in gene expression was provided by Cuffdiff (see 4.2 Materials and Methods). Significant fold changes are in bold (*Q*-value < 0.05). *Indicates genes with multiple transcriptomic gene entries, which had their FPKM values summed to calculate total fold change and designated significant if at least one gene entry exhibited a significant fold change.

4.3.3.4 Expression of Target Genes of the AAR Pathway

Activation of the amino acid response (AAR) pathway will also lead to increased expression of the xCT transporter (discussed in Chapter 2). The AAR pathway has been shown to be stimulated by amino acid depletion in multiple CHO cell lines (Fomina-Yadlin et al., 2013). To investigate if increased xCT expression at stationary phase is a consequence of AAR activation the expression of additional genes known to be regulated via this pathway was examined (Table 4.3). Of the 12 AAR target genes identified from the literature (Fomina-Yadlin et al., 2013; Kilberg et al., 2009; Lee et al., 2008), 3 were missing from the transcriptome data sets. Of the remaining 9 genes, ASNS, ATF3, and TRIB3 were significantly upregulated in addition to SLC7A11 in all cell lines. DDIT3 was upregulated in CAT-S and GS-Null cells only. There was no change in the 4 remaining genes for any cell line. In summary, of the AAR pathway target genes examined, increased expression was observed in only half of them in response to transition into stationary phase.

Table 4.3 Differential expression of genes regulated by the AAR pathway in response to transition from exponential to stationary growth phase of culture

		Log2 (fold change)		
Gene symbol	**Gene description**	**CAT-S**	**GS-Null**	**T127**
ASNS	Asparagine synthetase	**0.46**	**0.76**	**0.56**
ATF3	Activating transcription factor 3	**1.00**	**0.98**	**0.77**
DDIT3	DNA-damage-inducible transcript 3	**1.12**	**1.43**	0.18
SLC7A1	Solute carrier family 7 (cationic amino acid transporter, y+ system), member 1; CAT-1	0.10	0.02	0.12
TRIB3	Tribbles homolog 3	**0.82**	**1.00**	**1.21**
VEGFA	Vascular endothelial growth factor A	0.26	0.08	-0.01
ATF4*	Activating transcription factor 4	0.20	-0.04	0.12
SLC7A11*	Solute carrier family 7 (anionic amino acid transporter light chain, xc- system), member 11	**2.41**	**1.26**	**3.06**
SLC38A2*	Solute carrier family 38, member 2; SNAT2	0.26	0.23	0.47
CEBPB	CCAAT/enhancer binding protein (C/EBP), beta	-	-	-
EIF4EBP1	Eukaryotic translation initiation factor 4E binding protein 1	-	-	-
HERPUD1	Homocysteine-inducible, endoplasmic reticulum stress-inducible, ubiquitin-like domain member 1	-	-	-

Average (n = 2) log2 fold change in gene expression was provided by Cuffdiff (see 4.2 Materials and Methods). Significant fold changes are in bold (Q-value < 0.05). *Indicates genes with multiple transcriptomic gene entries, which had their FPKM values summed to calculate total fold change and designated significant if at least one gene entry exhibited a significant fold change.

4.3.3.5 Expression of Non-Proteinogenic Transporters

Expression of transporters belonging to the three groups of non-proteinogenic transporters (orphan, di/tripeptide, and other) were also filtered to identify transporters whose expression is in the top 75% percentile (Table 4.4). Three transporters were found to be highly expressed in all three cell lines at both growth phases: SLC38A10 (orphan transporter), SLC15A3 (PhT2, di/tripeptide transporter), and SLC6A6 (TauT, taurine transporter). The substrate profile and biological function of SLC38A10 is unknown, however it shares a high degree of protein homology to SLC38 family transporters that includes the highly expressed SLC38A2 transporter (Schiöth et al., 2013). PhT2 transports dipeptides, tripeptides, and histidine (Smith et al., 2013). Interestingly, feeding histidine- and tyrosine-dipeptides to antibody-producing CHO cells in fed-batch processes has been shown to enhance productivity and culture viability by ~40% and ~70% respectively (Kang et al., 2012). Also, TauT overexpression has been shown to enhance the viability and productivity of CHO cells (Tabuchi et al., 2010).

Table 4.4 Non-proteinogenic amino acid transporters with medium or high expression at exponential and stationary growth phase

		FPKM					
		Exponential			Stationary		
SLC ID	Protein name	CAT-S	GS-Null	T127	CAT-S	GS-Null	T127
Orphan transporters:							
SLC38A10		103.11	91.86	62.90	130.61	146.91	93.22
SLC38A6	SNAT6	15.38	18.60	20.65	15.55	14.76	17.19
SLC38A9		7.41	9.27	6.47	9.84	9.99	9.46
Di/Tripeptide transporters:							
SLC15A3	PhT2	36.95	44.78	44.34	43.88	58.50	26.97
SLC15A4	PhT1	12.50	11.45	12.04	20.46	17.04	14.36
Other amino acid transporters:							
SLC6A6	TauT	82.25	41.07	57.82	87.67	32.55	77.54

All FPKM values are the average of two independently sequenced samples.

4.3.4 Amino Acid Transport Rate Analysis

Extracellular amino acid concentrations were measured for the three cell lines (Appendix Figure A1) and net transport rates were calculated at days 4, 6, 8, and 10 to see if they reflect observations in transporter expression (Figure 4.6 and Table 4.5). Transport rates were grouped by amino acid charge and size as transporters typically facilitate the movement of multiple amino acids based upon these two properties. This was done to help maximise biological interpretation from the data sets.

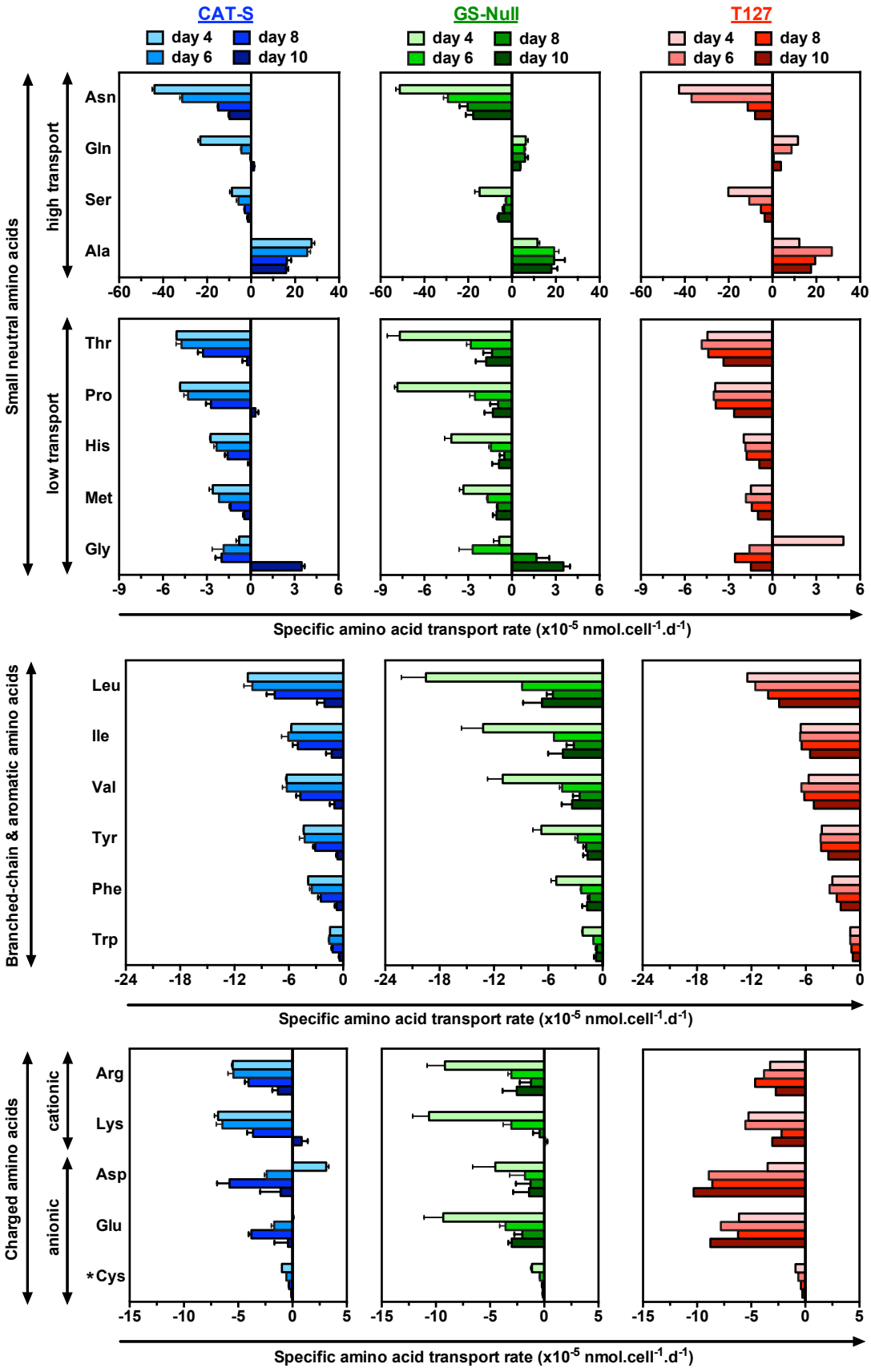

Figure 4.6 Comparison of specific amino acid transport rates throughout culture for CAT-S, GS-Null, and T127 cells. CAT-S (blue) and GS-Null (green) rates are measured from parallel duplicate 1-L bioreactors (mean + SEM, n = 2). T127 (red) rates

are from a single bioreactor. Negative and positive rates represent consumption and production respectively. Amino acids are grouped by charge and size. *Cystine is included with the anionic group due its transport dependence upon glutamate via the xCT transporter.

Table 4.5 Total specific amino acid transport rates throughout culture for CAT-S, GS-Null, and T127 cells

	Total specific amino acid transport rate					
	Small neutral amino acids			Charged amino acids		
Day	High transport	Low transport	BCAA and AAA	Cationic	Anionic*	Total
CAT-S:						
4	103.2 ± 0.4	16 ± 0.0	32.1 ± 0.1	12.4 ± 0.4	4.2 ± 0.3	**168.0 ± 0.1**
6	67.0 ± 1.8	15.4 ± 1.6	31.6 ± 3.1	11.9 ± 1.1	4.6 ± 0.5	**130.4 ± 7.1**
8	34.4 ± 1.9	10.9 ± 1.4	24.0 ± 2.6	7.7 ± 0.9	9.9 ± 1.4	**87.0 ± 8.2**
10	28.6 ± 0.3	4.7 ± 0.1	6.0 ± 2.4	2.2 ± 0.0	3.2 ± 1.5	**44.8 ± 4.1**
GS-Null:						
4	83.9 ± 4.0	23.9 ± 1.4	57.8 ± 8.3	19.8 ± 3.1	15.0 ± 4.0	**200.4 ± 20.9**
6	56.7 ± 4.4	11.1 ± 1.8	24.9 ± 0.7	6.1 ± 1.1	5.8 ± 1.9	**104.5 ± 1.1**
8	49.1 ± 9.2	5.5 ± 0.6	15.1 ± 2.8	1.8 ± 1.5	3.6 ± 2.1	**75.1 ± 2.2**
10	45.6 ± 6.8	8.5 ± 1.6	18.5 ± 6.1	2.8 ± 1.4	4.6 ± 1.7	**80.0 ± 14.2**
T127:						
4	86.7	16.6	33.1	8.5	10.5	**155.5**
6	83.2	14.1	33.5	9.4	17.4	**157.6**
8	36.5	14.0	30.7	6.8	15.2	**103.2**
10	32.9	9.3	26.1	5.8	19.4	**93.4**

The absolute value is taken of negative consumption rates in calculating total transport rates (nmol 10^{-5} $cells^{-1}$ day^{-1}). Amino acids are grouped by charge and size. ***BCAA***, branched-chain amino acids; ***AAA***, aromatic amino acids. *Anionic group includes cystine due its transport dependence upon glutamate via the xCT transporter.

Total amino acid transport rates were approximately equivalent in the CAT-S and T127 cell lines at day 4 (168.0 ± 0.1 versus 155.5 $x10^{-5}$ $nmol.cell^{-1}.d^{-1}$; Table 4.5). The GS-Null cell line had a higher transport rate (200.4 ± 20.9 $x10^{-5}$ $nmol.cell^{-1}.d^{-1}$)

despite achieving comparable growth rates, suggesting poor amino acid utilisation efficiency in these cells. Kyriakopoulos et al. (2013) reported a similar obsevation in their GS-Null cell line. A breakdown analysis of total transport revealed GS-Null cells to be consuming branched-chain, aromatic, and cationic amino acids at rates approximately twice that of the CAT-S and T127 cell lines (Table 4.5). Both GS-Null and T127 cells were found to have increased transport of aspartate and glutamate compared to CAT-S cells, correlating well with a higher expression of GLAST in these cell lines (Figure 4.2). At day 6 CAT-S and T127 cells remained in exponential growth. Total amino acid transport stayed constant in T127 cells but dropped slightly for CAT-S cells as glutamine availability became limited (Appendix Figure A1).

Total amino acid transport rates decrease as cells transition into stationary phase: 87.0 ± 8.2 for CAT-S cells at day 8, 103.2 for T127 cells at day 8, and 104.5 ± 1.1 for GS-Null cells at day 6 (Table 4.5). A drop in asparagine consumption largely caused the reduction in total transport for CAT-S and T127 cells at day 8 compared to day 4 as its availability became limited (Appendix Figure A1). Total transport rates are approximately equivalent across the three cell lines at stationary phase despite T127 cells producing an antibody with a high specific productivity, suggesting amino acid consumption is in excess of protein synthesis requirements. However, breakdown analysis of total transport also reveals that T127 cells were best able to maintain their consumption rate of certain small neutral amino acids (histidine, methionine, proline, serine, and threonine) as well as the branched-chain and aromatic amino acids at day 8. At day 10, the consumption rate of these amino acids continued to remain high in T127 cells but dropped drastically in CAT-S cells. This observation correlates with the previously described significant upregulation of SLC7A5 (branched-chain/aromatic amino acid transporter) and SLC1A4 (high affinity transporter of threonine) expression at day 8 for T127 cells. The SLC1A4 transporter also has a high affinity for serine, whose transport rate is greatest in T127 cells at all culture time points.

Transcriptomic data found the xCT transporter to be significantly upregulated in all three cell lines during stationary phase. This antiporter imports extracellular cystine in exchange for intracellular glutamate with a 1:1 stoichiometry, suggesting an increased cellular requirement for cystine during stationary growth. Cystine consumption was however found to decrease during stationary phase in all three cell lines (Figure 4.6).

4.3.5 Amino Acid Analysis of Two Additional IgG-Producing Cell Lines

Two further cell lines producing the same human IgG mAb (T29 and T48) were grown in duplicate fed-batch operations independently of the three cell lines already described (Figure 4.7). The three IgG producing cells lines vary in productivity. Average cell specific productivity (pg mAb.cell^{-1}.d^{-1}) of T127 cells is approximately double that of T29 cells (17.7 versus 7.5 ± 0.7, mean ± SEM) but approximately equal to T48 cells (17.7 versus 15.0 ± 1.1, mean ± SEM). Extracellular amino acid concentrations were measured for both cell lines to calculate net transport rates that were then compared to those in T127 cells (Figure 4.8 and Table 4.6).

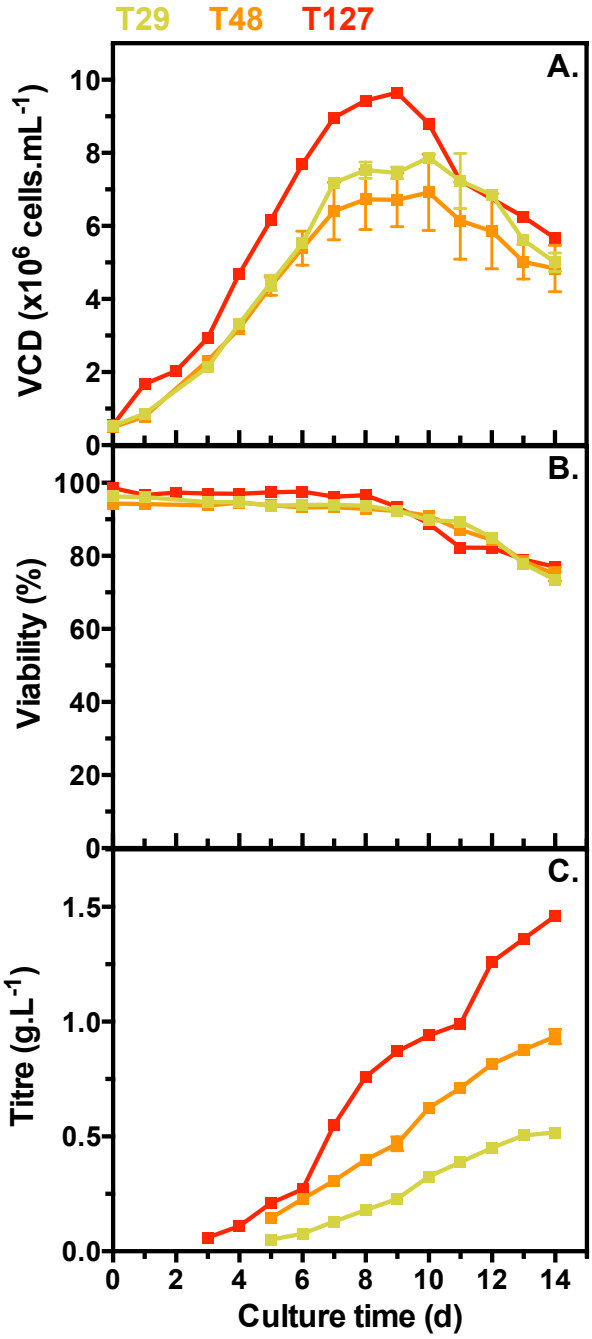

Figure 4.7 Production characteristics of T29, T48, and T127 cells grown in a 14-day fed-batch operation. T29 (yellow) and T48 (orange) cells were grown in parallel duplicate 1-L bioreactors (mean ± SEM, n = 2). T127 cells (red) were grown in a single bioreactor. (**A.**) Viable cell density (VCD). (**B.**) Culture viability. (**C.**) IgG titre across the culture period.

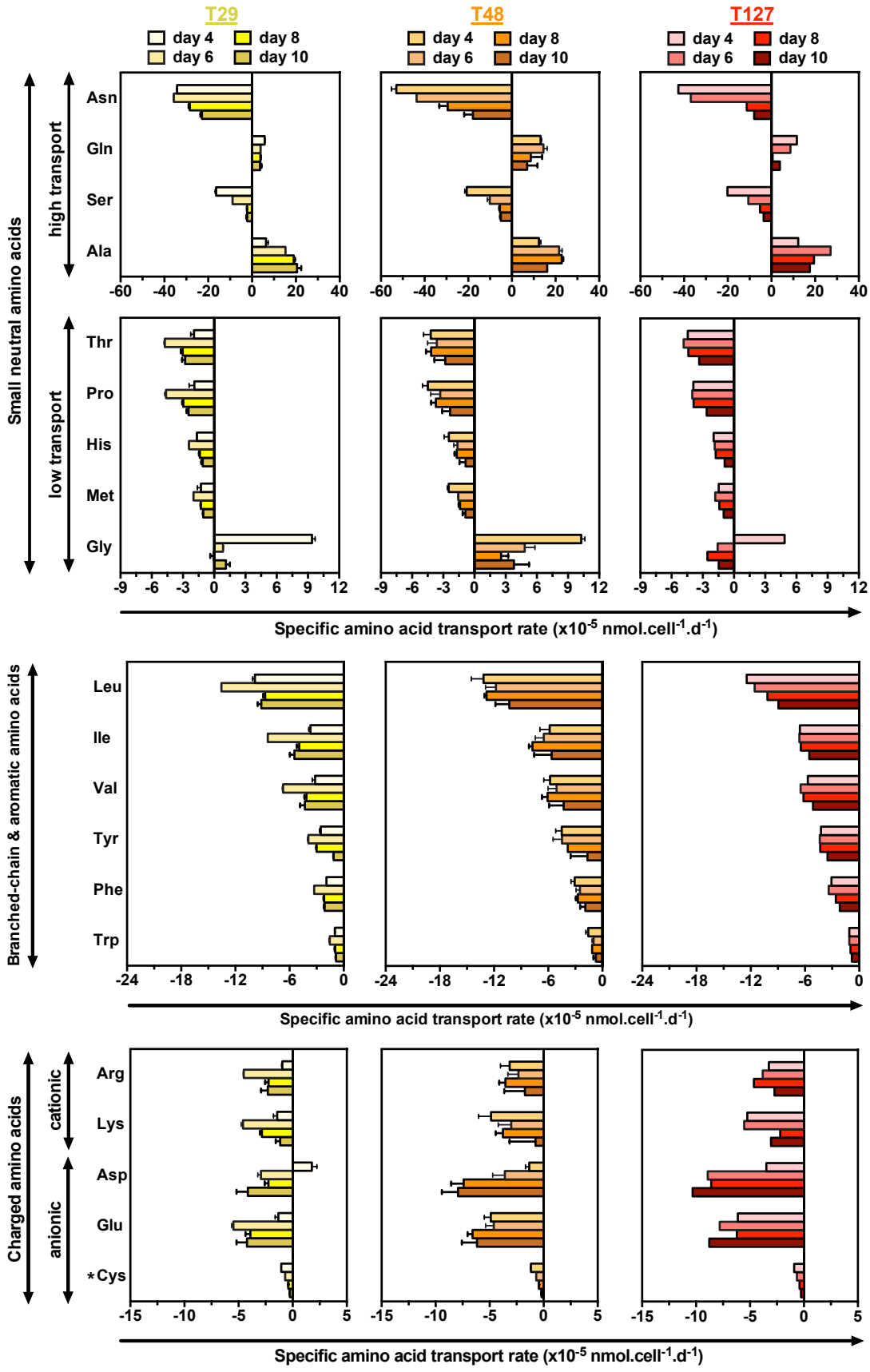
T29
T48
T127
day 4
day 6
day 8
day 10
Small neutral amino acids
high transport
low transport
Asn
Gln
Ser
Ala
Thr
Pro
His
Met
Gly
Specific amino acid transport rate (x10-5 nmol.cell-1.d-1)
Branched-chain & aromatic amino acids
Leu
Ile
Val
Tyr
Phe
Trp
Specific amino acid transport rate (x10-5 nmol.cell-1.d-1)
Charged amino acids
cationic
anionic
Arg
Lys
Asp
Glu
*Cys
Specific amino acid transport rate (x10-5 nmol.cell-1.d-1)

Figure 4.8 Comparison of specific amino acid transport rates throughout culture for T29, T48, and T127 cells. T29 (yellow) and T48 (orange) rates are measured from parallel duplicate 1-L bioreactors (mean + SEM, n = 2). T127 (red) rates are from a single bioreactor. Negative and positive rates represent consumption and production respectively. Amino acids are grouped by charge and size. *Cystine is included with the anionic group due its transport dependence upon glutamate via the xCT transporter.

Table 4.6 Total specific amino acid transport rates throughout culture for T29, T48, and T127 cells

	Total specific amino acid transport rate					
	Small neutral amino acids			Charged amino acids		
Day	High transport	Low transport	BCAA and AAA	Cationic	Anionic*	Total
T29:						
4	62.7 ± 0.6	16.2 ± 0.9	22.1 ± 0.6	2.4 ± 0.3	4.1 ± 0.2	**107.5 ± 0.4**
6	63.7 ± 0.4	14.6 ± 0.2	37.4 ± 0.1	9.1 ± 0.1	9.1 ± 0.4	**134.0 ± 0.2**
8	53.5 ± 1.2	9.0 ± 0.4	23.9 ± 0.8	5.1 ± 0.5	6.6 ± 0.8	**98.1 ± 1.3**
10	49.3 ± 2.7	8.5 ± 0.3	23.0 ± 1.5	3.4 ± 1.0	8.6 ± 2.0	**92.9 ± 2.1**
T48:						
4	99.3 ± 4.4	23.9 ± 1.9	34.0 ± 4.5	8.0 ± 2.0	7.4 ± 1.0	**172.5 ± 13.7**
6	89.9 ± 1.9	14.9 ± 1.1	31.3 ± 4.6	5.3 ± 2.2	8.9 ± 1.9	**150.4 ± 7.9**
8	66.4 ± 8.1	13.6 ± 0.6	34.4 ± 1.4	7.3 ± 1.3	14.4 ± 1.6	**136.1 ± 3.2**
10	46.1 ± 8.4	10.7 ± 1.2	24.7 ± 7.6	4.3 ± 2.5	14.3 ± 2.9	**100.1 ± 5.8**
T127:						
4	86.7	16.6	33.1	8.5	10.5	**155.5**
6	83.2	14.1	33.5	9.4	17.4	**157.6**
8	36.5	14.0	30.7	6.8	15.2	**103.2**
10	32.9	9.3	26.1	5.8	19.4	**93.4**

The absolute value is taken of negative consumption rates in calculating total transport rates (nmol 10^{-5} $cells^{-1}$ day^{-1}). Amino acids are grouped by charge and size. *BCAA*, branched-chain amino acids; *AAA*, aromatic amino acids. *Anionic group includes cystine due its transport dependence upon glutamate via the xCT transporter.

Total amino acid transport rates were higher in the two high producers (T48 and T127) during exponential growth (days 4 and 6; Table 4.6). This was a result of increased asparagine consumption and glutamine production in these cell lines compared to the low producer (T29). Amino acid transport profiles were otherwise very similar between the three producing cell lines. Total transport rates were approximately equivalent at stationary phase (days 8 and 10) across the three cell lines despite T29 cells having a lower Q_{mAb}, again suggesting that amino acid consumption may be in excess of protein synthesis requirements. Of noticeable difference is that the two high producers were consuming anionic amino acids at rates approximately twice that of the T29 cell line during stationary growth. As with T127 cells, both T29 and T48 cells are able to maintain their consumption rate of histidine, methionine, proline, and threonine as well as the branched-chain and aromatic amino acids during stationary growth.

4.4 Discussion

CHO membrane transporters control the availability of intracellular amino acids and are expected to have an essential role in supporting cell growth and high product titres. However, an analysis of transporter function during fed-batch CHO cultures has never been performed. The work presented here is the first chapter of two whose objective is to explore the first aim of this thesis: to characterise amino acid transport processes in CHO cells and understand how they might support culture performance. In this first characterisation chapter, Illumina next-generation sequencing was used to measure transporter expression in three CHO cell lines at exponential and stationary growth of a fed-batch process. Data on amino acid transporter expression were extracted from transcriptomic data sets and analysed by assessment of (i) transcript abundance (FPKM value), and (ii) fold-change (log2 value) in expression between cell lines and culture phase. Extracellular amino acid concentrations were measured and converted to transport rates that were then mapped to expression data. A number of transporters have been identified as having a key role in supporting culture performance and are discussed below. Three transporters: ASCT1, LAT1, and xCT are identified as potential targets for cell engineering strategies to improve cell line productivity.

4.4.1 LAT1, ASCT1 and SNAT2 Transport Neutral Amino Acids

An analysis of transcript abundance identified seven highly expressed transporters that collectively can facilitate the transport of all 20 proteinogenic amino acids (Figure 4.5).

The results show that LAT1 is the main transporter of the previously identified system L transport in CHO cells (Bass et al., 1981; Shotwell et al., 1981). Four transporters (LAT1–4) belong to system L and exhibit comparable selectivity for branched-chain amino acids (isoleucine, leucine, and valine), although LAT1–2 have a wider substrate specificity that also includes the aromatic amino acids (see Chapter 2; Section 2.3). Expression was detected for SLC7A8 and SLC43A2 but this was markedly reduced compared to SLC7A5 throughout culture (Appendix Table A2–4), consistent with observations reported by Kyriakopoulos et al. (2013) who also reported low expression for SLC43A1. It is therefore assumed that LAT1 is mediating the majority of system L transport. In support of this, LAT1 is the only CHO system L transporter to be identified in a proteomic study (Baycin-Hizal et al., 2012). LAT1 is the primary entry route for essential amino acids in most transformed cell lines (Fuchs and Bode, 2004), and regulates leucine-mediated mTORC1 signaling (Nicklin et al., 2009). Activation of mTORC1 in CHO cells is therefore likely to also be dependent upon LAT1 activity.

LAT1 antiport activity can be functionally coupled to the system ASC antiporter ASCT2 (Nicklin et al., 2009) and possibly coupled to system A and N uniporters (Baird et al., 2009; Boer et al., 2002) (Figure 2.3). System A and ASC transport has been previously demonstrated in CHO cells (Bass et al., 1981; Shotwell et al., 1981). SLC1A5 was missing from the transcriptomic data sets but the second system ASC transporter SLC1A4 (see Chapter 2; Table 2.1) was present and highly expressed (Table 4.1). The expression of both transporters has however been reported at the transcript (Kyriakopoulos et al. 2013) and protein level (Baycin-Hizal et al., 2012). Five transporters make up systems A and N (see Chapter 2; Section 2.3). The results show that expression of SLC38A2 (system A) was markedly higher than the other four transporters throughout culture (Appendix Table A2–4), making it the primary entry route for small neutral amino acids such as asparagine and glutamine through these two systems. This is consistent with transcript measurements reported by Kyriakopoulos et al. (2013). Furthermore, SLC38A2 is the only transporter of systems A and N whose expression has been confirmed at the protein level (Baycin-Hizal et al., 2012). A striking conclusion from this assessment of neutral transporters is that CHO cells heavily rely on a single transporter for the uptake of all branched-chain and aromatic amino acids, i.e. those amino acids that cannot be synthesised *de novo* and are designated as essential within multicellular organisms. Whereas for smaller neutral amino acids (e.g. asparagine, glutamine and serine) - the cellular requirement of which typically exceeds the cells capability for *de novo* synthesis making them conditionally

essential amino acids in CHO cell line manufacturing platforms - is divided over two transporters with distinct transport mechanisms. This redundancy in transport of smaller neutral amino acids suggests their intracellular availability is of a greater importance to cell growth than larger branched-chain and aromatic amino acids. As discussed in Chapter 2, glutaminolysis and asparagine metabolism have been shown to provide CHO cells with a carbon source that gets directed towards the TCA cycle to support macromolecule synthesis (e.g. fatty acids) and energy production. It is therefore hypothesised that expression of multiple transporters for smaller neutral amino acids in CHO cells is an adaptive response to support this metabolism which was reflected by a 2-3 fold increased consumption rate of these amino acids compared to essential amino acids (Table 4.5 and 4.6). The flux of amino acid derived carbon into the TCA cycle is associated with the production of ammonia as a byproduct while glutaminolysis is closely associated with aerobic glycolysis and associated lactate production (see Chapter 2). In addition to measurements of amino acid concentrations, glucose, lactate and ammonia were also measured throughout the fed-batch cultures described in this chapter. Glucose measurements were used to feed back glucose to ensure that it was never growth limiting while the pH was controlled to minimise the negative effects of lactate and ammonia on growth (see 4.2 Materials and Methods). No analysis was performed on glucose/lactate consumption/production rates due to the unknown contribution that other carbon sources expected to be found in the undisclosed media such as pyruvate may make to aerobic glycolysis.

4.4.2 GLAST, CAT-1 and y^+LAT2 Transport Charged Amino Acids

Anionic transport (aspartate and glutamate) is predominantly through system X_{AG}^-, and cationic transport (arginine and lysine) is predominantly through systems y^+ and y^+L in mammalian cells (see Chapter 2; Section 2.3). Five transporters belong to system X_{AG}^- and have near identical transport kinetics (Danbolt, 2001). All transporters were expressed but expression of SLC1A3 markedly exceeded expression of the other four transporters throughout culture (Appendix Table A2–4). GLAST is therefore assumed to be mediating the function of system X_{AG}^- transport previously identified in CHO cells (Ash et al., 1993). Kyriakopoulos et al. (2013) similarly detected substantial expression of SLC1A3 with an additional small contribution to X_{AG}^- from SLC1A2. GLAST has also been detected at the protein level (Baycin-Hizal et al., 2012).

The three uniporters of system y^+ provide a high-affinity influx route for arginine and lysine (Fotiadis et al., 2013). CAT-1 exhibits the highest substrate affinity

of the three transporters and is preferentially expressed (Appendix Table A2–4), suggesting it is mediating the previously identified y^+ transport in CHO cells (Rotoli et al., 1989). Kyriakopoulos et al. (2013) similarly detected transcript expression for SLC7A1 only and it is also the only y^+ transporter detected at the protein level (Baycin-Hizal et al., 2012). The two transporters belonging to system y^+L are antiporters that preferentially export arginine and lysine for the influx of neutral amino acids such as glutamine or leucine (see Chapter 2; Table 2.1). It has therefore been proposed that systems y^+ and y^+L are functionally coupled in mammalian cells (Fotiadis et al., 2013). Both SLC7A6 and SLC7A7 were expressed with higher expression of the latter (Table 4.1). Cell surface expression of these two transporters, as well as SLC7A5, was supported by high expression of SLC3A2 throughout culture for all cell lines (Table 4.1). Interestingly, abundance of SLC7A1 and SLC7A6 was equivalent in the three cell lines across culture. Functional coupling of these two transporters may help support the function of system L by providing an additional influx route for leucine and subsequent mTORC1 activation in CHO cells.

4.4.3 ASCT1, LAT1 and xCT Are Potential Markers for Antibody Production

Differences in transporter expression between cell lines and across culture were then explored to identify how expression compares with performance parameters such as growth rate, cell viability, and productivity (Figure 4.5).

Of the neutral transporters, SLC38A2 expression was high and approximately equivalent across the three cell lines, changing little throughout culture. However, SLC1A4 is the only transporter whose expression was significantly upregulated in T127 cells compared to the other two cell lines at both exponential (2-fold increase) and stationary (3-fold increase) phase making it a potential marker of productivity throughout culture. SLC1A4 expression was also regulated within culture, being significantly upregulated at stationary phase for all cell lines. Kyriakopoulos et al. (2013) made the same observation in their GS-Null and two antibody-producing cell lines. ASCT1 may therefore have a key functional role at stationary phase such as supporting cell viability. SLC7A5 expression was significantly upregulated at stationary phase in T127 cells only (3-fold), suggesting increased system L activity may be required to support antibody production late in culture.

Expression of the cationic transporters SLC7A1 and SLC7A6 was moderate and approximately equivalent across the three cell lines, changing little throughout culture. This is in contrast to measurements made by Kyriakopoulos et al. (2013) that

demonstrate SLC7A1 and SLC7A6 was upregulated and downregulated respectively in antibody-producers compared to their non-producer, a combination of transporter expression that would function to maximise arginine and lysine influx for their antibody-producers.

The aspartate and glutamate transporter SLC1A3 was found to be significantly upregulated in the two glutamine synthetase expressing cell lines compared to the host throughout culture. This indicates a necessary remodeling of transporter function for increased aspartate and glutamate uptake to support glutamine synthetase activity and growth in glutamine-free media. GS-Null and T127 cells also demonstrated significant upregulation of SLC6A9 and SLC7A11 compared to the host throughout culture. Collectively, these three transporters provide the glutamate, glycine, and cysteine required for GSH synthesis, indicating that both GS-Null and T127 cells may have an increased requirement for GSH throughout culture. Consistent with observations by Kyriakopoulos et al. (2013), SLC7A11 expression was also regulated within culture, being significantly upregulated at stationary phase for all cell lines. Expression of SLC7A11 at stationary phase in T127 cells is 3-fold and 2-fold higher than the host and GS-Null cells respectively, making it a third potential marker of productivity.

4.4.4 Increased SLC7A11 Expression During Stationary Growth Forms Part of An Adaptive Response That Supports Cellular Availability of GSH

The upregulation of SLC7A11 at stationary phase was the largest change in expression of any transporter for CAT-S (5-fold), GS-Null (2.5-fold), and T127 (8-fold) cells. Likewise, Kyriakopoulos et al. (2013) found upregulation of SLC7A11 at stationary phase to be their biggest change in expression across all cell lines (up to 16-fold). The xCT transporter is the primary influx route for cystine in cultured mammalian cells (Ganapathy et al., 2009) and its activity is closely associated with GSH synthesis (Chung et al., 2005; Shih et al., 2006) (reviewed in Chapter 2; Section 2.4). Upregulation of SLC7A11 is suggestive of an increased requirement for cellular GSH at stationary phase in all cell lines. In support of this the GSH/GSSG ratio has been reported to decrease considerably during stationary phase (Templeton et al., 2013). This could be a consequence of increased cellular ROS resulting from a shift in TCA cycle function towards oxidative phosphorylation during this phase of culture as reported in other CHO cell lines (reviewed in Chapter 2; Section 2.1). The expression of enzymes involved in regulating cellular GSH levels was examined to investigate this hypothesis further (Section 4.3.3.3; Table 4.2). Interestingly, culture viability correlated well with

the number of expression changes made to maximise cellular GSH levels, such that T127 cells with three changes were best able to maintain high culture viability throughout late-stage culture. Unique to the T127 cell line was the 1.6-fold increase in glutathione reductase. Sengupta et al. (2011) hypothesised that increased flux through the PPP at stationary phase (reviewed in Chapter 2; Section 2.1) functions to support NADPH production for glutathione reductase activity. The data presented in this chapter suggests the relationship between SLC7A11 expression and GSH synthesis warrants further investigation. Future studies would benefit from measuring GSH and ROS levels, SLC7A11 expression, and GSH related enzyme expression/activity throughout culture.

4.4.5 Changes in ASCT1, LAT1, and xCT Expression Could be an Adaptive Response to Support Antibody Production

This chapter also examined amino acid transport rates throughout culture in all cell lines to investigate how they correlate with changes in transporter expression.

ASCT1, identified above as a potential marker for productivity, is a high-affinity transporter of serine and threonine (see Chapter 2; Table 2.1), whose consumption rates remained high late in T127 culture compared to the other two non-producing cell lines (Figure 4.6). An analysis of the amino acid composition of a typical mammalian cell and IgG antibody (Table 4.7) reveals threonine and serine to be amongst the most abundant amino acids in an IgG. Furthermore, serine is a major requirement for cell biomass such that the cells must increase serine consumption to meet both biomass demands, as observed during exponential growth. Upregulation of SLC1A4 may therefore be a necessary adaptive response to support IgG production, explaining why this transporter represents a good marker for productivity throughout culture. The IgG also has a high requirement for leucine, tyrosine, and valine, all of which continued to be consumed at a high rate up to day 10 in T127 cells only. These amino acids are transported through LAT1 and may explain its 3-fold upregulation in T127 cells at stationary phase. A further two antibody-producing cell lines (T29 and T48) also maintained high consumption rates for leucine, threonine, tyrosine, serine, and valine at stationary phase, providing additional support for this hypothesis.

Interestingly, cystine consumption was found to decrease late in culture in all cell lines despite significant upregulation of SLC7A11 expression. The explanation for this is not clear, however the extracellular concentration of cystine was an order of magnitude lower than the other 19 amino acids throughout culture across the three cell

lines (Appendix Figure A1). As the fed-batch culture progressed and the media became increasingly amino acid rich, the cells may have struggled to acquire the additional cystine that they require. Cystine transport is therefore a bottleneck and represents an attractive cell engineering target. Alternatively, improved media design may boost cytosolic levels of cysteine. For example, feeding chemically synthesised cysteine-containing di/tripeptides. Kang et al. (2012) demonstrated that tyrosine-containing dipeptides had a significantly higher solubility than free tyrosine and feeding these dipeptides enhanced productivity and viability of an antibody-producing cell line. More recently, Kishishita et al. (2015) found that supplementing CHO cultures with a cysteine-serine-tyrosine tripeptide could significantly improve cell growth and productivity. High expression of SLC15A3 (Table 4.4) suggests the transport mechanism is in place for a variety of di/tripeptides to be experimentally tried out.

Cysteine is also required for IgG production. Despite the IgG requirement being low, it represents a 8-fold increase in composition percentage compared to the cell biomass (Table 4.7). Consequently, there is an increased demand for cysteine in antibody-producing cells to support both antibody production and GSH synthesis during late-stage phase. This may explain why this transporter as suggested above represents a good additional marker for productivity late in culture.

Table 4.7 Amino acid composition of a mammalian cell and an IgG antibody

Amino Acid	Percentage (%)		
	Cell Composition	Standard IgG Composition	mAb-109 Composition
Ala	9.0	5.3	5.3
Arg	4.7	2.4	3.2
Asn	10.1	3.5	3.9
Asp		4.0	3.9
Cys	0.3	2.4	2.4
Gln	12.6	5.0	4.5
Glu		5.2	4.4
Gly	9.1	7.0	7.2
His	2.2	1.7	1.7
Ile	5.7	2.4	2.3
Leu	9.0	6.8	7.7
Lys	6.9	7.0	6.6
Met	2.3	1.4	0.8
Phe	3.7	3.5	3.3
Pro	5.5	7.1	6.6
Ser	6.2	12.9	14.1
Thr	5.4	7.7	7.4
Trp	-	-	1.5
Tyr	2.7	4.1	4.8
Val	6.5	9.1	8.6

Mammalian cell and standard IgG composition was taken from Hu, 2012.

4.4.6 Summary

In this chapter, transcriptomic analysis of three CHO cell lines has identified seven highly expressed transporters that can collectively facilitate the transport of all 20 proteinogenic amino acids: ASCT1, CAT-1, GLAST, LAT1, SNAT2, xCT, and

y^+LAT2. An analysis of transporter expression within culture and between cell lines, together with measured amino acid transport data, has identified three transporters whose functional contribution towards culture performance warrants further investigation: ASCT1, LAT1, and xCT. All three represent possible markers for productivity, while xCT may also have a critical role in maintaining culture viability late in culture. It should however also be noted that the three CHO cell lines examined are non-clonal and thus are functionally heterogeneous. Consequently, the measurements reported in this chapter represent population averages. As discussed in Chapter 1, high-throughput screening technology is used to isolate rare highly productive clonal cell lines from transfectant pools. It is therefore conceivable that amino acid transporter expression in these rare highly productive cells may diverge from the population average observations described in this chapter. Future studies would therefore benefit from looking at multiple clonal cell lines with different levels of productivity. Increased expression of SLC1A4, SLC1A5, and SLC7A11 in T127 cells was hypothesised above to support the influx of amino acids needed for IgG production. In support of this theory, Ley et al. (2015) compared the CHO transcriptomes of a high- and low-producer of erythropoietin (EPO), and found reduced expression of catabolic genes specific for the most abundant amino acids in EPO in the high-producer relative to the low-producer. Similarly, Dietmair et al. (2012b) found significant downregulation of metabolic pathways involved in isoleucine, leucine, lysine, and valine degradation in a recombinant HEK293 cell line producing an IgG fragment relative to the non-producing host. The results presented in this chapter demonstrate for the first time an additional mechanism by which CHO cells may be modifying amino acid metabolism to support recombinant protein production.

Chapter 5

Inhibition of Amino Acid Transport and its Effects on Cell Growth and Antibody Production

This chapter evaluates the functional contribution that amino acid transport systems make to growth, viability, and productivity of CHO cell lines. Inhibitors were used to block amino acid entry through discrete transport systems at exponential and stationary phase of batch cultures. LAT1, GlyT1, and xCT transport activity were found to support antibody production during late-stage culture. xCT transport activity was also found to be a key determinant of culture viability throughout culture. This knowledge can help guide future cell line development processes in order to improve cell line productivity.

5.1 Introduction

In Chapter 4, RNA-sequencing was used to profile amino acid transporter gene expression in three CHO cell lines throughout a fed-batch process. Hypotheses about transporter function during culture were made based upon abundance and differential expression of transcripts, mapped amino acid transport rates, and a knowledge of how transporters support cellular processes from the literature. Importantly, ASCT1, LAT1, and xCT were identified as potential markers for antibody production. However, this hypothesis and others require further investigation, particularly because the correlation between mRNA and protein abundance is often poor (Hedge et al., 2003). Baycin-Hizal et al. (2012) compared mRNA and protein expression in CHO cells and found a correlation of $r = 0.48$. Measurement of transporter proteins using proteomic analysis or Western blotting can verify expression but manipulating transporter activity itself is required to evaluate their functional contribution to culture performance and experimentally test the hypotheses put forward in Chapter 4.

Gene knockdown can be used to specifically target the expression of amino acid transporter genes. RNA interference (RNAi) has been used to downregulate the expression of ASCT2 (Hassanein et al., 2013; Nicklin et al., 2009; Wang et al., 2014),

LAT1 (Nicklin et al., 2009), SNAT1 (Kondoh et al., 2007), and xCT (Timmerman et al., 2013) transporters in cancer cell lines. Targeting individual transporters with RNAi allowed the authors to examine their functional contribution towards cell growth, amino acid transport, and other cellular processes such as activation of mTORC1 signaling. An alternative method of manipulating transporter activity is by treating cells with inhibitors that block amino acid entry through specific transporters. This approach is technically much simpler to implement than RNAi methods and can easily be used to evaluate transporter function at any time point in culture. Inhibitors have played a key role in the early identification of mammalian amino acid transport systems (Christensen et al., 1967; Oxender and Christensen, 1963) and are frequently used to investigate amino acid transport function in cancer cell lines (Chung et al., 2005; Gout et al., 2001; Hassaniein et al., 2013; Nicklin et al., 2009; Pinilla et al., 2011; Shennan et al., 2004; Timmerman et al., 2013). Inhibitors have helped identify the presence of system A and L transporters in adherent CHO-K1 cells (Bass et al., 1980; Shotwell et al., 1980) but have never been reported to be used with industrial CHO cell lines to investigate how amino acid transporter function contributes to culture performance.

This chapter evaluates the functional contribution that transporters belonging to systems A, ASC, L, X_C^-, as well as the GlyT1 transporter, make to critical culture performance parameters (growth rate, cell viability, and antibody production). Inhibitors specific for these transporters were applied to the three cell lines from Chapter 4 (CAT-S, GS-Null, and T127) at exponential and stationary phase of batch cultures. Two additional antibody-producing cell lines (T29 and T48) were also tested at exponential growth. A description of the inhibitors and hypotheses being tested from Chapter 4 are provided throughout the results section.

5.2 Materials and Methods

5.2.1 Inhibitor Treatment at Exponential Growth

All cell lines were seeded at of 2 x 10^5 cells.mL^{-1} in 10 mL of CD-CHO medium (Life Technologies, Paisley, UK) in 50 mL vented TubeSpin® Bioreactors (TPP, Trasadingen, Switzerland) shaking at 170 rpm in 37^{o}C and 5% CO_2 air (Infors UK, Reigate, UK). CAT-S cells were supplemented with 8 mM L-glutamine (Life Technologies). Recombinant cells were not supplemented with MSX for all inhibitor experiments. At 24 hr after seeding all cultures were spun at 200g for 5 min and the medium was replaced with fresh test CD-CHO medium (supplemented with 8 mM

glutamine for CAT-S cells). BCH (2-amino-2-norbornanecarboxylic acid) (Sigma-Aldrich, Dorset, UK) and MeAIB (α-(methylamino)isobutyric acid) (Sigma-Aldrich) were both diluted in CD-CHO medium. SAS (sulfasalazine) (Sigma-Aldrich), GPNA (L-γ-glutamyl-p-nitroanilide) (Sigma-Aldrich), and ALX 5407 HCL (Tocris, Bristol, UK) were all diluted in dimethyl sulfoxide (DMSO) (Sigma-Aldrich) before addition to CD-CHO medium.

5.2.2 Inhibitor Treatment at Stationary Phase

CAT-S, GS-Null, and T127 cell lines were seeded at of 2 x 10^5 cells.mL^{-1} in 140 mL of CD-CHO medium in 500 mL vented Erlenmeyer flasks (Corning, Surrey, UK) shaking at 140 rpm in 37^{o}C and 5% CO_2 air. CAT-S cells were supplemented with 8 mM L-glutamine. Recombinant cells were not supplemented with MSX for all inhibitor experiments. Cells were grown until they reached stationary phase on day 5-6 (see Figure 5.1) and 9 mL culture aliquots were then transferred to 50 mL vented TubeSpin® Bioreactors. All inhibitors were diluted as described above but in conditioned (day 5-6) medium and applied to cells by spinning the cultures at 200g for 5 min and replacing the medium with the test medium.

5.2.3 Analysis of Factorial Experimental Data

Design Expert 9 (Stat-Ease, Inc., Minneapolis, USA) was used to identify and model significant factors (both single and factor combinations) from the two-level factorial design. In brief, the effect of each factor was automatically calculated by subtracting the average response of all experiments at its –level from the average response of all experiments at its +level using equation 5.1:

$$\text{Effect} = \frac{\sum R_+}{n_+} - \frac{\sum R_-}{n_-}$$

Where R is the response variable being investigated. For each factor the absolute effect value was automatically plotted on a half-normal probability plot. Factors with a large effect that markedly deviated from the other factors were manually identified. An analysis of variance (ANOVA) was then used to test each factor for significance and automatically generate a predictive model for the response variable in terms of the significant factors. Design Expert 9 automatically tested the generated models for normality by calculating the residuals (difference between predictive and actual

response) for each level combination and plotting them on a normal probability plot. These plots were manually examined to confirm that the residuals were normally distributed.

5.3 Results

Five CHO cell lines were investigated in this chapter: CAT-S, GS-Null, T29, T48, and T127. The growth and production characteristics for these cell lines were described in Chapter 4, however a summary is provided in Table 5.1. Transporter activity was inhibited at either exponential or stationary growth phase of batch cultures with the inhibitors described in Figure 5.1. For exponential growth studies, the five cell lines were treated for 3-4 days with inhibitors applied at 24 hr after seeding. At this time point in culture, all cell lines were approaching the end of their lag phase but also reached approximately the same cell density ensuring that the inhibitor "dose-per-cell" was equivalent between the cell lines. This design ensured that a comparison of responses (cell growth, culture viability, and productivity) could readily be made between the cell lines. The effect of transport inhibition at stationary phase was tested in CAT-S, GS-Null, and T127 cells only. In these experiments cells were grown until they reached stationary phase in batch cultures (day 5 for CATS and GS-Null cells, and day 6 for T127 cells), then treated with the same inhibitor concentration ranges used during exponential growth. Consequently, the inhibitor "dose-per-cell" was lower than that of exponential phase experiments for all cell lines. Solubility issues with many of the inhibitors made it experimentally difficult to keep this variable equivalent between the two growth phases being examined. It should also be noted that the three cell lines all reached different peak densities at stationary phase. Therefore the inhibitor "dose-per-cell" varied between the cell lines and a comparison of responses between cell lines cannot easily be made.

Table 5.1 Summary of growth and production characteristics of five CHO cell lines as assessed in 14-day fed-batch operations

Cell line	*Average μ (d^{-1})	Max VCD ($x10^6$ cells.mL^{-1})	Max titre ($mg.L^{-1}$)	Average Q_{mAb} (pg mAb.$cell^{-1}$.d^{-1})
CAT-S	0.32 ± 0.08	9.15 ± 0.16	-	-
GS-Null	0.40 ± 0.10	6.55 ± 0.80	-	-
T29	0.33 ± 0.07	7.88 ± 0.16	518 ± 18	7.5 ± 0.7
T48	0.31 ± 0.07	6.92 ± 1.05	935 ± 32	15.0 ± 1.1
T127	0.36	9.65	1457	17.7

Data from all cell lines except T127 are from parallel duplicate 1-L bioreactors (mean ± SEM, n = 2). Data for T127 cells is from a single bioreactor. *Average μ calculated over 0–8 days for all cell lines except GS-Null cells, which are calculated over 0–6 days.

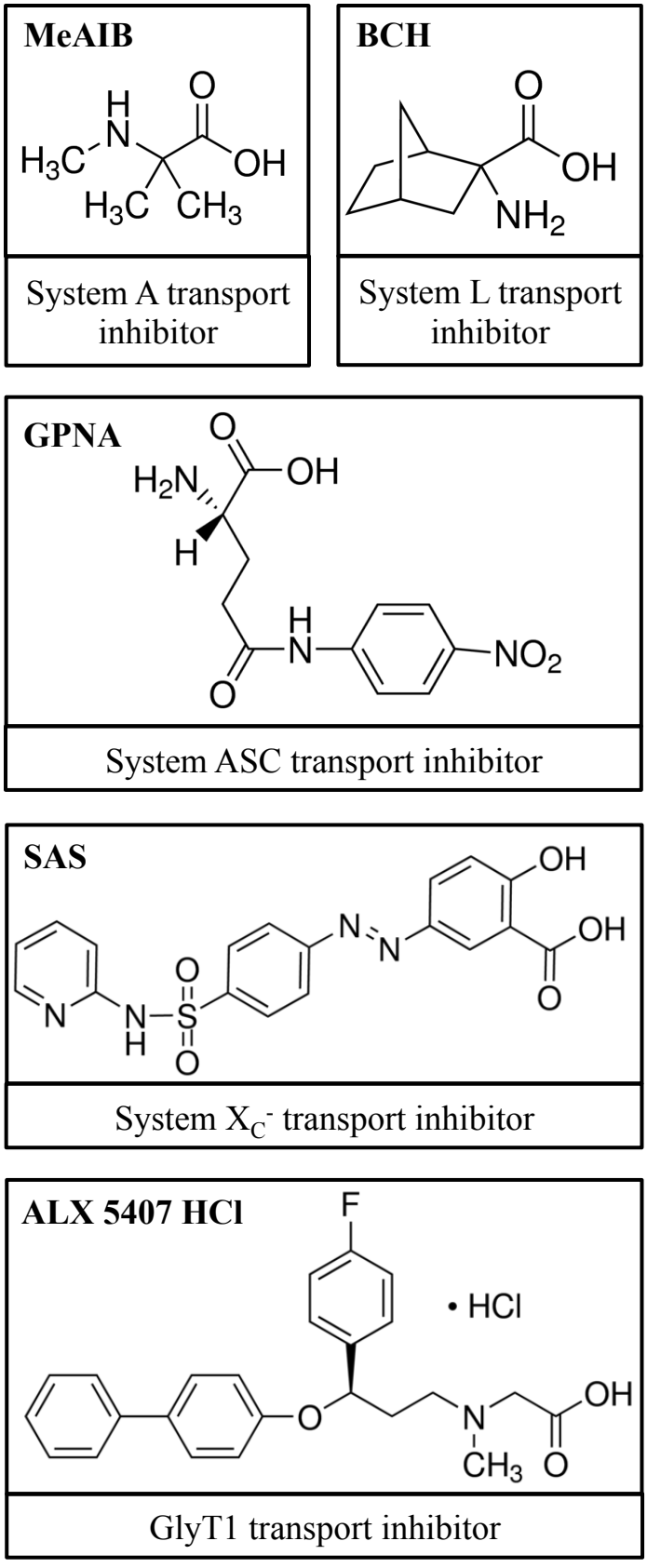

Figure 5.1 Inhibitors used to block amino acid transporter activity at exponential and stationary growth phases of batch cultures.

5.3.1 System L Transport Inhibition

The four transporters of system L (LAT1–4) facilitate the transport of essential neutral amino acids with large, branched or aromatic side-chains that include isoleucine, leucine, and valine (see Chapter 2; Table 2.1). From Chapter 4, LAT1 is hypothesised to be the primary entry route for this group of amino acids in all cell lines, with increased activity required during late-stage culture in T127 cells to support antibody production. The leucine analog, 2-amino-2-norbornanecarboxylic acid (BCH) is a highly specific transportable inhibitor for LAT1-4 (Babu et al., 2003; Bodoy et al., 2005; Kanai et al., 1998; Pineda et al., 1999) and has been used to examine LAT1 activity in a range of cancer cell lines (Nicklin et al., 2009; Shennan et al., 2004). BCH treatment is hypothesised to deplete cystosolic levels of essential amino acids leading to suppression of growth for all cell lines early in culture and inhibition of antibody production in T127 cells treated during late-stage culture.

Figure 5.2 shows the dose-response curves for cells treated with BCH during exponential growth. All cell lines exhibited a marked decrease in cell proliferation. However, small differences in sensitivity were apparent between the five cell lines as demonstrated by a comparison of their respective IC_{50} concentrations. T29 cells were most sensitive to BCH treatment with complete inhibition of growth at the higher concentrations tested. Both GS-Null and T48 cells had increased resistance to treatment, while CAT-S and T127 cells had the highest level of resistance. Culture viability measurements reflected these cell line differences with a high level of cell death observed in T29 cells, minor cell death observed in GS-Null and T48 cells, and no cell death observed in CAT-S and T127 cells (Figure 5.3 A–E).

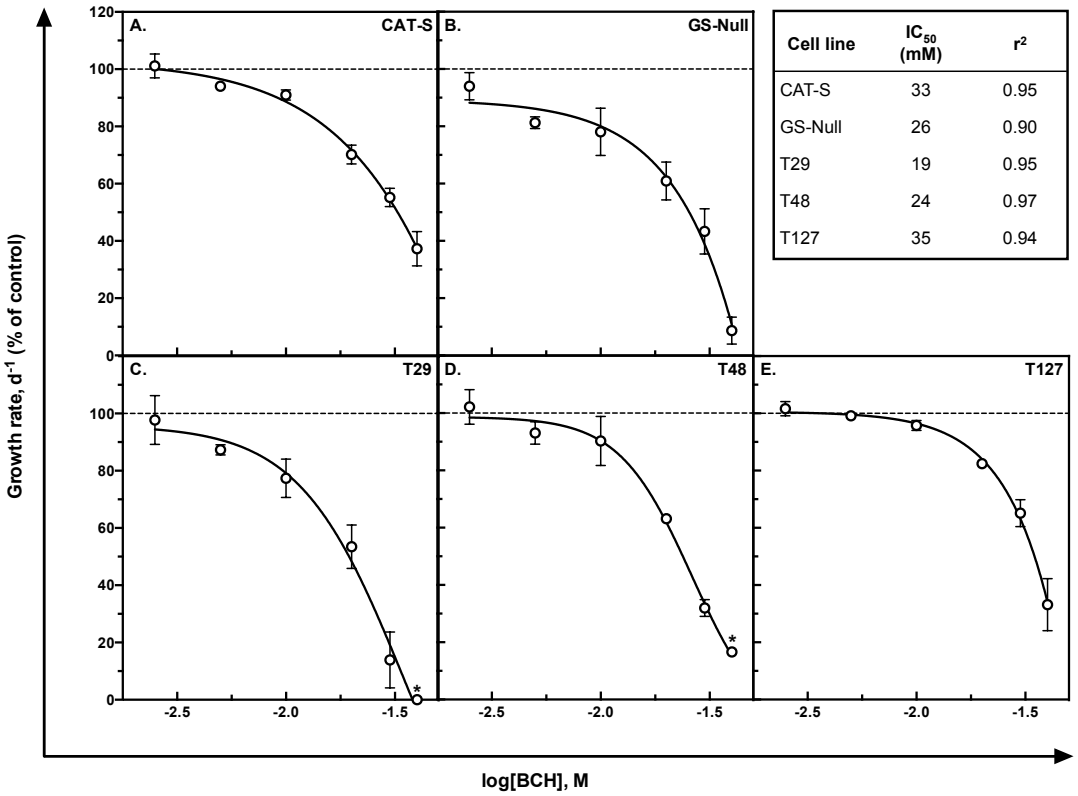

Figure 5.2 The effect of BCH treatment on cell proliferation during exponential growth phase. Cells were treated for 4 days with BCH. Growth rates (d^{-1}) were calculated and normalised to control cultures (0 mM BCH). Data is shown as the mean ± SEM of three independently performed experiments (**A.**, **B.**, **E.**) or two independently performed experiments (**C.** & **D.**). An asterisk indicates the data point is from a single experiment (40 mM cultures for **C.** & **D.**). Non-linear regression analysis was used to fit dose-response curves and calculate the IC_{50} concentrations (table insert).

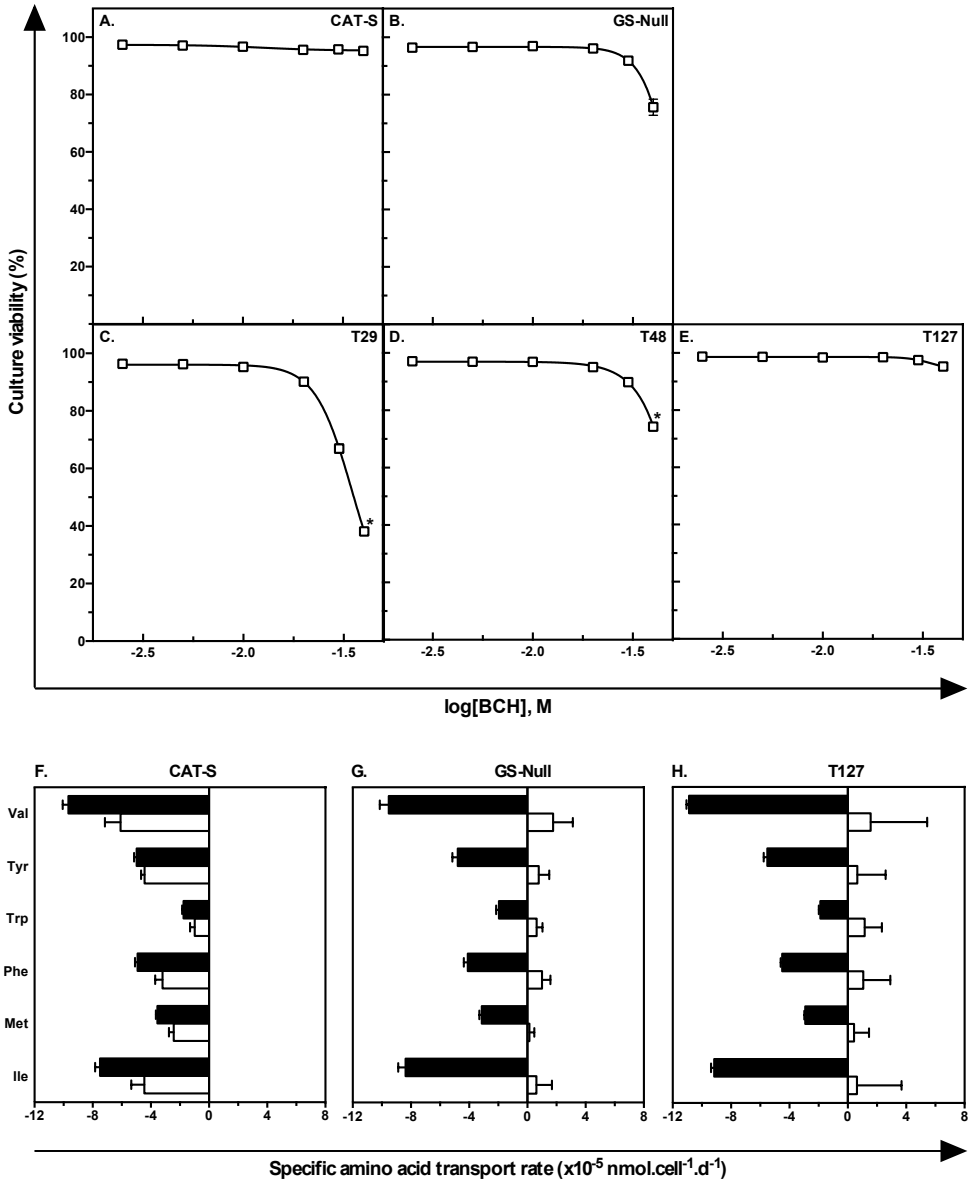

Figure 5.3 The effect of BCH treatment on culture viability and amino transport rates during exponential growth phase. Culture viability was measured on day 4 of BCH treatment. All control cultures (0 mM BCH) had viabilities >95%. Data is shown as the mean ± SEM of three independently performed experiments (**A.**, **B.**, **E.**) or two independently performed experiments (**C.** & **D.**). An asterisk indicates the data point is from a single experiment (40 mM cultures for **C.** & **D.**). Amino acid transport rates were calculated between days 1–3 for CAT-S cells (**F.**), and between days 1–4 for GS-Null (**G.**) and T127 cells (**H.**). Closed bars are rates from control cultures and open bars are rates at 30 mM (CAT-S and GS-Null) and 40 mM BCH (T127). Data is the mean + SEM of three independently performed experiments.

Transport rates of classic system L substrates were measured for CAT-S, GS-Null, and T127 cells in control and BCH treated cultures (Figure 5.3 F–H). Leucine transport rates could not be calculated as the amino acid quantification method (see Chapter 3; Section 3.2) measured BCH as leucine in treated cultures. Complete inhibition of uptake was observed for GS-Null and T127 cells at concentrations close to their IC_{50} (30 and 40 mM respectively). CAT-S cells continued to consume these amino acids around their IC_{50} (30 mM) but at a reduced rate with complete inhibition observed at 40 mM (data not shown).

Antibody production was examined in T29, T48, and T127 cells (Figure 5.4). Specific productivity remained relatively constant over the concentration range tested in all the three cell lines with titre decreasing in a dose-dependent manner in response to a drop in IVCD.

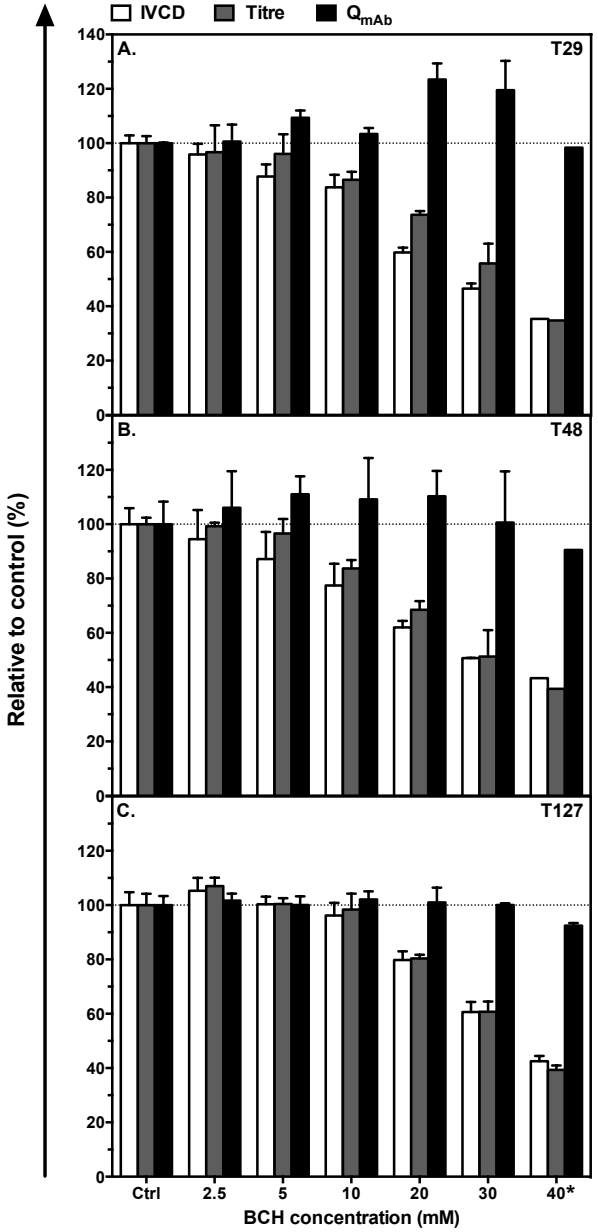

Figure 5.4 The effect of BCH treatment on antibody production during exponential growth phase. Cells were treated for 3 days (**A.** & **B.**) or 4 days (**C.**) with BCH. IVCD (white bars), titre (grey bars) and Q_{mAb} (black bars) was calculated and normalised to control cultures (0 mM BCH). Data is shown as the mean + SEM of two independently performed experiments (**A.** & **B.**) or three independently performed experiments (**C.**). The asterisk indicates the data is from a single experiment at 40 mM BCH with T29 (**A.**) and T48 (**B.**) cells.

The effect of BCH treatment during stationary phase was tested in CAT-S and T127 cells (Figure 5.5). For CAT-S cells, culture viability began to decrease at higher concentrations (30 and 40 mM BCH) after 24 hr of treatment. After 3 days, the viability of these two CAT-S cultures was markedly lower than control cultures. In contrast, viability of CAT-S cultures treated with lower concentrations of BCH (2.5, 5, 10, and 20 mM) was noticeably higher than control cultures, suggesting low levels of system L inhibition can prolong stationary growth in the host cell line. For T127 cells, no change in culture viability was observed after 24 hr of treatment. Analysis of antibody production over the same time period did however show specific productivity to decrease in a dose-dependent manner. T127 cells formed large rings of cell debris on the culture vessel wall after 24 hr in control cultures, preventing an accurate assessment of culture performance past this time point. Interestingly, addition of BCH prevented the formation of these cell debris rings and culture viability remained above 90% after 3 days for treated cultures at all concentrations (data not shown).

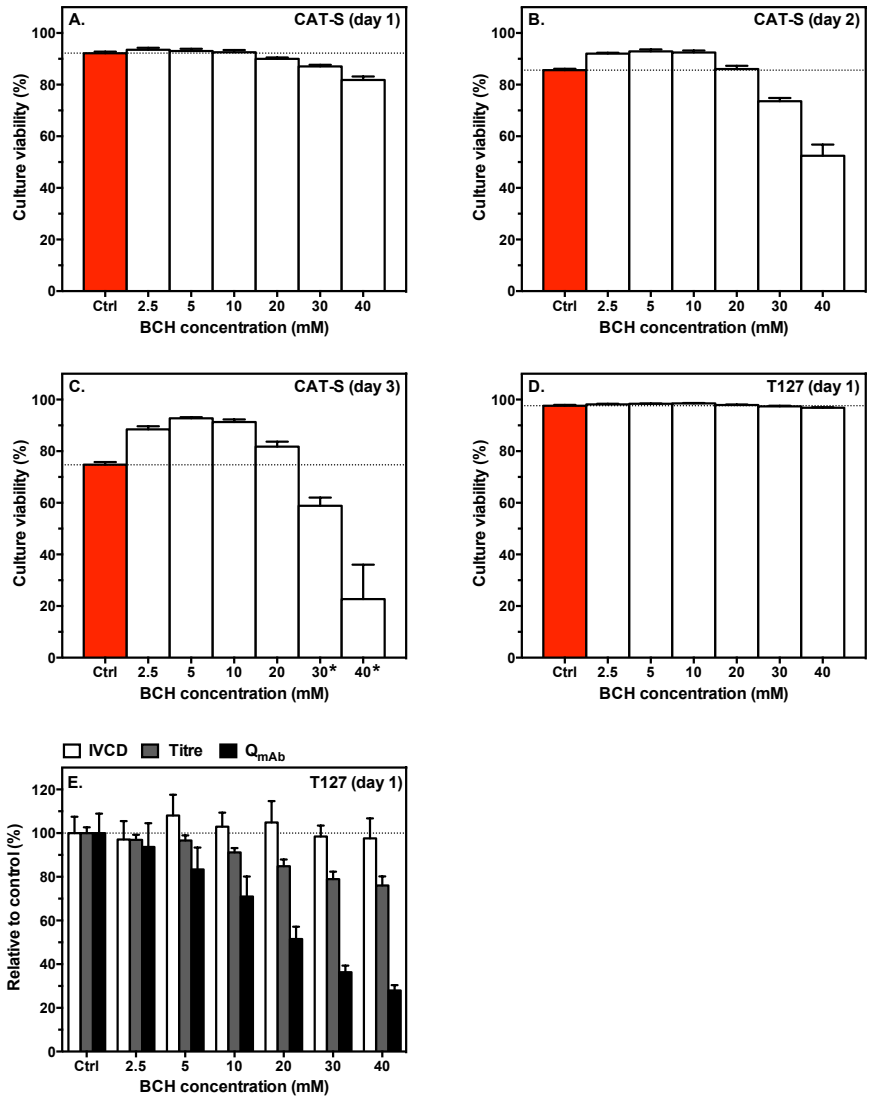

Figure 5.5 The effect of BCH treatment on CAT-S and T127 cells at stationary phase of batch culture. Culture viability was assessed for CAT-S cells at day 1 (**A.**), day 2 (**B**), and day 3 (**C.**) post-addition of BCH. T127 cells had their viability (**D.**) and antibody production (**E.**) assessed at day 1 post-addition of BCH. Control cultures represent cells incubated with 0 mM BCH. Data is shown as the mean + SEM of three independently performed experiments. An asterisk indicates data shown as the mean + SEM of two independently performed experiments.

5.3.2 System A Transport Inhibition

The three transporters of system A (SNAT1, 2, and 4) mediate the transport of small non-essential neutral amino acids such as alanine, asparagine, glutamine, and serine (see Chapter 2; Table 2.1). The alanine analog, α-(methylamino)isobutyric acid (MeAIB), is a highly specific transportable inhibitor for all system A transporters (Sugawara et al.,

2000; Varoqui et al., 2000; Yao et al., 2000), and has been used to examine SNAT2 activity in the MCF-7 breast cancer cell line (Pinilla et al., 2011). From Chapter 4, SNAT2 together with ASCT1 was hypothesised to be the main entry routes for this group of amino acids in all cell lines. Because of this transport redundancy, MeAIB treatment is hypothesised to reduce but not completely suppress cell growth for all cell lines early in culture.

Figure 5.6 shows the dose-response curves for cells treated with MeAIB during exponential growth. MeAIB markedly affected growth in all cell lines expressing glutamine synthetase, while growth of CAT-S cells was only slightly reduced. Blocking system A transport does not lead to complete inhibition of cell proliferation. For that reason IC_{25} concentrations were calculated for cell lines expressing glutamine synthetase. A comparison of these values shows T29 cells to be slightly more sensitive to system A inhibition. Culture viability measurements demonstrate that decreased cell proliferation was not accompanied by cell death in any cell line (Figure 5.7 A–E).

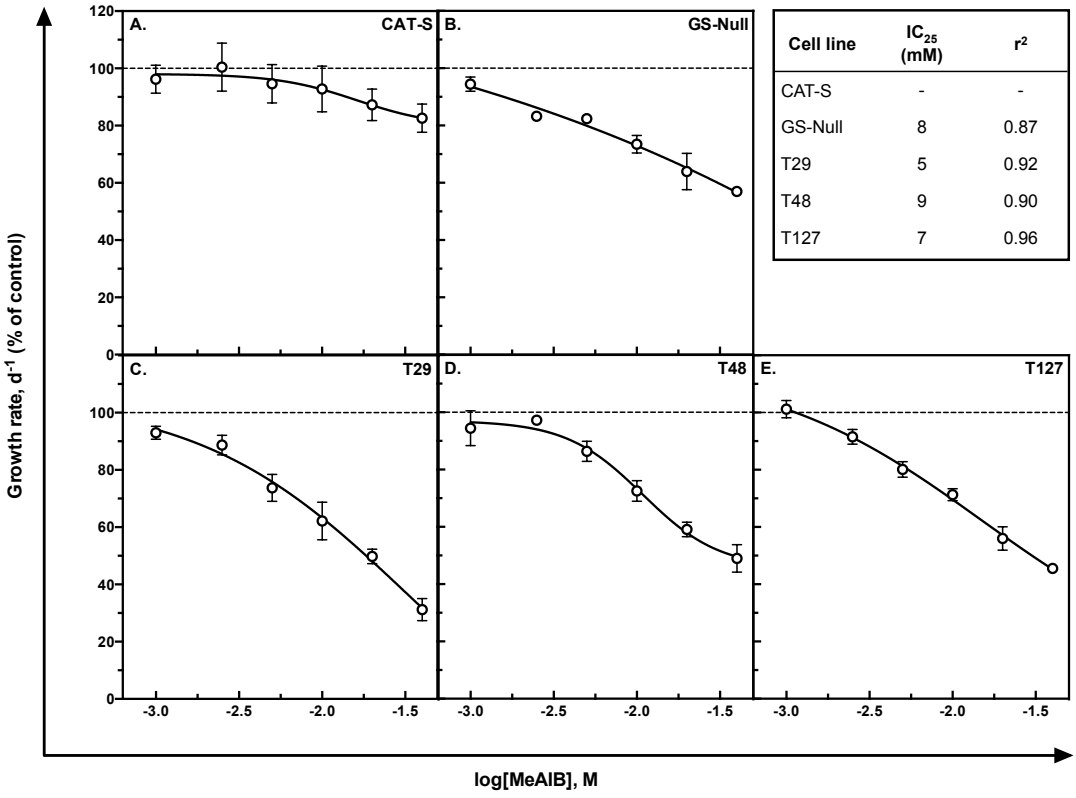

Figure 5.6 The effect of MeAIB treatment on cell proliferation during exponential growth phase. Cells were treated for 4 days with MeAIB. The specific growth rate (d^{-1}) was calculated and normalised to control cultures (0 mM MeAIB). Data is shown as the mean ± SEM of three independently performed experiments. Non-linear regression analysis was used to fit dose-response curves and calculate the IC_{25} values (table insert).

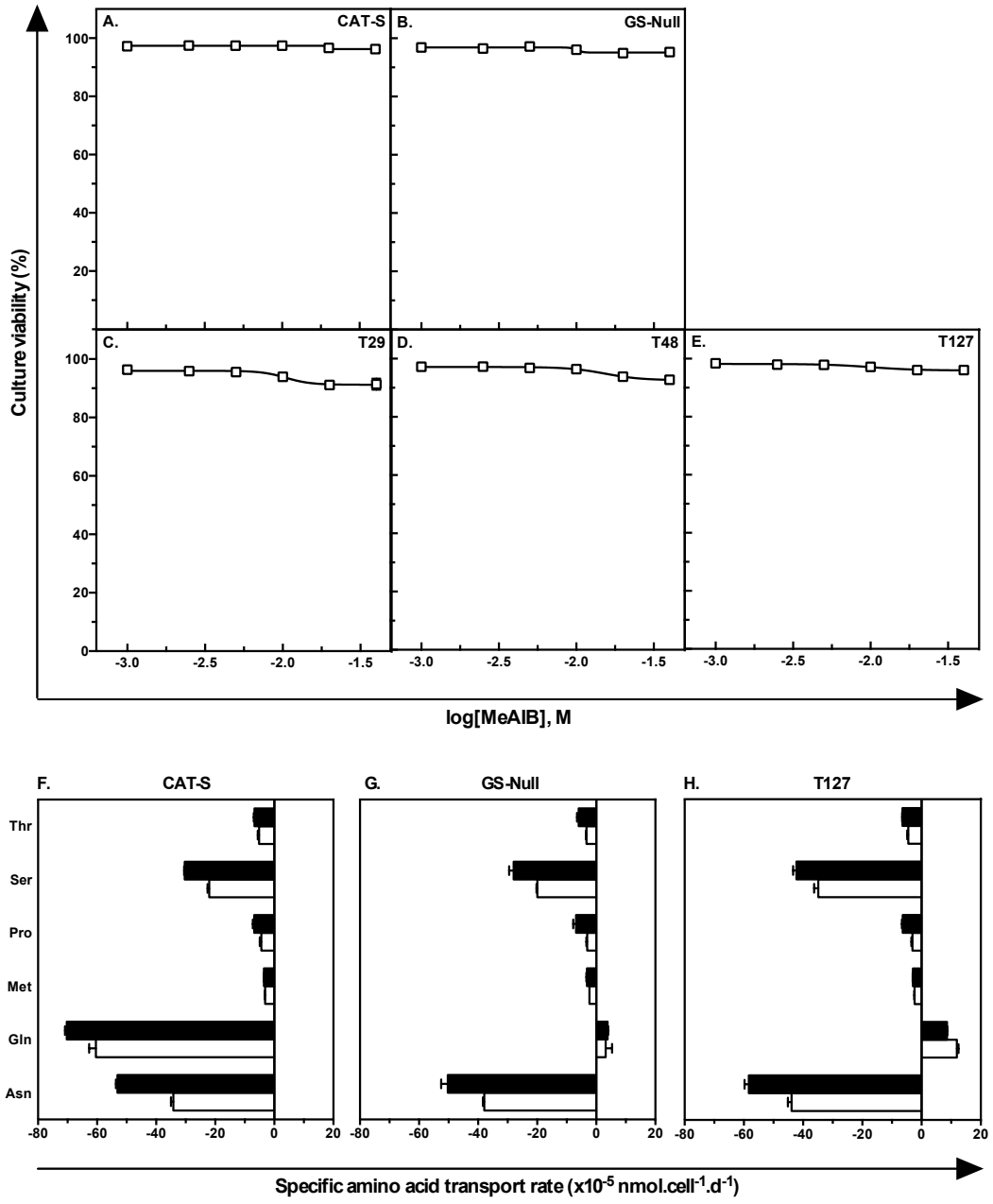

Figure 5.7 The effect of MeAIB treatment on culture viability and amino transport rates during exponential growth phase. Culture viability was measured on day 4 of MeAIB treatment (**A.** – **E.**). All control cultures (0 mM MeAIB) had viabilities >95%. Data is shown as the mean ± SEM of three independently performed experiments. Amino acid transport rates were calculated between days 1–3 for CAT-S cells (**F.**), and between days 1–4 for GS-Null (**G.**) and T127 cells (**H.**). Closed bars are rates from control cultures and open bars are rates at 40 mM (CAT-S), 10 mM (GS-Null), and 5 mM MeAIB (T127). Data is the mean + SEM of three independently performed experiments.

Transport rates of classic system A substrates were measured for CAT-S, GS-Null, and T127 cells in control and MeAIB treated cultures (Figure 5.7 F–H). Consumption of these amino acids was reduced but not completely inhibited in GS-Null and T127 cells at concentrations close to their IC_{25} (10 and 5 mM respectively). This was also observed in CAT-S cells at the maximum MeAIB concentration (40 mM). Significant consumption of asparagine and serine continued in GS-Null and T127 cells at 40 mM MeAIB demonstrating that complete inhibition of system A substrates did not occur in these two cell lines either (data not shown).

Antibody production was examined in T29, T48, and T127 cells (Figure 5.8). Specific productivity remained relatively constant over the concentration range tested in the low producer (T29) with titre decreasing in a dose-dependent manner in response to a drop in IVCD. The two high producers (T48 and T127) however showed a slight reduction in specific productivity in response to MeAIB treatment.

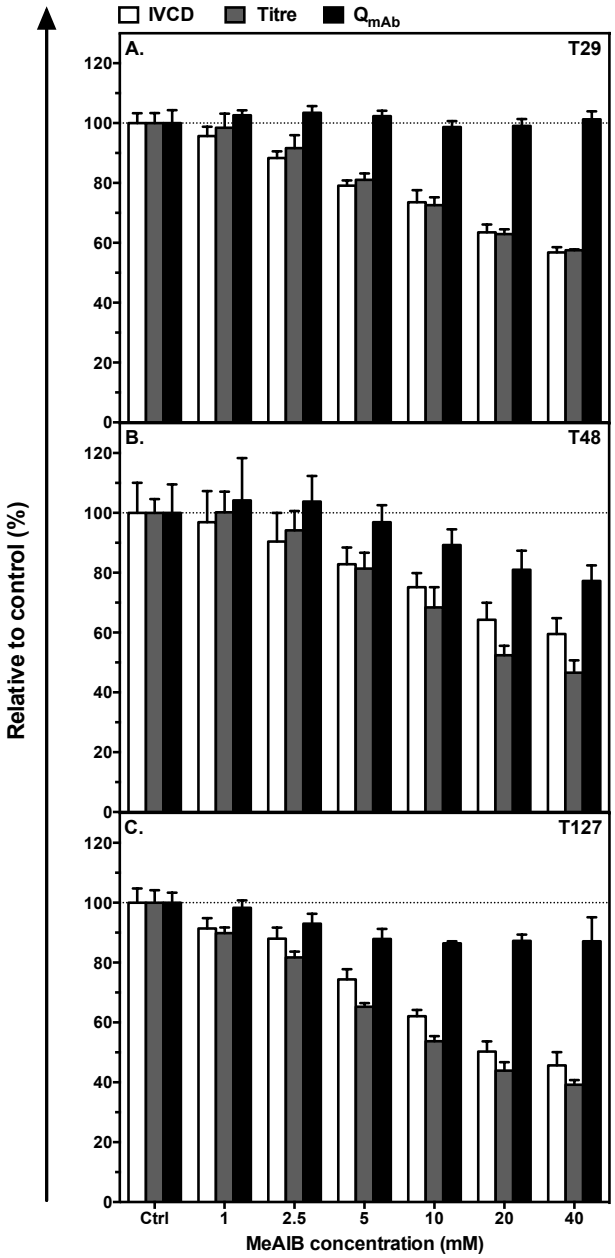

Figure 5.8 The effect of MeAIB treatment on antibody production during exponential growth phase. Cells were treated for 3 days (**A.** & **B.**) or 4 days (**C.**) with MeAIB. IVCD (white bars), titre (grey bars) and Q_{mAb} (black bars) was calculated and normalised to the control cultures (0 mM MeAIB). Data is shown as the mean + SEM of three independently performed experiments.

The effect of MeAIB treatment during stationary phase was tested in CAT-S, GS-Null, and T127 cells (Figure 5.9). For CAT-S and GS-Null cells, no change in culture viability was observed after 2 days of treatment. For T127 cells, no change in culture viability or antibody production was observed after 24 hr of treatment. T127

cells formed large rings of cell debris on the culture vessel wall after 24 hr in control and treated cultures, preventing an accurate assessment of culture performance past this time point

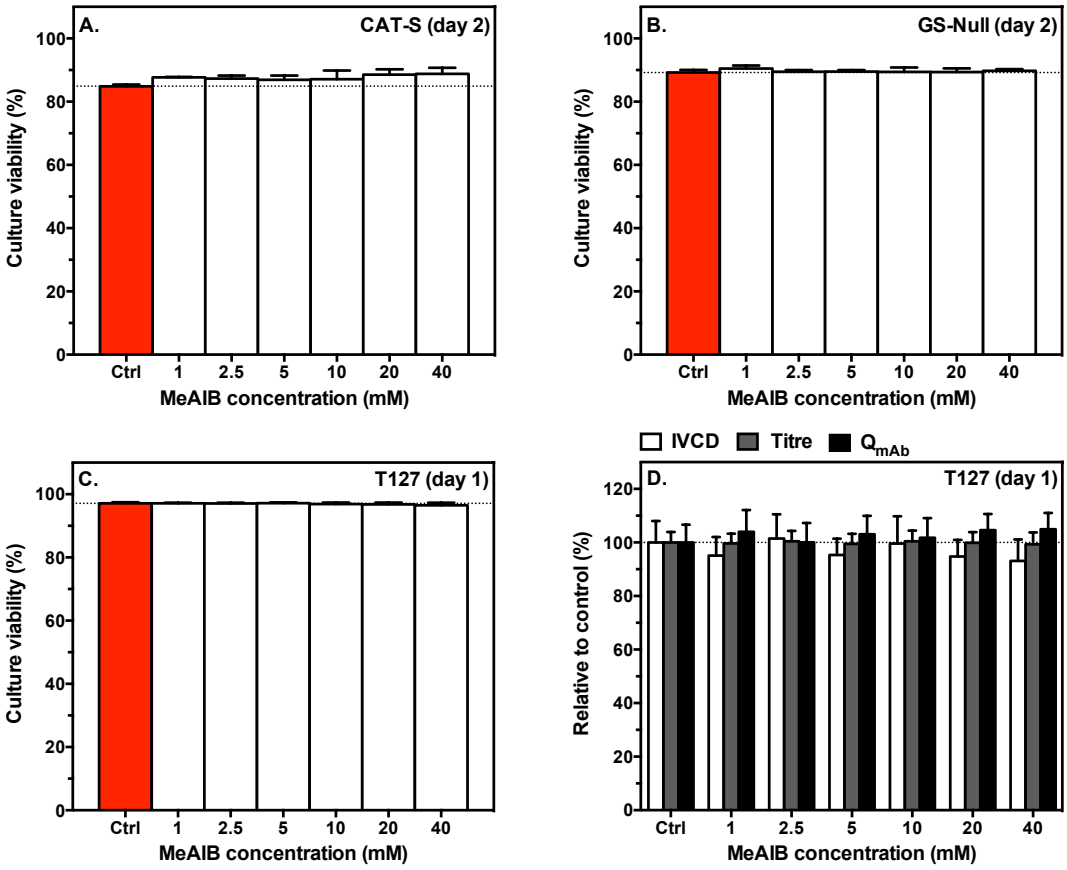

Figure 5.9 The effect of MeAIB treatment on CAT-S, GS-Null, and T127 cells at stationary phase of batch culture. Culture viability was assessed for CAT-S cells (**A.**) and GS-Null cells (**B.**) at day 2 post-addition of MeAIB. T127 cells had their viability (**C.**) and antibody production (**D.**) assessed at day 1 post-addition of MeAIB. Control cultures represent cells incubated with 0 mM MeAIB. Data is shown as the mean + SEM of three independently performed experiments.

5.3.3 System X_C^- Transport Inhibition

Chapter 4 hypothesised that the system X_C^- transporter xCT has a critical role in supporting cell viability in all cell lines. xCT activity was also hypothesised to support antibody production in T127 cells during late-stage culture. Sulfasalazine (SAS) is a clinically approved drug for the treatment of inflammatory bowel diseases and rheumatoid arthritis but has also been demonstrated as an effective inhibitor of cystine

uptake through the xCT transporter in a range of cancer cell lines (Chung et al., 2005; Gout et al., 2001; Timmerman et al., 2013). However, SAS also has two reported off-target effects. It can inhibit activation of the transcription factor nuclear factor-κB (NF-κB), which is involved in the activation of genes involved in cell proliferation and anti-apoptosis (Robe et al., 2004; Wahl et al., 1998). It can also inhibit glutathione S-transferases (GSTs), which catalyze the conjugation of GSH and electrophiles to prevent cell damage (Awasthi et al., 1994; Bach et al., 1985). Cells were treated with SAS to inhibit xCT activity, which is hypothesised to inhibit cystine uptake and induce cell death in all cell lines.

Figure 5.10 shows the dose-response curves for cells treated with SAS during exponential growth. All cell lines exhibited a marked decrease in cell proliferation. However, differences in sensitivity were apparent between the five cell lines as demonstrated by a comparison of their respective IC_{50} concentrations. CAT-S, GS-Null, and T29 cells were most sensitive to SAS treatment with both GS-Null and T29 cells showing complete inhibition of growth at 1 mM SAS. T48 cells were slightly more resistant to treatment, particularly at lower concentrations of SAS, while T127 cells were found to be most resistant. Interestingly, there was a small improvement in growth rate for T29 and T127 cells in response to treatment with 0.3 mM SAS compared to control cultures. T127 cells treated with 0.3 mM SAS continued to have a faster growth rate (21.9 ± 1.6%; mean ± SEM, n = 3) than control cultures by day 4 of treatment. Culture viability measurements on day 3 of inhibition demonstrate that moderate levels of cell death accompanied decreased cell proliferation for CAT-S, GS-Null, and T29 cells (Figure 5.11 A–E). Minor cell death was observed in the two high producers (T48 and T127). An assessment of culture viability after 4 days of treatment found substantial cell death in all cell lines with no obvious differences in sensitivity between them at higher SAS concentrations.

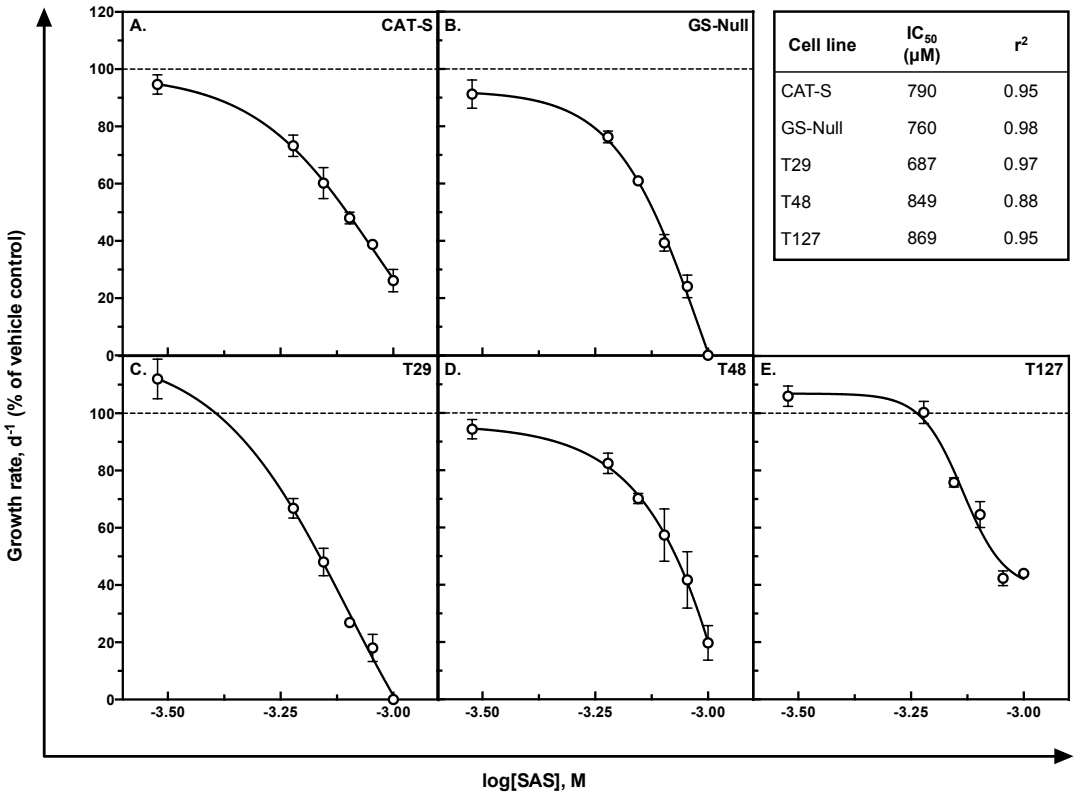

Cell line	IC_{50} (μM)	r^2
CAT-S	790	0.95
GS-Null	760	0.98
T29	687	0.97
T48	849	0.88
T127	869	0.95

Figure 5.10 The effect of SAS treatment on cell proliferation during exponential growth phase. Cells were treated for 3 days with SAS. The specific growth rate (d^{-1}) was calculated and normalised to the vehicle control cultures (0.2% DMSO v/v CD-CHO medium with 0 mM SAS). Data is shown as the mean ± SEM of three independent cultures. Non-linear regression analysis was used to fit dose-response curves and calculate the IC_{50} concentrations (table insert).

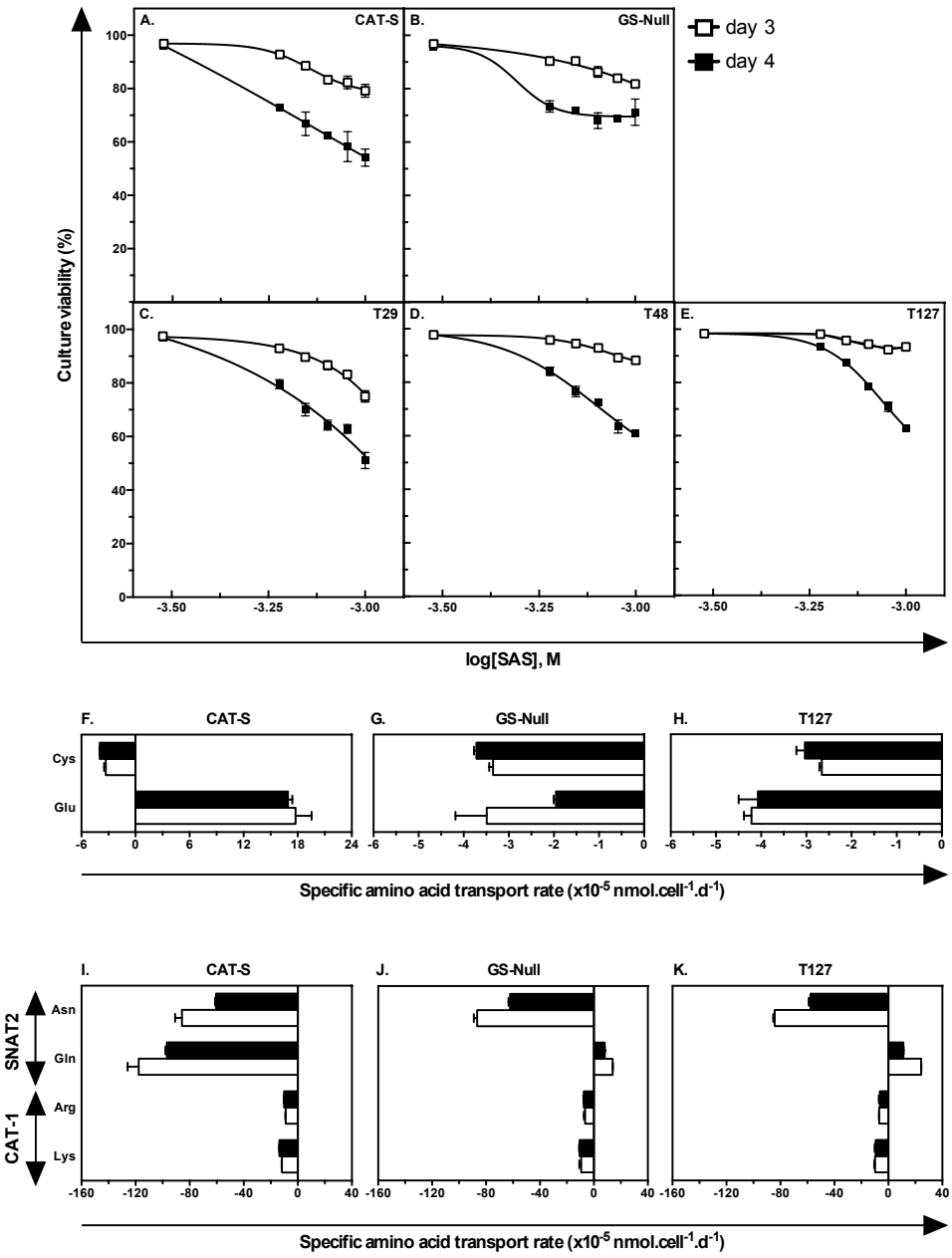

Figure 5.11 The effect of SAS treatment on culture viability and amino transport rates during exponential growth phase. Culture viability was measured on day 3 (open squares) and day 4 (closed squares) of SAS treatment (**A.** – **E.**). All vehicle control cultures (0.2% DMSO v/v CD-CHO medium with 0 mM SAS) had viabilities >95% on both days. Data is shown as the mean ± SEM of three independent cultures. Amino acid transport rates were calculated between days 1–3 (**F.** – **K.**). Closed bars are rates from vehicle control cultures and open bars are rates at 0.7 mM (CAT-S and GS-Null) and 0.8 mM SAS (T127). Data is the mean + SEM of three independently performed experiments.

Transport rates of cystine and glutamate were measured for CAT-S, GS-Null, and T127 cells in control and SAS treated cultures (Figure 5.11 F–H). All cell lines showed a small decrease in cystine consumption at concentrations close to their IC_{50}. No change in glutamate transport was observed in CAT-S and T127 cells but GS-Null cells demonstrated an increase in glutamate uptake. Cystine starvation has been shown to induce the amino acid response (AAR) signalling pathway in mammalian cells (Lee et al., 2008). The amino acid transporters SNAT2, CAT-1 as well as xCT itself are three well-studied target genes of the AAR pathway whose expression is upregulated in response to its activation. To investigate if this pathway was activated by system X_C^- inhibition, the transport rates of representative substrates for the SNAT2 and CAT-1 transporters were measured. SAS was found to increase the consumption of the SNAT2 substrate asparagine in a dose-dependent manner in the three cell lines (example data given at IC_{50} concentrations in Figure 5.11 I–K). Glutamine consumption in CAT-S cells increased in the same way. However, transport rates of the CAT-1 substrates arginine and lysine did not change in response to SAS treatment.

Antibody production was examined in T29, T48, and T127 cells (Figure 5.12). For T127 cells, day 4 titres decreased in a dose-dependent manner in response to a drop in both IVCD and specific productivity. The improvement in T127 growth rate observed with 0.3 mM SAS treatment led to an increased titre. For T29 and T48 cells, antibody data was measured in cultures treated with 0.3 and 0.8 mM SAS only. Day 3 titres decreased at the higher concentration for both cell lines in response to a drop in IVCD only. Treatment of 0.3 mM SAS in T29 cells boosted specific productivity in addition to growth resulting in ~40% increase in titre.

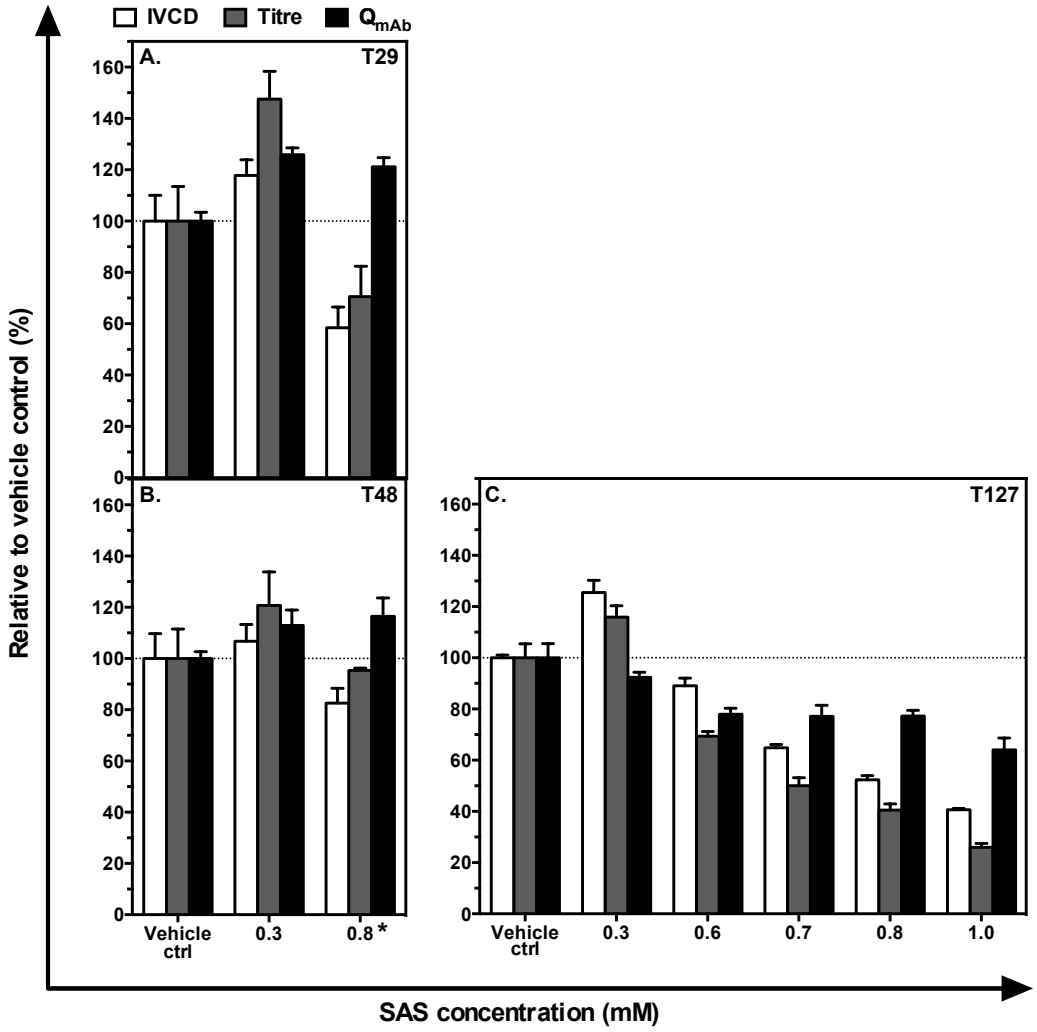

Figure 5.12 The effect of SAS treatment on antibody production during exponential growth phase. Cells were treated for 3 days (**A.** & **B.**) or 4 days (**C.**) with SAS. IVCD (white bars), titre (grey bars) and Q_{mAb} (black bars) was calculated and normalised to the vehicle control cultures (0.2% DMSO v/v CD-CHO medium with 0 mM SAS). Data is shown as the mean + SEM of three independent cultures. The asterisk indicates 0.8 mM data is shown as the mean + SEM of two independent cultures with (**A.**) T29 and (**B.**) T48 cells.

The effect of SAS treatment during stationary phase was tested in CAT-S, GS-Null, and T127 cells (Figure 5.13). The three cell lines displayed a striking increase in sensitivity to system X_C^- inhibition with cell death taking place just hours after SAS treatment. The reduced SAS "dose-per-cell" at stationary phase compared to exponential growth underscores this increase in sensitivity across the three cell lines.

Analysis of antibody production in T127 cells found specific productivity to decrease in a dose-dependent manner in response to SAS treatment at stationary phase.

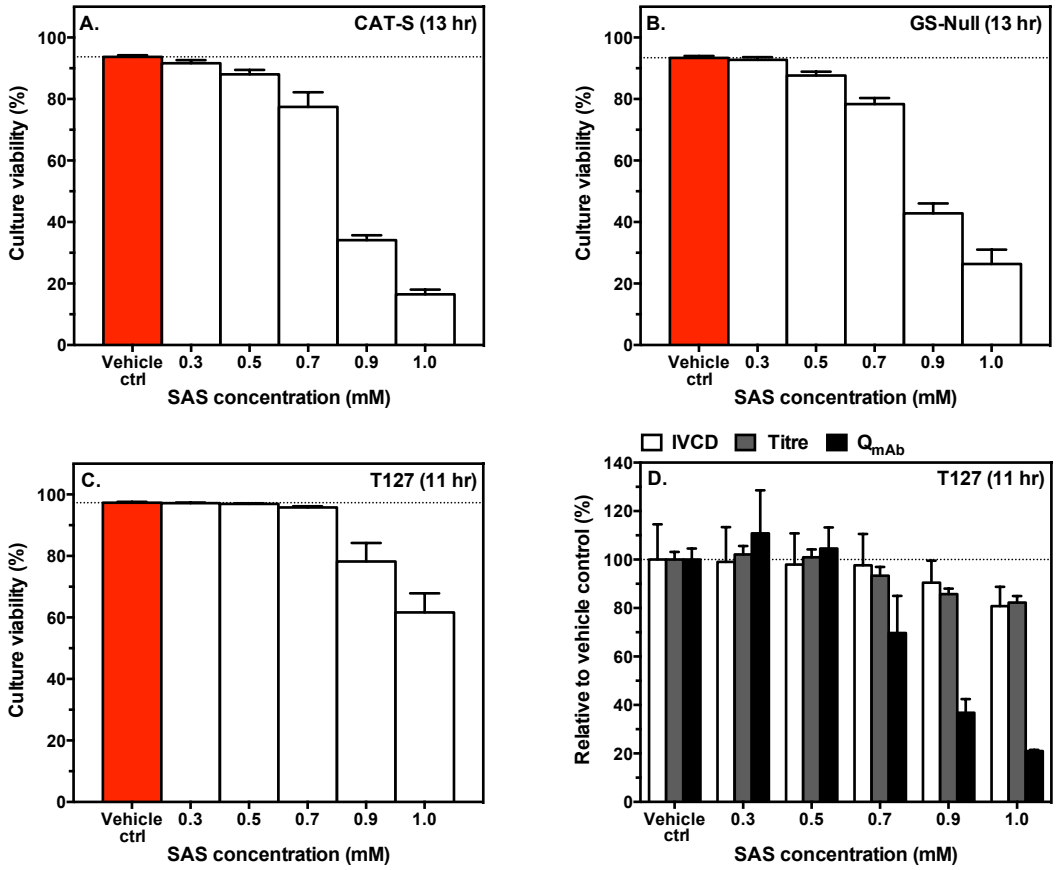

Figure 5.13 The effect of SAS treatment on CAT-S, GS-Null, and T127 cells at stationary phase of batch culture. Culture viability was assessed for CAT-S cells (**A.**) and GS-Null cells (**B.**) at 13 hrs post-addition of SAS. T127 cells had their viability (**C.**) and mAb production (**D.**) assessed at 11 hrs post-addition of SAS. Data is shown as the mean + SEM of three independently performed experiments, except Q_{mAb} (**D.**) where the data shown is the mean + SEM of two independently performed experiments at all concentrations.

5.3.4 System ASC Transport Inhibition

The two transporters of system ASC (ASCT1 and 2) mediate the transport of alanine, asparagine, glutamine, serine, and threonine (see Chapter 2; Table 2.1). As discussed above, ASCT1 alongside SNAT2 is hypothesised to be the main entry routes for this group of amino acids in all cell lines. In Chapter 4, ASCT1 was proposed as a potential marker of productivity throughout culture in T127 cells. Significant upregulation of

ASCT1 during late-stage culture in all cell lines also lead to the suggestion that it may have a key role in supporting cell viability. The glutamine analog, L-γ-glutamyl-p-nitroanilide (GPNA), contains a phenyl ring on the amide nitrogen group that mediates binding to the ASCT2 transporter (Esslinger et al., 2005). GPNA has been demonstrated as an effective inhibitor of glutamine uptake in HeLa cells (Nicklin et al., 2009) and the A549 lung cancer cell line (Hassaniein et al., 2013). Because ASCT1 and ASCT2 exhibit ~60% amino acid sequence identity with each other (Kanai et al., 2013), it is possible that GPNA may also bind to ASCT1. GPNA treatment is hypothesised to suppress cell growth during exponential phase and induce cell death at stationary phase in all cell lines. Treatment is also expected to have a negative effect on antibody production in T127 cells.

Figure 5.14 shows the dose-response curves for cells treated with GPNA during exponential growth. All cell lines exhibited a marked decrease in cell proliferation, however large differences in sensitivity exist. CAT-S and GS-Null cells were most sensitive to GPNA treatment sharing an IC_{50} concentration of 0.2 mM but having quite different dose-response curves. There was a considerable amount of variability in growth responses amongst the antibody producing cell lines, which did not correlate with productivity. T127 cells were by far the most resistant cell line of the five tested, having an IC_{50} concentration that is a magnitude higher than the host cell line. Whereas T48, also a high producer was very sensitive to GPNA treatment. The low producer T29 was found to be more resistant than T48 cells but also more sensitive than T127 cells. Culture viability measurements on day 3 of treatment reflected these cell line differences with T127 cells being most resistant to cell death (Figure 5.15 A–E). An assessment of culture viability after 4 days of treatment found substantial cell death in all cell lines except T127 cells, which continued to demonstrate a high level of resistance.

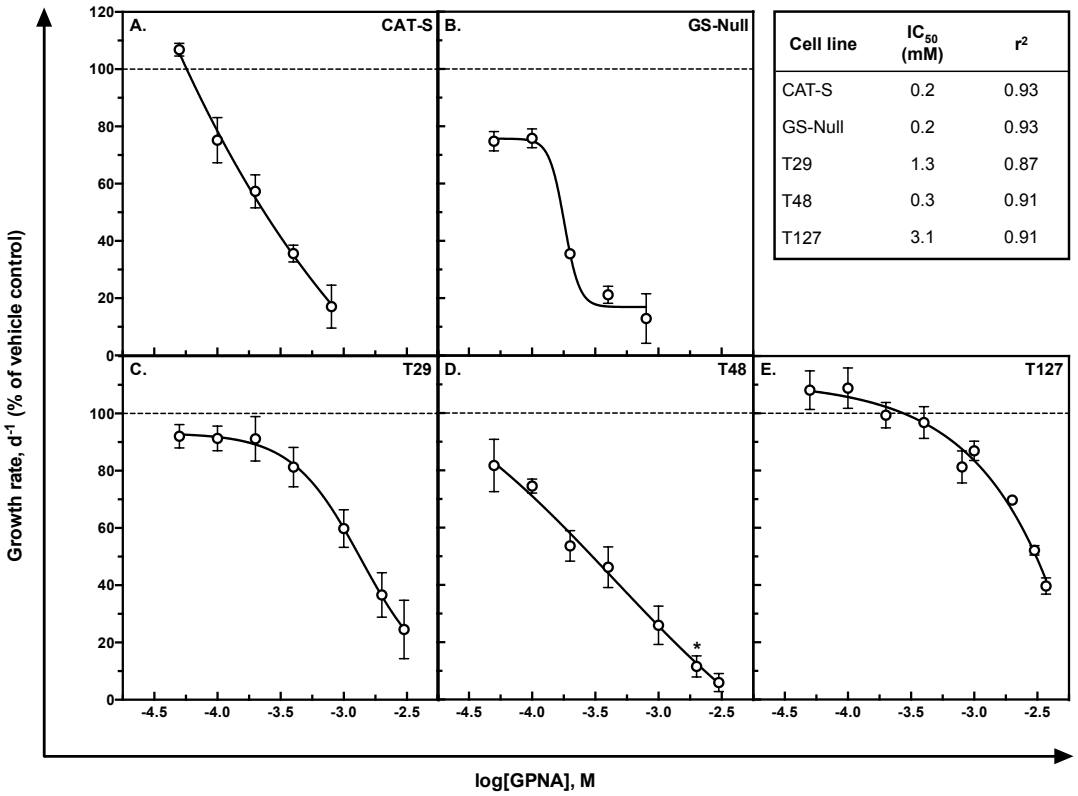

Figure 5.14 The effect of GPNA treatment on cell proliferation during exponential growth phase. Cells were treated for 3 days with GPNA. The specific growth rate (d^{-1}) was calculated and normalised to the vehicle control cultures (0.2% DMSO v/v CD-CHO medium with 0 mM GPNA). Data is shown as the mean ± SEM of three independent cultures. An asterisk indicates data shown as the mean ± SEM of two independent cultures (2 mM cultures for **D.** only). Non-linear regression analysis was used to fit dose-response curves and calculate the IC_{50} concentrations (table insert).

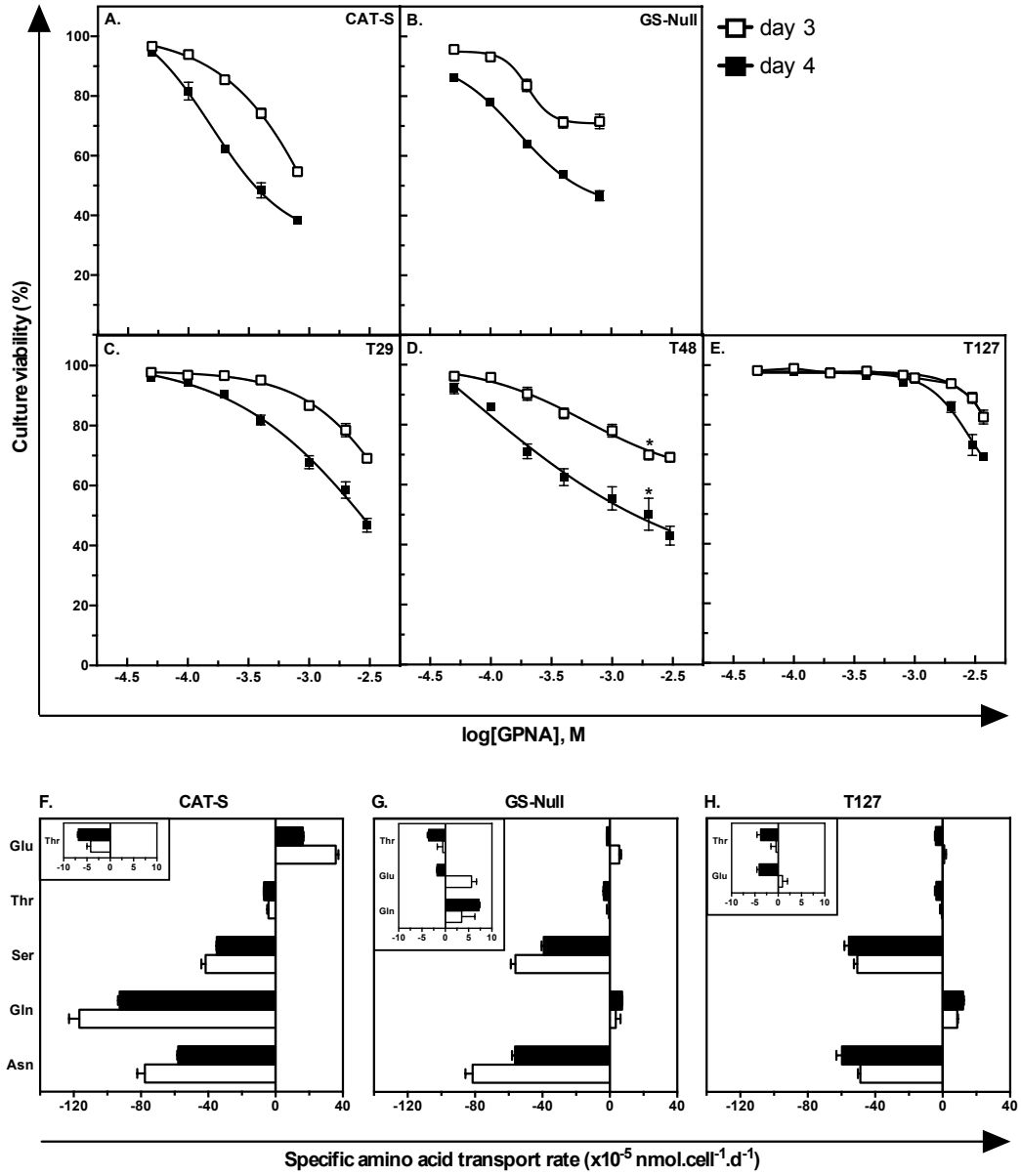

Figure 5.15 The effect of GPNA treatment on culture viability and amino transport rates during exponential growth phase. Culture viability was measured on day 3 (open squares) and day 4 (closed squares) of GPNA treatment. All vehicle control cultures (0.2% DMSO v/v CD-CHO medium with 0 mM GPNA) had viabilities >95% on both days. Data is shown as the mean ± SEM of three independent cultures. An asterisk indicates data shown as the mean ± SEM of two independent cultures (2 mM cultures for **D.** only). Amino acid transport rates were calculated between days 1–3 (**F.** – **H.**). Closed bars are rates from vehicle control cultures and open bars are rates at 0.2 mM (CAT-S and GS-Null) and 3.7 mM GPNA (T127). Data is the mean + SEM of three independent cultures

Transport rates of classic system ASC substrates were measured for CAT-S, GS-Null, and T127 cells in control and GPNA treated cultures (Figure 5.15 F–H). GPNA treatment was found to increase consumption of asparagine and serine in a dose-dependent manner in the sensitive CAT-S and GS-Null cell lines. Glutamine consumption in CAT-S cells increased in the same way. This counterintuitive observation may be explained by activation of the AAR pathway in these cells resulting in increased expression of SNAT2 but the simultaneous downregulation of global protein synthesis. In support of this, cystine uptake through the xCT transporter was also found to increase in a dose-dependent manner. At 0.2 mM GPNA, cystine consumption increased by 16.2 ± 6.2% and 48.6 ± 7.0% (mean ± SEM, n = 3) in CAT-S and GS-Null cells respectively. For resistant T127 cells, consumption of asparagine and serine was reduced but not completely inhibited at the maximum GPNA concentration (3.7 mM). Consumption of cystine was approximately equivalent in control and 3.7 mM GPNA treated T127 cells (-3.7 ± 0.2 versus -3.8 ± 0.1 $x10^{-5}$ $nmol.cell^{-1}.d^{-1}$; mean ± SEM, n = 3).

Antibody production was examined in T29, T48, and T127 cells (Figure 5.16). For T29 and T127 cells, which demonstrated a high level of resistance to GPNA, specific productivity remained constant over the concentration range tested and titre decreased in a dose-dependent manner in response to a drop in IVCD. For T48 cells, titre decreased in response to a drop in both IVCD and specific productivity.

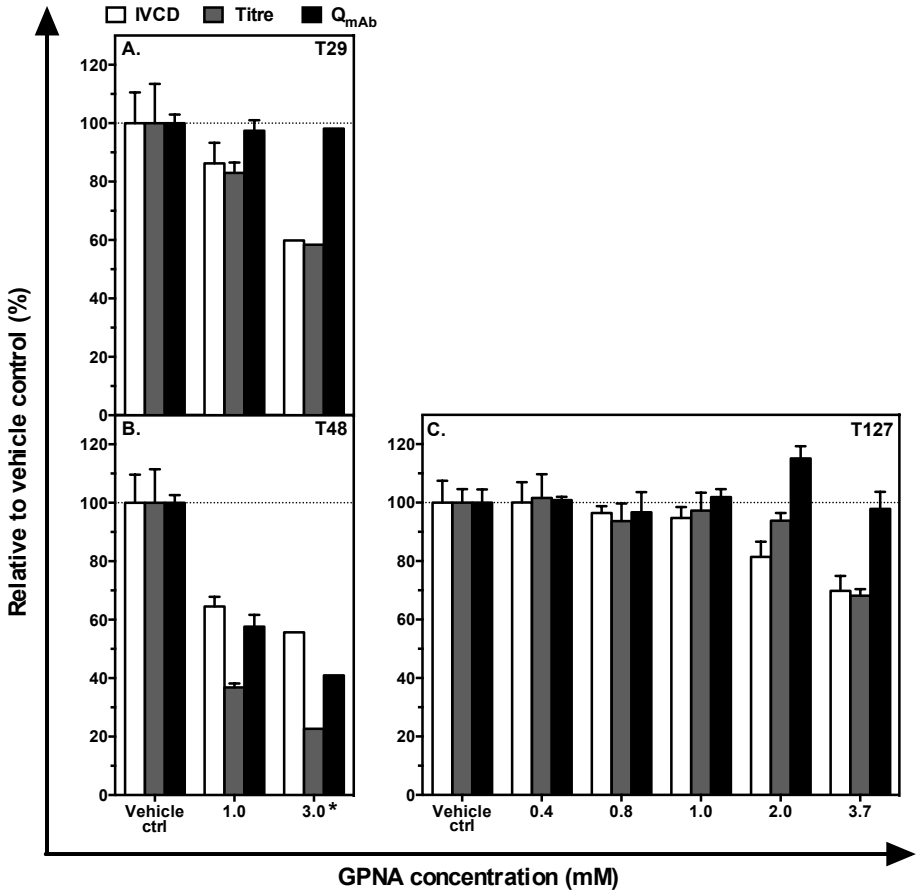

Figure 5.16 The effect of GPNA treatment on antibody production during exponential growth phase. Cells were treated for 3 days with GPNA. IVCD (white bars), titre (grey bars) and Q_{mAb} (black bars) was calculated and normalised to the vehicle control cultures (0.2% DMSO v/v CD-CHO medium with 0 mM GPNA). Data is shown as the mean + SEM of three independent cultures. The asterisk indicates data from a single experiment at 3.0 mM GPNA with T29 (**A.**) and T48 (**B.**) cells.

The effect of GPNA treatment during stationary phase was tested in CAT-S, GS-Null, and T127 cells (Figure 5.17). For CAT-S cells, no change in culture viability was observed after 2 days of treatment with the same concentration range used during exponential growth (0.05 – 0.8 mM GPNA). Increasing the concentration further (up to 3 mM) still did not induce cell death, suggesting they are no longer sensitive to system ASC inhibition. GS-Null cells remain sensitive to system ASC inhibition during stationary phase with cell death observed after 2 days of GPNA treatment. For T127 cells, no change in culture viability or antibody production was observed after 24 hr of treatment.

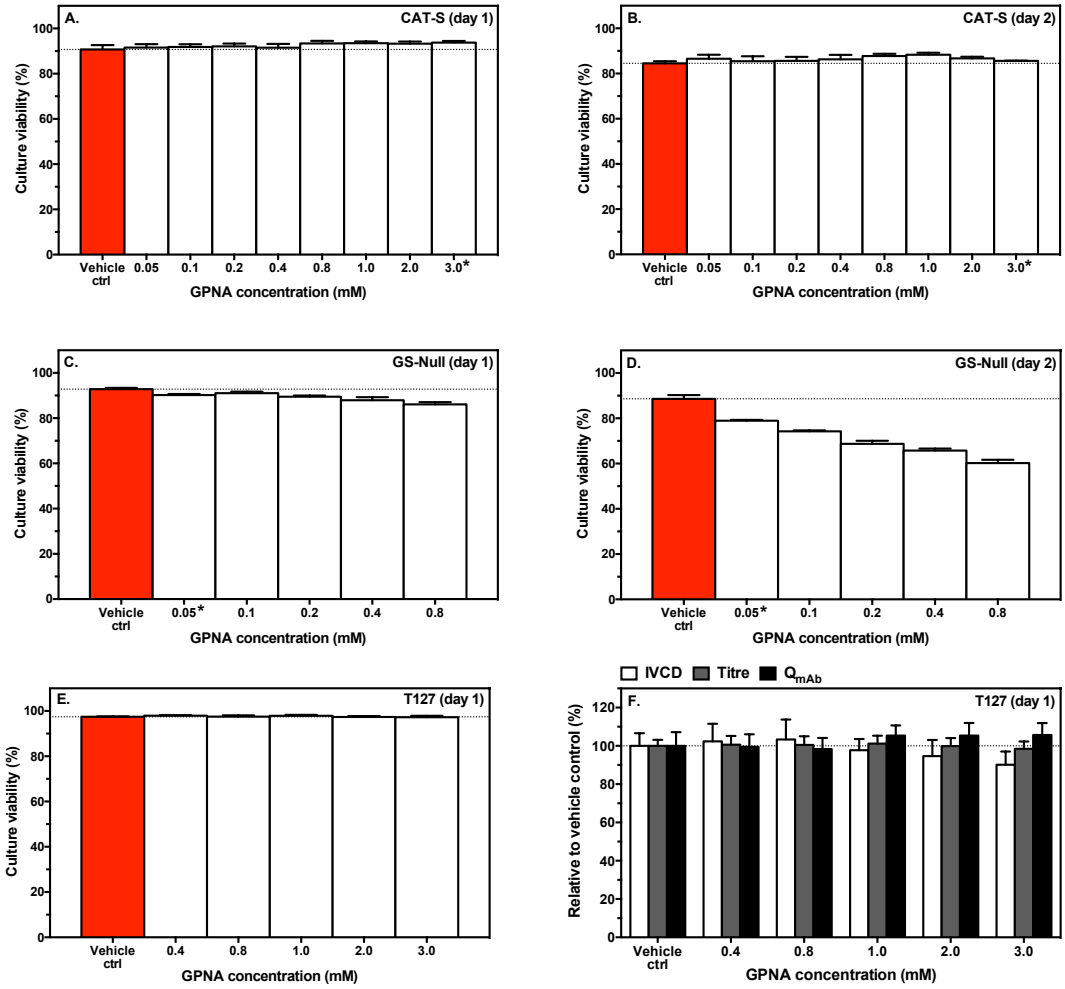

Figure 5.17 The effect of GPNA treatment on CAT-S, GS-Null, and T127 cells at stationary phase of batch culture. Culture viability was assessed at day 1 and day 2 post-addition of GPNA for CAT-S and GS-Null cells (**A. – D.**). T127 cells had their viability (**E.**) and mAb production (**F.**) assessed at day 1 post addition of GPNA. Data is shown as the mean + SEM of three independently performed experiments. An asterisk indicates data shown as the mean + SEM of two independently performed experiments (3 mM cultures for CAT-S only).

5.3.5 GlyT1 Transport Inhibition

Chapter 4 demonstrated that changes to GlyT1 expression correlated well with changes in expression of the cystine xCT transporter. It is therefore hypothesised that GlyT1 may be mediating the influx of glycine to support GSH synthesis. The glycine analog, sarcosine (N-methylglycine), is a weak selective transportable inhibitor of the GlyT1 transporter (Atkinson et al., 2001; Mallorga et al., 2003). However, it is also a metabolic intermediate in glycine synthesis making it unsuitable as an inhibitor in this work. ALX

5407 HCl (N-[(3R)-3-([1,1'-Biphenyl]-4-yloxy)-3-(4-fluorophenyl)propyl]-N-methylglycine hydrochloride), is a sarcosine analog that is a potent non-transportable inhibitor for GlyT1 (Atkinson et al., 2001). Because of the above observations with the transcriptomic data, ALX 5407 HCl treatment is hypothesised to induce cell death in all cell lines.

CAT-S, GS-Null, and T127 cells were treated with ALX 5407 HCl during exponential growth (Figure 5.18). Blocking GlyT1 transport reduced cell proliferation in all three cell lines but did not result in complete inhibition of growth (Figure 5.18 A–C). A comparison of IC_{25} values shows T127 cells to be slightly more resistant to GlyT1 inhibition. Culture viability measurements found no significant cell death for any of the three cell lines (Figure 5.18 D–F). Analysis of antibody production in T127 cells found specific productivity to remain constant over the concentration range tested with titre decreasing in response to a drop in IVCD (Figure 5.18 G).

Transport rates of glycine were measured for the three cell lines in control and ALX 5407 HCl treated cultures (Figure 5.18 H–J). ALX 5407 HCl treatment was found to increase production of glycine in the three cell lines. Glycine transport through GlyT1 is coupled to Na^+ and Cl^- transport making it effectively unidirectional for glycine import (see Chapter 2; Table 2.1). GlyT1 inhibition must therefore be limiting glycine consumption while glycine export via other transport processes continues thus demonstrating that glycine is simultaneously both produced and consumed within cells through different transporters.

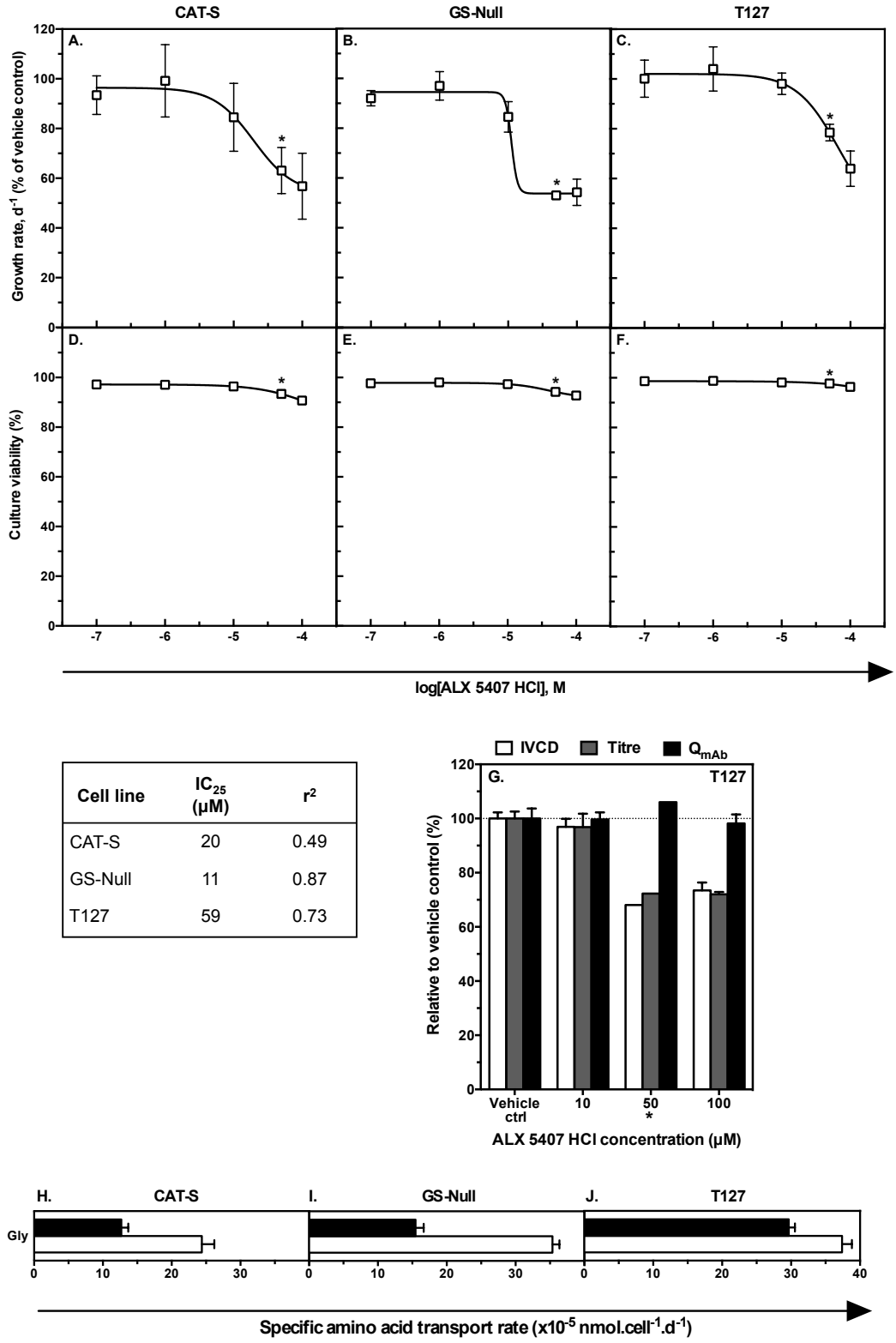

Cell line	IC_{25} (µM)	r^2
CAT-S	20	0.49
GS-Null	11	0.87
T127	59	0.73

Figure 5.18 The effect of ALX 5407 HCl treatment on CAT-S, GS-Null, and T127 cells during exponential growth phase. Cells were treated for 3 days with ALX 5407 HCl. The specific growth rate (d^{-1}) was calculated and normalised to the vehicle control cultures (0.2% DMSO v/v CD-CHO medium with 0 µM ALX 5407 HCl) (**A.** – **C.**). Non-linear regression analysis was used to fit dose-response curves and calculate the IC_{25} values (table insert). Culture viability was measured on day 3 of treatment (**D.** –

F.). All vehicle control cultures had viabilities >95%. Production of mAb was also assessed on day 3 of treatment for T127 cells (**G.**). Data is shown as the mean ± SEM of three independently performed experiments. An asterisk indicates data shown as the mean ± SEM of two independently performed experiments (50 μM cultures for **A. – F.**) and mAb data from a single experiment at 50 μM (**G.**). Amino acid transport rates were calculated between days 1–3 (**H. – J.**). Closed bars are rates from vehicle control cultures and open bars are rates at 50 μM GPNA ALX 5407 HCl.

The cell lines were also treated with ALX 5407 HCl during stationary phase (Figure 5.19). For CAT-S cells there was some minor cell death in treated cultures compared to control cultures. GS-Null cells had an increased sensitivity to GlyT1 inhibition at stationary phase, with moderate levels of cell death observed in treated cultures. For T127 cells, no change in culture viability was observed after 24 hr of treatment but an assessment of antibody production showed decreased specific productivity in treated cultures.

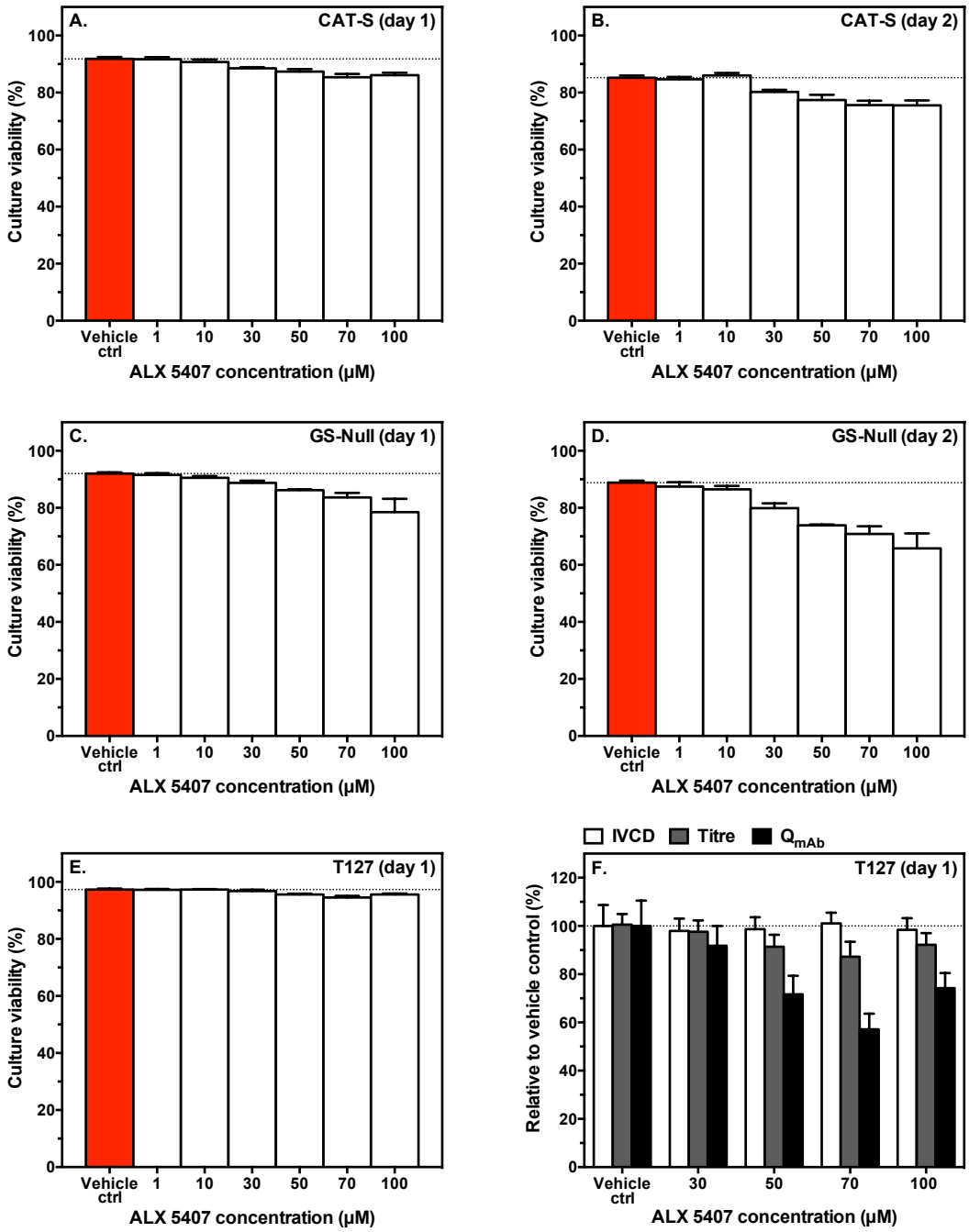

Figure 5.19 The effect of ALX 5407 HCl treatment on CAT-S, GS-Null, and T127 cells at stationary phase of batch culture. Culture viability was assessed at day 1 and day 2 post-addition of ALX 5407 HCl for CAT-S and GS-Null cells (**A. – D.**). T127 cells had their viability (**E.**) and mAb production (**F.**) assessed at day 1 post-addition of ALX 5407 HCl. Data is shown as the mean + SEM of three independently performed experiments.

5.3.6 Multi-Transporter Inhibition in T127 Cells During Exponential Growth

Finally, the effect of inhibiting multiple transport systems simultaneously on growth rate, culture viability, and specific productivity was investigated in the antibody-producing T127 cell line. Four transport systems (factors) were studied: A, ASC, L, and X_C^- using MeAIB, GPNA, BCH, and SAS respectively. A two-level factorial design was conducted as this can reveal interactions between the transport systems that would not otherwise be revealed through a one-factor-at-a-time (OFAT) experiment. Each inhibitor was applied at either 0 mM (– level) or its respective IC_{25} concentration (+ level) resulting in 16 ($=2^4$) level combinations (Appendix Table B1). IC_{25} concentrations were determined from the earlier dose-response curves (MeAIB = 5 mM; GPNA = 0.4 mM; BCH = 10 mM; SAS = 0.6 mM). Figure 5.20 shows the data for the three response variables.

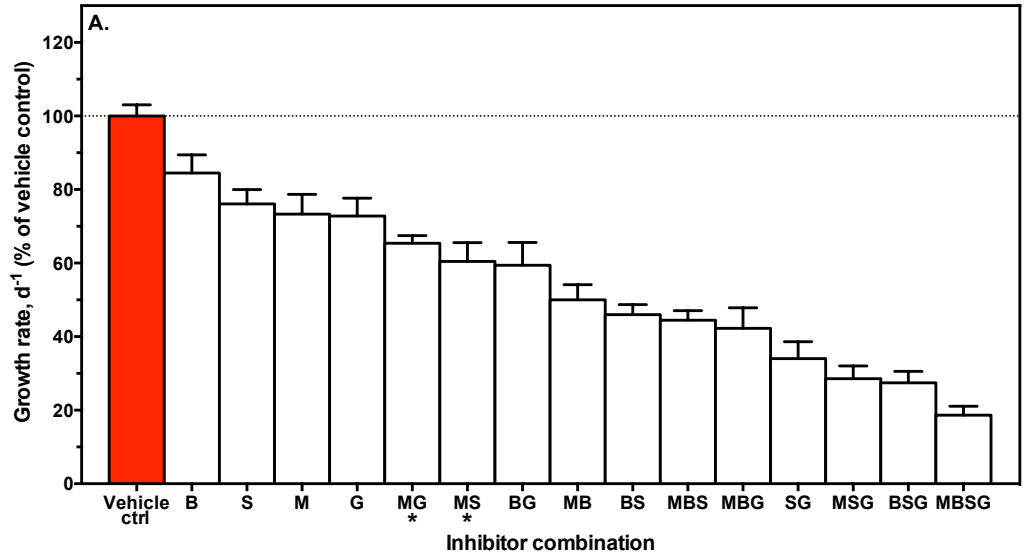
A.
Growth rate, d-1 (% of vehicle control)
120
100
80
60
40
20
0
Vehicle ctrl
B
S
M
G
MG *
MS *
BG
MB
BS
MBS
MBG
SG
MSG
BSG
MBSG
Inhibitor combination

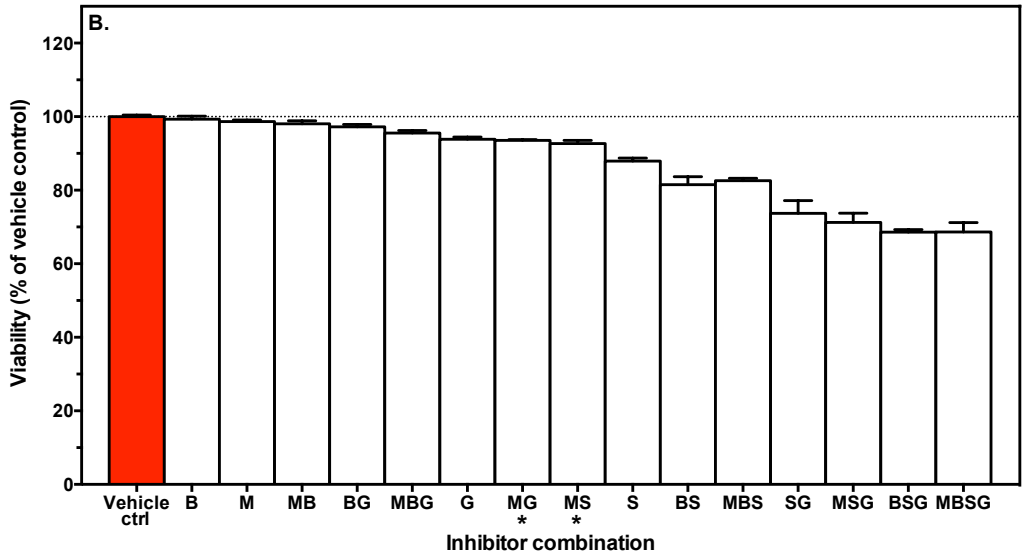
B.
Viability (% of vehicle control)
120
100
80
60
40
20
0
Vehicle ctrl
B
M
MB
BG
MBG
G
MG *
MS *
S
BS
MBS
SG
MSG
BSG
MBSG
Inhibitor combination

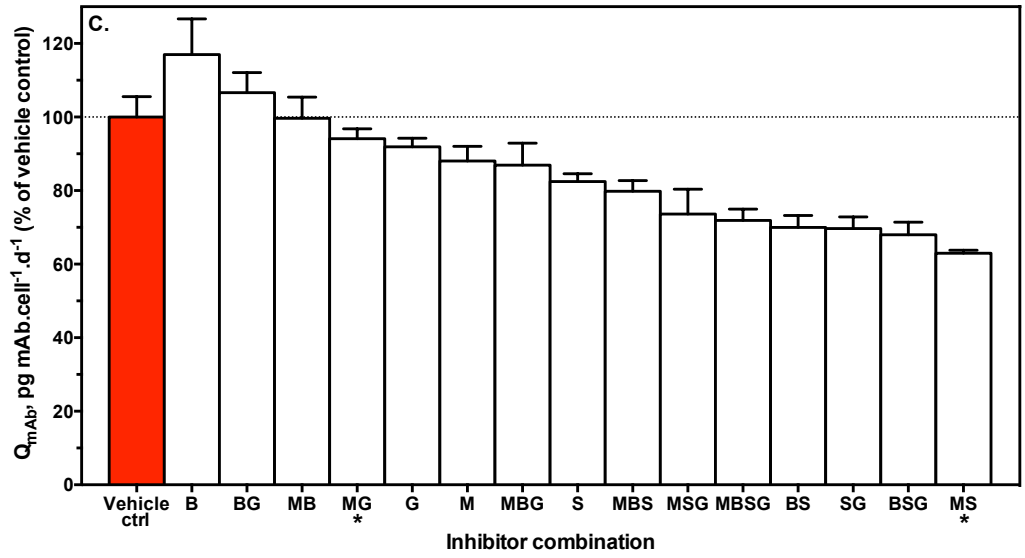
C.
QmAb, pg mAb.cell-1.d-1 (% of vehicle control)
120
100
80
60
40
20
0
Vehicle ctrl
B
BG
MB
MG *
G
M
MBG
S
MBS
MSG
MBSG
BS
SG
BSG
MS *
Inhibitor combination

Figure 5.20 The effect of multi-transporter inhibition on T127 cells during exponential growth phase. Cells were treated for 4 days with different combinations of transport system inhibitors. The specific growth rate (d^{-1}) (**A.**), culture viability (%) (**B.**) and specific antibody production (qmAb, pg mAb.cell^{-1}.d^{-1}) (**C.**) was calculated and normalised to the vehicle control cultures (0.2% DMSO v/v CD-CHO medium with no inhibitor). Inhibitors were applied at their IC_{25} values: ***B***, BCH (10 mM); ***S***, SAS (0.6 mM); ***M***, MeAIB (5 mM); ***G***, GPNA (0.4 mM). Data is shown as the mean + SEM of four independently performed experiments (**A.** & **B.**) or three independently performed experiments (**C.**). An asterisk indicate data shown as the mean + SEM of three independently performed experiments (**A.** & **B.**) or two independently performed experiments (**C.**).

5.3.6.1 Multi-Transporter Inhibition and Growth Rate

A half-normal probability plot created in Design Expert 9 (see 5.2 Materials and Methods) identified inhibition of systems A, ASC, L, and X_C^- alone as significant factors affecting growth rate in T127 cells (Appendix Figure B1). These significant factors were fitted to the following predictive model:

$$\text{Growth rate} = 55.2 - 7.3*\text{MeAIB} - 8.6*\text{BCH} - 13.3*\text{SAS} - 11.6*\text{GPNA}$$

An ANOVA confirmed that the model and each of the model terms is statistically significant (Model: $F_{(4,11)} = 26.73$, $P < 0.0001$; MeAIB: $F_{(1,11)} = 13.04$, $P = 0.0041$; BCH: $F_{(1,11)} = 18.08$, $P = 0.0014$; SAS: $F_{(1,11)} = 42.77$, $P < 0.0001$; GPNA: $F_{(1,11)} = 33.03$, $P = 0.0001$). A normal probability plot of residuals confirmed normality of residuals (Appendix Figure B2).

A comparison of the factor coefficients indicates that the inhibition of systems ASC and X_C^- has the biggest impact upon growth rate in T127 cells during exponential growth. Inhibition of systems A and L has an approximately equivalent negative impact upon growth that is less than that observed with the former two systems. Inhibiting multiple transport systems simultaneously demonstrates synergistic effects on growth rate in T127 cells (Figure 5.20 A). No interactions such as the inhibition of one transport system potentiating the inhibition of a second transport system were identified in the factorial experiment.

5.3.6.2 Multi-Transporter Inhibition and Culture Viability

A half-normal probability plot identified inhibition of systems L, X_C^-, and ASC alone, as well as interactions of systems L*X_C^-, L*ASC, and X_C^-*ASC as significant factors affecting culture viability in T127 cells (Appendix Figure B3). These significant factors were fitted to the following predictive model:

Culture viability = 88.0 – 1.5*BCH – 9.4*SAS – 4.8*GPNA – 1.7*BCH*SAS + 0.9*BCH*GPNA – 3.2*SAS*GPNA

An ANOVA confirmed that the model and each of the model terms is statistically significant (Model: $F_{(6,9)} = 204.01$, $P < 0.0001$; BCH: $F_{(1,9)} = 22.63$, $P = 0.0010$; SAS: $F_{(1,9)} = 850.46$, $P < 0.0001$; GPNA: $F_{(1,9)} = 219.78$, $P < 0.0001$; BCH*SAS: $F_{(1,9)} = 26.58$, $P = 0.0006$; BCH*GPNA: $F_{(1,9)} = 7.24$, $P = 0.0248$; SAS*GPNA: $F_{(1,9)} = 97.35$, $P < 0.0001$). A normal probability plot of residuals confirmed normality of residuals (Appendix Figure B4).

Inhibition of systems X_C^- has the biggest impact upon culture viability in T127 cells, followed by inhibition of system ASC. Interestingly, inhibiting system ASC at the same time as system X_C^- potentiates the negative effect the latter has on culture viability (Appendix Figure B5 A). System L inhibition makes a small but significant impact upon culture viability, however its inhibition can potentiate the effect of system X_C^- inhibition (Appendix Figure B5 B) or help minimise the effect of system ASC inhibition (Appendix Figure B5 C).

5.3.6.3 Multi-Transporter Inhibition and Specific Productivity

A half-normal probability plot identified only system X_C^- as a significant factor affecting specific productivity in T127 cells (Appendix Figure B6). This further confirms the observations above in which only SAS treatment induced a large effect on specific productivity. The dependence of specific productivity on X_C^- inhibition was predicted using:

Specific productivity = 85.2 – 12.9*SAS

An ANOVA confirmed that the model is statistically significant ($F_{(1,14)} = 37.23$, $P < 0.0001$). A normal probability plot of residuals confirmed normality of residuals (Appendix Figure B7).

5.4 Discussion

The work presented here is the second chapter of two that characterises the system of amino acid transporters in industrial CHO cell lines and complements the work of Chapter 4. In this second chapter, inhibitors were used to block amino acid entry through discrete transport systems in order to help understand how their transport function contributes to culture performance parameters. The inhibitors used were mostly analogs of natural proteinogenic amino acids and were selected based on prior use in the literature, their inability to be metabolised (e.g. ALX 5407 HCl over sarcosine for GlyT1 transporter), and had to be non-toxic to the cell itself (e.g. BCH over melphalan, a second inhibitor of system L transport which is also an alkylating agent). The exact mechanisms by which inhibiting a transport system induced changes to cell growth, viability or antibody production were not explored but hypotheses are provided in the discussion that follows.

5.4.1 System L Inhibition Blocks Essential Amino Acid Uptake, Suppresses Cell Growth, and Inhibits Antibody Production

BCH is a highly specific inhibitor for the four transporters that make up system L (Babu et al., 2003; Bodoy et al., 2005; Kanai et al., 1998; Pineda et al., 1999). In this chapter, BCH treatment completely inhibited the uptake of classic system L amino acids (Figure 5.3 F–H). This is consistent with the hypothesis put forward in Chapter 4 that system L is the major uptake route for essential amino acids. Many cancer cell lines preferentially increase their expression of LAT1 over the other three system L transporters to support increased growth rates (Fuchs and Bode, 2004), which was also seen in the three CHO cell lines examined in Chapter 4 (see Section 4.4.1). Based upon this, LAT1 is assumed to be mediating the majority of system L transport. The present results cannot confirm this but it could be investigated in future studies using siRNA knockdown of LAT1 mRNA as demonstrated previously in HeLa cells (Nicklin et al., 2009).

BCH treatment resulted in complete or near complete suppression of cell growth in the five cell lines tested during exponential growth (Figure 5.2) with varying degrees of cell death also observed (Figure 5.3). For the three antibody-producing cell lines, titre was coupled to cell growth with specific productivity unaffected (Figure 5.4). The mechanism of growth suppression was not investigated but system L inhibition was assumed to deplete cytosolic levels of essential amino acids including leucine. Previous work has demonstrated that BCH induced depletion of intracellular leucine induces caspase-mediated apoptotic cell death in cancer cells (Kim et al., 2008). Inhibiting

leucine uptake in HeLa cells with BCH suppresses mTORC1 signaling (Nicklin et al., 2009). Removing leucine, akin to BCH treatment, suppresses mTORC1 signaling and stimulates the AAR pathway in CHO cells (Fomina-Yadlin et al., 2014). This group also demonstrated downregulation of genes involved in cell cycle progression, DNA replication, nucleotide biosynthesis, and lipid biosynthesis in response to leucine withdrawal, which could explain the responses seen in this chapter. The present results found differences in sensitivity between the cell lines in response to BCH treatment as demonstrated by a comparison of their IC_{50} values. This cannot be readily explained. Similarly, Fomina-Yadlin et al. (2014) observed variable levels of growth inhibition and cell death in five antibody-producing and parental CHO cell lines in response to leucine withdrawal.

Chapter 4 identified LAT1 as a potential marker for productivity during late-stage culture, which was hypothesised to support an increased essential amino acid demand for antibody production. Consistent with this hypothesis, specific productivity decreased in a BCH dose-dependent manner at stationary phase (Figure 5.5). Interestingly, low concentrations of BCH prolonged the viability of CAT-S cultures during late-stage culture. This cannot be readily explained, however further work to elucidate the mechanism could benefit the design of nutrient feeds for fed-batch processes where manipulating the essential amino acid composition may lead to prolonged culture viability.

5.4.2 Dependence Upon System A and ASC Transport for Cell Growth Differs Between Cell Lines

Many cancer cell lines preferentially increase their expression of ASCT2 to support the uptake of small non-essential neutral amino acids (Fuchs and Bode, 2004; Ganapathy et al., 2009). Transcriptomic data from the three cell lines examined in Chapter 4 identified high expression of SNAT2 and ASCT1 (the second system ASC transporter). ASCT2 was missing from the reference genome but has been previously identified at the genomic, transcriptomic, and proteomic level in CHO cells by several groups (Appendix Table A1), and is therefore assumed to also be present. The conditionally essential requirement for asparagine and glutamine in CHO cells suggests that activity of these transporters must be critical to exponential growth, however their relative functional contribution to this phase of culture was previously unknown.

The present results found cell lines expressing glutamine synthetase to be more sensitive to system A inhibition than the parental host (Figure 5.6). Across the cell lines

MeAIB impacted upon asparagine consumption the most, yet it failed to completely inhibit the transport of this and other classic system A amino acids (Figure 5.7 F–H), confirming the existence of additional transport processes for these substrates and explains why there was no complete suppression of cell growth. Interestingly, MeAIB minimally inhibited glutamine consumption in the parental host, even at 40 mM, a concentration at which it would completely outcompete glutamine. Collectively, these data suggest that recombinant glutamine synthetase cells are more sensitive to system A inhibition due to their increased dependence on asparagine, whereas the parental host also has access to glutamine whose primary entry route is not through system A in these cells. In support of this it has been demonstrated that asparagine and glutamine both significantly contribute to TCA cycle replenishment during exponential growth (Dean and Reddy, 2013). Recombinant GS-CHO cells grown in glutamine free media increase their consumption of asparagine (Zhang et al., 2006), limitation of which has been shown to limit GS-CHO cell growth while its removal leads to complete suppression of growth (Duarte et al., 2014). Removing asparagine has been shown to induce G1-phase cell cycle arrest in CHO cells (Fomina-Yadlin et al., 2014), whereas serine limitation has been shown to have less of a negative impact on GS-CHO cell growth (Duarte et al., 2014).

In contrast to the lack of sensitivity observed with system A inhibition, the parental host was found to be highly sensitive to system ASC inhibition (Figure 5.14). GS-Null cells were equally sensitive and T127 cells were most resistant as demonstrated by a comparison of their IC_{50} concentrations. Resistance to GPNA however did not correlate with productivity (comparison of T29, T48, and T127) but did correlate with ASCT1 mRNA levels (see Chapter 4; Table 4.1). Assessment of amino acid transport rates indicated activation of the AAR pathway in CAT-S and GS-Null cells (Figure 5.15 F–H). Removal of asparagine or glutamine from CHO cells has previously been shown to activate the AAR pathway (Fomina-Yadlin et al., 2014). The present results cannot confirm GPNA mediated AAR activation but it could be investigated in future studies by measuring expression of AAR targets. ASCT1 was significantly upregulated at stationary phase in all cell lines leading to the hypothesis that it may be required to support cell viability. However, cell death in response to GPNA was observed with GS-Null cells only suggesting this hypothesis may not hold true for all cell lines.

Upregulation of ASCT1 in T127 cells compared to the two non-producing cell lines throughout culture also lead to the suggestion that this transporter acts as a marker

for antibody production. It was hypothesised that this was to due to a high abundance of serine and threonine in the antibody. Yet, specific productivity was unaffected at both exponential and stationary growth in response to GPNA treatment in T127 cells. However, system A inhibition did cause a slight reduction in specific productivity in the two high-producers T48 and T127 (Figure 5.8), suggesting this hypothesis may still hold true. It could be that the concentration range of GPNA was not high enough in T127 cells to induce a reduction in specific productivity. In support of this, GPNA sensitive high-producing T48 cells demonstrated a decrease in titre in response to a drop in both IVCD and specific productivity (Figure 5.16).

5.4.3 The xCT Transporter Supports Cell Viability in all Cell Lines and Antibody Production During Late-Stage Culture

Cystine uptake through the xCT transporter is a prerequisite for GSH synthesis in cultured mammalian cells. In Chapter 4, the xCT transporter is reported to be significantly upregulated at stationary phase in all cell lines. It was hypothesised that this formed part of an adaptive response to support the availability of GSH and help maintain cell viability. In this chapter, SAS treatment resulted in cell death confirming that xCT transporter activity supports cell viability. Cell death was almost immediate during late-stage culture (Figure 5.13), whereas it only became substantial after 3–4 days of treatment during early-stage culture for all cell lines (Figure 5.11 A–E). Chapter 4 also identified xCT expression in T127 cells to be significantly higher than CAT-S and GS-Null cells at stationary phase. It was hypothesised that this was to help support an increased demand for cysteine in these cells for antibody production. Consistent with this hypothesis, specific productivity decreased in a SAS dose-dependent manner at stationary phase (Figure 5.13). Furthermore, specific productivity was also inhibited in a similar manner in T127 cells during exponential growth phase (Figure 5.12). The ability for T127 cells to significantly increase their expression of xCT may explain why they have an increased resistance to SAS treatment compared to the other cell lines examined during exponential growth. The high-producing T48 cell line may also have the same capability.

SAS treatment reduced cystine uptake in all cell lines as expected (Figure 5.11 F–H) but the precise mechanism of cell death was not explored. Previous groups have demonstrated that SAS depletes GSH levels and increases ROS levels (Chung et al., 2005; Timmerman et al., 2013). Chung et al. (2005) investigated growth inhibition further and found SAS induced S-phase cell cycle arrest followed by caspase-mediated

apoptotic cell death in glioma cells. Cells treated with SAS during exponential growth in this chapter followed this pattern of an initial decrease in cell proliferation and then cell death suggesting a similar mechanism is taking place. The rapid cell death observed in cells treated later in culture suggest high ROS levels at the time of SAS treatment. A shift in TCA cycle function towards oxidative phosphorylation as reported in other CHO cell lines during stationary phase (Zagari et al., 2012) could be the source of increased ROS (reviewed in Chapter 2; Section 2.1).

Despite the cellular responses to xCT inhibition being in agreement with proposed hypotheses, a major limitation of this investigation is that the SAS off-target inhibition effects on NF-κB and GSTs were not investigated. A number of methods could be used in future work to investigate this such as testing whether the response to SAS can be repeated by a second xCT inhibitor such as the cyclic glutamate analog, S-4-carboxy-phenylglycine (S-4-CPG) (Chung and Sontheimer, 2009; Patel et al., 2004), or siRNA reduction of xCT mRNA (Timmerman et al., 2013).

5.4.4 The GlyT1 Transporter Supports Antibody Production During Late-Stage Culture

Expression of the GlyT1 transporter correlated reasonably well with xCT expression in CAT-S, GS-Null, and T127 cells and was hypothesised to help support GSH synthesis (see Chapter 4). Similarly, Kyriakopoulos et al. (2013) found significant upregulation of GlyT1 expression in all cell lines at stationary phase.

The present results found ALX 5407 HCl treatment mediated some inhibition of cell proliferation in all cell lines during exponential growth with minimal cell death (Figure 5.18). As with xCT inhibition, CAT-S and GS-Null cells were more sensitive to GlyT1 inhibition during late-stage culture demonstrating significant cell death after 2 days of treatment (Figure 5.19). Specific productivity decreased in response to ALX 5407 HCl treatment in T127 cells. Interestingly, glycine is the fifth most abundant amino acid in the IgG antibody (see Chapter 4; Table 4.7). This suggests that GlyT1 transport activity may help support antibody production during late-stage culture.

5.4.5 Conclusions and Future Perspectives

Inhibitors of individual amino acid transporters (GlyT1, xCT) and transport systems (A, ASC, L) were used to evaluate how transporter function contributes to CHO culture performance parameters (growth rate, viability, and specific productivity). The results demonstrate that GlyT1, xCT, and system L transport support antibody production

during late-stage culture in T127 cells. System A and xCT transport also support specific productivity during exponential growth in these cells. Transcriptomic data suggests that LAT1 and SNAT2 are the main mediators of system L and A activity respectively. xCT transport activity is also a key determinant of culture viability throughout culture for all cell lines. Increased sensitivity to xCT inhibition was observed during late-stage culture, which correlates with a significant upregulation in expression of this transporter and decreased cystine transport, suggesting that xCT transport represents a bottleneck for all cell lines. Of noticeable difference between the cell lines is the increased dependence of recombinant glutamine synthetase cells for system A transport activity. Whereas, the parental host has an increased dependence for system ASC transport activity compared to T127 cells. A factorial experiment with T127 cells during exponential growth showed that xCT was the only transporter to have a strong significant negative effect on growth rate, viability, and specific productivity. It also revealed an interaction between xCT and system ASC transport whereby simultaneous inhibition of the latter potentiates cell death.

It should also be noted that despite the specificity of the inhibitors used in this study (Figure 5.1), it cannot conclusively be said that the effect they have on growth, viability or productivity is directly related to the inhibition of their target transporters. As discussed in Chapter 2 (see 2.4 Amino Acid Transporters in Cancer), amino acid transporters can be functionally coupled such that the activity of a single transporter can limit/control the activity of a second. Therefore, transport inhibition of one transporter or transporter system may perturb the transport activity of a second, which may also have an impact upon cell line performance parameters. More targeted experimental approaches such as siRNA knock down or gene overexpression would generate the same concerns. Consequentially, results from inhibitor studies are actually more informative about how the activity of individual transporters operating within the context of a wider system of transporters contributes to cell line productivity.

The knowledge from this chapter can help guide future cell line development (CLD) processes in a number of ways. Firstly, screening transfectant pools or clones early in CLD. Both xCT and system ASC transport act as markers of productivity. Application of SAS and GPNA can be used to rapidly enrich or select for cells with these transport capabilities (explored further in Chapter 6). Secondly, improving transport capabilities of cystine or essential amino acid transport by genetically engineering the host cell line to make it better suited for antibody production. Thirdly, improve media design (explored further in chapter 7).

Chapter 6

Evolving Resistance to Amino Acid Transport Inhibition for Improved Cell Line Performance

Both ASCT1 and xCT transporters were previously identified as potential markers of antibody production, with xCT also found to be critical in facilitating cystine influx and supporting culture viability. In this chapter, a directed evolution strategy was developed to isolate sub-populations of parental CAT-S cells and antibody-producing T127 cells resistant to GPNA and SAS transport inhibition. Evolved cell lines were hypothesised to have an increased capability for system ASC or xCT transport. Compared to the unevolved host, SAS-resistant CAT-S cells demonstrated an increased capacity for GSH synthesis, increased resistance to a ROS insult, and a heritable improvement in cell growth. However, neither SAS- or GPNA-resistant CAT-S cells could outperform the unevolved host in the transient production of a recombinant IgG. For SAS-resistant T127 cells, long-term exposure to the DMSO vehicle was found to have a negative impact upon cell growth and specific productivity. However, when this was controlled for, evolved T127 cells were capable of increased specific productivity leading to an increase in overall titres. The work in this chapter demonstrates that it is possible to isolate cell lines with desirable characteristics for biomanufacturing through manipulation of amino acid transport processes.

6.1 Introduction

As discussed in Chapter 1, production of recombinant therapeutic antibodies requires the isolation of cell lines that can stably produce high product titres with the necessary quality attributes. Because the majority of antibody synthesis is uncoupled from cell growth, the cell line must be capable of rapidly generating high cell densities that can be maintained for extended periods at high viabilities. Strategies used to maximise the potential of recombinant cell lines include improved expression vector design, optimisation of bioreactor control parameters, media optimisation, and cell engineering

approaches. Amino acid transporter proteins are unique in that they interface with both the intra- and extracellular environment such that the knowledge gained in Chapters 4 and 5 can be used to improve media design (explored further in Chapter 7) or direct cell engineering strategies.

Mammalian cell engineering strategies have traditionally involved the over-expression or silencing of individual genes involved in cellular processes including metabolism, apoptosis and protein folding to introduce desirable characteristics for biomanufacturing (strategies reviewed in Lim et al., 2010). More recently, studies have explored the potential of exploiting the inherent heterogeneity of parental cell populations as an alternative to genetic manipulations. Davies et al. (2012) created a library of 199 untransfected clones from Lonza's proprietary parental CHOK1SV cell line and demonstrated significant clone-specific variation in cell growth rates and ability to transiently express either GFP or an IgG antibody. This panel of host clones was subsequently used to help isolate cell lines that can transiently and stably outperform the transfected parental CHOK1SV host (O'Callaghan et al., 2015). Genetic instability of the CHO-K1 cell line is the primary source of such heterogeneity in parental populations. Early karyotype studies demonstrated the existence of large-scale deletions and rearrangements of chromosomes between different CHO cell lines (reviewed in Wurm and Hacker, 2011), while recent genome sequencing projects has provided a deeper analysis of genetic instability detailing missing genes, single-nucleotide polymorphisms (SNPs), short insertions and deletions, as well as gene copy number variations (CNVs) between industrial CHO cell lines (Lewis et al., 2013; Xu et al., 2011). In addition to genetic alterations, DNA methylation has also been found to be a strong contributor to production instability in CHO cell populations resulting in gene silencing without loss of the gene itself (Kim et al., 2011; Yang et al., 2010b). Directed evolution of CHO cell lines (and any other genetically instable mammalian cell line) represents a method of exploiting genetic diversity to isolate sub-populations of cells with desirable phenotypic characteristics for biomanufacturing from a heterogeneous background. In this approach a selective pressure(s) is applied and resistant cells are selected. The process is typically repeated over many rounds until a stable population of cells with the required phenotype is obtained. Matsumura et al. (1991) demonstrated that by subjecting an antibody-producing hybridoma cell line to gradual increases in ammonia concentrations a sub-population of cells resistant to this stress could be isolated. Similarly, a human promyelocytic HL-60 cell line resistant to inhibitory levels of lactate and ammonia was isolated from a sensitive parental population (Schumpp and

Schlaeger, 1992). The resistant cells were capable of an extended stationary phase compared to non-resistant cells. Prentice et al. (2007) described a method of "bioreactor evolution" in which a parental and recombinant CHO cell line was adapted to the environmental conditions of decline phase in a fed-batch process. The evolved parental host cells attained a 2-fold increase in peak viable cell density, while the evolved recombinant cell line attained a ~40% increase in peak viable cell density resulting in a ~40% gain in final titre in fed-batch cultures over the respective non-evolved cells. Directed evolution has also been used to adapt CHO cells to growth in glutamine free media (Bort et al., 2010; Taschwer et al., 2012). For an untransfected parental host, the glutamine-free adapted cells exhibited increased consumption of aspartate, asparagine, and glutamate (Bort et al., 2010). These latter studies demonstrate that directed evolution is a useful alternative to genetic manipulations for metabolic engineering strategies.

The above evolution studies demonstrate that modifying the environmental conditions of CHO and other mammalian cell lines can successfully result in the isolation of sub-populations with improved manufacturing properties. This chapter examines the utility of directed evolution as a method of manipulating CHO amino acid transport processes with the aim to isolate cells with improved cell line manufacturing characteristics. In this chapter, inhibitors of amino acid transport from Chapter 5 (SAS and GPNA) are used as selective agents to isolate sub-populations of the parental CAT-S host and T127 non-clonal IgG expressing cell line resistant to the effects of these compounds with the hypothesis that these resistant cells will have an increased capability for system xCT or ASC transport. In Chapters 4 and 5, the cystine-glutamate xCT antiporter was identified as a key determinant of culture viability in all cell lines, particularly during stationary phase. This correlated with a significant upregulation of xCT expression for all cells at this point in culture. Transcriptomic data indicates that this forms part of an adaptive response to support the availability of GSH by ensuring the cell has a sufficient supply of cystine. Furthermore, xCT expression in antibody-producing T127 cells is significantly higher than the parental CAT-S host and the GS-Null cell line, indicating that cystine import through the xCT transporter may also be required to support antibody production. Inhibitor data supports this hypothesis with T127 cells demonstrating a SAS dose-dependent decrease in specific productivity at exponential and stationary phase. Engineering the cell to have increased xCT transport functionality may therefore enhance culture longevity and boost specific productivity. This chapter first describes a direction evolution method that uses SAS as a selective

pressure to isolate a resistant sub-population of cells from the parental CAT-S host. These cells were then characterised by examining their growth, capacity for GSH synthesis and ability to transiently produce a recombinant IgG antibody. This adaptation method was also applied to the antibody-producing T127 cell line to investigate if evolving further resistance to SAS could further improve productivity. Finally, this chapter also explores if an increased capability for system ASC transport can support antibody synthesis as hypothesised in Chapter 4. This was investigated by repeating the evolution process with the parental CAT-S but with GPNA as the selective pressure. The growth and capacity of these cells to transiently produce a recombinant IgG antibody was also assessed.

6.2 Materials and Methods

6.2.1 Transient Transfection

6.2.1.1 Expression Vectors

The mAb-109 vector containing genes for both the heavy and light chains of a human IgG monoclonal antibody was kindly provided by MedImmune. A vector encoding GFP (phCMV C-GFP; Genlantis, San Diego, USA) was used to assess transfection efficiency.

6.2.1.2 Lipofection

Prior to transfection cells were sub-cultured at 5 x 10^5 cells.mL^{-1} in 100 mL of CD-CHO medium supplemented with 8 mM L-glutamine (Life Technologies, Paisley, UK) in 500 mL vented Erlenmeyer flasks (Corning, Surrey, UK) for 24 hr until they reached 1 x 10^6 cells.mL^{-1}. Culture aliquots of 10 mL were then transferred to 50 mL vented TubeSpin® Bioreactors (TPP, Trasadingen, Switzerland). Cells were transfected using Lipofectamine® LTX with Plus™ Reagent (Life Technologies). For each transfection 12 μg of DNA was incubated with 24 μL of Lipofectamine® LTX Reagent and 12 μL of PLUS™ Reagent for 5 min at room temperature. Both DNA and Lipofectamine® LTX Reagent were diluted in Opti-MEM® I Reduced Serum Medium (Life Technologies) prior to incubation. The DNA-Lipid complex was then added to cultures and incubated at 37^{o}C in 5% CO_2 air shaking at 170 rpm (Infors UK, Reigate, UK). Cultures were maintained by feeding 10% of the initial culture volume of CHO CD EfficientFeed™ A and B (1:1 ratio) (Life Technologies) at 48 and 96 hr post-transfection.

6.2.2 Flow Cytometry

The Attune Autosampler® flow cytometer (Life Technologies) was used to measure GFP expression for transfection efficiency investigations. Cell events were plotted by measurements of both side-scatter (SSC; marker of granularity) and forward-scatter (FSC; marker of cell size) (Figure 6.1).

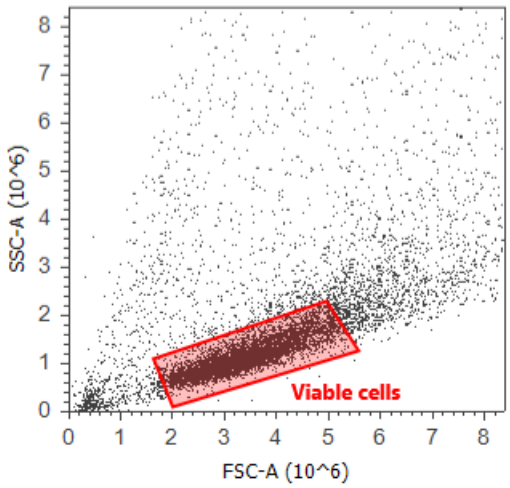

Figure 6.1 Gated population of viable cells. 10, 000 viable cells were used to measure GFP expression in all experiments.

The population of viable cells was gated and a daughter plot was generated to assess GFP expression. GFP was excited using a 488 nm laser passing through a 530/30 centre/bandpass filter (BL1). Non-transfected control cells were used to detect autofluorescence and gate the daughter plot for GFP expression (Figure 6.2). A sample of 10, 000 viable cells were used to measure GFP expression in all experiments. Data was analysed using Attune® Cytometric Software v2.1 (Life Technologies).

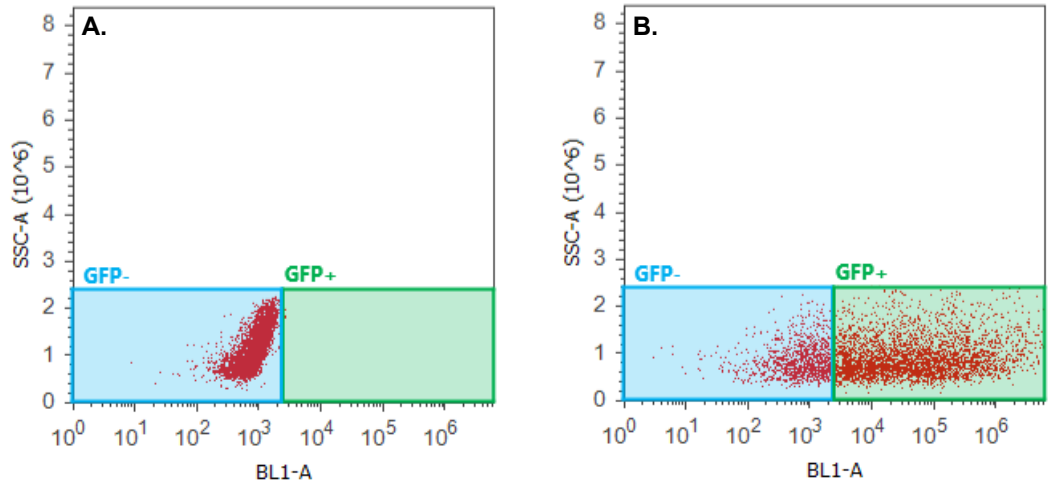

Figure 6.2 Example daughter plot for GFP expression. (**A.**) Non-transfected cells were used to detect autofluorescence (GFP-) and gate the daughter plot. (**B.**) Detection of GFP (GFP+) expression in transfected cells.

6.2.3 Cellular Glutathione Quantification

Samples of 3 x 10^6 cells were centrifuged at 200g for 5 min, washed once in PBS and recentrifuged. Cells were diluted in fresh PBS and triplicate 10, 000 cells were dispensed per well in 96-well plates. Intracellular GSH levels were then measured using a GSH-Glo™ Glutathione Assay kit (Promega, Southampton, UK). Luminescence was read using a Fluoroskan Ascent™ FL (Thermo Scientific, Loughborough, UK). TCEP (tris(2-carboxyethyl)phosphine hydrochloride) solution (Sigma-Aldrich, Dorset, UK) was used to reduced oxidised GSH (GSSG) and measure total intracellular GSH levels. Cells were preincubated in a final concentration of 1 mM TCEP for 30 min at room temperature before proceeding with the GSH-Glo™ Glutathione Assay.

6.2.4 Inhibitor Treatment

Cells were treated following the method described previously (see Chapter 5; Section 5.2.1). Hydrogen peroxide (Sigma-Aldrich) was diluted in CD-CHO medium (Life Technologies).

6.2.5 Batch Overgrow Shake Flask Cultures

Cells were seeded at 3 x 10^5 cells.mL^{-1} in 35 mL of CD-CHO medium (Life Technologies) in 125 mL vented Erlenmeyer flasks (Corning) shaking at 140 rpm in 37^{o}C and 5% CO_2 air (Infors UK). CAT-S cells and evolved sub-populations were

supplemented with 8 mM L-glutamine (Life Technologies). T127 cells and evolved sub-populations were supplemented with 50 μM L-methionine sulfoximine (Sigma-Aldrich) and grown in a humidified incubator.

6.2.6 Fed-Batch Overgrow Shake Flask Cultures

Cells were seeded at 3 x 10^5 cells.mL^{-1} in 35 mL of CD-CHO medium (Life Technologies) in 125 mL vented Erlenmeyer flasks (Corning) shaking at 140 rpm at 37^{o}C in 5% CO_2 air (Infors UK). Cultures were supplemented with 8 mM glutamine at day 0 and then maintained by feeding 10% of the initial culture volume of CHO CD EfficientFeed™ A and B (1:1 ratio) (Life Technologies) every 72 hr from day 3 onwards.

6.3 Results

6.3.1 Creation of a SAS-Resistant CAT-S Cell Line (CAT-R-S700)

A sub-population of cells resistant to SAS mediated inhibition of the xCT transporter was isolated from the parental CAT-S host over an eight-week period (CAT-R-S700; Figure 6.3 A). A vehicle control cell line (CAT-CTRL) was created in parallel by sub-culturing the parental host over the same time period with 0.2% DMSO v/v CD-CHO medium. SAS resistance was initiated by sub-culturing the parental host every 3–4 days with CD-CHO medium supplemented with 500 μM SAS. After 10 generations the viability of SAS treated cultures recovered to >90% (data not shown) and the SAS concentration was increased to 700 μM. Following a further 20 generations the growth rate of SAS treated cultures was comparable to equivalently aged CAT-CTRL cells over 3–4 day sub-culturing periods. Yet, routine batch overgrows during sub-culturing demonstrated that maximal cell densities and culture viabilities were still significantly reduced in SAS treated cultures at day 6 (data not shown). After 50 generations growth had completely recovered and the CAT-R-S700 cell line was established. The CAT-R-S700 cell line was characterised by performing a SAS dose-response study during exponential growth and comparing it to the curve generated for the parental host in Chapter 5 (Figure 6.3 B–C). The IC_{50} SAS concentration for the parental host was previously determined as 790 μM. However, SAS treatment had no effect on cell proliferation and culture viability in CAT-R-S700 cells at all concentrations tested.

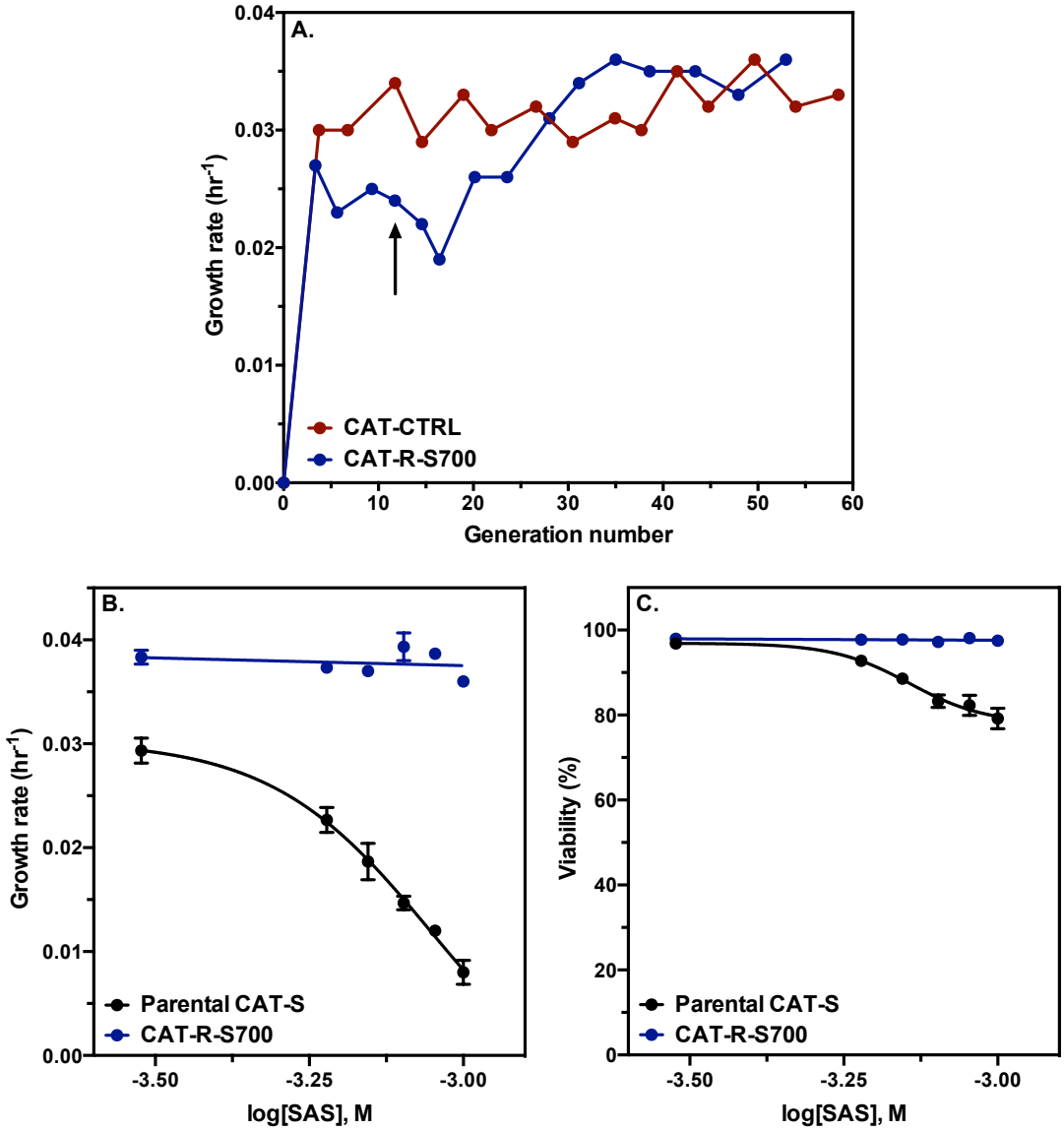

Figure 6.3 Creation of a SAS-resistant CAT-S cell line. (**A.**) Parental CAT-S host cells were initially treated with 500 μM SAS that was increased to 700 μM SAS as indicated by the arrow (CAT-R-S700; blue line). A vehicle control cell line was created in parallel by sub-culturing the host with 0.2% DMSO v/v CD-CHO medium (CAT-CTRL; red line). (**B. – C.**) Parental (black) and CAT-R-S700 (blue) cells were treated for 3 days with SAS. The specific growth rate (hr^{-1}) was calculated and culture viability was measured on day 3 of treatment. Data is shown as the mean ± SEM of three independently performed experiments.

6.3.1.1 Growth Profile of the CAT-R-S700 Cell Line

A comparison of the CAT-R-S700 and parental CAT-S dose-response curves demonstrates that the former has a higher specific rate of cell proliferation at a non-

inhibitory SAS concentration (300 μM) over 3 days (Figure 6.3 B–C). The growth performance of the parental and CAT-R-S700 cell lines was explored further in batch and fed-batch overgrow shake flask cultures (Figure 6.4). Batch growth profiles for both cell lines grown under control conditions (0% DMSO v/v CD-CHO medium with 0 μM SAS) found CAT-R-S700 cells to exhibit a 15% and 40% increase in average specific proliferation rate and cumulative IVCD respectively. The CAT-R-S700 cell line also demonstrated enhanced cell growth over the parental host in fed-batch cultures. However, it has previously been shown that CHO cells will typically increase their proliferation rate over extended sub-culturing regimes (Davies et al., 2012). To confirm that the improved ability of CAT-R-S700 cells to accumulate biomass is a consequence of SAS resistance rather than an artifact of the evolution method the growth profile of the CAT-CTRL cell line was also assessed. CAT-CTRL cells exhibited an equivalent growth profile to the parental host and remained sensitive to SAS treatment in batch culture. It is therefore concluded that the improved growth properties of CAT-R-S700 cells is due to an evolved resistance to the inhibitory effect of SAS rather than a consequence of an extended sub-culturing regime or long-term DMSO vehicle exposure. Distinct from the improved performance observed during early culture, the CAT-R-S700 cell line was found to perform poorly late in culture compared to the parental host. It exhibited a shorter stationary phase and a higher magnitude of cell death during the decline phase, which was more noticeable in fed-batch overgrow cultures. For batch cultures this is expected to be a consequence of nutrient depletion and a build-up of waste products (e.g. ammonia and lactate). In fed-batch cultures, it is expected that re-optimisation of the feeding regime would lead to an improved performance for CAT-R-S700 cells.

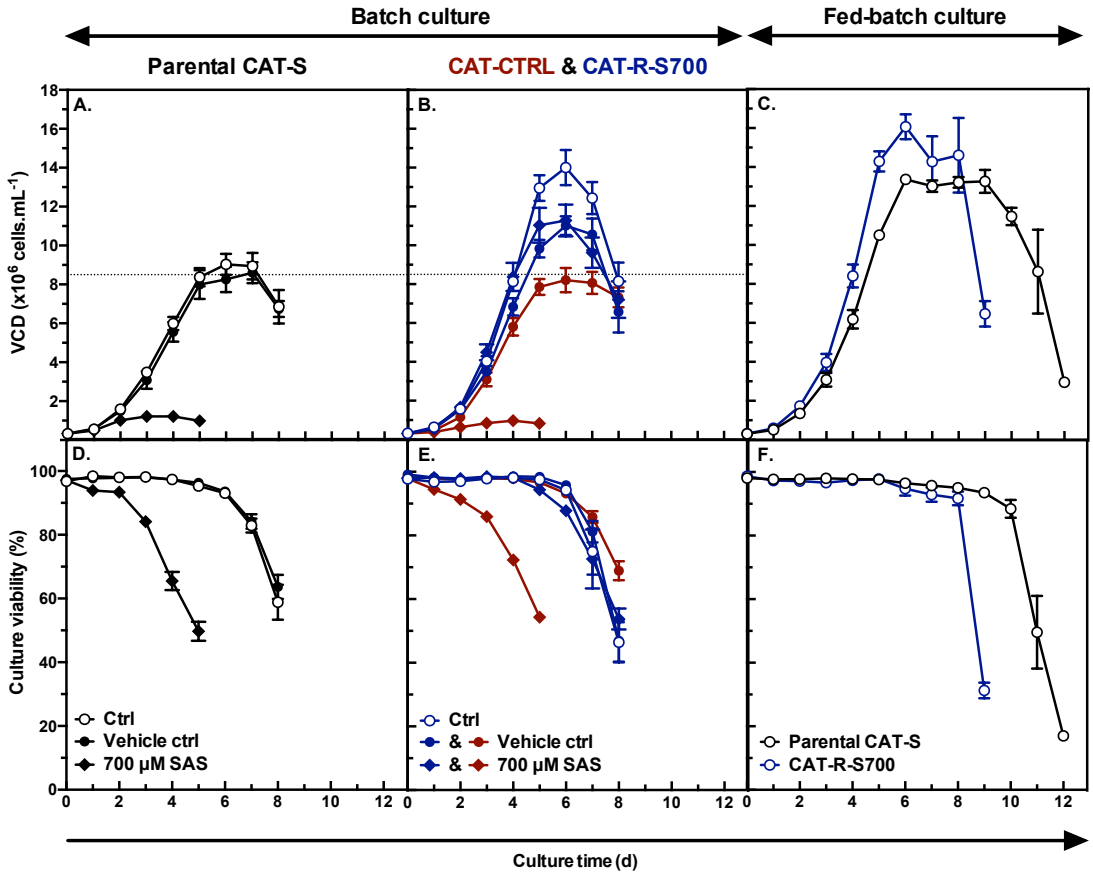

Cell line	Average µ (d^{-1})	IVCD (10^6 cells.hr.mL^{-1})
Batch		
Parental CAT-S	0.55 ± 0.01	996 ± 39
CAT-R-S700	0.62 ± 0.01	1362 ± 36
Fed-batch		
Parental CAT-S	0.65 ± 0.01	1310 ± 10
CAT-R-S700	0.67 ± 0.02	1596 ± 44

Figure 6.4 Batch and fed-batch culture growth curves for parental, CAT-CTRL and CAT-R-S700 cells. (**A. – C.**) Viable cell density (VCD). (**D. – F.**) Culture viability. Open circles are control cultures (0% DMSO v/v CD-CHO medium), closed circles are vehicle control cultures (0.2% DMSO v/v CD-CHO medium), and closed squares are cultures treated with 700 µM SAS at seeding. Black, red and blue lines are parental, CAT-CTRL, and CAT-R-S700 cell lines respectively. Table insert compares average µ calculated over 0–6 days and cumulative IVCD over 8 days for batch and fed-batch control cultures. Data is shown as the mean ± SEM of four independently performed experiments.

6.3.1.2 Intracellular Glutathione Content and Cell Line Responses to Reactive Oxygen Species Exposure

It is hypothesised that resistance to SAS is mediated by increased expression of the xCT transporter. This should provide CAT-R-S700 cells with an improved ability for cystine import and GSH synthesis. Cystine transport rates were not measured but the intracellular concentration of reduced (GSH) and oxidised glutathione (GSSG) was measured in both the parental and CAT-R-S700 cell lines at day 3 of exponential growth in batch cultures (Figure 6.5 A). Total glutathione (GSH and GSSG) is 40% higher in the CAT-R-S700 cell line indicating a higher rate of GSH synthesis for these cells. Furthermore, the parental host had a lower ratio of GSH:GSSG than the CAT-R-S700 cell line (0.62 ± 0.04 versus 1.02 ± 0.27; mean ± SEM, n = 4) suggesting increased levels of oxidative stress in the parental host. Unexpectedly, neither GSH nor GSSG was detected in the CAT-R-S700 cell line at stationary phase (day 6) of batch cultures. This could however be due to a depletion of nutrients resulting from the improved growth rate. GSSG was detected in the parental host but this was considerably reduced compared to exponential growth measurements and extremely variable between experiments (41.0 ± 33.7 $x10^{-5}$ $pg.\mu m^{-3}$ cell volume; mean ± SEM, n = 3). To assess if increased GSH synthesis in CAT-R-S700 cells offers a protective effect against reactive oxygen species (ROS) both cell lines were exposed to H_2O_2 during exponential growth (Figure 6.5 B–C). CAT-R-S700 cells were found to be more resistant to ROS exposure than the parental host as demonstrated by a comparison of their IC_{50} H_2O_2 concentrations (450 versus 278 μM H_2O_2 for CAT-R-S700 and parental cells respectively; Figure 6.5 B). Collectively, these data reveal that evolved resistance to SAS treatment has increased rates of GSH synthesis, which provides protection from oxidative stress.

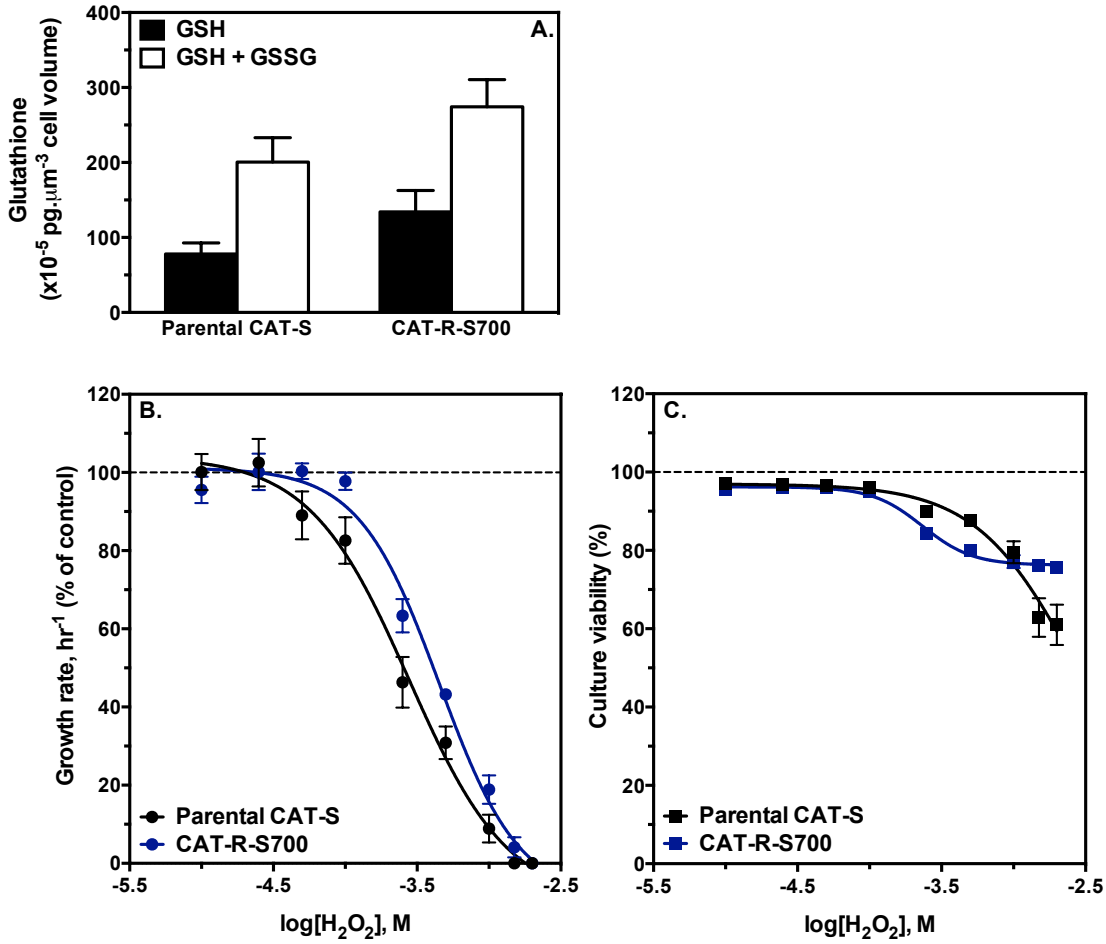

Figure 6.5 Glutathione content and effect of H_2O_2 treatment on parental and CAT-R-S700 cells during exponential growth phase. (**A.**) Glutathione content was measured on day 3 of batch cultures and normalised by cell volume. Black bars are reduced glutathione (GSH) and white bars are total glutathione (reduced and oxidised glutathione; GSH and GSSG). Data is shown as the mean + SEM of four independently performed experiments. (**B. – C.**) Parental (black) and CAT-R-S700 (blue) cells were treated for 2 days with H_2O_2. The specific growth rate (hr^{-1}) was calculated and normalised to control cultures (0 mM H_2O_2). Culture viability was measured on day 2 of H_2O_2 treatment with all control cultures having viabilities >95%. Data is shown as the mean ± SEM of four independently performed experiments.

6.3.1.3 Heritability of the CAT-R-S700 Phenotype

The CAT-R-S700 cell line was next grown for over 100 generations under control conditions (0% DMSO v/v CD-CHO medium with 0 µM SAS) to examine if it could retain its enhanced growth performance during extended sub-culture without the 700 µM SAS selective pressure (Figure 6.6). After every 17 generations 8-day batch

overgrow shake flask cultures were performed to assess growth rate, cumulative IVCD, and culture viability under non-treated and SAS-treated conditions. The improved ability of the CAT-R-S700 cell line to accumulate biomass was retained over 100 generations in non-treated cultures. However, after 50 generations SAS treatment began to inhibit both cell proliferation and maximum attainable viable cell densities indicating that SAS resistance was gradually being lost.

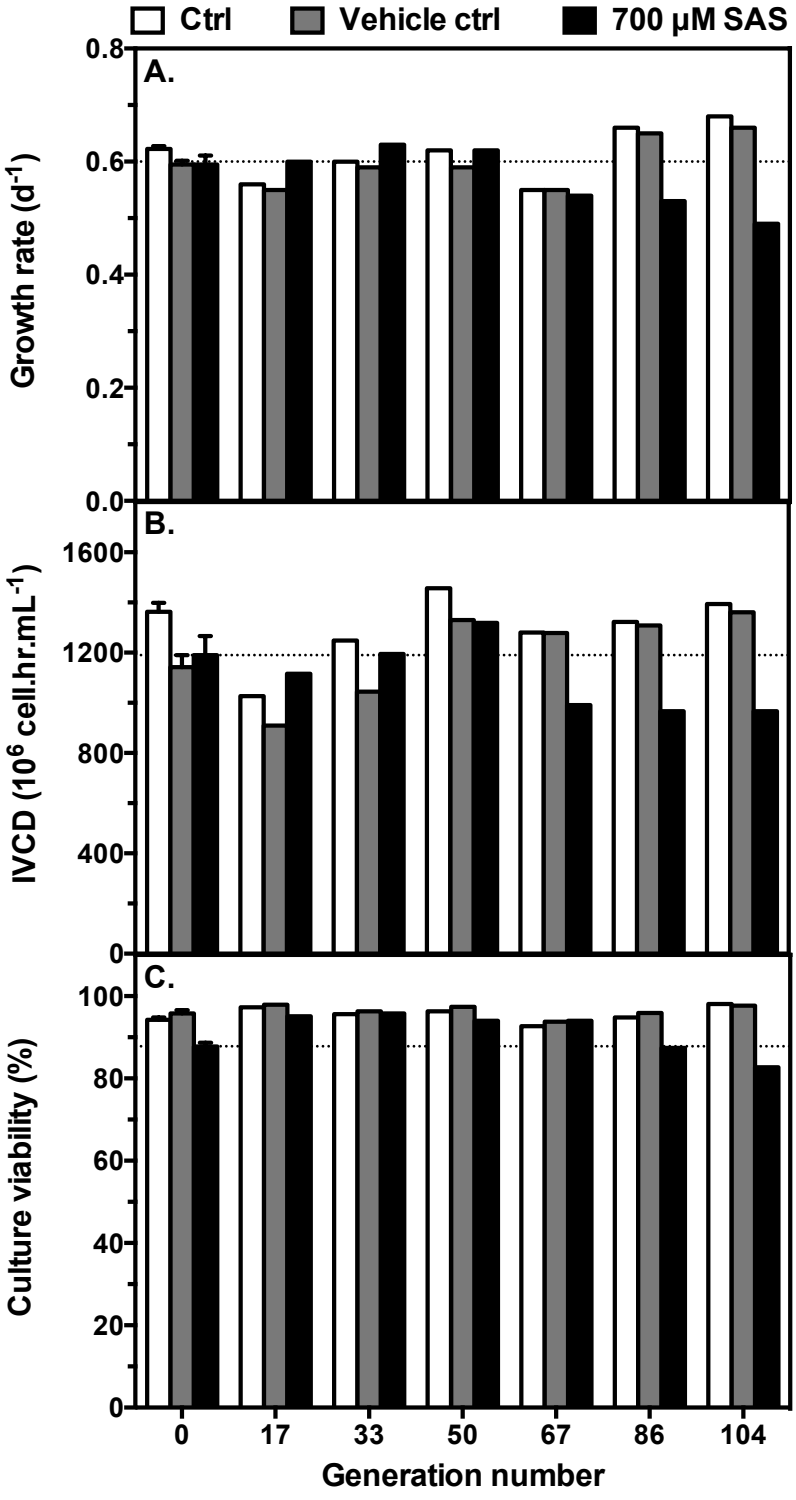

Figure 6.6 Heritability of the CAT-R-S700 phenotype. The CAT-R-S700 cell line was sub-cultured for over 100 generations without the 700 μM SAS selective pressure. Batch growth curves were performed at approximately every 17 generations. White bars are control cultures (0% DMSO v/v CD-CHO medium), grey bars are vehicle control cultures (0.2% DMSO v/v CD-CHO medium) and black bars are cultures treated with 700 μM SAS at seeding. (**A.**) Average μ calculated over 0–6 days. (**B.**) Cumulative IVCD over 8 days. (**C.**) Culture viability on day 6. Data at generation 0 is shown as the mean + SEM of four independently performed experiments.

6.3.2 Creation of a GPNA-Resistant CAT-S Cell Line (CAT-R-G200)

In Chapter 4, it is reported that ASCT1 is significantly upregulated in antibody-producing T127 cells at both growth phases of culture compared to CAT-S and GS-Null cells (see Chapter 4; Section 4.3.3). It was hypothesised that ASCT1 may be upregulated to support serine and threonine consumption for antibody synthesis. Yet, inhibition of system ASC with GPNA inhibited specific productivity in antibody-producing T48 cells but not T127 cells (see Chapter 5; Section 5.3.4). Evolving resistance to GPNA treatment in the CAT-S host and examining its ability to transiently produce an antibody was therefore performed to further investigate the role of system ASC transport and antibody production.

A sub-population of cells with increased resistance to GPNA mediated inhibition of system ASC transport was isolated from the parental CAT-S host over a ten-week period (CAT-R-G200; Figure 6.7 A). As before, a vehicle control cell line (CAT-CTRL) was created in parallel by sub-culturing the parental host over the same time period with 0.2% DMSO v/v CD-CHO medium. GPNA resistance was initiated by sub-culturing the parental host every 4 days with CD-CHO medium supplemented with 50 μM GPNA. After 30 generations the growth rate of GPNA treated cultures was comparable to equivalently aged CAT-CTRL cells over 4 day sub-culturing periods and the GPNA concentration was then increased to 200 μM. Growth deteriorated over the subsequent 10 generations before gradually recovering. After 70 generations growth had completely recovered and the CAT-R-G200 cell line was established. The CAT-R-G200 cell line was characterised by performing a GPNA dose-response study during exponential growth and comparing it to the curve generated for the parental host in Chapter 5 (Figure 6.7 B–C). The CAT-R-G200 cell line was less sensitive to GPNA treatment than the parental host as demonstrated by a comparison of their IC_{50} GPNA

concentrations (1.3 mM versus 0.2 mM GPNA; Figure 6.7 B). However, this was still considerably lower than the antibody-producing T127 cell line (IC_{50} = 3.1 mM; see Chapter 5, Figure 5.14). These data therefore confirm that the CAT-R-G200 cell line has evolved a degree of resistance to the inhibitory effect of GPNA but with a longer period of evolution it should be possible to isolate a sub-population with improved resistance.

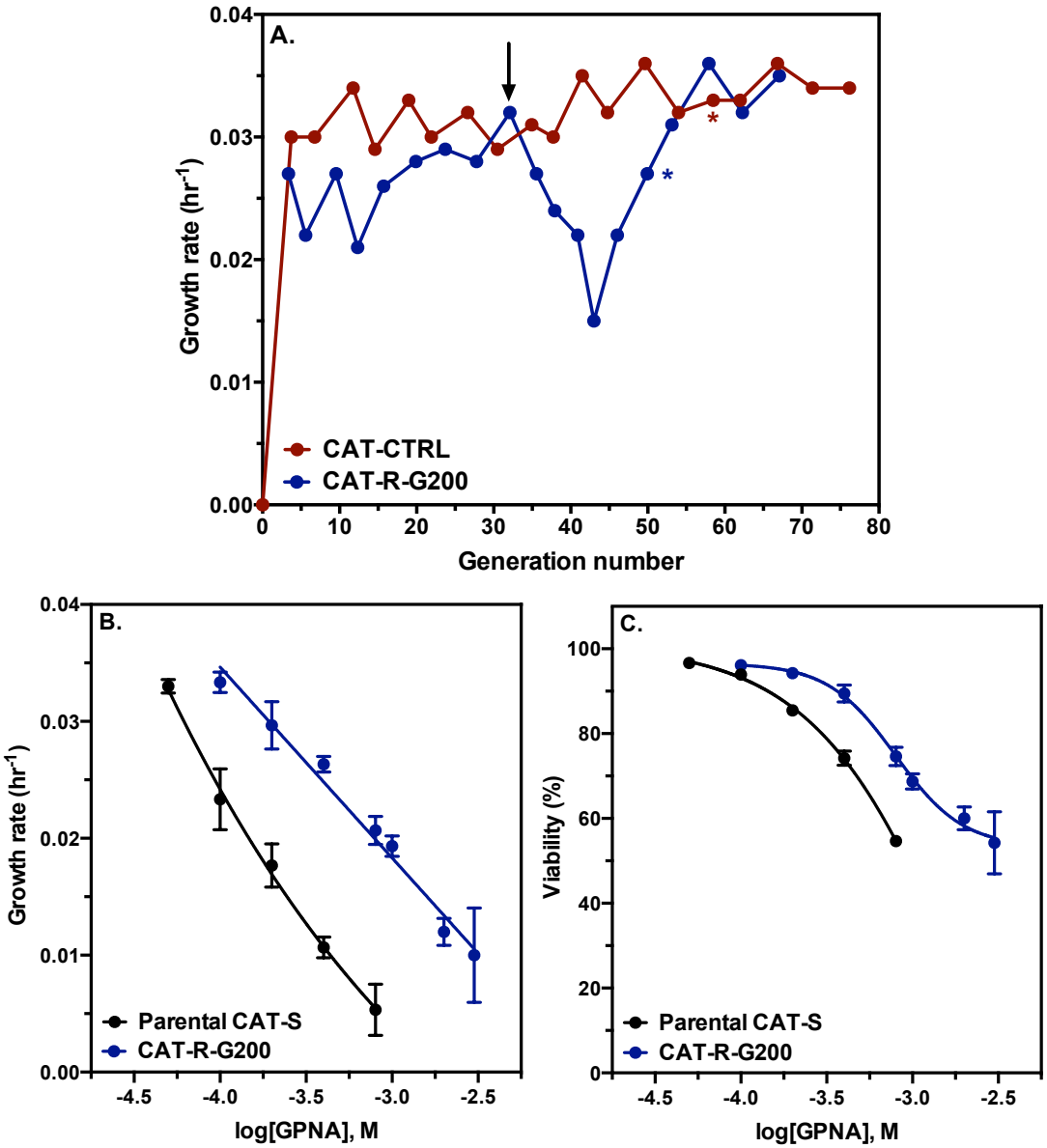

Figure 6.7 Creation of the GPNA-resistant CAT-S cell line. (**A.**) Parental CAT-S host cells were initially treated with 50 μM GPNA that was increased to 200 μM GPNA as indicated by the arrow (CAT-R-G200; blue line). A vehicle control (0.2% DMSO v/v CD-CHO medium) cell line (CAT-CTRL; red line) was also created. An asterisk indicates a freeze/thaw event. (**B. – C.**) Parental (black line) and CAT-R-G200 (blue

line) cells were treated for 3 days with GPNA. The specific growth rate (hr^{-1}) was calculated and culture viability was measured on day 3 of treatment. Data is shown as the mean ± SEM of three independently performed experiments.

6.3.2.1 Growth Profile of the CAT-R-G200 Cell Line

The growth performance of the CAT-R-G200 cell line was explored further in batch and fed-batch overgrow shake flask cultures (Figure 6.8). Growth profiles of the parental and CAT-R-G200 cell lines grown under control conditions (0% DMSO v/v CD-CHO medium with 0 μM GPNA) in batch culture were identical. However, the CAT-R-G200 cell line demonstrated an enhanced ability to accumulate biomass in fed-batch cultures, exhibiting a 9% and 20% increase in average specific proliferation rate and cumulative IVCD respectively. CAT-CTRL cells remained sensitive to GPNA treatment in batch cultures confirming that an extended sub-culturing regime or long-term DMSO vehicle exposure is not the cause of GPNA resistance in the CAT-R-G200 cell line.

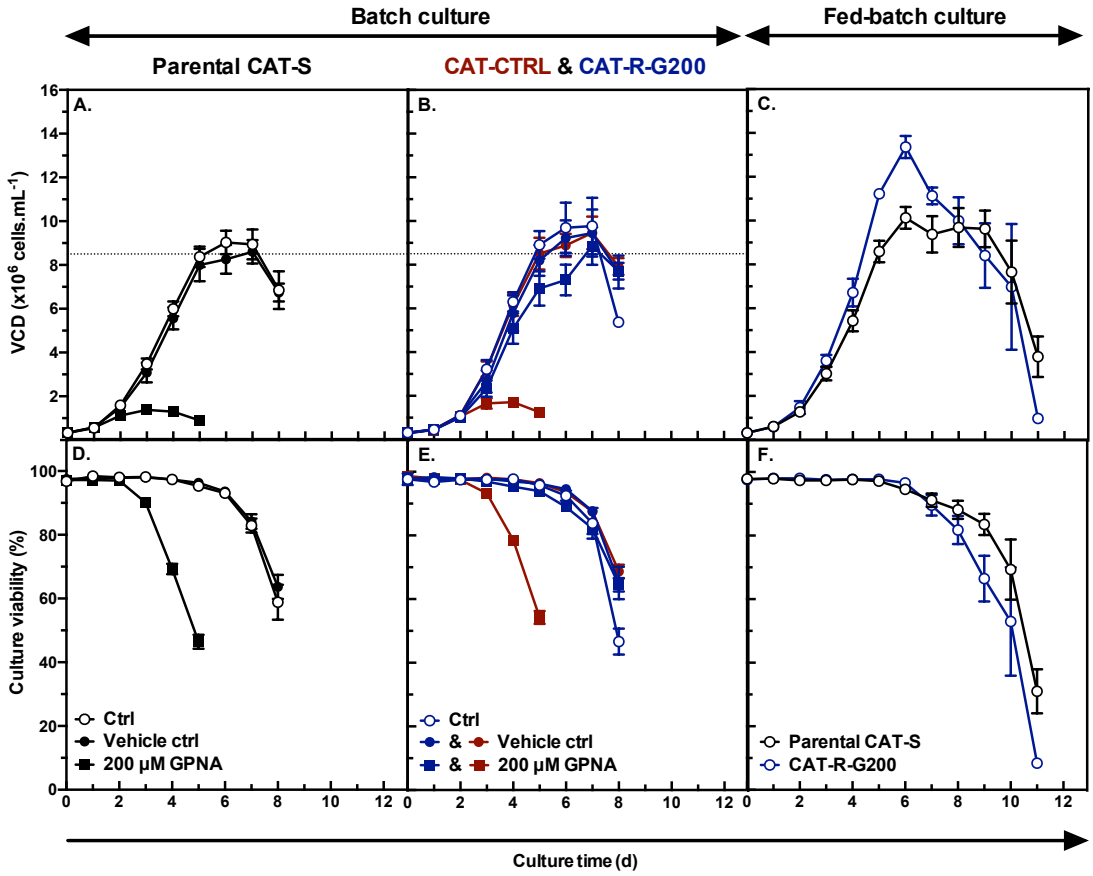

Cell line	Average µ (d^{-1})	IVCD (10^6 cells.hr.mL^{-1})
Batch		
Parental CAT-S	0.55 ± 0.01	996 ± 39
CAT-R-G200	0.57 ± 0.01	988 ± 56
Fed-batch		
Parental CAT-S	0.57 ± 0.00	1041 ± 77
CAT-R-G200	0.62 ± 0.01	1270 ± 60

Figure 6.8 Batch and fed-batch culture growth curves for parental, CAT-CTRL and CAT-R-G200 cells. (**A. – C.**) Viable cell density (VCD). (**D. – F.**) Culture viability. Open circles are control cultures (0% DMSO v/v CD-CHO medium), closed circles are vehicle control cultures (0.2% DMSO v/v CD-CHO medium), and closed squares are cultures treated with 200 µM GPNA at seeding. Black, red, and blue lines are parental, CAT-CTRL, and CAT-R-G200 cell lines respectively. Table insert compares average µ calculated over 0–6 days and cumulative IVCD over 8 days for batch and fed-batch control cultures. Data is shown as the mean ± SEM of four independently performed experiments (except the CAT-R-G200 control batch culture data, which is shown as the mean ± SEM of three independently performed experiments).

6.3.2.2 Heritability of the CAT-R-G200 Phenotype

The heritability of the CAT-R-G200 phenotype was examined by sub-culturing the cell line over 28 generations without the 200 μM GPNA selective pressure (Figure 6.9). 8-day batch overgrow shake flask cultures were performed to assess growth rate, cumulative IVCD and culture viability under non-treated and GPNA-treated conditions after 20 and 28 generations. Resistance to GPNA treatment had declined within 20 generations but was not completely lost. These data indicate that GPNA resistance is unstable in the evolved cell line.

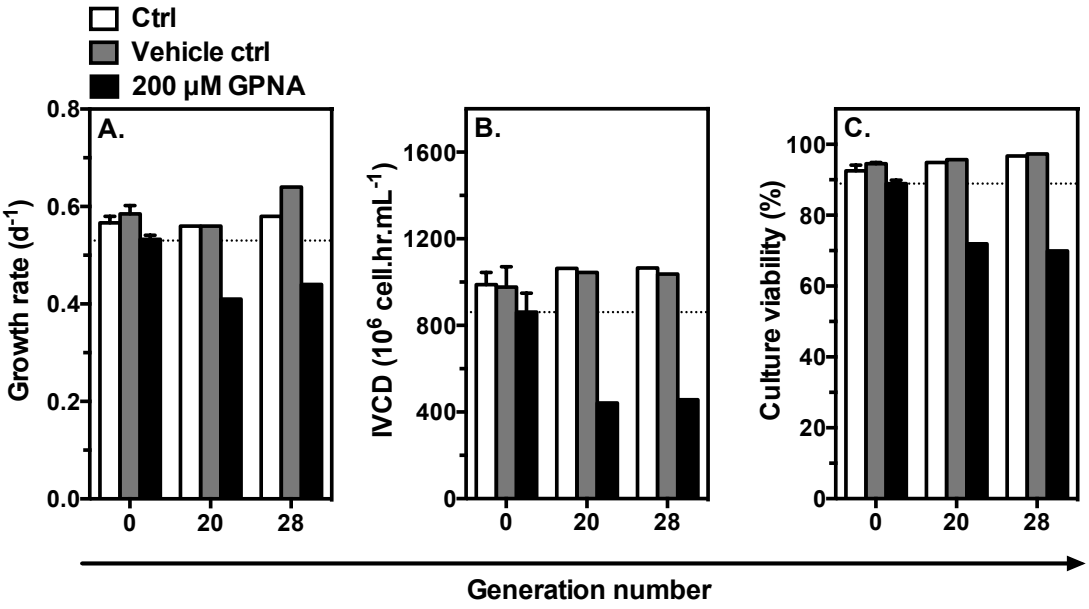

Figure 6.9 Heritability of the CAT-R-G200 phenotype. The CAT-R-G200 cell line was sub-cultured for 28 generations without the 200 μM GPNA selective pressure. Batch growth curves were performed after 20 and 28 generations. White bars are control cultures (0% DMSO v/v CD-CHO medium), grey bars are vehicle control cultures (0.2% DMSO v/v CD-CHO medium) and black bars are cultures treated with 200 μM GPNA at seeding. (**A.**) Average μ calculated over 0–6 days. (**B.**) Cumulative IVCD over 8 days. (**C.**) Culture viability on day 6. Data at generation 0 is shown as the mean + SEM of four independently performed experiments (except the control batch culture data, which is shown as the mean + SEM of three independently performed experiments).

6.3.3 Transfection Efficiency and Transient Production of a Recombinant IgG Antibody in Parental and Resistant Cell Lines

The evolved cell lines were examined to see if they have an improved ability to produce a recombinant IgG antibody. 12 μg of a vector containing genes for both the heavy and light chains of a human IgG monoclonal antibody was transfected by lipofection into the parental, CAT-R-G200 and CAT-R-S700 cell lines. For each transfection cell growth and viability was assessed at 48, 72, and 96 hr post-transfection (Figure 6.10 A–F). Transfection efficiency was also determined for each cell line at the same time points by performing an additional transfection with 12 μg of a GFP vector (see 6.2 Materials and Methods; Figure 6.10 G–I). The effect of DNA transfection on cell growth and viability was equivalent between GFP and antibody transfections for each cell line at all time points (Figure 6.10 A–F; comparison of green and black bars). Growth and viability was inhibited to the same degree in transfected parental and CAT-R-G200 cells but the CAT-R-S700 cell line was noticeably more resistant to transfection conditions. This observation was reflected in measurements of transfection efficiency which was approximately 80% in the parental and CAT-R-G200 cell lines at all time points but 60% in CAT-R-S700 cells at 48 hr post-transfection decreasing to 50% after 96 hr (Figure 6.10 G–I). Collectively, these data indicate that evolved resistance to SAS treatment has made this cell line more resistant to DNA:lipid complex based transfections.

Measurement of antibody production demonstrated no differences in titre or specific productivity between the parental and CAT-R-G200 cell lines at all time points post-transfection (Figure 6.11). However, the CAT-R-S700 cell line was markedly poor at antibody production compared to the parental host.

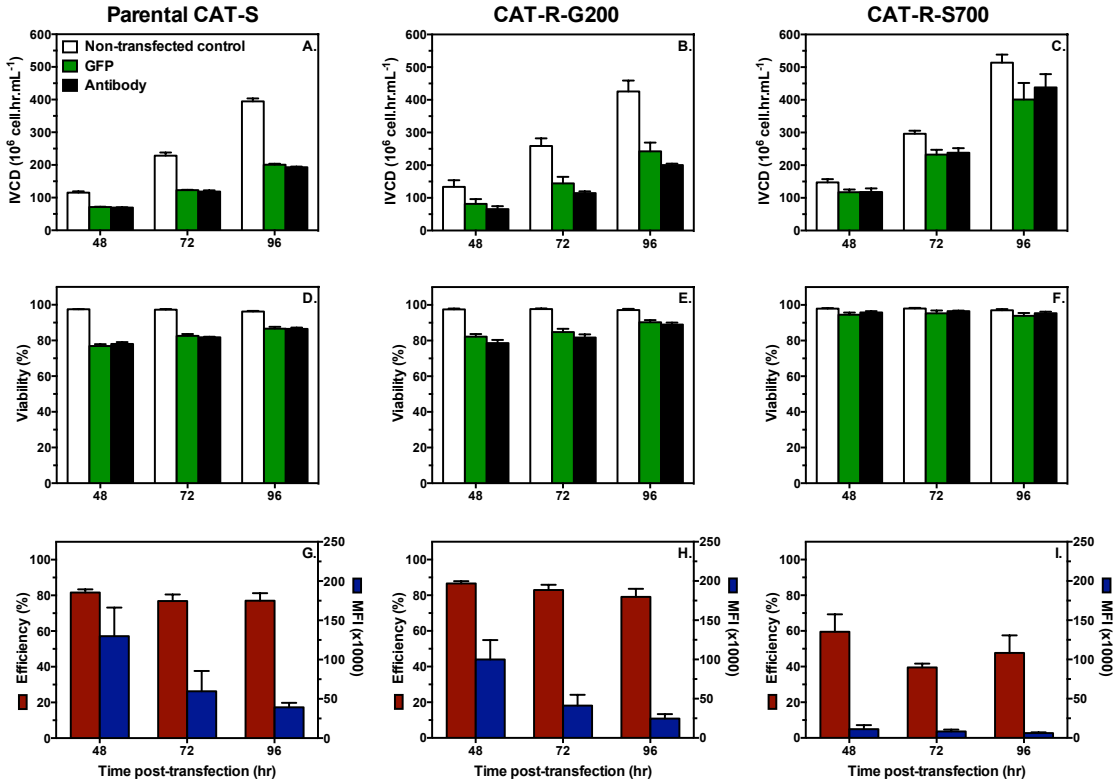

Figure 6.10 Growth characteristics of parental and resistant CAT-S cells transiently expressing GFP and an IgG monoclonal antibody. Each cell line was transfected with either the phCMV C-GFP vector (green bars) or mAb-109 vector (black bars) by lipofection. Cumulative IVCD (**A. – C.**) and culture viability (**D. – F.**) was compared within cell lines at 48, 72 and 96 hr post-transfection. Non-transfected cells (white bars) were performed as a control. Transfection efficiency and median fluorescence intensity (MFI) of GFP transfections was also assessed over the same time points (**G. – I.**). Non-transfected and GFP data shown is the mean + SEM of three independent experiments. Antibody data shown is the mean + SEM of two independent experiments, where in a single experiment antibody transfections were performed in duplicate and measurements were averaged.

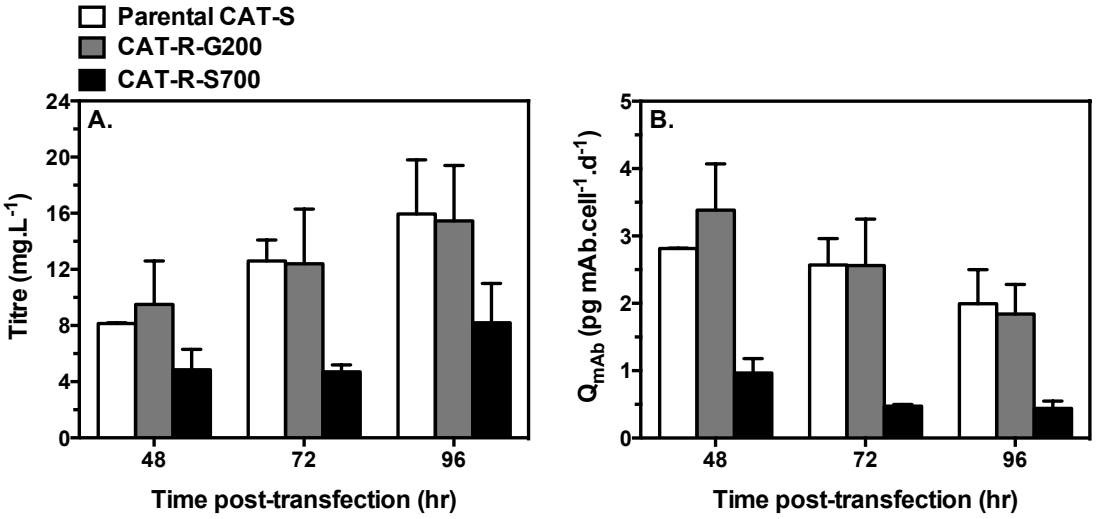

Figure 6.11 Transient production of an IgG monoclonal antibody in parental and resistant CAT-S cells. Each cell line was transfected with the mAb-109 vector by lipofection. Volumetric titres (**A.**) and cell specific production rates (**B.**) were measured at 48, 72 and 96 hr post-transfection. Data shown is the mean + SEM of two independent experiments, where in a single experiment antibody transfections were performed in duplicate and measurements were averaged.

6.3.4 Creation of SAS-Resistant T127 Cell Lines

The T127 antibody-producing cell line is a stable transfectant pool (non-clonal) and is hypothesised to be functionally heterogeneous. The SAS evolution method was therefore applied to the T127 cell line to investigate if a sub-population of cells could be isolated with improved performance characteristics. Two resistant cell lines were isolated from T127 cells over a twenty-week period (T127-R-S500 & T127-R-S700; Figure 6.12). The T127-R-S500 cell line was created by sub-culturing T127 cells every 4 days with CD-CHO medium supplemented with 500 μM SAS for 120 generations. After the first 20 generations a second shake flask was initiated from T127-R-S500 cells and sub-cultured with 700 μM SAS for a further 100 generations to create the T127-R-S700 cell line. As with the parental host, a vehicle control cell line (T127-CTRL) was created in parallel by sub-culturing T127 cells over 120 generations with 0.2% DMSO v/v CD-CHO medium. All cell lines were supplemented with 50 μM MSX throughout the evolution process.

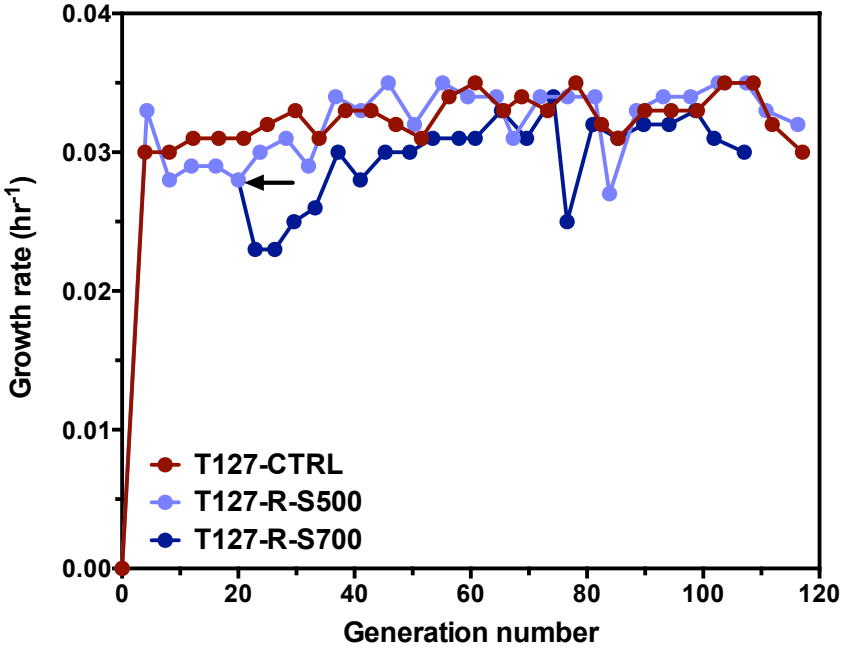

Figure 6.12 Creation of SAS-resistant T127 cell lines. Recombinant T127 cells stably expressing an IgG antibody were treated with 500 μM SAS over an extended sub-culturing regime (T127-R-S500; light blue line). After 20 generations, a second shake flask was initiated from T127-R-S500 cells (as indicated by the arrow) and sub-cultured with 700 μM SAS (T127-R-S700; dark blue line). A vehicle control cell line was created in parallel by sub-culturing the T127 cell line with 0.2% DMSO v/v CD-CHO medium (T127-CTRL; red line).

6.3.4.1 Growth and Antibody Production Characteristics for Non-Evolved and Resistant T127 Cell Lines

Performance of the non-evolved and two resistant T127 cell lines were assessed in batch overgrow shake flask cultures (Figure 6.13 & 6.14). T127-CTRL cells exhibited a lower growth rate and achieved a reduced maximal viable cell density than non-evolved T127 cells, indicating a prolonged exposure to DMSO has a negative impact on cell growth. In support of this, non-evolved T127 cells treated with DMSO achieved a slightly lower maximal viable cell density than those without DMSO (Figure 6.13 A). Both T127-R-S500 and T127-R-S700 cells demonstrated resistance to SAS that was not due to an extended sub-culturing regime (non-evolved versus T127-CTRL cells) or prolonged exposure to DMSO (resistant cells versus T127-CTRL cells). T127-R-S500 cells demonstrate a small increase in both growth rate and IVCD compared to non-evolved T127 cells when cultured in the presence of SAS but exhibit a shorter stationary phase.

However, compared to the T127-CTRL cells, average growth rate and IVCD is enhanced by 20% and 40% respectively in T127-R-S500 cells. T127-R-S700 cells exhibit comparable growth to T127-CTRL cells when cultured in the presence of SAS. For cultures without SAS treatment, the cells became visibly clumpy from day 5 onwards preventing accurate assessment of cell densities passed day 7.

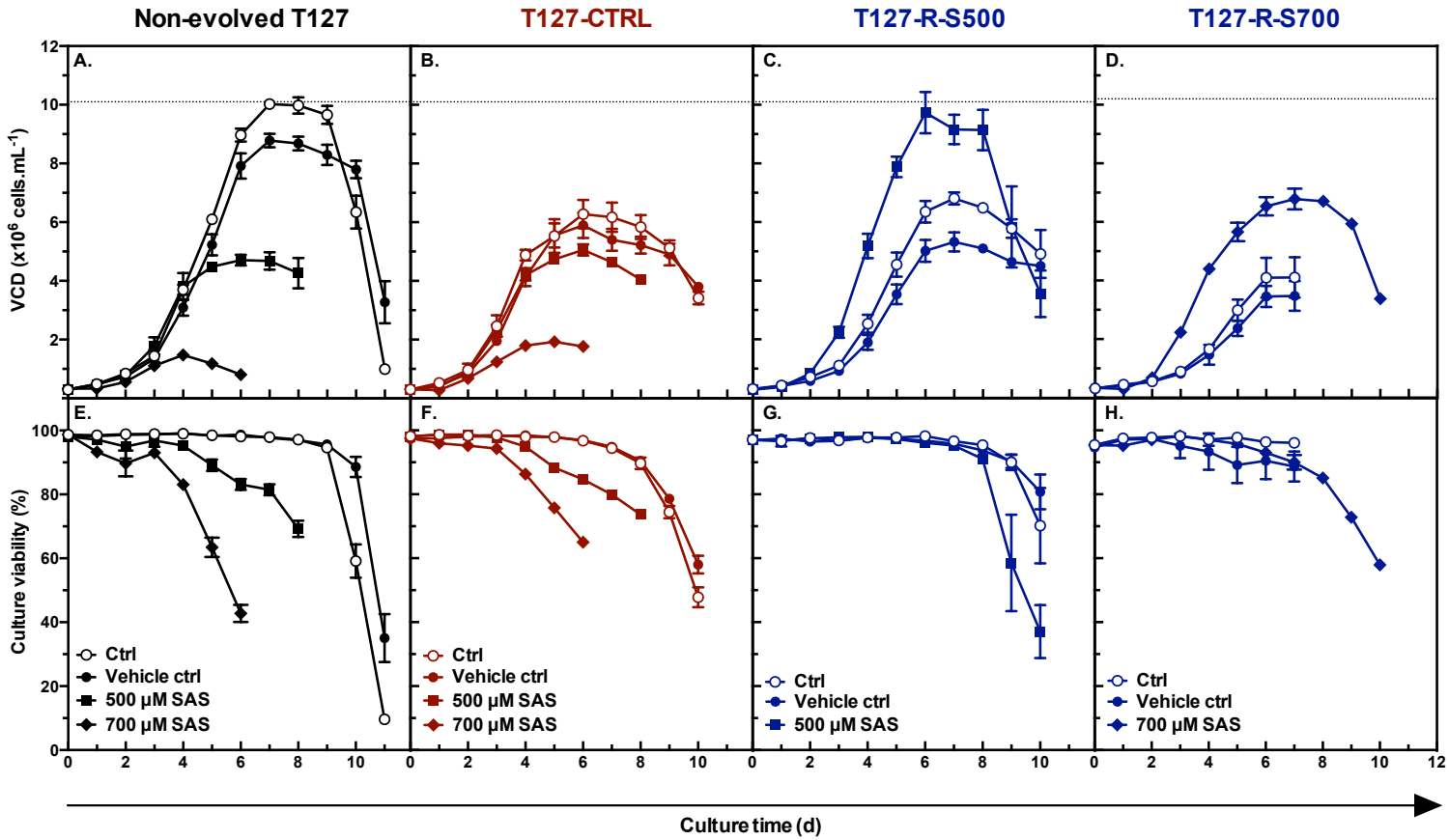

Figure 6.13 Batch culture growth curves for non-evolved T127, T127-CTRL, T127-R-S500 and T127-R-S700 cells. (**A. – D.**) Viable cell density (VCD). (**E. – H.**) Culture viability. Open circles are control cultures (0% DMSO v/v CD-CHO medium), closed circles are vehicle control cultures (0.2% DMSO v/v CD-CHO medium), and squares and diamonds are cultures treated with 500 µM and 700 µM SAS respectively at seeding. Data is shown as the mean ± SEM of three independently performed experiments.

Antibody production in the two resistant cell lines was measured and compared to production in the non-evolved (Figure 6.14 A) and T127-CTRL cells (Figure 6.14 B.). The latter comparison was made due to the inhibitory effect of prolonged exposure to DMSO on growth. Specific productivity is reduced in T127-R-S500 cells compared to non-evolved cells leading to a decrease in overall titre. Yet, specific productivity in T127-R-S500 cells was equivalent to that in T127-CTRL cells indicating that prolonged DMSO exposure has a negative effect on this performance parameter in addition to growth. When compared to the T127-CTRL cells, T127-R-S500 cells have an increased titre resulting from an increased IVCD. Interestingly, T127-R-S700 cells have an increased titre compared to T127-CTRL cells resulting from a higher specific productivity. This indicates that adaptation to higher concentrations of SAS may have a positive effect on antibody productivity.

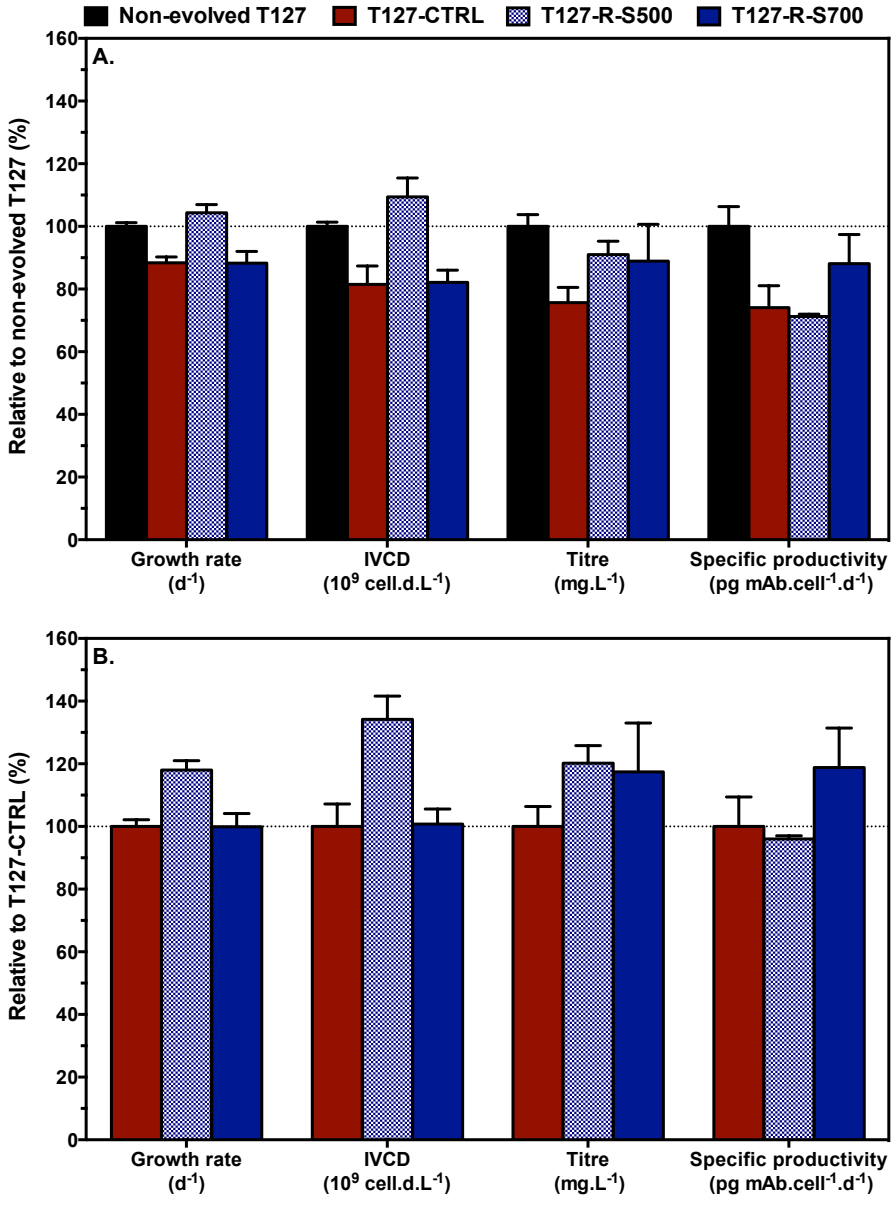

Figure 6.14 Comparison of growth and production characteristics for non-evolved T127, T127-CTRL, T127-R-S500 and T127-R-S700 cells as assessed in batch cultures. Average growth rate (μ; d^{-1}) was calculated over 0–6 days. Integral viable cell density (IVCD; 10^9 cell.d.L^{-1}) is the cumulative IVCD over 8 days. IgG titre (mg.L^{-1}) is taken at day 6. Specific productivity (Q_{mAb}; pg mAb.$cell^{-1}$.d^{-1}) is taken between days 3 and 6. (**A.**) Parameter values normalised to non-evolved T127 cells. (**B.**) Parameter values normalised to T127-CTRL cells. Data is shown as the mean + SEM of three independently performed experiments.

6.4 Discussion

The initial objective of this chapter was to isolate a sub-population of CAT-S cells with increased xCT transport activity using directed evolution. These cells would be expected to have a greater capacity for cystine import, which is predicted to support increased rates of GSH and antibody synthesis than unevolved CAT-S cells. The directed evolution method used SAS as a selective pressure during an extended sub-culturing regime of the parental CAT-S host. A population of CAT-S cells resistant to SAS treatment was isolated within eight weeks (CAT-R-S700). The CAT-R-S700 cell line demonstrated higher rates of GSH synthesis and was better able to cope with an oxidative stress insult than the non-adapted parental host. It is hypothesised that this is due to increased xCT transporter expression in CAT-R-S700 cells although this was not measured. In support of this, overexpression of the xCT transporter has previously been shown to increase GSH synthesis and provide protection from oxidative stress in astrocytes (Shih et al., 2006).

Unexpectedly, CAT-R-S700 cells demonstrated an improved growth rate and attained higher cell densities than the non-adapted parental host in batch and fed-batch cultures. The reason for this growth advantage is not clear. However, it is hypothesised that in addition to increased xCT transporter expression the evolution process also selected for other genes involved in amino acid transport and biosynthesis via activation of the amino acid response (AAR) pathway. SAS inhibits cystine uptake in a variety of mammalian cell lines (Chung et al., 2005; Gout et al., 2001; Timmerman et al., 2013), including the parental CAT-S cell line (see Chapter 5; Figure 5.11). Cystine starvation is known to induce the AAR pathway in mammalian cells (Lee et al., 2008), a cellular process that inhibits global protein synthesis but simultaneously upregulates a number of genes via activating transcription factor 4 (ATF4) including the amino acid

transporters xCT, SNAT2 and CAT-1, as well as asparagine synthetase (Kilberg et al., 2009). The expression of these four genes has previously been shown to be upregulated in response to AAR pathway activation in industrial CHO cell lines (Fomina-Yadlin et al., 2014). In Chapter 5, treating CAT-S cells with SAS was found to increase average consumption of the SNAT2 substrates asparagine and glutamine by 25% and 20% respectively (see Chapter 5; Figure 5.11), indicating SAS exposure stimulates the AAR pathway in the parental host. It is therefore hypothesised that early in the creation of the CAT-R-S700 cell line, the AAR pathway was activated and there was upregulation of all or some of these four metabolic genes. As CAT-R-S700 cells developed resistance to SAS treatment, cytosolic concentrations of cysteine was restored and the AAR pathway was suppressed. However, cell proliferation is the primary selective pressure during sub-culture and increased expression of SNAT2, CAT-1 and asparagine synthetase may have been selected for to support cell growth (e.g. increased glutamine consumption capacity). This would make their increased expression a stable feature of the CAT-R-S700 cell line. In agreement with this, the improved growth performance of CAT-R-S700 cells was heritable over 100 generations in the absence of the SAS selective pressure. Yet, resistance to SAS treatment began to decrease after 50 generations. A possible explanation for this latter observation is that in the absence of SAS, oxidative stress would act as the main selection pressure for maintenance of high xCT expression to support GSH synthesis. However, this is typically experienced during stationary phase of culture (see Chapter 2; Section 2.1). Expression of xCT would therefore be expected to decrease over successive generations during sub-culture where cells are kept in exponential growth. Loss of SAS resistance after 50 generations also provides further evidence to suggest that the mechanism conferring the growth advantage in CAT-R-S700 cells is distinct from SAS resistance.

Transient production of a recombinant IgG antibody was tested in CAT-R-S700 cells. CAT-R-S700 cells were found to be extremely poor at producing an antibody compared to the non-adapted parental host. However, this reflected the low transfection efficiency measured with this cell line. Davies et al. (2012) demonstrated considerable clone-specific variation in “transfectability” using lipofection than electroporation. This suggests that transient transfections in both the parental and CAT-R-S700 cell lines should be repeated using electroporation to help achieve equivalent transfection efficiencies.

The evolution process was repeated but with GPNA as the selective pressure until a sub-population of parental CAT-S cells with increased resistance to GPNA

inhibition was isolated (CAT-R-G200). GPNA resistance has previously been shown to correlate well with ASCT1 mRNA levels (Chapters 4 & 5). It is therefore assumed that increased expression of system ASC transporters (ASCT1 and/or ASCT2) is the source of resistance in these cells although this was not measured. In Chapter 4, it was hypothesised that system ASC transport is upregulated in T127 cells to support serine and threonine consumption for antibody synthesis. CAT-R-G200 cells with an increased capability for system ASC transport may therefore be able to produce higher quantities of antibody than unevolved CAT-S cells. Transient production of a recombinant IgG antibody was performed in CAT-R-G200 cells and compared to the performance of the CAT-S host to test this hypothesis. Antibody production was equivalent in the two cell lines indicating that the CAT-R-G200 cell line is not able to outperform the CAT-S host in a transient system. However, transient systems have previously been demonstrated to be a poor predictor of stable transfection performance (O'Callaghan et al., 2015). Future work would benefit from creating and comparing the performance of stable transfectant pools before this hypothesis is rejected. The growth performance of the CAT-R-G200 cell line was also characterised. In fed-batch cultures CAT-R-G200 cells exhibited an increased growth rate and achieved a higher IVCD than the CAT-S host. This indicates that the nutrient feed composition complements the evolved metabolic capabilities of the CAT-R-G200 cells. Compared to the CAT-R-S700 cell line, the CAT-R-G200 cell line took longer to create and resistance was unstable. It is hypothesised that this is because the GPNA-based directed evolution process was selecting for a small sub-population of cells that inherently have increased expression levels of ASCT1-2. In contrast, the SAS-based directed evolution process is fast as the whole cell population is being adapted via the AAR pathway. Fluorescence activated cell sorting (FACS) and magnetic activated cell separation (MACS) have been demonstrated as useful techniques in reducing the time length of CHO evolution strategies by sorting out viable cells (Bort et al., 2010; Taschwer et al., 2012). Therefore the use of FACS and/or MACS could help create a more stable GPNA resistant cell line in a shorter time period.

The SAS selection process was also applied to the T127 antibody-producing cell line. Interestingly, it took longer for growth and viability to recover in T127 cells than the CAT-S host (120 versus 60 generations). This could be due to the negative effects of both MSX and SAS on GSH metabolism. MSX is known to inhibit γ-glutamylcysteine synthetase, the first enzymatic step in GSH synthesis (Richman et al., 1973), while SAS has an off-target inhibition effect on glutathione S-transferases (GSTs), which catalyse the conjugation of GSH and electrophiles (Awasthi et al., 1994; Bach et al., 1985).

Together they may impede adaptation but using FACS or MACS in future studies as discussed above could speed this up. In batch cultures both T127-R-S500 and T127-R-S700 cells were able to achieve higher IgG antibody titres than T127-CTRL cells. This was due to either an increase in IVCD (T127-R-S500) or specific productivity (T127-R-S700). However, the evolved cell lines were unable to outperform the non-evolved T127 cell line. This is believed to be a result of prolonged exposure to DMSO, which had an inhibitory effect on both growth and specific productivity. Future evolution strategies would benefit from circumventing the need to solubilise SAS in this vehicle. An alternative method of getting SAS into solution involves dissolving the drug in NaOH and adjusting the pH with HCl (correspondence with Professor Sontheimer's lab, The University of Alabama, USA). However, the osmolarity of the solution would need to be checked as well as the balance between ions as the activity of many amino acid transporters is ion dependent. In contrast to the CAT-R-S700 cell line, growth of T127-R-S500 and T127-R-S700 cells was dependent upon supplementation with SAS. The reason for this is not clear. One hypothesis is that these two isolated sub-populations may have a very high capacity for xCT transport activity that may increase cystine influx and/or glutamate efflux in a way that disrupts growth. For example, high intracellular levels of cysteine have been shown to induce cell death in mammalian cells (Ji et al., 2016), whereas a high intracellular availability of glutamate is essential during cell proliferation to replenish TCA cycle intermediates (see 2.1 Mammalian Cell Metabolism). However, in the presence of SAS there remains an inhibitory block on excessive xCT activity. This hypothesis would suggest that xCT transport activity must be finely tuned in CHO cells and that the directed evolution method can select for sub-populations with increased xCT transport function that has adverse effects on cell growth. Further work characterising these cell lines is required to explore this hypothesis.

Directed evolution is a process in which a selective pressure is used to isolate a population of cells with a desired phenotype from a heterogeneous background. In contrast to single gene changes using genetic engineering tools, directed evolution has the potential to alter the expression of multiple genes simultaneously (Majors et al., 2009). In this chapter it has been hypothesised that SAS and GPNA have selected for cell populations with increased xCT and system ASC transporter expression respectively. Activation of the AAR pathway has been postulated as one mechanism by which the xCT transporter is upregulated. However, as discussed above (see 6.1 Introduction), CHO cell populations are genetically diverse and certain nucleotide

variations inside and outside of the coding sequence may have been selected for that affect transporter expression or function. SNPs outside the coding sequence for example can impact gene expression by affecting cellular processes such as mRNA stability, gene splicing, or promoter activity. SNPs inside the coding region may however result in silent or missense mutations. One way in which silent mutations may affect gene expression is by switching to more or less abundant codons that speed-up or slow-down protein synthesis respectively. Conversely, missense mutations may lead to an increase or decrease in transporter function, particularly if the amino acid change is in the site of the transporter involved in translocation of amino acid substrates across the cell membrane. The directed evolution process may therefore have selected sub-populations of cells with missense mutations in the coding sequence resulting in increased transporter activity rather than cells with increased transporter expression as postulated so far. Future work could look at the cDNA of the xCT and system ASC transporters to look for potential sequence variants in the evolved cell lines compared to the parental population.

In this chapter, a directed evolution method is described that was able to isolate cell lines with desirable characteristics for biomanufacturing. Evolution of the parental CAT-S host using SAS as a selective agent proved to be particularly successful with a stable improvement in growth performance achieved. This study would benefit from further characterisation of the evolved cell lines such as measurements of amino acid transport rates and expression of amino acid transporters, particularly with the CAT-R-S700 cell line. A priority for future work should be to compare the relative performance of the CAT-S host and CAT-R-S700 cells to transiently and stably produce an IgG antibody using electroporation as the preferred transfection method.

Chapter 7

Rational Design of Culture Media From an Understanding of Amino Acid Transport Mechanisms

In this chapter, a mechanistic model to describe essential amino acid transport processes in CHO cells is constructed from transcriptomic (Chapter 4) and inhibitor (Chapter 5) data. This model demonstrates how the consumption rate of aromatic, branched-chain and cationic amino acids is dependent upon their extracellular concentrations. This model can be used to direct the optimisation of amino acid concentrations in basal and feed media to maximise cell growth and antibody production.

7.1 Introduction

The optimisation of basal and feed media is a key activity in the development of fed-batch processes. For example, variations in nutrient composition have been demonstrated to have a significant effect on cell growth, culture longevity and IgG production in a single CHO cell line (Yu et al., 2011). Design of experiments (DoE) is a statistical method frequently used in media development (Jiang et al., 2012; Parampalli et al., 2008; Zhang et al., 2013). In this approach factorial experiments are used to screen for nutrients and other media components that either alone or in combination have a statistically significant effect on cell growth and/or antibody production. Regression models and response surface methodology (RSM) is then used to find the optimal levels of media components to improve cell line productivity.

Optimisation of amino acid concentrations is arguably one of the most important goals in CHO cell media development because of their role in central metabolism (Dean and Reddy, 2013; Duarte et al., 2014), signaling to pathways that regulate global protein synthesis (Fomina-Yadlin et al., 2014) and synthesis of recombinant proteins with correct glycosylation profiles (Chen and Harcum, 2005; Fan et al., 2014). Spent media

analysis (SMA) is one approach commonly used to optimise amino acid concentrations (Altamirano et al., 2004; Kishishita et al., 2015; Kyriakopoulos and Kontoravdi, 2014; Ma et al., 2009; Sellick et al., 2011). In this approach cell lines are first grown in batch culture and amino acid concentrations are measured. A feed is then designed in which selected amino acids are fed-back at concentrations found in the basal medium (Sellick et al., 2011) or based upon specific consumption rates and predicted cell growth (Altamirano et al., 2004; Kyriakopoulos and Kontoravdi, 2014). CHO metabolic models have also been used to optimise amino acid concentrations (Xing et al., 2011) or suggest further improvements to a SMA optimised process (Kyriakopoulos and Kontoravdi, 2014). Metabolic models have an advantage over DoE and SMA methods in that they take into account biomass and recombinant protein composition within the reaction network.

However, none of the above approaches consider potential limitations in amino acid transport that may affect uptake. Individual transporters typically facilitate the movement of multiple amino acids (see Chapter 2; Section 2.3) such that extracellular concentrations can influence which amino acids are preferentially transported. Furthermore, functional relationships exist between individual transporters (Nicklin et al., 2009). Yang et al. (2010) examined alanine, glutamine and serine transport competition through system A transporters in cultured hepatocytes and constructed equations from empirical data that can predict the transport rate of these amino acids in terms of their concentrations in the culture medium. A similar better understanding of the relationship between CHO transporter activity and amino acid uptake would be a major benefit to future developments of culture media for improved cell line productivity. This chapter explores how the data generated in Chapters 4 and 5 can be used to optimise amino acid concentrations in culture media based upon knowledge of biomass composition (cell and product) as well as the transport capabilities of the CHO cell line.

7.2 Materials and Methods

7.2.1 Generation of Amino Acid Transport Profile Data

CAT-S, GS-Null and T127 cells were all treated with BCH, MeAIB, SAS, GPNA and ALX 5407 HCl during exponential growth of batch cultures in Chapter 5. Transport rates for each of the 20 amino acids was measured in control and treated cultures, and are analysed in this chapter.

7.2.1.1 CAT-S Transport Profiles

62 individual transport profiles for the 20 amino acids were generated for CAT-S cells from the following culture conditions: BCH (0, 10, 20, 30 and 40 mM), MeAIB (10, 20 and 40 mM), SAS (0, 300, 600, 700 and 1000 μM), GPNA (50, 100, 200, 400 and 800 μM) and ALX 5407 HCl (0, 10 and 50 μM).

7.2.1.2 GS-Null Transport Profiles

64 individual transport profiles for the 20 amino acids were generated for GS-Null cells from the following culture conditions: BCH (0, 5, 20, 30 and 40 mM), MeAIB (1, 5, 10 and 40 mM), SAS (0, 300, 600, 700 and 1000 μM), GPNA (50, 100, 200, 400 and 800 μM) and ALX 5407 HCl (0, 10 and 50 μM).

7.2.1.3 T127 Transport Profiles

71 individual transport profiles for the 20 amino acids were generated for T127 from the following culture conditions: BCH (0, 10, 20, 30 and 40 mM), MeAIB (2.5, 5, 10 and 40 mM), SAS (0, 300, 600, 700, 800 and 1000 μM), GPNA (0, 0.4, 0.8, 1.0, 2.0 and 3.7 mM) and ALX 5407 HCl (0, 10 and 50 μM).

7.2.3 Statistical Analysis

Spearman's rank correlation was performed in RStudio (R Core Team, 2014) using the corr.test function in the psych package (Revelle, 2014) unless otherwise stated. Correlation coefficients (ρ), raw probability, and adjusted probability values to account for multiple tests were reported. The Holm (1979) method was used to calculate adjusted probability values. The corrplot package (Wei, 2013) was used to plot a correlogram of the statistical outputs from the Spearman rank correlation test.

7.3 Results

In Chapter 5, inhibitors of amino acid transport were applied to five CHO cell lines during exponential growth of batch cultures. The transport rates for each of the 20 amino acids was measured for each perturbation in CAT-S, GS-Null, and T127 cells. A total of 62, 64, and 71 individual transport profiles were measured for these three cell lines respectively (see 7.2 Materials and Methods). The total specific transport rate (sum

of absolute consumption and production rates of all amino acids) for each profile was plotted against the growth rate resulting from that perturbation (Figure 7.1).

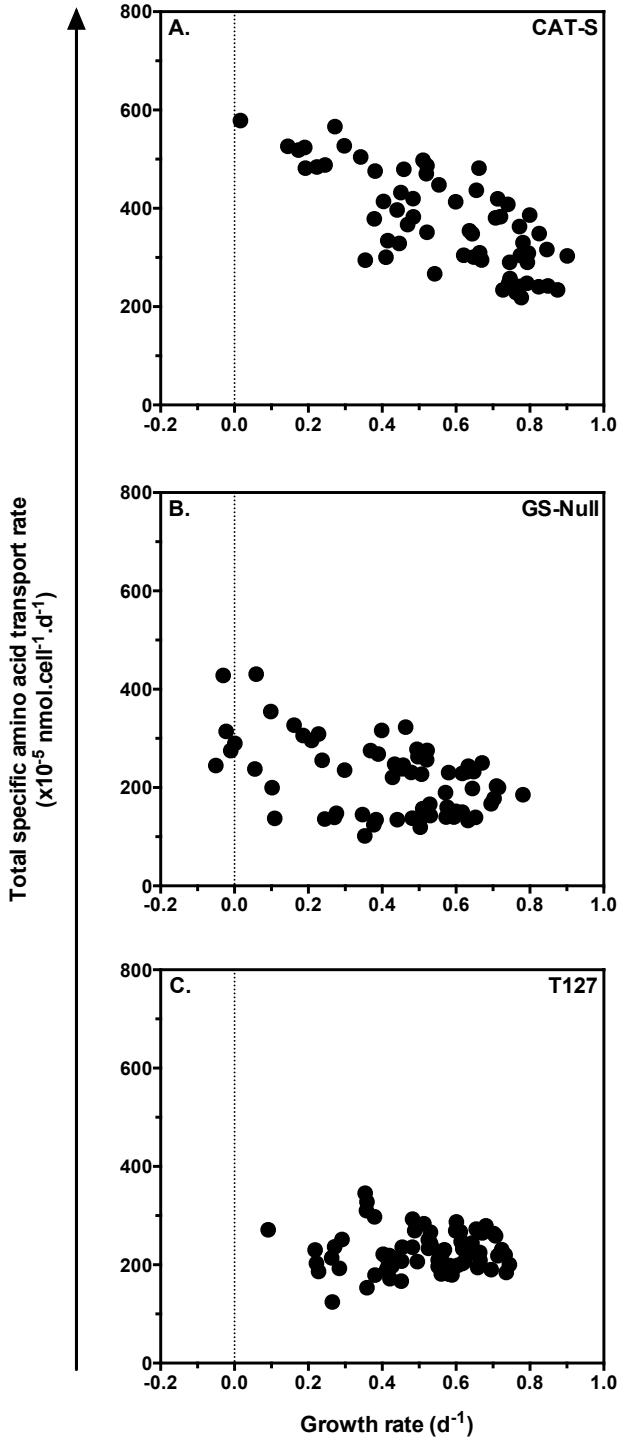

Figure 7.1 Relationships between total specific amino acid transport rates and growth rates in CAT-S, GS-Null and T127 cells. Each data point represents an individual amino acid transport profile in which absolute consumption and production rates of the 20 amino acids were summed. A total of 62, 64 and 71 transport profiles are plotted for (**A.**) CAT-S, (**B.**) GS-Null, and (**C.**) T127 cells respectively. Section 7.2

Materials and Methods provides further details on the source of these profiles. Spearman's rank correlation was performed using GraphPad Prism v6.0 (GraphPad Software, San Diego, USA) to analyse these relationships (outputs in main body of text).

For CAT-S cells, there is a significantly strong negative correlation between growth rate and total specific transport rate (ρ = -0.71; P = < 0.0001). This correlation is weak in GS-Null cells but still significant (ρ = -0.37; P = 0.003), while no correlation exists in T127 cells (ρ = 0.06; P = 0.6). These relationships were explored further for each cell line by plotting the specific transport rates of each amino acid against growth rates (Appendix Figure C1). CAT-S cells were found to increase their consumption and metabolism of amino acids associated with energy production as cell proliferation decreased. Consumption of asparagine, cystine, glutamine and serine, and production of alanine, aspartate, glutamate and glycine all increased with decreasing growth rates. These changes primarily came from the perturbations made by GPNA (system ASC inhibitor) and SAS (system X_C^- inhibitor). Asparagine, glutamine and serine are all substrates of the SNAT2 transporter, while cystine is a substrate of the xCT transporter. Both transporters are well known targets of the amino acid response (AAR) pathway, which is activated by depletion of intracellular amino acid levels (see Chapter 2; Section 2.2.2). For GS-Null cells, consumption of asparagine, cystine and serine, and production of alanine, aspartate, glutamate, glutamine and glycine all increased with decreasing growth rates. Again, these changes primarily came from GPNA and SAS inhibited cultures. While for T127 cells, only alanine, aspartate and glycine production increased with decreasing growth rates. However, these cells were more resistant to GPNA and SAS inhibition (see Chapter 5).

Many of the amino acids in Appendix Figure C1 showed very similar patterns of correlation against growth rate, suggestive of shared amino acid transport processes. These were therefore explored further. For each profile, the specific transport rate for an individual amino acid was plotted against the specific transport rate of the remaining 19 amino acids generating 190 unique amino acid comparisons. Strong linear relationships were found to exist between many amino acids in each of the three cell lines (data not shown). The strength of these relationships was analysed further using Spearman's rank correlation with the statistical outputs plotted as a correlogram for visual interpretation (Figure 7.2; numerical values are also provided in Appendix Table C1–3).

A. CAT-S

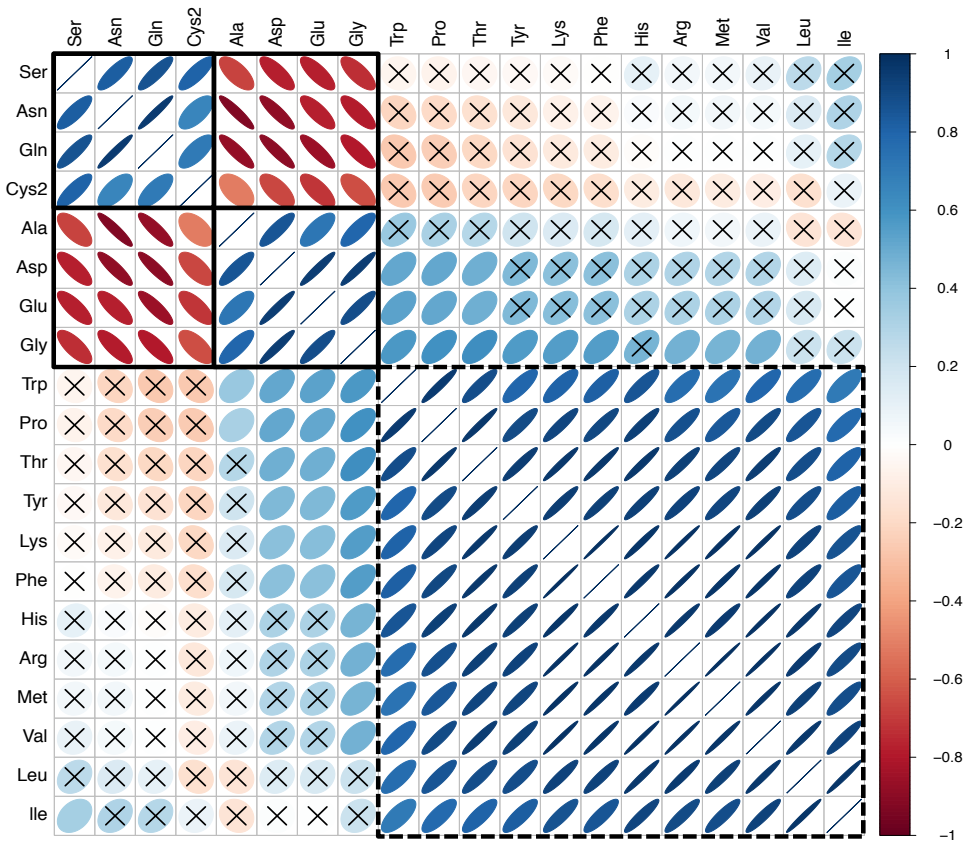

B. GS-Null

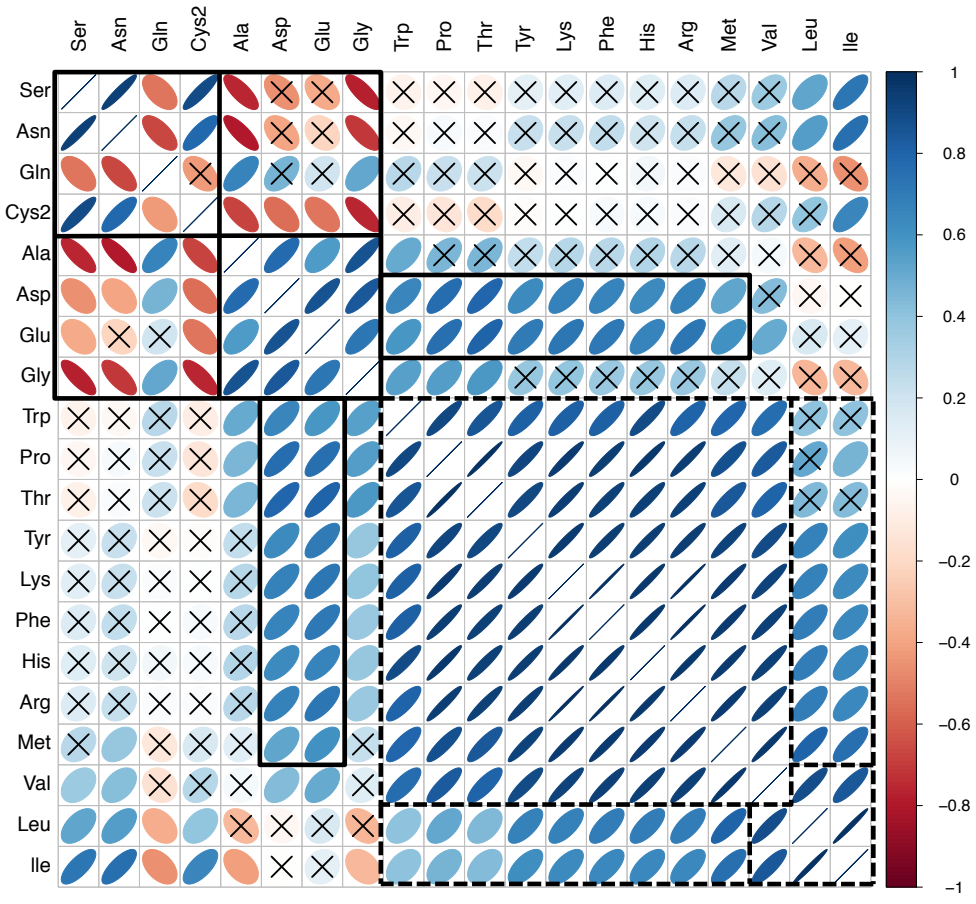

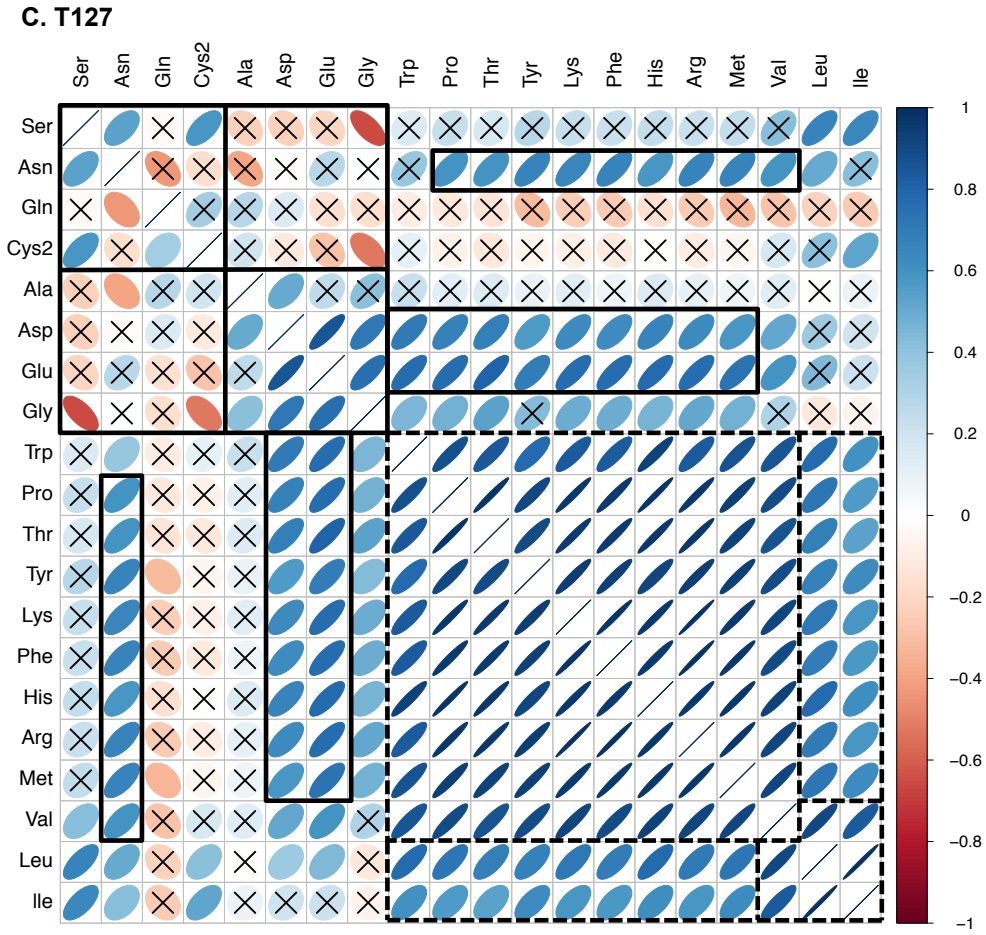

Figure 7.2 Correlations between the 20 proteinogenic amino acids in CAT-S, GS-Null and T127 cells. Data was analysed using Spearman's rank correlation and the statistical output visualised as correlograms. Ellipses represent correlation coefficients (ρ) with the width and colour signifying the strength of the coefficient. Crosses indicate non-significant correlation coefficients (significant if $P < 0.01$). Raw and adjusted probabilities are used above and below the diagonal respectively. Black boxes are used to group key correlations discussed in the main body of text. Broken boxes group correlations between essential amino acids. Solid boxes group correlations between non-essential amino acids.

7.3.1 Essential Amino Acid Correlations

For CAT-S cells, the transport of cationic (arginine and lysine), branched-chain (isoleucine, leucine and valine), and aromatic (histidine, phenylalanine, tryptophan and tyrosine) amino acids, in addition to methionine, threonine, and proline all have significantly strong positive correlations (typically $\rho \geq 0.9$). These correlations are highly conserved in recombinant glutamine synthetase cell lines (GS-Null and T127)

with all but isoleucine and leucine. Both isoleucine and leucine maintain a significantly strong positive correlation with each other (ρ = 1.0) and to valine (ρ = 0.8 – 0.9) but have a weak-moderate correlation to the other essential amino acids in these cells (ρ = 0.4 – 0.8). These positive correlations imply essential amino acids must share some common transport mechanism. A mechanistic model of transport for these amino acids is inferred from literature (Chapter 2), transcriptomic (Chapter 4) and inhibitor (Chapter 5) data and summarised in Figure 7.3.

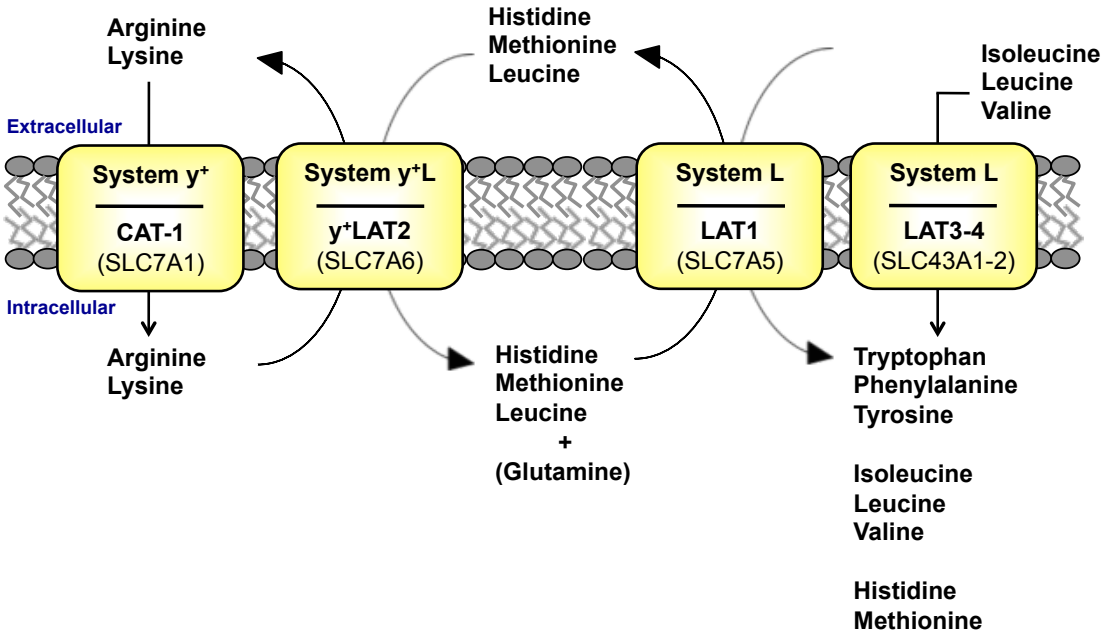

Figure 7.3 Proposed mechanistic model of essential amino acid transport in CAT-S, GS-Null and T127 cells. Growth of GS-Null and T127 cells in glutamine free media is proposed to recruit the activity of either (or both) LAT3 or LAT4 uniporters to support consumption of isoleucine, leucine and valine through LAT1.

The four transporters of system L (LAT1–4) facilitate the transport of branched-chain amino acids with the LAT1–2 antiporters also capable of transporting the four aromatic amino acids (see Chapter 2; Table 2.1). BCH (system L inhibitor) treatment results in complete inhibition of uptake for these amino acids (see Chapter 5; Section 5.3.1) and transcriptomic data demonstrate that the LAT1 transporter is preferentially expressed over LAT2 (see Chapter 4; Section 4.3.3). In contrast, intracellular accumulation of the two cationic amino acids is facilitated by the uniporters of system y^+ (see Chapter 2; Table 2.1) of which CAT-1 is preferentially expressed across the three CHO cell lines (see Chapter 4; Section 4.3.3). The two transporters belonging to system y^+L (y^+LAT1–

2) have an obligatory antiport transport mechanism in which intracellular arginine and lysine are exported for the import of glutamine, histidine, leucine, and methionine, thereby connecting the activities of LAT1 and CAT-1 (see Chapter 2; Table 2.1). Transcriptomic data demonstrate that y^+LAT2 is preferentially expressed over y^+LAT1 (see Chapter 4; Section 4.3.3). In support of such a mechanism intracellular histidine, leucine, and methionine have been shown to strongly trans-stimulate amino acid influx through LAT1 (Meier et al., 2002). Glutamine is a poor efflux substrate of LAT1 (Meier et al., 2002) but its high intracellular concentration means its export is preferentially coupled to amino acid influx through LAT1 (Nicklin et al., 2009). Interestingly, influx of isoleucine and leucine is no longer coupled to aromatic amino acid transport in GS-Null and T127 cells grown in glutamine free media indicating that they must instead be entering the cell through a separate transporter. BCH data implies that this must still be a system L transporter, and therefore must be through either (or both) the LAT3 or LAT4 system L uniporters.

To help validate the model, the relationship between consumption and medium composition of essential amino acids was investigated. The magnitude of transport rate for a given amino acid through a single transporter will be dependent upon the extracellular concentrations of competing amino acids and the kinetic parameters (K_m and V_{max}) that each of those amino acids has for that transporter. If the aromatic, branched-chain, and cationic amino acids are transported through two distinct transporters as proposed in Figure 7.3 then their consumption rates relative to one another should match their extracellular concentrations (assuming equivalent kinetic properties). The concentration of amino acids in the cell culture medium was measured and transport rates were calculated using control cultures (i.e. inhibitor free cultures) from Chapter 5 (Table 7.1).

Table 7.1 Specific transport rates of amino acids in CAT-S, GS-Null and T127 cells grown under control conditions

	Specific transport rate ($x10^{-5}$ $nmol.cell^{-1}.d^{-1}$)		
Amino acid	**CAT-S**	**GS-Null**	**T127**
1. Neutral			
A. Branched-chain amino acids			
Ile	-7.9 ± 1.4	-9.4 ± 1.4	-9.9 ± 1.6
Leu	-13.7 ± 2.4	-15.4 ± 1.8	-17.0 ± 2.9
Val	-9.9 ± 1.3	-9.9 ± 0.9	-10.6 ± 1.7
B. Aromatic amino acids			
His	-4.3 ± 0.5	-3.7 ± 0.4	-3.2 ± 0.9
Phe	-4.9 ± 0.5	-4.1 ± 0.3	-4.0 ± 0.8
Trp	-1.6 ± 0.3	-1.8 ± 0.3	-1.5 ± 0.6
Tyr	-5.3 ± 0.8	-4.8 ± 0.8	-5.3 ± 1.0
C. Amide, hydroxyl, sulfur, cyclic and small amino acids			
Asn	-56.5 ± 3.7	-55.3 ± 5.8	-58.5 ± 3.8
Gln	-80.3 ± 12.8	4.3 ± 3.6	10.0 ± 1.2
Thr	-6.7 ± 1.0	-5.1 ± 1.2	-5.3 ± 1.5
Ser	-33.0 ± 3.0	-35.1 ± 6.9	-49.8 ± 6.9
Met	-3.6 ± 0.3	-3.2 ± 0.2	-2.6 ± 0.6
Cys2	-3.6 ± 0.5	-3.0 ± 0.7	-3.0 ± 0.4
Pro	-6.7 ± 1.1	-6.0 ± 1.5	-4.8 ± 2.6
Gly	12.9 ± 1.9	16.0 ± 6.9	27.1 ± 7.0
Ala	35.6 ± 4.5	2.5 ± 1.8	2.4 ± 1.6
2. Cationic			
Arg	-9.5 ± 1.0	-7.5 ± 0.6	-6.8 ± 1.5
Lys	-12.7 ± 1.3	-10.7 ± 1.0	-10.0 ± 2.2
3. Anionic			
Asp	15.0 ± 2.3	3.2 ± 1.2	0.8 ± 1.9
Glu	13.2 ± 3.0	-3.1 ± 1.1	-4.5 ± 2.0

All values are shown as mean ± SD (n = 9). Amino acids are grouped by their overall charge with neutral amino acids further divided into three groups based upon the chemical nature of their side-chain. Negative and positive rates represent consumption and production respectively.

The aromatic and branched-chain amino acids proposed to be transported exclusively by system L, ranked in order of concentration, is Leu > Val > Ile > Tyr ≈ Phe > Trp (data not shown). Kinetic parameters for these amino acids through LAT1 have been shown to be approximately equivalent (Yanagida et al., 2001) indicating that their transport rate should match their concentration order. The transport rates for these six amino acids do indeed match this order exactly in CAT-S, GS-Null and T127 cells (Table 7.1). Similarly for cationic amino acids, the concentration of Lys is greater than Arg (data not shown) and both amino acids have approximately equivalent kinetic parameters through the CAT-1 transporter (Closs et al., 2006). The transport rate of lysine is consistently higher than arginine in CAT-S, GS-Null and T127 cells (Table 7.1). This understanding of essential amino acid transport has important implications in medium design to maximise cell or antibody synthesis (discussed in Section 7.4).

7.3.2 Non-Essential Amino Acid Correlations

The non-essential amino acids alanine, aspartate, asparagine, glutamate, glutamine, glycine, and serine are closely associated with central metabolic pathways that support energy metabolism in addition to the biosynthesis of macromolecules other than proteins (e.g. lipids and nucleic acids) during exponential growth (see Chapter 2; Section 2.1). For CAT-S cells, these amino acids form a group of statistically significant linear relationships distinct from the essential amino acids (Figure 7.2 A). Strong positive correlations ($\rho \geq 0.8$) exist between the consumption of asparagine, serine, and glutamine, and the production of alanine, asparatate, glutamate, and glycine. The transport rates for these seven amino acids are also inversely correlated. This is hypothesised to be a consequence of metabolic reactions that mediate the interconversion of these seven amino acids, for example deamination and transamination reactions. These interconversion reactions mean that unlike essential amino acid relationships, positive correlations do not necessarily imply a common transport process. For CAT-S and GS-Null cells, the xCT substrate cystine has a significantly moderate-strong positive correlation with the SNAT2 substrates asparagine, glutamine (CAT-S only) and serine ($\rho = 0.7 – 0.9$). This correlation reflects the increased consumption of these amino acids in response to decreasing growth rates as discussed above.

The linear relationships between non-essential amino acids are severely disrupted in recombinant glutamine synthetase cell lines grown in glutamine free media (Figure 7.2 B–C). Furthermore, correlation loss is greatest in T127 cells, associating

well with glutamine synthetase gene expression, which is 8-fold higher in T127 cells than GS-Null cells (3220 versus 440 FPKM). Despite these differences a significantly strong positive correlation between aspartate and glutamate (ρ = 0.9) is highly conserved across the three cell lines. Additionally, in both GS-Null and T127 cells these two anionic amino acids also now have a significantly moderate positive correlation with all essential amino acids except isoleucine, leucine, and valine (ρ = 0.6 – 0.8). The same essential amino acids also have a significantly moderate positive correlation with asparagine in T127 cells (ρ = 0.6 – 0.7).

7.4 Discussion

An analysis of amino acid profiles generated in Chapter 5 identified linear relationships between amino acids in CAT-S, GS-Null and T127 cells. Correlation matrices were used to further analyse these profiles and in conjunction with data from previous chapters a mechanistic model for essential amino acid transport was devised (Figure 7.3). Importantly, this analysis reveals that consumption rates of aromatic, branched-chain and cationic amino acids is dependent upon the concentration of these amino acids in culture medium. It is therefore hypothesised that by modulating the extracellular concentrations of these amino acids it should be possible to control which amino acids are preferentially consumed. This would represent an important benefit in the optimisation of basal and feed media to meet the changing biomass objectives throughout a fed-batch process.

Essential amino acids such as isoleucine, leucine and valine play an important role in supporting cell growth by directing their carbon atoms towards intermediates of the TCA cycle and stimulating the mTORC1 signaling pathway whose activation promotes cell growth (see Chapter 2 and Figure 2.1). However, ^{13}C-MFA studies with CHO cells provide evidence that glucose, asparagine and glutamine are the main donors of carbon to the TCA cycle (see 2.1.1 Aerobic Glycolysis and Glutaminolysis Support Cell Proliferation). The bulk of consumed essential amino acids are therefore likely to be directed towards protein synthesis to support growth. Host cell protein synthesis is hypothesised to dominate over antibody production to support cell growth and division during exponential growth. Selvarasu et al. (2012) analysed the amino acid composition of five industrially relevant CHO cell lines including CHO-K1, CHO DG44 and CHO DXBII. For aromatic and branched-chained amino acids the relative concentration of these amino acids from highest to lowest was found to follow as Leu > Val > Ile > Phe

> Tyr > Trp. For cationic amino acids this was Lys > Arg. This order of abundance corresponds well with the composition of the cell culture medium indicating that these amino acids are already optimised for host cell protein synthesis. However, antibody production is hypothesised to dominate protein synthesis late in culture and has a very different composition of essential amino acids to host cell proteins. For the IgG antibody used throughout the work in this thesis the order of essential amino acids is now Val > Leu > Tyr > Phe > Ile > Trp (see Chapter 4; Table 4.7). For the cationic amino acids Lys remains greater than Arg but the relative difference is now 2-fold compared to 1.5-fold for host cell proteins. Therefore, in order to optimise the productivity of a fed-batch process, feed additions during exponential growth should be designed to maintain the relative essential amino acid composition observed in the cell culture medium. However, feed additions during late exponential-stationary growth phase should have an altered essential amino acid composition to help maximise antibody synthesis. BCH (system L inhibitor) treatment during late-stage culture decreases specific antibody productivity in a dose-dependent manner (see Chapter 5; Section 5.3.1) highlighting the importance of optimising essential amino acid consumption.

Expanding this mechanistic model to include transport of the seven non-essential amino acids (alanine, asparagine, aspartate, cysteine, glutamine, glutamate, and glycine) is highly desirable for media design and development of feeding regimes. Asparagine and glutamine consumption rates far exceed that of the other amino acids in CHO cell lines (see Figure 4.6 and Figure 4.8) and ^{13}C-MFA studies with CHO cells demonstrate that these two amino acids significantly contribute to TCA cycle replenishment via aspartate and glutamate to support cell proliferation (see 2.1.1 Aerobic Glycolysis and Glutaminolysis Support Cell Proliferation and Figure 2.1). However, deamination of these amino acids results in high secretion of ammonia, which is toxic to cell growth and antibody production. Maintenance of ammonia levels at low concentrations is a key objective of fed-batch processes and is primarily achieved through careful control of asparagine and glutamine feeding. The correlation matrices revealed that aspartate and glutamate transport is highly conserved irrespective of extracellular glutamine or the expression level of recombinant glutamine synthetase (Figure 7.2). Only transporters belonging to system X_{AG}^- are capable of facilitating the transport of both anionic amino acids (see Chapter 2; Table 2.1), and transcriptomic data demonstrate that GLAST (SLC1A3) is preferentially expressed (see Chapter 4; Section 4.3.3). Functional coupling between transporters of non-essential and essential

amino acids has also been demonstrated in HeLa cells (Nicklin et al., 2009). In GS-Null and T127 cells anionic amino acid transport is correlated with consumption of most essential amino acids suggesting some mechanistic link may exist between GLAST, CAT-1, and LAT1 transporters. However, further work is required to elucidate the interplay of essential and non-essential transporters as well as the role of media components (e.g. extracellular glutamine presence) and metabolic reactions of non-essential amino acids (including recombinant glutamine synthetase expression).

In summary, this is the first time that an understanding of CHO transport processes has been used to direct the hypothetical optimisation of amino acid concentrations in culture media. The mechanistic model described here serves as a starting point for the development of a mathematical model that can predict transport rates of essential amino acids. Further characterisation of essential amino acid transport would aid this. For example, performing a DoE experiment in which the extracellular concentrations of essential amino acids are varied.

Chapter 8

Conclusions and Future Work

8.1 Conclusion

8.1.1 Characterisation of Amino Acid Transport Processes

The first aim of this thesis was to understand how the function of CHO amino acid transporters might support culture performance parameters such as cell growth, culture viability and specific productivity. To investigate this, transporter gene expression was first measured using Illumina next-generation sequencing in a parental host and two recombinant cell lines throughout a fed-batch process (Chapter 4). In agreement with previously reported transcriptomic (Kyriakopoulos et al., 2013) and proteomic (Baycin-Hizal et al., 2012) CHO cell measurements, the following seven transporters were found to be highly expressed across the three cell lines: ASCT1 (SLC1A4, system ASC), CAT-1 (SLC7A1, system y^+), GLAST (SLC1A3, system X_{AG}^-), LAT1 (SLC7A5, system L), SNAT2 (SLC38A2, system A), xCT (SLC7A11, system X_C^-) and y^+LAT2 (SLC7A6, system y^+L). Collectively, these seven transporters facilitate the transport of all 20 proteinogenic amino acids. By increasing the expression of just a few transporters, CHO cells can access all extracellular amino acids at a reduced metabolic burden to the cell.

Building upon Chapter 4, inhibitors of amino acid transport were then used to evaluate transporter function at exponential and stationary phase of batch cultures (Chapter 5). The xCT cystine transporter was found to be essential for culture viability in all CHO cell lines examined. In agreement with observations by Kyriakopoulos et al. (2013), transcriptomic data revealed upregulation of xCT at stationary phase to be the largest change in expression for any transporter in any cell line. xCT activity is closely associated with GSH synthesis (Chung et al., 2005; Shih et al., 2006) and the results in Chapter 4 revealed that xCT upregulation forms part of a larger adaptive response that can support the cellular availability of GSH during late culture. Surprisingly, upregulation of xCT did not result in increased cystine consumption and all cell lines demonstrated increased sensitivity to xCT inhibition late in culture compared to early in

culture. Collectively, the results presented suggest that despite the inclusion of antioxidants in culture media (Whitford, 2006) CHO cells continue to depend on *de novo* GSH synthesis to maintain high culture viabilities. Yet, cystine influx could be a bottleneck in GSH synthesis. Future work is required to explore this further (discussed in Section 8.2).

Previous studies have found producer cells downregulate the expression of catabolic genes specific for amino acids that are abundant in the composition of a recombinant protein (Dietmier et al., 2012b; Ley et al., 2015). This thesis proposes for the first time that upregulation of amino acid transporter expression also supports productivity by increasing consumption rates of amino acids that are abundant in an IgG antibody. Antibody-producing cells (T29, T48 and T127) maintained high consumption rates of leucine, threonine, tyrosine, serine and valine throughout stationary phase, all of which are abundant amino acids in the IgG antibody. This correlated with upregulation of ASCT1 (serine and threonine) and LAT1 (leucine, tyrosine and valine) transporters in T127 cells. Furthermore, inhibition of LAT1 (in addition to GlyT1 and xCT) transport during late-stage culture negatively impacted upon specific productivity. Transport activity of ASCT1, GlyT1, LAT1 and xCT transporters is therefore concluded to be important in supporting antibody production. Kyriakopoulos et al. (2013) proposed LAT4 (SLC43A2) and GLT-1 (SLC1A2) as potential markers of productivity based upon gene expression measurements. Like LAT1, LAT4 also belongs to system L but transports branched-chain amino acids only. The biological significance of GLT-1 upregulation is unclear.

Overall, the combination of RNA-sequencing and amino acid transport inhibition has helped to achieve the first aim of this thesis. Yet both experimental approaches have their limitations. For transcriptomic data, the correlation between mRNA and protein expression can often be poor with a correlation of $r = 0.48$ previously reported for CHO cells (Baycin-Hizal, 2012). Ideally, Western blots should be performed to verify expression of the main transporters reported in this thesis at the protein level (discussed further in Section 8.2). Inhibitors have the disadvantage of being non-specific such that they i) commonly target transport systems (multiple transporters), and ii) can have off-target effects on other biological processes. Transfection of cells with small inhibitory RNA (siRNA) molecules can be used in future work as a more targeted alternative method to inhibitors. The knockdown in expression of specific transporters with siRNA can help verify how their biological function supports key culture performance parameters (discussed further in Section 8.2).

8.1.2 Improving Cell Growth and Productivity

The second aim of this thesis was to use the above knowledge of CHO amino acid transport processes as a basis for exploring ways to improve cell growth and antibody production. Chapter 6 explored a directed evolution strategy to isolate sub-populations of the host cell line with increased resistance to system ASC or X_C^- transport inhibition. It was expected that these cells would have an improved capability to produce an antibody. However, evolved cells were unable to outperform the non-evolved host in the transient production of a recombinant IgG antibody. Yet for X_C^- evolved cells the results also demonstrated that transfection conditions were sub-optimal. It is suggested that future work should address this as well as compare stable transfection performance in both evolved and non-evolved parental cell lines. Interestingly, X_C^- evolved cells demonstrated a substantial improvement in growth performance over non-evolved host cells in batch and fed-batch cultures. Importantly for biomanufacturing, this phenotype was heritable for over 100 generations. It is suggested that enhanced cell growth is due to the evolution process selecting for increased expression of additional genes involved in amino acid transport and biosynthesis via activation of the AAR pathway. The X_C^- evolution process was also applied to the antibody-producing T127 cell line to see if a sub-population of cells with improved productivity could be isolated. The results from this work were inconclusive. Evolved T127 cells were unable to outperform non-evolved T127 cells, however long-term exposure to DMSO was found to have a negative impact on cell growth and specific productivity. When this was controlled for, evolved T127 cells were demonstrated to be capable of achieving higher titres due to increased specific productivity. The work in this chapter demonstrates that it is possible to isolate cell lines with desirable characteristics for biomanufacturing through manipulation of amino acid transport processes. However, this chapter would vastly benefit from further characterisation of the evolved cell lines. In particular, the measurement of transporter expression at the transcript (qRT-PCR) or protein (Western blot) level, and a comparison of amino acid transport profiles in evolved and non-evolved cells.

Finally, Chapter 7 presented a mechanistic model to describe essential amino acid transport processes in CHO cells. Constructed from data generated in Chapters 4 and 5, this model provides a hypothetical approach to controlling the consumption rate of essential amino acids through simple modulations to their extracellular concentrations. This model can therefore be used to optimise amino acid concentrations in basal and feed media to match the changing biomass requirements throughout

culture. This is the first time to my knowledge that an understanding of transport capabilities has been used to direct the optimisation of culture media for CHO cells.

8.2 Future Work

Future work should primarily focus on validating several of the results in this thesis to help strengthen the conclusions made. RNA-sequencing identified ASCT1, CAT-1, GLAST, LAT1, SNAT2, xCT, and y^+LAT2 as the key transporters supporting culture performance. Furthermore, significant differences in expression of ASCT1, GLAST, LAT1 and xCT existed either between cell lines, within culture or both. A number of conclusions regarding the function of these transporters were made based upon these observations. Western blots should be performed to i) verify the expression of these seven transporters at the protein level, and ii) determine if significant differences in mRNA levels are reflected at the protein level. The work in Chapters 4 and 5 also identified ASCT1, GlyT1, LAT1 and xCT transporters as having an important role in supporting antibody production. siRNA knockdown of these transporters in the antibody-producing T127 cell line can be used to verify this result. The transcriptomic analysis performed in this thesis was limited in that it only looked at the transporter component of amino acid metabolism. However, as discussed above, previous studies have found downregulation of catabolic genes for amino acids that are abundant in the recombinant protein (Dietmier et al., 2012b; Ley et al., 2015). To build a more complete picture of amino acid metabolism, expression data for genes involved in amino acid metabolic pathways should be extracted and mapped to transporter data.

Further work is also required to characterise the relationship between xCT transporter activity, GSH synthesis, and culture viability. This is particularly important, as extended periods of high culture viability are required during stationary phase to maximise antibody production. Western blots can first confirm if upregulation of xCT mRNA levels at stationary phase is translated to changes at the protein level. Whereas targeted manipulation of xCT expression can be used to verify its functional role. siRNA knockdown can be performed at exponential and stationary phase of cultures, followed by examination of GSH synthesis, GSH/GSSG ratios, cystine transport, ROS levels, as well as culture performance (e.g. cell viability). Similarly, xCT overexpression can also be performed followed by measurement of the above parameters. Collectively, these experiments would provide a detailed description of xCT function in CHO cells. Amino acid measurements in this thesis also identified

cystine transport as a potential bottleneck to GSH synthesis. It was suggested that this is due to the low solubility of this amino acid. Previous work has demonstrated that tyrosine-containing dipeptides have a significantly higher solubility than free tyrosine and feeding these dipeptides can enhance culture viability and productivity (Kang et al., 2012). More recently, Kishishita et al. (2015) found that supplementing CHO cultures with a cysteine-serine-tyrosine tripeptide could significantly improve cell growth and productivity. Future work should explore the utility of di/tripeptides as a means of increasing cytosolic levels of cysteine and whether this can have a positive effect upon culture viability.

The amino acid transport model described in Chapter 7 opens up two engineering possibilities that can be explored for improving CHO cell growth and productivity, i) optimised media formulations, and ii) modulation of transporter expression. For the first engineering avenue, optimised media formulation, the mechanistic model and correlation matrices serve as a starting point for the development of a mathematical model that can predict transport rates of essential amino acids as a function of their extracellular concentrations. Such a model can then be used to optimise the concentrations of essential amino acids in basal and feed media to maximise cell growth and antibody production. Expanding the mechanistic model to include non-essential amino acid (NEAA) transport is highly desirable. Work from Chapters 4 and 5 indicate that GLAST, SNAT2 and system ASC transporters facilitate NEAA transport in CHO cells. However, the relative contribution that each transporter makes to NEAA transport differs between cell lines. siRNA knockdown of these transporters can help verify their function in each cell line. The second possible engineering avenue, modulation of transporter expression, involves increasing the diversity of transport options for essential amino acid uptake. The transport rate of any branched-chain or aromatic amino acid is currently constrained by the transport of other similar essential amino acids as they compete with one another to enter the cell through LAT1 (overlapping selectivity). Engineering the cell to express additional transporters with the intent of minimising overlapping substrate selectivity can help maximise the transport rate of these amino acids. For example, overexpression of LAT3 or LAT4 (branched-chain amino acid transporters) can help increase the uptake of aromatic amino acids through LAT1.

Appendix A

Table A1 CHO amino acid transporters identified in genome, transcriptome and proteome studies

Gene name (SLC ID)	Protein name	NCBI gene ID	Transcript literature	Protein literature
Proteinogenic amino acid transporters:				
SLC1A1	EAAC1, EAAT3	100760895	Birzele et al., 2010; Kyriakopoulos et al., 2013	-
SLC1A2	GLT-1, EAAT2	100752285	Birzele et al., 2010; Kyriakopoulos et al., 2013	-
SLC1A3	GLAST, EAAT1	100689464	Becker et al., 2011; Birzele et al., 2010; Ji et al., 2007; Kyriakopoulos et al., 2013	Baycin-Hizal et al., 2012
SLC1A4	ASCT1, SATT	100689351	Birzele et al., 2010; Clarke et al., 2011; Doolan et al., 2010; Kyriakopoulos et al., 2013; Marin et al., 2003	Baycin-Hizal et al., 2012
SLC1A5	ASCT2, AAAT	100763902	Becker et al., 2011; Birzele et al., 2010; Clarke et al., 2011; Kyriakopoulos et al., 2013; Shen et al., 2010	Baycin-Hizal et al., 2012
SLC1A6	EATT4	100770833	-	-
SLC1A7	EATT5	100767052	-	Baycin-Hizal et al., 2012
SLC3A1	rBAT	100765887	Birzele et al., 2010; Kyriakopoulos et al., 2013	-
SLC3A2	4F2hc	100689315	Becker et al., 2011; Birzele et al., 2010; Clarke et al., 2011; Fenczik et al., 1997; Kyriakopoulos et al., 2013	Baycin-Hizal et al., 2012
SLC6A5	GlyT2	100761450	Kyriakopoulos et al., 2013	-
SLC6A7	PROT	100764967	-	-
SLC6A9	GlyT1	100774471	Birzele et al., 2010; Kyriakopoulos et al., 2013	-
SLC6A14	ATB0,+	100751194	-	-
SLC6A15	B0AT2, v7-3, NTT7-3	100758864	Becker et al., 2011; Birzele et al., 2010; Kyriakopoulos et al., 2013	-
SLC6A17	XT1, NTT4	100769158	-	-
SLC6A18	B0AT3, XT2	100762871	-	-
SLC6A19	B0AT1, HND	100762288	Kyriakopoulos et al., 2013	-
SLC6A20	XT3, Xtrp3	-	Kyriakopoulos et al., 2013	-
SLC7A1	CAT-1, ATRC1	100689176	Becker et al., 2011; Birzele et al., 2010; Kyriakopoulos et al., 2013	Baycin-Hizal et al., 2012
SLC7A2	CAT-2A and -2B, ATRC2	100772617	Kyriakopoulos et al., 2013	-
SLC7A3	CAT-3, ATRC3	100771829	Birzele et al., 2010; Kyriakopoulos et al., 2013	-
SLC7A5/SLC3A2	LAT1/4F2hc	100768667	Becker et al., 2011; Kyriakopoulos et al., 2013	Baycin-Hizal et al., 2012
SLC7A6/SLC3A2	y+LAT2/4F2hc	100760403	Becker et al., 2011; Birzele et al., 2010; Kyriakopoulos et al., 2013	-

Gene name (SLC ID)	Protein name	NCBI gene ID	Transcript literature	Protein literature
SLC7A7/SLC3A2	y+LAT1/4F2hc	100768258	Birzele et al., 2010; Kyriakopoulos et al., 2013	-
SLC7A8/SLC3A2	LAT2/4F2hc	100770731	Birzele et al., 2010; Kyriakopoulos et al., 2013	-
SLC7A9/SLC3A1	b0,+AT/rBAT	100759612	Kyriakopoulos et al., 2013	-
SLC7A10/SLC3A2	Asc-1/4F2hc	100769905	Kyriakopoulos et al., 2013	-
SLC7A11/SLC3A2	xCT/4F2hc	100764546	Becker et al., 2011; Birzele et al., 2010; Kyriakopoulos et al., 2013	-
SLC7A12	Asc-2	-	-	-
SLC7A13	AGT-1, XAT2	-	-	-
SLC7A15	ArpAT	-	-	-
SLC16A10	TAT1, MCT10	100774015	Kyriakopoulos et al., 2013	-
SLC36A1	PAT1	-	Birzele et al., 2010; Kyriakopoulos et al., 2013	-
SLC36A2	PAT2	100765800	Kyriakopoulos et al., 2013	-
SLC36A4	PAT4	100752115	Becker et al., 2011; Birzele et al., 2010; Kyriakopoulos et al., 2013	-
SLC38A1	SNAT1	100769511	-	-
SLC38A2	SNAT2	100689188	Becker et al., 2011; Birzele et al., 2010; Kyriakopoulos et al., 2013; Lopez-Fontanals et al., 2003; Shen et al., 2010	Baycin-Hizal et al., 2012
SLC38A3	SNAT3	100754504	Birzele et al., 2010; Kyriakopoulos et al., 2013	-
SLC38A4	SNAT4	100769795	Birzele et al., 2010; Kyriakopoulos et al., 2013	-
SLC38A5	SNAT5	100767098	Birzele et al., 2010; Kyriakopoulos et al., 2013	-
SLC38A7	SNAT7	100762550	Becker et al., 2011; Birzele et al., 2010	Baycin-Hizal et al., 2012
SLC43A1	LAT3	100757617	Kyriakopoulos et al., 2013	-
SLC43A2	LAT4	100767730	Becker et al., 2011; Birzele et al., 2010; Kyriakopoulos et al., 2013	-
Orphan transporters:				
SLC7A4	CAT-4	100757506	-	-
SLC7A14		100764763	Birzele et al., 2010	-
SLC36A3	PAT3	100759799	Kyriakopoulos et al., 2013	-
SLC38A6	SNAT6	100752560	Birzele et al., 2010	-
SLC38A8		100750441	-	-
SLC38A9		100767955	Becker et al., 2011; Birzele et al., 2010	-
SLC38A10		100763275	Becker et al., 2011; Birzele et al., 2010	-
SLC38A11		100753232	-	-

Gene name (SLC ID)	Protein name	NCBI gene ID	Transcript literature	Protein literature
SLC43A3	EEG1	100760704	-	-
Di/Tripeptide transporters:				
SLC15A1	PepT1	100760826	Birzele et al., 2010	-
SLC15A2	PepT2	100766001	-	-
SLC15A3	PhT2	100775005	Birzele et al., 2010; Kyriakopoulos et al., 2013	-
SLC15A4	PhT1	100761469	Birzele et al., 2010; Kyriakopoulos et al., 2013	-
Other amino acid transporters:				
SLC6A1	GAT1	100760370	Birzele et al., 2010	-
SLC6A6	TauT	100765478	Birzele et al., 2010; Kyriakopoulos et al., 2013	Baycin-Hizal et al., 2012
SLC6A11	GAT-B, GAT-3	100752493	Birzele et al., 2010	-
SLC6A12	BGT1	100752445	-	-
SLC6A13	GAT2	100752749	Birzele et al., 2010	-

Dash entries indicate that no data exists.

Table A2 Transcript abundance of CAT-S amino acid transporter genes at exponential and stationary growth phase of culture

SLC ID	Protein name	Gene ID	FPKM		Log2 (fold change)
			Exponential	Stationary	
Proteinogenic amino acid transporters:					
SLC1A1	EAAC1, EAAT3	CHOv3_017091	0.00	0.01	0.00
SLC1A2	**GLT-1, EAAT2**	**CHOv3_000503**	**0.99**	**2.22**	**1.17**
SLC1A3	GLAST, EAAT1	CHOv3_015276	11.09	13.38	0.27
		CHOv3_015277	15.83	19.36	0.29
		Total:	26.91	32.74	0.28
SLC1A4	**ASCT1, SATT**	**CHOv3_014644**	**39.08**	**70.68**	**0.86**
SLC1A5	ASCT2, AAAT	-	-	-	-
SLC1A6	EATT4	CHOv3_005410	0.00	0.00	0.00
SLC1A7	EATT5	CHOv3_000133	0.08	0.11	0.49
SLC3A1	rBAT	CHOv3_015117	0.11	0.10	-0.22
SLC3A2	4F2hc	CHOv3_012684	113.23	128.09	0.18
SLC6A5	GlyT2	CHOv3_015162	0.00	0.04	0.00
SLC6A7	PROT	-	-	-	-
SLC6A9	**GlyT1**	**CHOv3_001777**	**4.65**	**8.40**	**0.85**
SLC6A14	ATB0,+	-	-	-	-
SLC6A15	**B0AT2, v7-3, NTT7-3**	**CHOv3_006384**	**21.29**	**28.16**	**0.40**
SLC6A17	XT1, NTT4	-	-	-	-
SLC6A18	B0AT3, XT2	CHOv3_013987	0.27	0.17	-0.70
SLC6A19	B0AT1, HND	CHOv3_001277	0.06	0.03	-1.03
		CHOv3_005126	0.00	0.00	0.00
		CHOv3_012010	0.73	1.00	0.45
		CHOv3_013987	0.27	0.17	-0.70
		Total:	1.06	1.19	0.17
SLC6A20	XT3, Xtrp3	CHOv3_001648	0.12	0.17	0.55
SLC7A1	CAT-1, ATRC1	CHOv3_017350	23.07	24.65	0.10
SLC7A2	CAT-2A and -2B, ATRC2	-	-	-	-
SLC7A3	CAT-3, ATRC3	CHOv3_005547	0.74	0.73	-0.02
SLC7A5	**LAT1**	**CHOv3_013995**	**58.57**	**77.31**	**0.40**

SLC7A6	y+LAT2	CHOv3_017011	23.98	23.86	-0.01
SLC7A7	y+LAT1	CHOv3_014453	7.88	9.48	0.27
SLC7A8	LAT2	CHOv3_013127	0.07	0.11	0.61
SLC7A9	b0,+AT	-	-	-	-
SLC7A10	Asc-1	-	-	-	-
SLC7A11	**xCT**	**CHOv3_014733**	**0.49**	**2.71**	**2.45**
		CHOv3_014734	**2.40**	**12.65**	**2.40**
		Total:	**2.89**	**15.36**	**2.41**
SLC7A12	Asc-2	-	-	-	-
SLC7A13	AGT-1, XAT2	-	-	-	-
SLC7A15	ArpAT	CHOv3_011147	11.64	12.54	0.11
SLC16A10	TAT1, MCT10	CHOv3_014950	0.00	0.00	0.00
SLC36A1	PAT1	CHOv3_008024	7.57	9.97	0.40
SLC36A2	PAT2	-	-	-	-
SLC36A4	**PAT4**	**CHOv3_011956**	**14.06**	**19.67**	**0.48**
SLC38A1	SNAT1	-	-	-	-
SLC38A2	**SNAT2**	**CHOv3_000065**	**28.24**	**38.04**	**0.43**
		CHOv3_000066	61.63	69.43	0.17
		Total:	**89.87**	**107.48**	**0.26**
SLC38A3	SNAT3	CHOv3_006952	0.03	0.00	0.00
SLC38A4	**SNAT4**	**CHOv3_000064**	**3.38**	**5.92**	**0.81**
SLC38A5	SNAT5	CHOv3_006268	0.02	0.06	1.73
SLC38A7	SNAT7	CHOv3_017260	19.29	22.08	0.19
SLC43A1	LAT3	-	-	-	-
SLC43A2	LAT4	CHOv3_013395	28.42	26.07	-0.12
Orphan transporters:					
SLC7A4	CAT-4	-	-	-	-
SLC7A14		CHOv3_013091	0.00	0.02	0.00
SLC36A3	PAT3	-	-	-	-
SLC38A6	SNAT6	CHOv3_017371	15.38	15.55	0.02

SLC38A8		CHOv3_013991	0.00	0.02	0.00
SLC38A9		**CHOv3_015616**	**7.41**	**9.84**	**0.41**
SLC38A10		**CHOv3_013664**	**103.11**	**130.61**	**0.34**
SLC38A11		CHOv3_000880	0.00	0.00	0.00
SLC43A4	EEG1	-	-	-	-
Di/Tripeptide transporters:					
SLC15A1	PepT1	CHOv3_004436	0.00	0.00	0.00
SLC15A2	PepT2	CHOv3_014577	0.02	0.22	3.76
SLC15A3	PhT2	CHOv3_008787	36.95	43.88	0.25
SLC15A4	**PhT1**	**CHOv3_000890**	**12.50**	**20.46**	**0.71**
Other amino acid transporters:					
SLC6A1	GAT1	-	-	-	-
SLC6A6	TauT	CHOv3_017568	82.25	87.67	0.09
SLC6A11	GAT-B, GAT-3	CHOv3_016377	0.00	0.02	0.00
SLC6A12	BGT1	CHOv3_011902	0.01	0.01	0.10
SLC6A13	GAT2	-	-	-	-

All FPKM values are the average of two independently sequenced samples. Significant fold changes are in bold (Q-value < 0.05). Transporters with multiple gene entries had their FPKM values summed to calculate total fold change, which was designated significant if at least one gene entry exhibited a significant fold change. Dash entries indicate that no transcriptomic data exists.

Table A3 Transcript abundance of GS-Null amino acid transporter genes at exponential and stationary growth phase of culture

SLC ID	Protein name	Gene ID	FPKM		Log2 (fold change)
			Exponential	Stationary	
Proteinogenic amino acid transporters:					
SLC1A1	EAAC1, EAAT3	CHOv3_017091	0.00	0.01	0.00
SLC1A2	**GLT-1, EAAT2**	**CHOv3_000503**	**2.25**	**4.01**	**0.83**
SLC1A3	GLAST, EAAT1	CHOv3_015276	19.42	21.50	0.15
		CHOv3_015277	27.22	29.49	0.12
		Total:	46.64	50.99	0.13
SLC1A4	**ASCT1, SATT**	**CHOv3_014644**	**39.76**	**80.95**	**1.03**
SLC1A5	ASCT2, AAAT	-	-	-	-
SLC1A6	EATT4	CHOv3_005410	0.00	0.00	0.00
SLC1A7	EATT5	CHOv3_000133	0.07	0.20	1.62
SLC3A1	rBAT	CHOv3_015117	0.07	0.27	1.83
SLC3A2	4F2hc	CHOv3_012684	136.64	138.43	0.02
SLC6A5	GlyT2	CHOv3_015162	0.00	0.00	0.00
SLC6A7	PROT	-	-	-	-
SLC6A9	GlyT1	CHOv3_001777	10.31	12.25	0.25
SLC6A14	ATB0,+	-	-	-	-
SLC6A15	B0AT2, v7-3, NTT7-3	CHOv3_006384	27.38	31.66	0.21
SLC6A17	XT1, NTT4	-	-	-	-
SLC6A18	B0AT3, XT2	CHOv3_013987	0.23	0.16	-0.55
SLC6A19	B0AT1, HND	CHOv3_001277	0.00	0.06	0.00
		CHOv3_005126	0.00	0.00	0.00
		CHOv3_012010	0.81	0.66	-0.30
		CHOv3_013987	0.23	0.16	-0.55
		Total:	1.04	0.88	-0.25
SLC6A20	XT3, Xtrp3	CHOv3_001648	0.06	0.22	1.96
SLC7A1	CAT-1, ATRC1	CHOv3_017350	25.71	26.00	0.02
SLC7A2	CAT-2A and -2B, ATRC2	-	-	-	-
SLC7A3	CAT-3, ATRC3	CHOv3_005547	1.21	1.48	0.29
SLC7A5	LAT1	CHOv3_013995	81.76	82.27	0.01

SLC7A6	y+LAT2	CHOv3_017011	23.54	21.69	-0.12
SLC7A7	y+LAT1	CHOv3_014453	12.05	12.73	0.08
SLC7A8	LAT2	CHOv3_013127	0.06	0.06	0.02
SLC7A9	b0,+AT	-	-	-	-
SLC7A10	Asc-1	-	-	-	-
SLC7A11	**xCT**	**CHOv3_014733**	**1.41**	**3.91**	**1.47**
		CHOv3_014734	**8.04**	**18.67**	**1.22**
		Total:	**9.45**	**22.58**	**1.26**
SLC7A12	Asc-2	-	-	-	-
SLC7A13	AGT-1, XAT2	-	-	-	-
SLC7A15	ArpAT	CHOv3_011147	9.65	12.31	0.35
SLC16A10	TAT1, MCT10	CHOv3_014950	0.01	0.04	2.12
SLC36A1	PAT1	CHOv3_008024	9.53	12.40	0.38
SLC36A2	PAT2	-	-	-	-
SLC36A4	**PAT4**	**CHOv3_011956**	**17.43**	**23.72**	**0.44**
SLC38A1	SNAT1	-	-	-	-
SLC38A2	SNAT2	CHOv3_000065	45.01	54.82	0.28
		CHOv3_000066	82.21	94.28	0.20
		Total:	127.22	149.09	0.23
SLC38A3	SNAT3	CHOv3_006952	0.00	0.00	0.00
SLC38A4	**SNAT4**	**CHOv3_000064**	**5.01**	**8.40**	**0.75**
SLC38A5	SNAT5	CHOv3_006268	0.02	0.23	3.70
SLC38A7	SNAT7	CHOv3_017260	20.14	16.74	-0.27
SLC43A1	LAT3	-	-	-	-
SLC43A2	LAT4	CHOv3_013395	18.41	14.62	-0.33
Orphan transporters:					
SLC7A4	CAT-4	-	-	-	-
SLC7A14		CHOv3_013091	0.00	0.01	0.00
SLC36A3	PAT3	-	-	-	-
SLC38A6	SNAT6	CHOv3_017371	18.60	14.76	-0.33

SLC38A8		CHOv3_013991	0.00	0.01	0.00
SLC38A9		CHOv3_015616	9.27	9.99	0.11
SLC38A10		**CHOv3_013664**	**91.86**	**146.91**	**0.68**
SLC38A11		CHOv3_000880	0.01	0.03	1.77
SLC43A4	EEG1	-	-	-	-
Di/Tripeptide transporters:					
SLC15A1	PepT1	CHOv3_004436	0.00	0.02	0.00
SLC15A2	PepT2	CHOv3_014577	0.01	0.03	2.37
SLC15A3	**PhT2**	**CHOv3_008787**	**44.78**	**58.50**	**0.39**
SLC15A4	**PhT1**	**CHOv3_000890**	**11.45**	**17.04**	**0.57**
Other amino acid transporters:					
SLC6A1	GAT1	-	-	-	-
SLC6A6	TauT	CHOv3_017568	41.07	32.55	-0.34
SLC6A11	GAT-B, GAT-3	CHOv3_016377	0.00	0.01	0.00
SLC6A12	BGT1	CHOv3_011902	0.00	0.02	0.00
SLC6A13	GAT2	-	-	-	-

All FPKM values are the average of two independently sequenced samples. Significant fold changes are in bold (Q-value < 0.05). Transporters with multiple gene entries had their FPKM values summed to calculate total fold change, which was designated significant if at least one gene entry exhibited a significant fold change. Dash entries indicate that no transcriptomic data exists.

Table A4 Transcript abundance of T127 amino acid transporter genes at exponential and stationary growth phase of culture

SLC ID	Protein name	Gene ID	FPKM		Log2 (fold change)
			Exponential	Stationary	
Proteinogenic amino acid transporters:					
SLC1A1	EAAC1, EAAT3	CHOv3_017091	0.00	0.00	0.00
SLC1A2	**GLT-1, EAAT2**	**CHOv3_000503**	**0.90**	**2.55**	**1.50**
SLC1A3	**GLAST, EAAT1**	**CHOv3_015276**	**8.04**	**23.44**	**1.54**
		CHOv3_015277	31.31	36.51	0.22
		Total:	**39.35**	**59.95**	**0.61**
SLC1A4	**ASCT1, SATT**	**CHOv3_014644**	**76.81**	**243.63**	**1.67**
SLC1A5	ASCT2, AAAT	-	-	-	-
SLC1A6	EATT4	CHOv3_005410	0.00	0.00	0.00
SLC1A7	EATT5	CHOv3_000133	0.03	0.11	1.78
SLC3A1	rBAT	CHOv3_015117	0.18	0.16	-0.12
SLC3A2	**4F2hc**	**CHOv3_012684**	**161.58**	**215.08**	**0.41**
SLC6A5	GlyT2	CHOv3_015162	0.00	0.04	0.00
SLC6A7	PROT	-	-	-	-
SLC6A9	**GlyT1**	**CHOv3_001777**	**7.07**	**13.14**	**0.89**
SLC6A14	ATB0,+	-	-	-	-
SLC6A15	B0AT2, v7-3, NTT7-3	CHOv3_006384	16.66	20.06	0.27
SLC6A17	XT1, NTT4	-	-	-	-
SLC6A18	B0AT3, XT2	CHOv3_013987	0.34	0.27	-0.34
SLC6A19	B0AT1, HND	CHOv3_001277	0.00	0.00	0.00
		CHOv3_005126	0.00	0.00	0.00
		CHOv3_012010	0.68	0.81	0.25
		CHOv3_013987	0.34	0.27	-0.34
		Total:	1.02	1.08	0.08
SLC6A20	XT3, Xtrp3	CHOv3_001648	0.10	0.14	0.39
SLC7A1	CAT-1, ATRC1	CHOv3_017350	26.09	28.31	0.12
SLC7A2	CAT-2A and -2B, ATRC2	-	-	-	-
SLC7A3	CAT-3, ATRC3	CHOv3_005547	0.65	0.42	-0.63
SLC7A5	**LAT1**	**CHOv3_013995**	**30.85**	**91.26**	**1.56**

SLC7A6	y+LAT2	CHOv3_017011	23.25	20.53	-0.18
SLC7A7	y+LAT1	CHOv3_014453	11.77	13.70	0.22
SLC7A8	LAT2	CHOv3_013127	0.06	0.07	0.21
SLC7A9	b0,+AT	-	-	-	-
SLC7A10	Asc-1	-	-	-	-
SLC7A11	**xCT**	**CHOv3_014733**	**0.73**	**8.26**	**3.51**
		CHOv3_014734	**5.26**	**41.60**	**2.98**
		Total:	**5.99**	**49.86**	**3.06**
SLC7A12	Asc-2	-	-	-	-
SLC7A13	AGT-1, XAT2	-	-	-	-
SLC7A15	ArpAT	CHOv3_011147	12.76	14.12	0.15
SLC16A10	TAT1, MCT10	CHOv3_014950	0.00	0.02	0.00
SLC36A1	**PAT1**	**CHOv3_008024**	**5.70**	**10.30**	**0.85**
SLC36A2	PAT2	-	-	-	-
SLC36A4	**PAT4**	**CHOv3_011956**	**10.89**	**19.91**	**0.87**
SLC38A1	SNAT1	-	-	-	-
SLC38A2	**SNAT2**	**CHOv3_000065**	**17.27**	**42.06**	**1.28**
		CHOv3_000066	75.92	87.34	0.20
		Total:	**93.19**	**129.40**	**0.47**
SLC38A3	SNAT3	CHOv3_006952	0.03	0.06	0.73
SLC38A4	SNAT4	CHOv3_000064	7.68	7.57	-0.02
SLC38A5	SNAT5	CHOv3_006268	0.05	0.20	2.14
SLC38A7	SNAT7	CHOv3_017260	19.62	22.06	0.17
SLC43A1	LAT3	-	-	-	-
SLC43A2	LAT4	CHOv3_013395	18.87	19.74	0.07
Orphan transporters:					
SLC7A4	CAT-4	-	-	-	-
SLC7A14		CHOv3_013091	0.00	0.00	0.00
SLC36A3	PAT3	-	-	-	-
SLC38A6	SNAT6	CHOv3_017371	20.65	17.19	-0.26

SLC38A8		CHOv3_013991	0.00	0.00	0.00
SLC38A9		**CHOv3_015616**	**6.47**	**9.46**	**0.55**
SLC38A10		**CHOv3_013664**	**62.90**	**93.22**	**0.57**
SLC38A11		CHOv3_000880	0.01	0.01	-0.13
SLC43A4	EEG1	-	-	-	-
Di/Tripeptide transporters:					
SLC15A1	PepT1	CHOv3_004436	0.01	0.04	2.46
SLC15A2	PepT2	CHOv3_014577	0.04	0.23	2.59
SLC15A3	PhT2	**CHOv3_008787**	**44.34**	**26.97**	**-0.72**
SLC15A4	PhT1	CHOv3_000890	12.04	14.36	0.25
Other amino acid transporters:					
SLC6A1	GAT1	-	-	-	-
SLC6A6	TauT	**CHOv3_017568**	**57.82**	**77.54**	**0.42**
SLC6A11	GAT-B, GAT-3	CHOv3_016377	0.00	0.01	0.00
SLC6A12	BGT1	CHOv3_011902	0.00	0.02	0.00
SLC6A13	GAT2	-	-	-	-

All FPKM values are the average of two independently sequenced samples. Significant fold changes are in bold (Q-value < 0.05). Transporters with multiple gene entries had their FPKM values summed to calculate total fold change, which was designated significant if at least one gene entry exhibited a significant fold change. Dash entries indicate that no transcriptomic data exists.

Table A5 FPKM boundaries for low, medium and high gene expression in CAT-S, GS-Null and T127 cells at exponential and stationary growth phase

	CAT-S	
Expression level	**Exponential**	**Stationary**
Low (bottom 25th percentile)	FPKM ≤ 3.67	FPKM ≤ 2.99
Medium (middle 50th percentile)	3.67 < FPKM ≤ 41.03	2.99 < FPKM ≤ 39.16
High (top 25th percentile)	FPKM > 41.03	FPKM > 39.16

	GS-Null	
Expression level	**Exponential**	**Stationary**
Low (bottom 25th percentile)	FPKM ≤ 4.22	FPKM ≤ 3.07
Medium (middle 50th percentile)	4.22 < FPKM ≤ 41.49	3.07 < FPKM ≤ 38.16
High (top 25th percentile)	FPKM > 41.49	FPKM > 38.16

	T127	
Expression level	**Exponential**	**Stationary**
Low (bottom 25th percentile)	FPKM ≤ 3.55	FPKM ≤ 3.25
Medium (middle 50th percentile)	3.55 < FPKM ≤ 40.70	3.25 < FPKM ≤ 39.06
High (top 25th percentile)	FPKM > 40.70	FPKM > 39.06

Small neutral amino acids

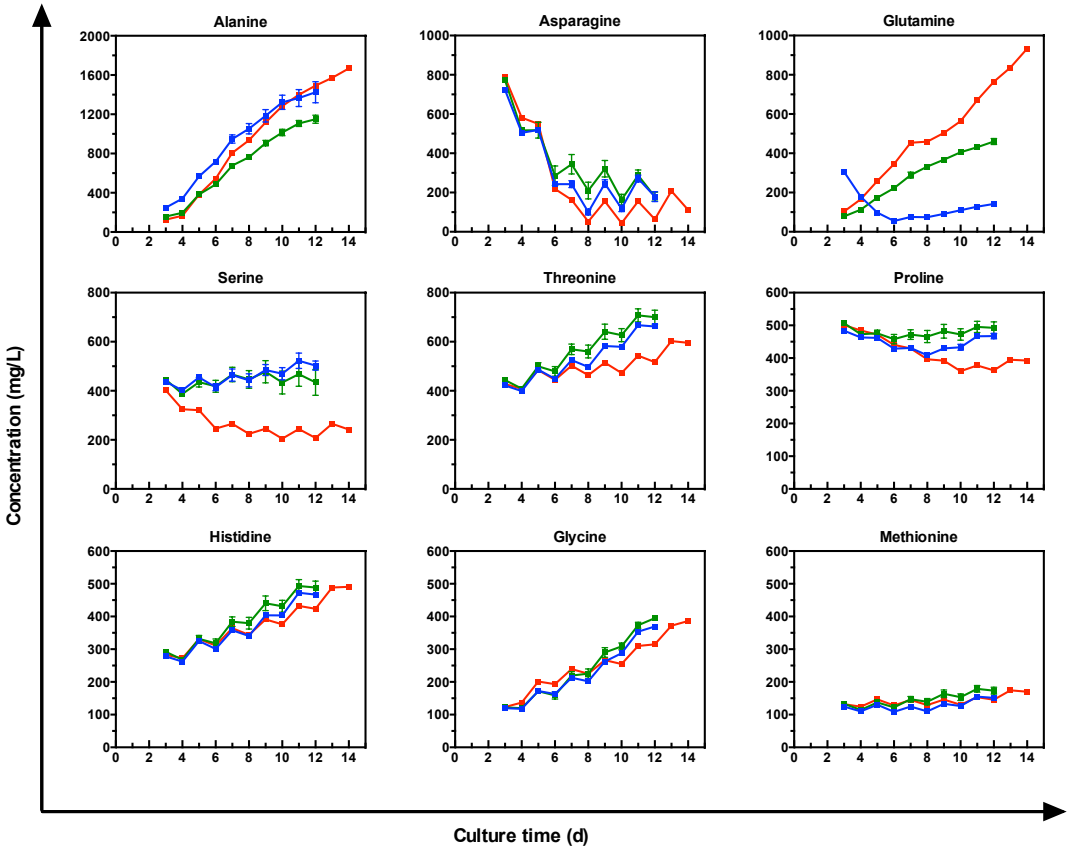

Branch-chained and aromatic amino acids

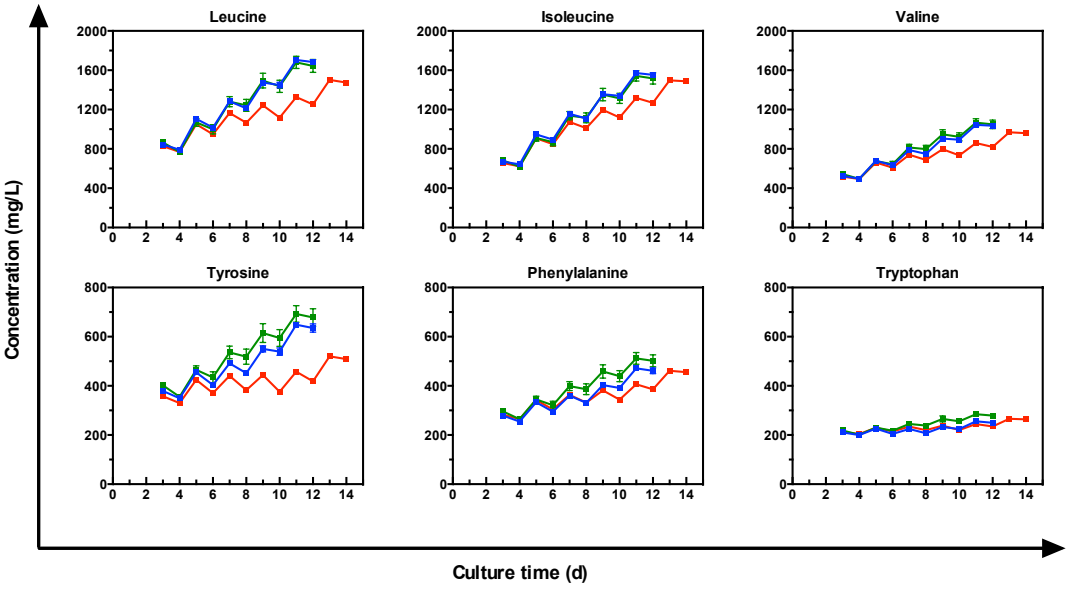

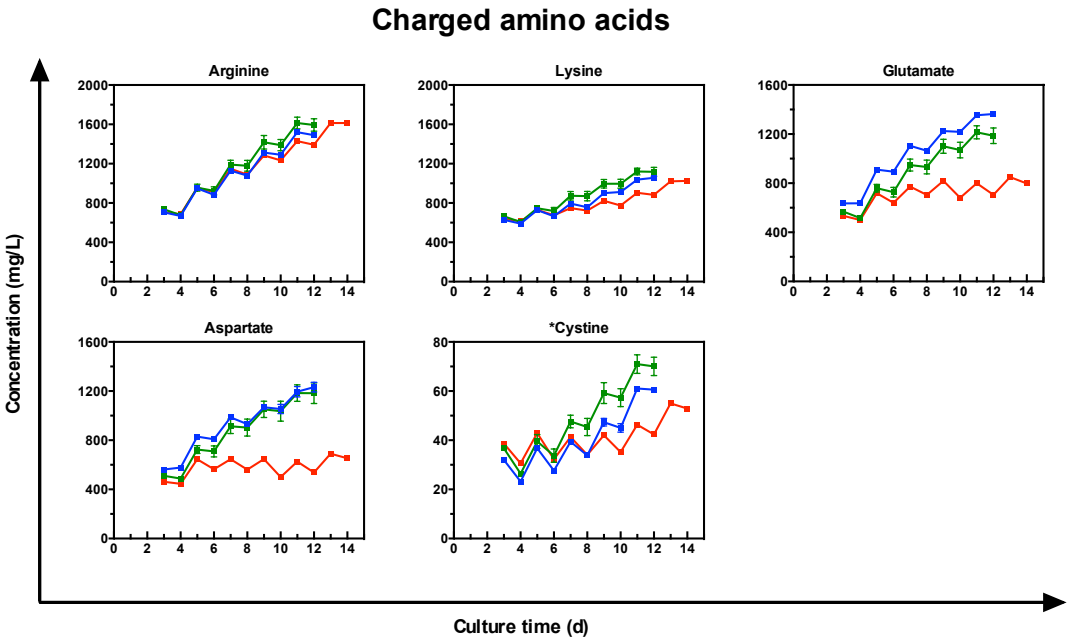

Figure A1 Extracellular amino acid concentrations for CAT-S, GS-Null, and T127 cells throughout fed-batch culture. CAT-S (blue) and GS-Null (green) concentrations are measured from parallel duplicate 1-L bioreactors (mean ± SEM, n = 2). T127 (red) concentrations are from a single bioreactor. Amino acids are grouped by charge and size. *Cystine is included with the anionic group due its transport dependence upon glutamate via the xCT transporter.

Appendix B

Table B1 Design matrix for the two-level factorial experiment showing factor interactions, response variable data and calculated effects

		Indvidual factors				Factor combinations (interactions)											Response variables (% of vehicle control)		
Standard	Run	M	B	S	G	MB	MS	MG	BS	BG	SG	MBS	MBG	BSG	MSG	MBSG	Growth rate	Culture viability	Specific productivity
11	1	-	+	-	+	-	+	-	-	+	-	+	-	-	+	+	59.4	97.3	106.6
16	2	+	+	+	+	+	+	+	+	+	+	+	+	+	+	+	18.7	68.7	71.9
10	3	+	-	-	+	-	-	+	+	-	-	+	-	+	-	+	65.4	95.1	94.1
2	4	+	-	-	-	-	-	-	+	+	+	+	+	-	+	-	73.3	98.7	88.1
15	5	-	+	+	+	-	-	-	+	+	+	-	-	+	-	-	27.5	68.6	68.0
1	6	-	-	-	-	+	+	+	+	+	+	-	-	-	-	+	100.0	100.0	100.0
8	7	+	+	+	-	+	+	-	+	-	-	+	-	-	-	-	44.5	82.6	79.8
13	8	-	-	+	+	+	-	-	-	-	+	+	+	-	-	+	34.0	73.7	69.7
9	9	-	-	-	+	+	+	-	+	-	-	-	+	+	+	-	72.8	95.4	91.9
7	10	-	+	+	-	-	-	+	+	-	-	-	+	-	+	+	46.0	81.5	70.0
12	11	+	+	-	+	+	-	+	-	+	-	-	+	-	-	-	42.3	95.5	86.9
14	12	+	-	+	+	-	+	+	-	-	+	-	-	-	+	-	28.6	71.2	73.6
3	13	-	+	-	-	-	+	+	-	-	+	+	+	+	-	-	84.5	99.3	117.0
4	14	+	+	-	-	+	-	-	-	-	+	-	-	+	+	+	50.0	98.1	99.7
6	15	+	-	+	-	-	+	+	-	+	-	-	+	+	-	+	60.5	92.7	63.0
5	16	-	-	+	-	+	-	-	-	+	-	+	-	+	+	-	76.1	89.4	82.5
Growth rate effect:		-14.63	-17.23	-26.5	-23.29	-0.84	6.78	4.93	1.6	3.98	-6.3	3.54	-2.42	3.41	-4.22	-1.94			
Viability effect:		-0.33	-3.08	-18.87	-9.59	-0.13	0.81	-0.79	-3.33	1.74	-6.38	0.21	0.41	0.82	-0.93	0.79			
Productivity effect:		-6.07	4.63	-25.73	-4.65	0.25	5.62	3.66	-4.39	-3.61	1.66	7.07	-5.74	1.67	0.72	-1.61			

The factorial experiment was set up by following the randomised run order. The response variables show the average data taken from Figure 5.20. +, inhibitor applied at IC_{25} concentration; -, inhibitor applied at 0 mM; *M*, MeAIB (5 mM); *B*, BCH (10 mM); *S*, SAS (0.6 mM); *G*, GPNA (0.4 mM).

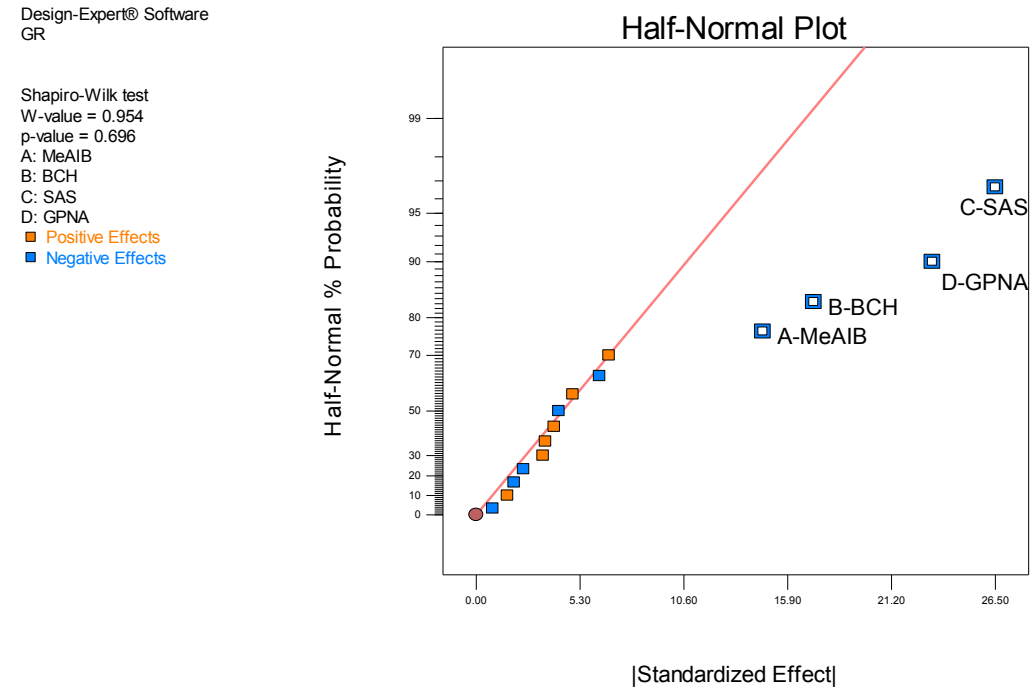

Figure B1 Half-normal probability plot of absolute effects for growth response. Factors identified as significant are labeled.

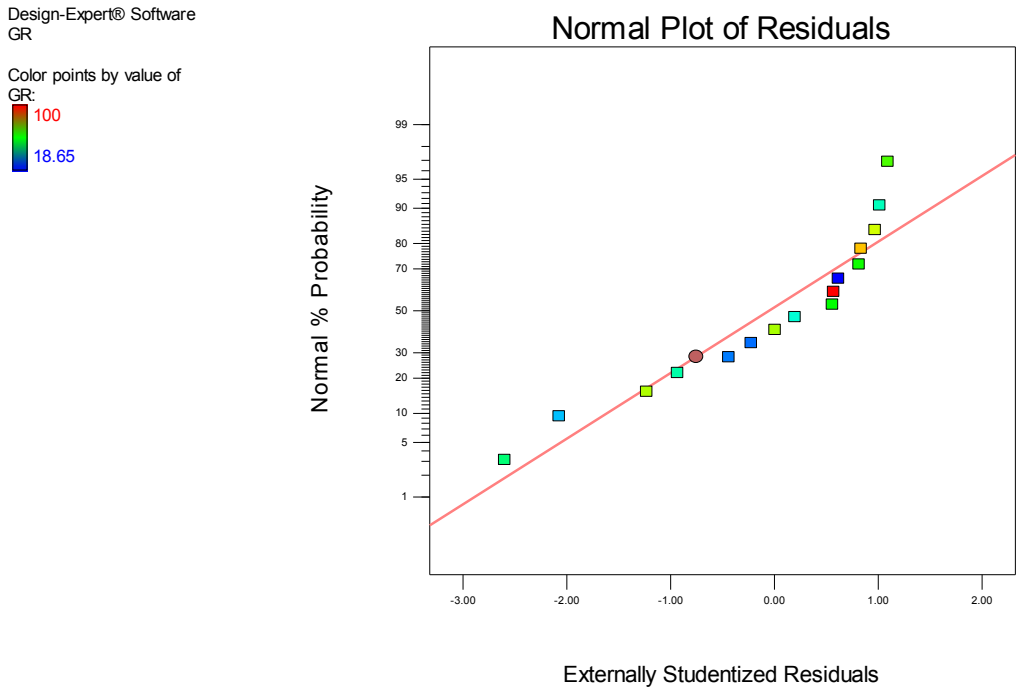

Figure B2 Normal probability plot of residuals for growth rate.

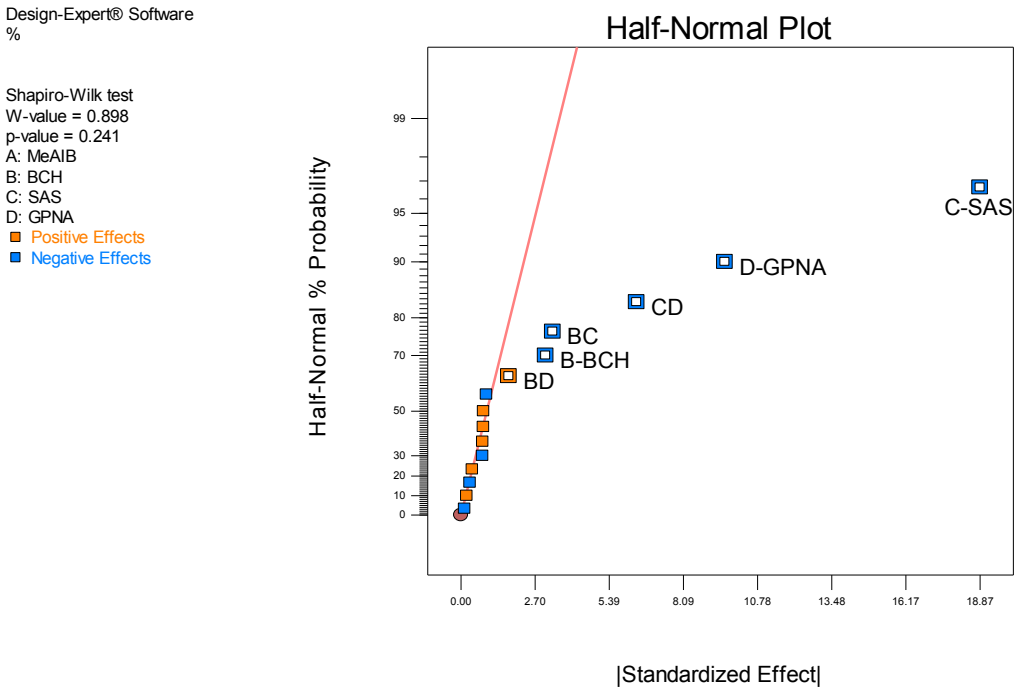

Figure B3 Half-normal probability plot of absolute effects for culture viability. Factors identified as significant are labeled.

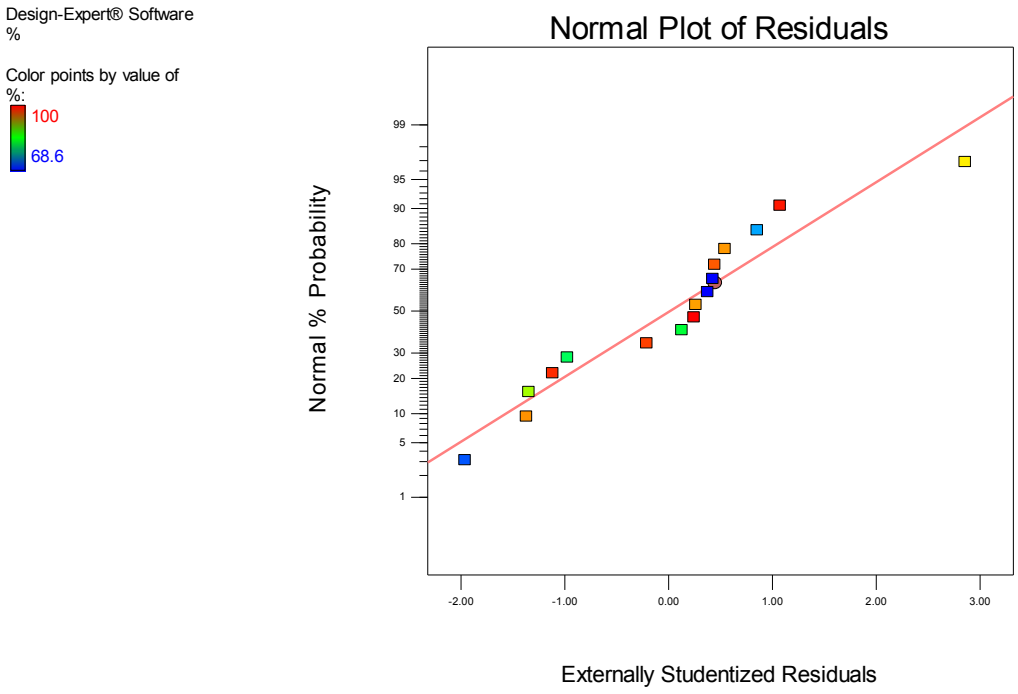

Figure B4 Normal probability plot of residuals for culture viability.

A

Design-Expert® Software
Factor Coding: Actual
%

X1 = C: SAS
X2 = D: GPNA

Actual Factors
A: MeAIB = 0
B: BCH = 0

■ D- -1
▲ D+ 1

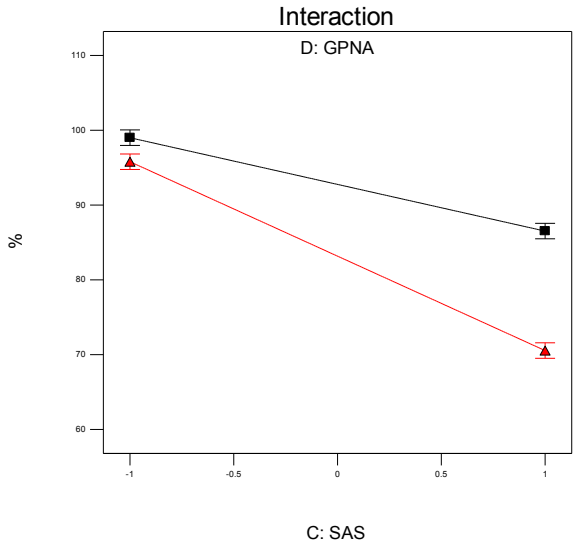

B

Design-Expert® Software
Factor Coding: Actual
%

X1 = B: BCH
X2 = C: SAS

Actual Factors
A: MeAIB = 0
D: GPNA = 0

■ C- -1
▲ C+ 1

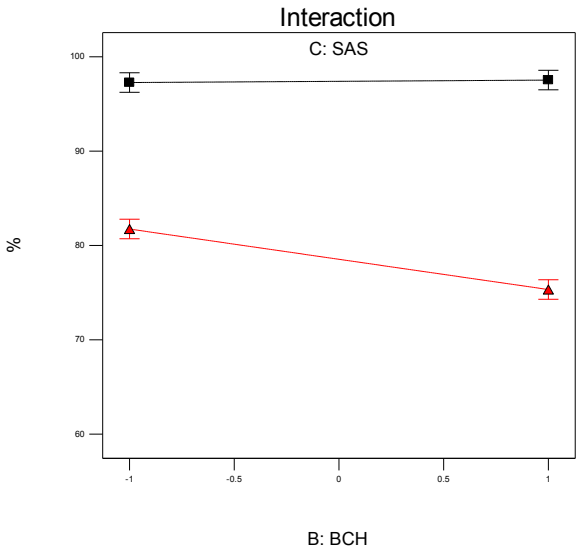

C

Design-Expert® Software
Factor Coding: Actual
%

X1 = B: BCH
X2 = D: GPNA

Actual Factors
A: MeAIB = 0
C: SAS = 0

■ D- -1
▲ D+ 1

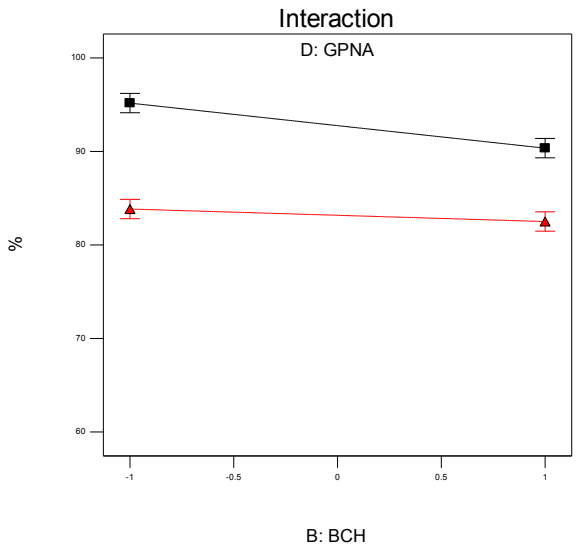

Figure B5 Interactions between systems ASC, L, and X_C^- for culture viability. (**A**.) Interaction of systems X_C^- and ASC; (**B.**) Interaction of systems L and X_C^-; (**C.**) Interaction of systems L and ASC.

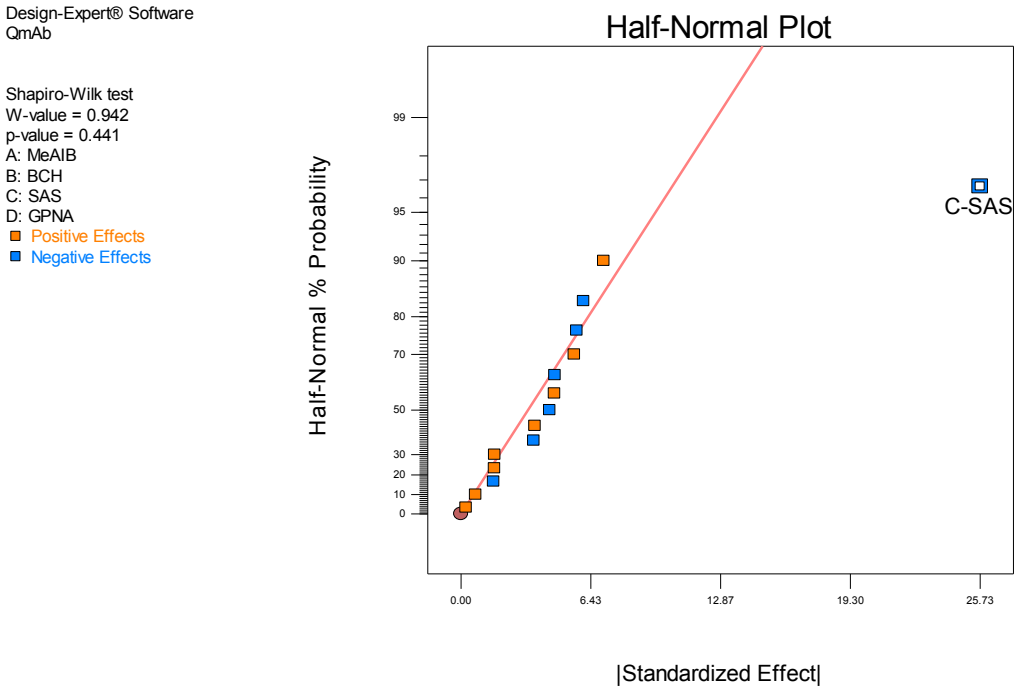

Figure B6 Half-normal probability plot of absolute effects for specific productivity. SAS factor identified as significant is labeled.

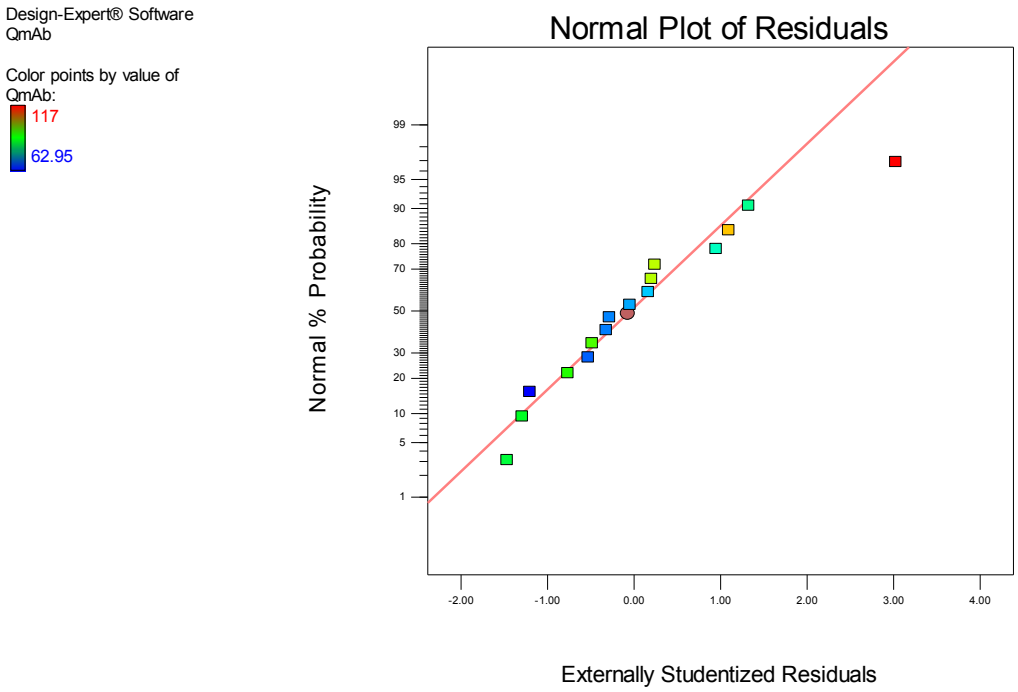

Figure B7 Normal probability plot of residuals for specific productivity.

Appendix C

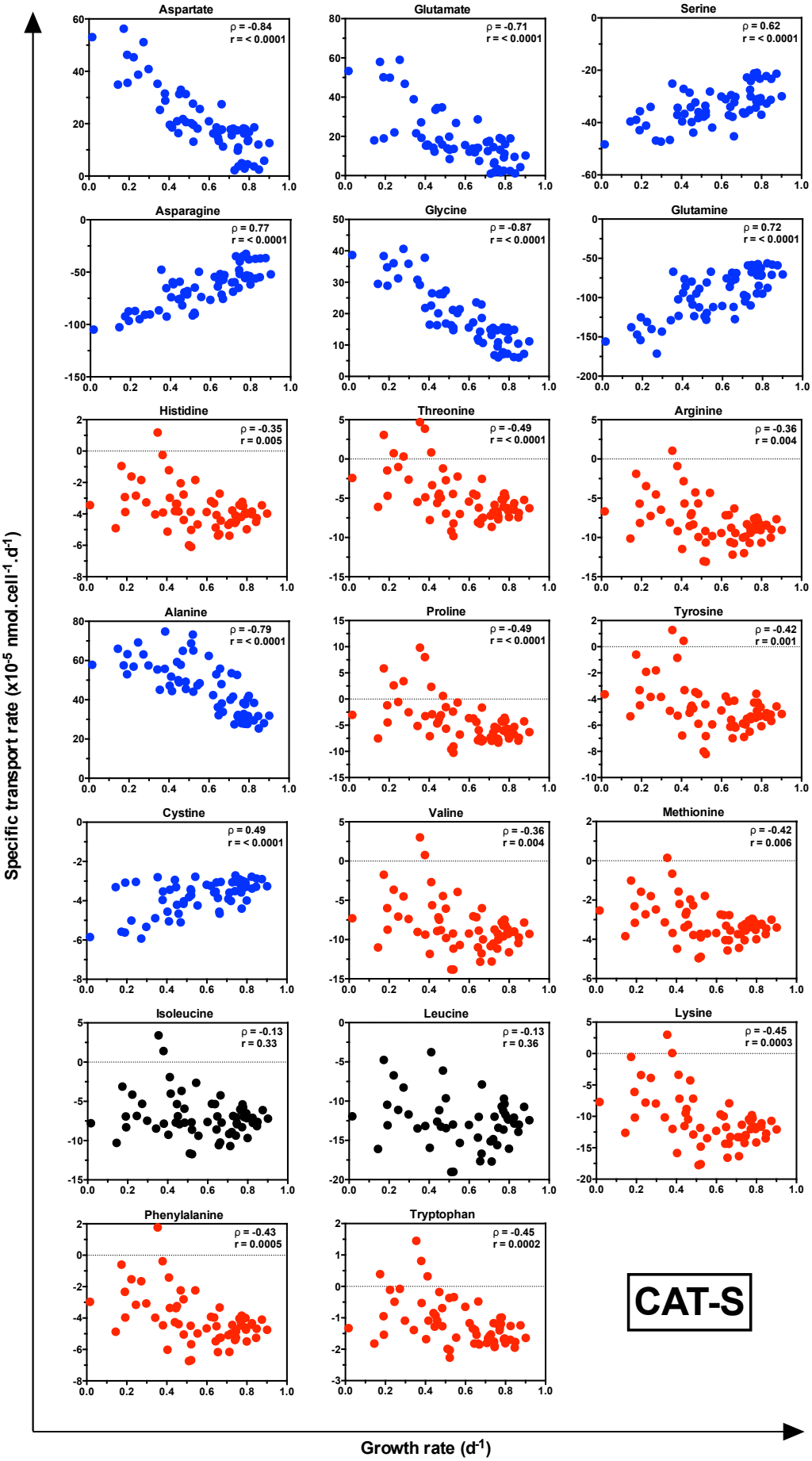
Aspartate
ρ = -0.84
r = < 0.0001
Glutamate
ρ = -0.71
r = < 0.0001
Serine
ρ = 0.62
r = < 0.0001
Asparagine
ρ = 0.77
r = < 0.0001
Glycine
ρ = -0.87
r = < 0.0001
Glutamine
ρ = 0.72
r = < 0.0001
Histidine
ρ = -0.35
r = 0.005
Threonine
ρ = -0.49
r = < 0.0001
Arginine
ρ = -0.36
r = 0.004
Alanine
ρ = -0.79
r = < 0.0001
Proline
ρ = -0.49
r = < 0.0001
Tyrosine
ρ = -0.42
r = 0.001
Cystine
ρ = 0.49
r = < 0.0001
Valine
ρ = -0.36
r = 0.004
Methionine
ρ = -0.42
r = 0.006
Isoleucine
ρ = -0.13
r = 0.33
Leucine
ρ = -0.13
r = 0.36
Lysine
ρ = -0.45
r = 0.0003
Phenylalanine
ρ = -0.43
r = 0.0005
Tryptophan
ρ = -0.45
r = 0.0002
CAT-S
Specific transport rate (x10-5 nmol.cell-1.d-1)
Growth rate (d-1)

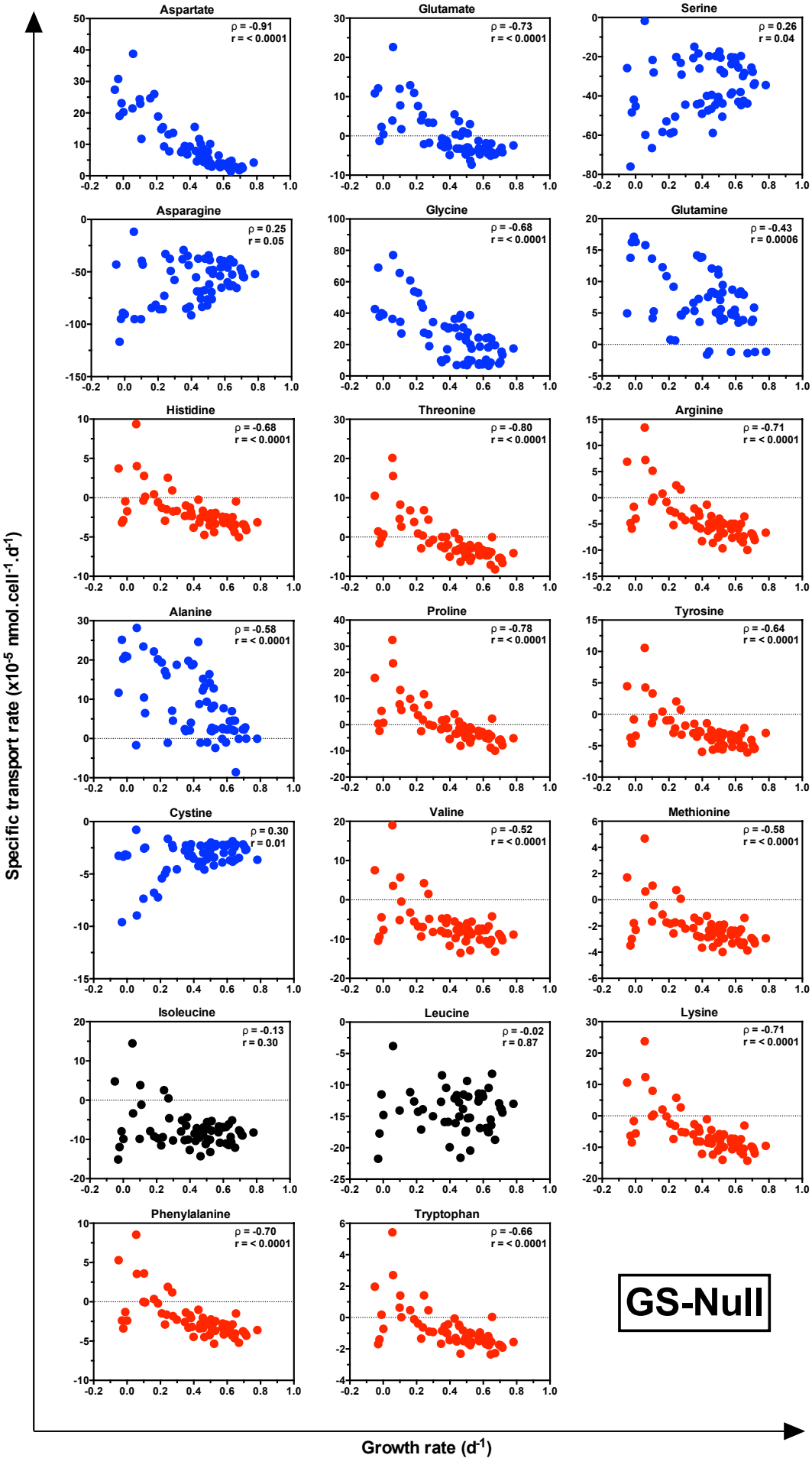
Aspartate
ρ = -0.91
r = < 0.0001
Glutamate
ρ = -0.73
r = < 0.0001
Serine
ρ = 0.26
r = 0.04
Asparagine
ρ = 0.25
r = 0.05
Glycine
ρ = -0.68
r = < 0.0001
Glutamine
ρ = -0.43
r = 0.0006
Histidine
ρ = -0.68
r = < 0.0001
Threonine
ρ = -0.80
r = < 0.0001
Arginine
ρ = -0.71
r = < 0.0001
Alanine
ρ = -0.58
r = < 0.0001
Proline
ρ = -0.78
r = < 0.0001
Tyrosine
ρ = -0.64
r = < 0.0001
Cystine
ρ = 0.30
r = 0.01
Valine
ρ = -0.52
r = < 0.0001
Methionine
ρ = -0.58
r = < 0.0001
Isoleucine
ρ = -0.13
r = 0.30
Leucine
ρ = -0.02
r = 0.87
Lysine
ρ = -0.71
r = < 0.0001
Phenylalanine
ρ = -0.70
r = < 0.0001
Tryptophan
ρ = -0.66
r = < 0.0001
GS-Null
Specific transport rate (x10-5 nmol.cell-1.d-1)
Growth rate (d-1)

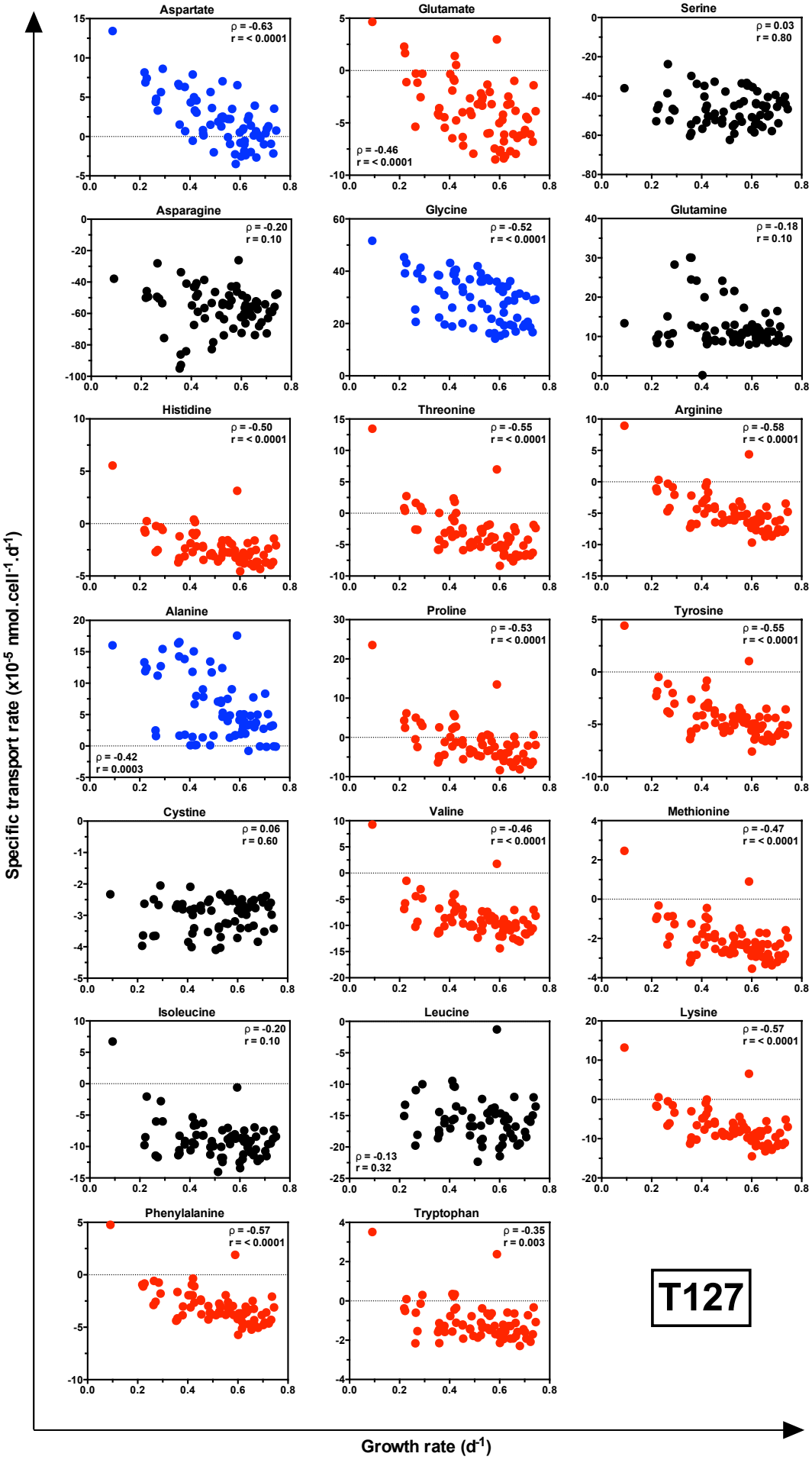
Aspartate
ρ = -0.63
r = < 0.0001
Glutamate
ρ = -0.46
r = < 0.0001
Serine
ρ = 0.03
r = 0.80
Asparagine
ρ = -0.20
r = 0.10
Glycine
ρ = -0.52
r = < 0.0001
Glutamine
ρ = -0.18
r = 0.10
Histidine
ρ = -0.50
r = < 0.0001
Threonine
ρ = -0.55
r = < 0.0001
Arginine
ρ = -0.58
r = < 0.0001
Alanine
ρ = -0.42
r = 0.0003
Proline
ρ = -0.53
r = < 0.0001
Tyrosine
ρ = -0.55
r = < 0.0001
Cystine
ρ = 0.06
r = 0.60
Valine
ρ = -0.46
r = < 0.0001
Methionine
ρ = -0.47
r = < 0.0001
Isoleucine
ρ = -0.20
r = 0.10
Leucine
ρ = -0.13
r = 0.32
Lysine
ρ = -0.57
r = < 0.0001
Phenylalanine
ρ = -0.57
r = < 0.0001
Tryptophan
ρ = -0.35
r = 0.003
T127
Specific transport rate (x10-5 nmol.cell-1.d-1)
Growth rate (d-1)

Figure C1 Relationships between transport rates of individual amino acids and growth rates in CAT-S, GS-Null and T127 cells. For each of the 62, 64 and 71 transport profiles for CAT-S, GS-Null and T127 cells respectively, the specific transport rate for an individual amino acid was plotted against growth rate. Spearman's rank correlation was performed using GraphPad Prism v6.0 (GraphPad Software, San Diego, USA) to analyse these relationships. Blue and red data points indicate amino acids with significant ($P < 0.05$) increased and decreased transport rates respectively as a function of decreasing growth rates.

Table C1 Spearman's rank correlation coefficient values for CAT-S cells

	Asp																			
Asp	1.00	**Glu**																		
Glu	0.95	1.00	**Ser**																	
Ser	-0.77	-0.78	1.00	**Asn**																
Asn	-0.88	-0.78	0.82	1.00	**Gly**															
Gly	0.94	0.89	-0.73	-0.78	1.00	**Gln**														
Gln	-0.90	-0.86	0.87	0.96	-0.80	1.00	**His**													
His	0.31	0.31	0.11	0.02	0.47	-0.01	1.00	**Thr**												
Thr	0.49	0.49	-0.05	-0.16	0.62	-0.21	0.96	1.00	**Arg**											
Arg	0.30	0.31	0.06	0.05	0.48	0.00	0.97	0.93	1.00	**Ala**										
Ala	0.85	0.72	-0.67	-0.92	0.80	-0.87	0.11	0.28	0.06	1.00	**Pro**									
Pro	0.51	0.52	-0.06	-0.19	0.60	-0.24	0.93	0.97	0.87	0.33	1.00	**Tyr**								
Tyr	0.45	0.45	-0.03	-0.13	0.57	-0.16	0.94	0.94	0.92	0.20	0.89	1.00	**Cys2**							
Cys2	-0.66	-0.72	0.81	0.65	-0.64	0.71	-0.10	-0.22	-0.13	-0.51	-0.26	-0.21	1.00	**Val**						
Val	0.30	0.29	0.09	0.05	0.47	0.01	0.99	0.94	0.99	0.08	0.90	0.93	-0.10	1.00	**Met**					
Met	0.30	0.31	0.05	0.06	0.47	0.01	0.95	0.92	0.99	0.05	0.85	0.91	-0.10	0.98	1.00	**Ile**				
Ile	0.01	0.01	0.33	0.30	0.21	0.29	0.92	0.81	0.90	-0.14	0.77	0.83	0.09	0.93	0.89	1.00	**Leu**			
Leu	0.14	0.17	0.26	0.15	0.22	0.10	0.97	0.89	0.95	-0.14	0.86	0.88	-0.17	0.97	0.94	0.98	1.00	**Lys**		
Lys	0.41	0.42	-0.03	-0.07	0.56	-0.12	0.97	0.97	0.99	0.15	0.91	0.94	-0.20	0.98	0.98	0.87	0.92	1.00	**Phe**	
Phe	0.41	0.42	-0.01	-0.07	0.56	-0.11	0.97	0.97	0.98	0.18	0.91	0.94	-0.17	0.97	0.97	0.85	0.92	0.99	1.00	**Trp**
Trp	0.52	0.54	-0.06	-0.22	0.57	-0.27	0.85	0.89	0.76	0.38	0.95	0.80	-0.26	0.80	0.74	0.70	0.76	0.80	0.82	1.00

Table C2 Spearman's rank correlation coefficient values for GS-Null cells

	Asp																			
Asp	1.00	**Glu**																		
Glu	0.87	1.00	**Ser**																	
Ser	-0.46	-0.37	1.00	**Asn**																
Asn	-0.39	-0.22	0.94	1.00	**Gly**															
Gly	0.84	0.73	-0.78	-0.70	1.00	**Gln**														
Gln	0.46	0.19	-0.54	-0.66	0.52	1.00	**His**													
His	0.64	0.66	0.13	0.21	0.39	0.05	1.00	**Thr**												
Thr	0.80	0.80	-0.07	0.03	0.58	0.22	0.93	1.00	**Arg**											
Arg	0.68	0.73	0.15	0.24	0.37	0.02	0.97	0.94	1.00	**Ala**										
Ala	0.77	0.56	-0.76	-0.80	0.86	0.67	0.30	0.46	0.28	1.00	**Pro**									
Pro	0.76	0.76	-0.04	0.04	0.56	0.23	0.96	0.98	0.95	0.46	1.00	**Tyr**								
Tyr	0.63	0.71	0.12	0.22	0.38	-0.03	0.95	0.90	0.95	0.25	0.91	1.00	**Cys2**							
Cys2	-0.55	-0.54	0.89	0.79	-0.75	-0.42	0.04	-0.18	0.02	-0.68	-0.14	-0.01	1.00	**Val**						
Val	0.44	0.51	0.37	0.43	0.14	-0.16	0.93	0.80	0.93	0.04	0.84	0.89	0.28	1.00	**Met**					
Met	0.53	0.60	0.28	0.38	0.24	-0.13	0.96	0.85	0.96	0.12	0.88	0.93	0.17	0.97	1.00	**Ile**				
Ile	-0.01	0.12	0.73	0.75	-0.33	-0.46	0.64	0.43	0.64	-0.42	0.47	0.62	0.66	0.84	0.76	1.00	**Leu**			
Leu	-0.05	0.17	0.52	0.56	-0.33	-0.37	0.70	0.45	0.70	-0.33	0.51	0.67	0.40	0.89	0.81	0.98	1.00	**Lys**		
Lys	0.67	0.73	0.12	0.23	0.39	0.02	0.97	0.94	0.99	0.28	0.95	0.95	0.01	0.93	0.96	0.63	0.68	1.00	**Phe**	
Phe	0.66	0.72	0.14	0.24	0.38	0.01	0.96	0.94	0.99	0.28	0.95	0.95	0.03	0.93	0.96	0.65	0.69	1.00	1.00	**Trp**
Trp	0.65	0.59	-0.07	-0.04	0.54	0.28	0.90	0.85	0.81	0.50	0.91	0.82	-0.10	0.76	0.79	0.41	0.41	0.82	0.81	1.00

Table C3 Spearman's rank correlation coefficient values for T127 cells

	Asp																			
Asp	1.00	**Glu**																		
Glu	0.86	1.00	**Ser**																	
Ser	-0.24	-0.22	1.00	**Asn**																
Asn	-0.02	0.27	0.53	1.00	**Gly**															
Gly	0.71	0.75	-0.65	0.01	1.00	**Gln**														
Gln	0.15	-0.17	-0.02	-0.43	-0.17	1.00	**His**													
His	0.67	0.77	0.24	0.59	0.47	-0.16	1.00	**Thr**												
Thr	0.68	0.81	0.18	0.60	0.53	-0.14	0.96	1.00	**Arg**											
Arg	0.64	0.77	0.22	0.66	0.52	-0.25	0.97	0.97	1.00	**Ala**										
Ala	0.51	0.26	-0.24	-0.40	0.41	0.29	0.15	0.14	0.11	1.00	**Pro**									
Pro	0.67	0.77	0.23	0.60	0.48	-0.13	0.98	0.97	0.97	0.13	1.00	**Tyr**								
Tyr	0.56	0.69	0.29	0.67	0.43	-0.32	0.91	0.90	0.94	0.10	0.91	1.00	**Cys2**							
Cys2	-0.11	-0.28	0.59	-0.17	-0.52	0.34	0.00	-0.13	-0.11	0.20	-0.08	-0.06	1.00	**Val**						
Val	0.52	0.60	0.43	0.60	0.30	-0.29	0.92	0.87	0.91	0.13	0.89	0.89	0.18	1.00	**Met**					
Met	0.58	0.73	0.24	0.66	0.47	-0.33	0.97	0.92	0.97	0.07	0.93	0.94	-0.06	0.92	1.00	**Ile**				
Ile	0.21	0.21	0.65	0.42	-0.07	-0.26	0.62	0.53	0.59	0.09	0.57	0.63	0.53	0.83	0.63	1.00	**Leu**			
Leu	0.36	0.44	0.67	0.50	-0.12	-0.22	0.78	0.69	0.70	-0.01	0.72	0.68	0.42	0.90	0.72	0.99	1.00	**Lys**		
Lys	0.64	0.77	0.24	0.65	0.50	-0.25	0.96	0.96	0.99	0.13	0.97	0.94	-0.09	0.91	0.96	0.59	0.71	1.00	**Phe**	
Phe	0.63	0.76	0.23	0.67	0.50	-0.25	0.96	0.95	0.98	0.08	0.95	0.94	-0.11	0.90	0.97	0.58	0.70	0.98	1.00	**Trp**
Trp	0.70	0.76	0.15	0.39	0.45	-0.10	0.92	0.85	0.84	0.23	0.88	0.78	0.10	0.85	0.87	0.60	0.78	0.83	0.84	1.00

References

Aggarwal, R. S. (2014) What's fueling the biotech engine-2012 to 2013. *Nature Biotechnology*, 32(1), pp. 32-39.

Ahn, W. S. & Antoniewicz, M. R. (2011) Metabolic flux analysis of CHO cells at growth and non-growth phases using isotopic tracers and mass spectrometry. *Metabolic Engineering,* 13(5), pp. 598-609.

Ahn, W. S. & Antoniewicz, M. R. (2012) Towards dynamic metabolic flux analysis in CHO cell cultures. *Biotechnology Journal,* 7(1), pp. 61-74.

Altamirano, C., Paredes, C., Illanes, A., Cairó, J. J. & Gòdia, F. (2004) Strategies for fed-batch cultivation of t-PA producing CHO cells: substitution of glucose and glutamine and rational design of culture medium. *Journal of Biotechnology*, 110(2), pp. 171-179.

Arriza, J. L., Kavanaugh, M. P., Fairman, W. A., Wu, Y. N., Murdoch, G. H., North, R. A. & Amara, S. G. (1993) Cloning and expression of a human neutral amino acid transporter with structural similarity to the glutamate transporter gene family. *Journal of Biological Chemistry*, 268(21), pp. 15329-15332.

Ash, J. F., Igo, R. P. Jr., Morgan, M. & Grey, A. (1993) Selection of Chinese hamster ovary cells (CHO-K1) with reduced glutamate and aspartate uptake. *Somatic Cell and Molecular Genetics*, 19(3), pp. 231-243.

Atkinson, B. N., Bell, S. C., De Vivo, M., Kowalski, L. R., Lechner, S. M., Ognyanov, V. I., Tham, C. S., Tsai, C., Jia, J., Ashton, D. & Klitenick, M. A. (2001). ALX 5407: a potent, selective inhibitor of the hGlyT1 glycine transporter. *Molecular Pharmacology,* 60(6), pp. 1414-1420.

Awasthi, S., Sharma, R., Singhal, S. S., Herzog, N. K., Chaubey, M. & Awasthi, Y. C. (1994). Modulation of cisplatin cytotoxicity by sulphasalazine. *British Journal of Cancer*, 70(2), pp. 190-194.

Babu, E., Kanai, Y., Chairoungdua, A., Kim, D. K., Iribe, Y., Tangtrongsup, S., Jutabha, P., Li, Y., Ahmed, N., Sakamoto, S., Anzai, N., Nagamori, S. & Endou, H. (2003) Identification of a novel system L amino acid transporter structurally distinct from heterodimeric amino acid transporters. *Journal of Biological Chemistry*, 278(44), pp. 43838-43845.

Bach, M. K., Brashler, J. R. & Johnson, M. A. (1985) Inhibition by sulfasalazine of LTC synthetase and of rat liver glutathione S-transferases. *Biochemical Pharmacology*, 34(15), 2695-2704.

Baird, F. E., Bett, K. J., Maclean, C., Tee, A. R., Hundal, H. S. & Taylor, P. M. (2009) Tertiary active transport of amino acids reconstituted by coexpression of System A and L transporters in *Xenopus* oocytes. *American Journal of Physiology: Endocrinology and Metabolism,* 297(3), pp. E822-9.

Barnes, L. M., Bentley, C. M. & Dickson, A. J. (2000) Advances in animal cell recombinant protein production: GS-NS0 expression system. *Cytotechnology,* 32(2), pp. 109-123.

Bass, R., Hedegaard, H. B., Dillehay, L., Moffett, J. & Englesberg, E. (1981 The A, ASC, and L systems for the transport of amino acids in Chinese hamster ovary cells (CHO-K1). *The Journal of Biological Chemistry,* 256(20), pp. 10259-10266.

Baycin-Hizal, D., Tabb, D. L., Chaerkady, R., Chen, L., Lewis, N. E., Nagarajan, H., Sarkaria, V., Kumar, A., Wolozny, D., Colao, J., Jacobson, E., Tian, Y., O'Meally, R. N., Krag, S. S., Cole, R. N., Palsson, B. O., Zhang, H. & Betenbaugh, M. (2012) Proteomic analysis of Chinese hamster ovary cells. *Journal of Proteome Research*, 11(11), pp. 5265-5276.

Becker, J., Hackl, M., Rupp, O., Jakobi, T., Schneider, J., Szczepanowski, R., Bekel, T., Borth, N., Goesmann, A., Grillari, J., Kaltschmidt, C., Noll, T., Pühler, A. Tauch, A. & Brinkrolf, K. (2011) Unraveling the Chinese hamster ovary cell line transcriptome by next-generation sequencing. *Journal of Biotechnology*, 156(3), pp. 227-235.

Berg, J. M., Tymoczko, J. L. & Stryer, L. (2007) *Biochemistry*. 6th Edition. New York, W. H. Freeman and Company.

Birch, J. R. & Racher, A. J. (2006) Antibody production. *Advanced Drug Delivery Reviews,* 58(5-6), pp. 671-85.

Birzele, F., Schaub, J., Rust, W., Clemens, C., Baum, P., Kaufmann, H., Weith, A., Schulz, T. W. & Hildebrandt, T. (2010) Into the unknown: expression profiling without genome sequence information in CHO by next generation sequencing. *Nucleic Acids Research*, 38(12), pp. 3999-4010.

Bodoy, S., Martín, L., Zorzano, A., Palacín, M., Estevez, R. & Bertran, J. (2005) Identification of LAT4, a novel amino acid transporter with system L activity. *Journal of Biological Chemistry*, 280(12), pp. 12002-12011.

Bodoy, S., Fotiadis, D., Stoeger, C., Kanai, Y. & Palacín, M. (2013) The small SLC43 family: Facilitator system L amino acid transporters and the orphan EEG1. *Molecular Aspects of Medicine*, 34(2-3), pp. 638-645.

Böhmer, C., Bröer, A., Munzinger, M., Kowalczuk, S., Rasko, J. E., Lang, F. & Bröer, S. (2005) Characterization of mouse amino acid transporter B0AT1 (slc6a19). *Biochemical Journal*, 389(Pt 3), pp. 745-751.

Bort, J. A., Stern, B. & Borth, N. (2010) CHO-K1 host cells adapted to growth in glutamine-free medium by FACS-assisted evolution. *Biotechnology Journal*, 5(10), pp. 1090-1097.

Bröer, A., Wagner, C. A., Lang, F. & Bröer, S. (2000) The heterodimeric amino acid transporter 4F2hc/y+LAT2 mediates arginine efflux in exchange with glutamine. *Biochemical Journal*, 349(Pt 3), pp. 787-795.

Bröer, A., Tietze, N., Kowalczuk, S., Chubb, S., Munzinger, M., Bak, L.K. & Bröer, S. (2006). The orphan transporter v7-3 (slc6a15) is a Na+-dependent neutral amino acid transporter (B0AT2). *Biochemical Journal*, 393(Pt 1), pp. 421-430.

Bröer, S. (2002) Adaptation of plasma membrane amino acid transport mechanisms to physiological demands. *Pflugers Archiv: European Journal of Physiology,* 444(4)**,** pp. 457- 466.

Chairoungdua, A., Kanai, Y., Matsuo, H., Inatomi, J., Kim, D. K. & Endou, H. (2001) Identification and characterization of a novel member of the heterodimeric amino acid transporter family presumed to be associated with an unknown heavy chain. *Journal of Biological Chemistry*, 276(52), pp. 49390-49399.

Chen, P. & Harcum, S. W. (2005) Effects of amino acid additions on ammonium stressed CHO cells. *Journal of Biotechnology*, 117(3), pp. 277-286.

Chillarón, J., Estevez, R., Mora, C., Wagner, C. A., Suessbrich, H., Lang, F., Gelpl, J. L., Testar, X., Busch, A. E., Zorzano, A. & Palacin, M. (1996) Obligatory amino acid exchange via systems bo,+-like and y+L-like. A tertiary active transport mechanism for renal reabsorption of cystine and dibasic amino acids. *The Journal of Biological Chemistry,* 271(30), pp. 17761-17770.

Christensen, H. N., Liang, M. & Archer, E. G. (1967) A distinct Na^+-requiring transport system for alanine, serine, cysteine, and similar amino acids. *The Journal of Biological Chemistry,* 242(22), pp. 5237-5246.

Christie, G. R., Hajduch, E., Hundal, H. S., Proud, C. G. & Taylor, P. M. (2002) Intracellular sensing of amino acids in Xenopus laevis oocytes stimulates p70 S6 kinase in a target of rapamycin-dependent manner. *The Journal of Biological Chemistry,* 277(12), pp. 9952-9957.

Chung, W. J., Lyons, S. A., Nelson, G. M., Hamza, H., Gladson, C. L., Gillespie, G. Y. & Sontheimer, H. (2005) Inhibition of cystine uptake disrupts the growth of primary brain tumors. *The Journal of Neuroscience,* 25(31), pp. 7101-7110.

Chung, W. J. & Sontheimer, H. (2009) Sulfasalazine inhibits the growth of primary brain tumors independent of nuclear factor-kappaB. *Journal of Neurochemistry*, 110(1), pp. 182-193.

Clarke, C., Doolan, P., Barron, N., Meleady, P., O'Sullivan, F., Gammell, P., Melville, M., Leonard, M. & Clynes, M. (2011) Large scale microarray profiling and coexpression network analysis of CHO cells identifies transcriptional modules associated with growth and productivity. *Journal of Biotechnology*, 155(3), pp. 350-359.

Closs, E. I., Boissel, J. P., Habermeier, A. & Rotmann, A. (2006) Structure and function of cationic amino acid transporters (CATs). *Journal of Membrane Biology*, 213(2), pp. 67-77.

Danbolt, N. C. (2001) Glutamate uptake. *Progress in Neurobiology*, 65(1), pp. 1-105.

Davies, S. L., Lovelady, C. S., Grainger, R. K., Racher, A. J., Young, R. J. & James, D. C. (2013) Functional heterogeneity and heritability in CHO cell populations. *Biotechnology and Bioengineering*, 110(1), pp. 260-274.

Dean, J. & Reddy, P. (2013) Metabolic Analysis of Antibody Producing CHO Cells in Fed-Batch Production. *Biotechnology and Bioengineering*, 110(6), pp. 1735-1747.

DeBerardinis, R. J., Mancuso, A., Daikhin, E., Nissim, I., Yudkoff, M., Wehrli, S. & Thompson, C. B. (2007) Beyond aerobic glycolysis: transformed cells can engage in glutamine metabolism that exceeds the requirement for protein and nucleotide synthesis. *PNAS,* 104(49), pp. 19345-19350.

De Jesus, M. & Wurm, F. M. (2011) Manufacturing recombinant proteins in kg-ton quantities using animal cells in bioreactors. *European Journal of Pharmaceutics and Biopharmaceutics,* 78(2), pp.184-188.

Demain, A. L. & Vaishnav, P. (2009) Production of recombinant proteins by microbes and higher organisms. *Biotechnology Advances,* 27(3), pp. 297-306.

Dietmair, S., Hodson, M. P., Quek, L. E., Timmins, N. E., Chrysanthopoulos, P., Jacob, S. S., Gray, P. & Nielsen, L. K. (2012a) Metabolite profiling of CHO cells with different growth characteristics. *Biotechnology and Bioengineering,* 109(6), pp. 1404-1414.

Dietmair, S., Hodson, M. P., Quek, L. E., Timmins, N. E., Gray, P. & Nielsen, L. K. (2012b) A multi-omics analysis of recombinant protein production in Hek293 cells. *PLoS One*, 7(8).

Doolan, P., Meleady, P., Barron, N., Henry, M., Gallagher, R., Gammell, P., Melville, M., Sinacore, M., McCarthy, K., Leonard, M., Charlebois, T. & Clynes, M. (2010) Microarray and proteomics expression profiling identifies several candidates, including the valosin-containing protein (VCP), involved in regulating high cellular growth rate in production CHO cell lines. *Biotechnology and Bioengineering,* 106(1), pp. 42-56.

Dreesen, I. A. & Fussenegger, M. (2011) Ectopic expression of human mTOR increases viability, robustness, cell size, proliferation, and antibody production of chinese hamster ovary cells. *Biotechnology and Bioengineering,* 108(4), pp. 853-866.

Duarte, T. M., Carinhas, N., Barreiro, L. C., Carrondo, M. J., Alves, P. M. & Teixeira, A. P. (2014) Metabolic responses of CHO cells to limitation of key amino acids. *Biotechnology and Bioengineering,* 111(10), pp. 2095-2106.

Esslinger, C. S., Cybulski, K. A. & Rhoderick, J. F. (2005) Ngamma-aryl glutamine analogues as probes of the ASCT2 neutral amino acid transporter binding site. *Bioorganic & Medicinal Chemistry,* 13(4) 1111-1118.

Fan, Y., Jimenez Del Val, I., Muller, C., Wagtberg Sen, J., Rasmussen, S. K., Kontoravdi, C., Weilguny, D. & Andersen, M. R. (2015) Amino acid and glucose metabolism in fed-batch CHO cell culture affects antibody production and glycosylation. *Biotechnology and Bioengineering*, 112(3), pp. 521-535.

Fenczik, C. A., Sethi, T., Ramos, J. W., Hughes, P. E. & Ginsberg, M. H. (1997) Complementation of dominant suppression implicates CD98 in integrin activation. *Nature*, 390(6655), pp. 81–85.

Fernández, E., Torrents, D., Zorzano, A., Palacin, M. & Chillarón, J. (2005) Identification and functional characterization of a novel low affinity aromatic-preferring amino acid transporter (arpAT). One of the few proteins silenced during primate evolution. *Journal of Biological Chemistry*, 280(19), pp. 19364-19372.

Fogolín, M. B., Wagner, R., Etcheverrigaray, M. & Kratje, R. (2004) Impact of temperature reduction and expression of yeast pyruvate carboxylase on hGM-CSF-producing CHO cells. *Journal of Biotechnology*, 109(1-2), pp. 179-191.

Fomina-Yadlin, D., Gosink, J. J., McCoy, R., Follstad, B., Morris, A., Russell, C. B. & McGrew, J. T. (2014) Cellular responses to individual amino-acid depletion in antibody-expressing and parental CHO cell lines. *Biotechnology and Bioengineering,* 111(5), pp. 965-979.

Fotiadis, D., Kanai, Y. & Palacín, M. (2013) The SLC3 and SLC7 families of amino acid transporters. *Molecular Aspects of Medicine*, 34(2-3), pp. 139-158.

Fuchs, B. C. & Bode, B. P. (2005) Amino acid transporters ASCT2 and LAT1 in cancer: partners in crime? *Seminars in Cancer Biology,* 15(4), pp. 254-266.

Fukasawa, Y., Segawa, H., Kim, J. Y., Chairoungdua, A., Kim, D. K., Matsuo, H., Cha, S. H., Endou, H. & Kanai, Y. (2000) Identification and characterization of a Na(+)-independent neutral amino acid transporter that associates with the 4F2 heavy chain and exhibits substrate selectivity for small neutral D- and L-amino acids. *Journal of Biological Chemistry*, 275(13), pp. 9690-9698.

Ganapathy, V., Thangaraju, M. & Prasad, P. D. (2009) Nutrient transporters in cancer: relevance to Warburg hypothesis and beyond. *Pharmacology and Therapeutics,* 121(1), pp. 29- 40.

Gout, P. W., Buckley, A. R., Simms, C. R. & Bruchovsky, N. (2001) Sulfasalazine, a potent suppressor of lymphoma growth by inhibition of the x(c)- cystine transporter: a new action for an old drug. *Leukemia*, 15(10), pp. 1633-1640.

Griffith, O. W. (1999) Biologic and pharmacologic regulation of mammalian glutathione synthesis. *Free Radical Biology and Medicine*, 27(9-10), pp. 922-935.

Hara, K., Yonezawa, K., Weng, Q. P., Kozlowski, M.T., Belham, C. & Avruch, J. (1998) Amino Acid Sufficiency and mTOR Regulate p70 S6 Kinase and eIF-4E BP1 through a Common Effector Mechanism. *The Journal of Biological Chemistry,* 273(33), pp. 14484-14494.

Harreither, E., Hackl, M., Pichler, J., Shridhar, S., Auer, N., Labaj, P. P., Scheideler, M., Karbiener, M., Grillari, J., Kreil, D. P. & Borth, N. (2015) Microarray profiling of preselected CHO host cell subclones identifies gene expression patterns associated with increased production capacity. *Biotechnology Journal*, 10(10), pp. 1625-1638.

Hassanein, M., Hoeksema, M. D., Shiota, M., Qian, J., Harris, B. K., Chen, H., Clark, J. E., Alborn, W. E., Eisenberg, R. & Massion, P. P. (2013) SLC1A5 mediates glutamine transport required for lung cancer cell growth and survival. *Clinical Cancer Research*, 19(3), pp. 560-570.

Hedge, P. S., White, I. R. & Debouck, C. (2003) Interplay of transcriptomics and proteomics. *Current Opinion in Biotechnology*, 14(6), pp. 647-651.

Hediger, M. A., Romero, M. F., Peng, J. B., Rolfs, A., Takanaga, H. & Bruford, E. A. (2004) The ABCs of solute carriers: physiological, pathological and therapeutic implications of human membrane transport proteins. *Pflugers Archiv: European Journal of Physiology,* 447(5), pp. 465-468.

Holm, S. (1979) A simple sequentially rejective multiple test procedure. *Scandinavian Journal of Statistics* 6(2), pp. 65–70.

Hu, W. S. (2012) Cell culture bioprocess engineering. Minneapolis, Wei-Shou, Hu.

Igo, R. P. Jr. & Ash, J. F. (1998) The Na^+-dependent glutamate and aspartate transporter supports glutathione maintenance and survival of CHO-K1 cells. *Somatic Cell and Molecular Genetics*, 24(6), pp. 341-352.

Irani, N., Wirth, M., van den Heuvel, J. & Wagner, R. (1999) Improvement of the primary metabolism of cell cultures by introducing a new cytoplasmic pyruvate carboxylase reaction. *Biotechnology and Bioengineering,* 66(4), pp. 238-246.

Jain, E. & Kumar, A. (2008) Upstream processes in antibody production: evaluation of critical parameters. *Biotechnology Advances*, 26(1), pp. 46-72.

Jayapal, K. P., Wlaschin, K. F., Hu, W. S. & Yap, M. G. S. (2007) Recombinant protein therapeutics from CHO cells - 20yrs and counting. *Chemical Engineering Progress,* 103(7), pp. 40-47.

Jewell, J. L., Kim, Y.C., Russell, R. C., Yu, F. X., Park, H. W., Plouffe, S. W., Tagliabracci, V. S. & Guan, K. L. (2015) Differential regulation of mTORC1 by leucine and glutamine. *Science*, 347(6218), pp. 194-198.

Ji, X., Jin, Y., Chen, Y., Li, C. & Guo, L. (2007) Existence of an endogenous glutamate and aspartate transporter in Chinese hamster ovary cells. *Acta Biochimica et Biophysica Sinica,* 39(11), pp. 851-856.

Ji, Y., Wu, Z., Dai, Z., Zhang, Q. & Wu, G. (2016) Excessive L-cysteine induces vacuole-like cell death by activating endoplasmic reticulum stress and mitogen-activated protein kinase signaling in intestinal porcine epithelial cells. *Amino Acids*, 48(1), pp. 149-156.

Jiang, Z., Droms, K., Geng, Z., Casnocha, S., Xiao, Z., Gorfien, S. & Jacobia, S. J. (2012) Fed-batch cell culture process optimization. *BioProcess International,* 10, pp. 40- 45.

Kanai, Y., Segawa, H., Miyamoto, K., Uchino, H., Takeda, E. & Endou, H. (1998) Expression cloning and characterization of a transporter for large neutral amino acids activated by the heavy chain of 4F2 antigen (CD98). *The Journal of Biological Chemistry,* 273(37) 23629-23632.

Kanai, Y., Fukasawa, Y., Cha, S. H., Segawa, H., Chairoungdua, A., Kim, D. K., Matsuo, H., Kim, J. Y., Miyamoto, K., Takeda, E. & Endou, H. (2000) Transport properties of a system y+L neutral and basic amino acid transporter. Insights into the mechanisms of substrate recognition. *The Journal of Biological Chemistry,* 275(27) 20787-20793.

Kanai, Y., Clémençon, B., Simonin, A., Leuenberger, M., Lochner, M., Weisstanner, M. & Hediger, M. A. (2013) The SLC1 high-affinity glutamate and neutral amino acid transporter family. *Molecular Aspects of Medicine*, 34(2-3), pp. 108-120.

Kang, S., Mullen, J., Miranda, L. P. & Deshpande, R. (2012) Utilization of tyrosine- and histidine-containing dipeptides to enhance productivity and culture viability. *Biotechnology and Bioengineering*, 109(9), pp. 2286-2294.

Kantardjieff, A., Jacob, N. M., Yee, J. C., Epstein, E., Hoh, Y. J., Philip, R., Betenbaugh, M. & Hu, W. S. (2010) Transcriptome and proteome analysis of Chinese hamster ovary cells under low temperature and butyrate treatment. *Journal of Biotechnology*, 145(2), pp. 143-159.

Karunakaran, S., Ramachandran, S., Coothankandaswamy, V., Elangovan, S., Babu, E., Periyasamy-Thandavan, S., Gurav, A., Gnanaprakasam, J. P., Singh, N., Schoenlein, P. V., Prasad, P. D., Thangaraju, M. & Ganapathy, V. (2011) SLC6A14 ($ATB^{0,+}$) protein, a highly concentrative and broad specific amino acid transporter, is a novel and effective drug target for treatment of estrogen receptor-positive breast cancer. *The Journal of Biological Chemistry,* 286(36), pp. 31830-31838.

Kelley, B. (2009) Industrialization of mAb production technology: the bioprocessing industry at a crossroads. *MAbs,* 1(5), pp. 443-452.

Kilberg, M. S., Shan, J. & Su, N. (2009) ATF4-dependent transcription mediates signaling of amino acid limitation. *Trends in Endocrinology and Metabolism*, 20(9), pp. 436-443.

Kim, C. S., Cho, S. H., Chun, H. S., Lee, S. Y., Endou, H., Kanai, Y. & Kim D. K. (2008) BCH, an inhibitor of system L amino acid transporters, induces apoptosis in cancer cells. *Biological & Pharmaceutical Bulletin*, 31(6), pp. 1096-1100.

Kim, D. K., Kanai, Y., Chairoungdua, A., Matsuo, H., Cha, S. H. & Endou, H. (2001) Expression cloning of a Na+-independent aromatic amino acid transporter with structural similarity to H+/monocarboxylate transporters. *Journal of Biological Chemistry*, 276(20), pp. 17221-17228.

Kim, J. & Guan, K. L. (2011) Amino acid signaling in TOR activation. *Annual Review of Biochemistry,* 80, pp. 1001-1032.

Kim, M., O'Callaghan, P. M., Droms, K. A. & James, D. C. (2011) A Mechanistic Understanding of Production Instability in CHO Cell Lines Expressing Recombinant Monoclonal Antibodies. *Biotechnology and Bioengineering*, 108(10), pp. 2434-2446.

Kim, S. H. & Lee, G. M. (2007) Functional expression of human pyruvate carboxylase for reduced lactic acid formation of Chinese hamster ovary cells (DG44). *Applied Microbiology and Biotechnology*, 76(3), pp. 659-665.

Kishishita, S., Katayama, S., Kodaira, K., Takagi, Y., Matsuda, H., Okamoto, H., Taksuma, S., Hirashima, C. & Aoyagi, H. (2015) Optimization of chemically defined feed media for monoclonal antibody production in Chinese hamster ovary cells. *Journal of Bioscience and Bioengineering*, 120(1), pp. 78-84.

Kondoh, N., Imazeki, N., Arai, M., Hada, A., Hatsuse, K., Matsuo, H., Matsubara, O., Ohkura, S. & Yamamoto, M. (2007). Activation of a system A amino acid transporter, ATA1/SLC38A1, in human hepatocellular carcinoma and preneoplastic liver tissues. *International Journal of Oncology*, 31(1), pp. 81-87.

Kyriakopoulos, S, Polizzi, K. M. & Kontoravdi, C. (2013) Comparative analysis of amino acid metabolism and transport in CHO variants with different levels of productivity. *Journal of Biotechnology*, 168(4), pp. 543-551.

Kyriakopoulos, S. & Kontoravdi, C. (2014) A framework for the systematic design of fed-batch strategies in mammalian cell culture. *Journal of Biotechnology and Bioengineering*, 111(12), pp. 2466-2476.

Lee, J. I., Dominy, J. E. Jr., Sikalidis, A. K., Hirschberger, L. L., Wang, W. & Stipanuk, M. H. (2008) HepG2/C3A cells respond to cysteine deprivation by induction of the amino acid deprivation/integrated stress response pathway. *Physiological Genomics*, 33(2), pp. 218-229.

Lewerenz, J., Klein, M. & Methner, A. (2006) Cooperative action of glutamate transporters and cystine/glutamate antiporter system X_c^- protects from oxidative glutamate toxicity. *Journal of Neurochemistry*, 98(3), pp. 916-925.

Lewis, N. E., Liu, X., Li, Y., Nagarajan, H., et al. (2013) Genomic landscapes of Chinese hamster ovary cell lines as revealed by the Cricetulus griseus draft genome. *Nature Biotechnology*, 31(8), pp. 759-765.

Ley, D., Seresht, A. K., Engmark, M., Magdenoska, O., Nielsen, K. F., Kildegaard, H. F. & Andersen, M. R. (2015) Multi-omic profiling of EPO-producing Chinese hamster ovary cell panel reveals metabolic adaptation to heterologous protein production. *Biotechnology and bioengineering*, doi: 10.1002/bit.25652 [Epub ahead of print].

Lim, Y., Wong, N. S., Lee, Y. Y., Ku, S. C., Wong, D. C. & Yap, M. G. (2010) Engineering mammalian cells in bioprocessing – current achievements and future perspectives. *Biotechnology and Applied Biochemistry,* 55(5), pp. 175-189.

López-Fontanals, M., Rodríguez-Mulero, S., Casado, F. J., Dérijard, B. & Pastor-Anglada, M. (2003) The osmoregulatory and the amino acid-regulated responses of system A are mediated by different signal transduction pathways. *The Journal of General Physiology*, 122(1), pp. 5-16.

Lunt, S. Y. & Vander Heiden, M. G. (2011) Aerobic glycolysis: meeting the metabolic requirements of cell proliferation. *Annual Review of Cell and Developmental Biology,* 27, pp. 441-464.

Luo, J., Vijayasankaran, N., Autsen, J., Santuray, R., Hudson, T., Amanullah, A. & Li, F. (2012) Comparative metabolite analysis to understand lactate metabolism shift in Chinese hamster ovary cell culture process. *Biotechnology and Bioengineering,* 109(1), pp. 146-156.

Ma, N., Ellet, J., Okediadi, C., Hermes, P., McCormick, E. & Casnocha, S. (2009) A single nutrient feed supports both chemically defined NS0 and CHO fed-batch processes: Improved productivity and lactate metabolism. *Biotechnology Progress*, 25(5), pp. 1353-1363.

Majors, B. S., Chiang, G. G. & Betenbaugh, M. J. (2009) Protein and genome evolution in Mammalian cells for biotechnology applications. *Molecular Biotechnology*, 42(2), pp. 216-223.

Mallorga, P. J., Williams, J. B., Jacobson, M., Marques, R., Chaudhary, A., Conn, P. J., Pettibone, D. J. & Sur, C. (2003) Pharmacology and expression analysis of glycine transporter GlyT1 with [3H]-(N-[3-(4'-fluorophenyl)-3-(4'phenylphenoxy)propyl])sarcosine. *Neuropharmacology*, 45(5), pp. 585-593.

Marin, M., Lavillette, D., Kelly, S. M. & Kabat, D. (2003) N-linked glycosylation and sequence changes in a critical negative control region of the ASCT1 and ASCT2 neutral amino acid transporters determine their retroviral receptor functions. *Journal of Virology*, 77(5), pp. 2936-2945.

Matsumura, M., Shimoda, M., Aril, T. & Kataoka, H. (1991) Adaptation of hybridoma cells to higher ammonia concentration. *Cytotechnology*, 7(2), pp. 103-112.

Matsuo, H., Kanai, Y., Kim, J. Y., Chairoungdua, A., Kim, D. K., Inatomi, J., Shigeta, Y., Ishimine, H., Chaekuntode, S., Tachampa, K., Choi, H. W., Babu, E., Fukuda, J. & Endou, H. (2002) Identification of a novel Na+-independent acidic amino acid transporter with structural similarity to the member of a heterodimeric amino acid transporter family associated with unknown heavy chains. *Journal of Biological Chemistry*, 277(23), pp. 21017-21026.

Meier, C., Ristic, Z., Klauser, S. & Verrey, F. (2002) Activation of system L heterodimeric amino acid exchangers by intracellular substrates. *The EMBO Journal,* 21(4), pp. 580-589.

Melville, M., Doolan, P., Mounts, W., Barron, N., Hann, L., Leonard, M., Clynes, M., & Charlebois, T. (2011) Development and characterization of a Chinese hamster ovary cell-specific oligonucleotide microarray. *Biotechnology Letters*, 33(9), pp. 1773-1779.

Nakauchi, J., Matsuo, H., Kim, D. K., Goto, A., Chairoungdua, A., Cha, S. H., Inatomi, J., Shiokawa, Y., Yamaguchi, K., Saito, I., Endou, H. & Kanai, Y. (2000) Cloning and characterization of a human brain Na(+)-independent transporter for small neutral amino acids that transports D-serine with high affinity. *Neuroscience Letters*, 287(3), pp. 231-235.

Nicklin, P., Bergman, P., Zhang, B., Triantafellow, E., Wang, H., Nyfeler, B., Yang, H., Hild, M., Kung, C., Wilson, C., Myer, V. E., Mackeigan, J. P., Porter, J. A., Wang, Y. K., Cantley, L. C., Finan, P. M. & Murphy, L. O. (2009) Bidirectional transport of amino acids regulates mTOR and autophagy. *Cell,* 136(3), pp. 521-534.

O'Callaghan, P. M., Berthelot, M. E., Young, R. J., Graham, J. W., Racher, A. J. & Aldana, D. (2015) Diversity in host clone performance within a Chinese hamster ovary cell line. *Biotechnology Progress*, doi: 10.1002/btpr.2097. [Epub ahead of print].

Oxender, D.L. & Christensen, H. N. (1963) Distinct mediating systems for the transport of neutral amino acids by the ehrlich cell. *The Journal of Biological Chemistry,* 238, pp. 3686-3699.

Parampalli, A., Eskridge, K., Smith, L., Meagher, M. M., Mowry, M. C. & Subramanian, A. (2007) Developement of serum-free media in CHO-DG44 cells using a central composite statistical design. *Cytotechnology*, 54(1), pp. 57-68.

Paredes, C., Prats, E., Cairó, J. J., Azorín, F., Cornudella, L. & Gòdia, F. 1(999) Modification of glucose and glutamine metabolism in hybridoma cells through metabolic engineering. *Cytotechnology*, 30(1-3), pp. 85-93.

Patel, S. A., Warren, B. A., Rhoderick, J. F. & Bridges, R. J. (2004) Differentiation of substrate and non-substrate inhibitors of transport system xc(-): an obligate exchanger of L-glutamate and L-cystine. *Neuropharmacology*, 46(2), pp. 273-284.

Pineda, M., Fernandez, E., Torrents, D., Estevez, R., Lopez, C., Camps, M., Lloberas, J., Zorzano, A. & Palacin, M. (1999) Identification of a membrane protein, LAT-2, that Co-expresses with 4F2 heavy chain, an L-type amino acid transport activity with broad specificity for small and large zwitterionic amino acids. *The Journal of Biological Chemistry,* 274(28) 19738-19744.

Pinilla, J., Aledo, J. C., Cwiklinski, E., Hyde, R., Taylor, P. M. & Hundal, H. S. (2011) SNAT2 transceptor signalling via mTOR: a role in cell growth and proliferation? *Frontiers in Bioscience*, 3, pp. 1289-1299.

Pramod, A. B., Foster, J., Carvelli, L. & Henry, L. K. (2013) SLC6 transporters: structure, function, regulation, disease association and therapeutics. *Molecular Aspects of Medicine*, 34(2-3), pp. 197-219.

Prentice, H. L., Ehrenfels, B. N. & Sisk, W. P. (2007) Improving performance of mammalian cells in fed-batch processes through "bioreactor evolution". *Biotechnology Progress*, 23(2), pp. 458–464.

Puck, T. T., Cieciura, S. J. & Robinson, A. (1958) Genetics of somatic mammalian cells. III. Long-term cultivation of euploid cells from human and animal subjects. *Journal of Experimental Medicine*, 108(6), pp. 945-956.

Quek, L., Dietmair, S., Krömer, J. O. & Nielsen, L. K. (2010) Metabolic flux analysis in mammalian cell culture. *Metabolic Engineering*, 12(2), pp. 161-171.

R Core Team (2014). R: A language and environment for statistical computing. R Foundation for Statistical Computing, Vienna, Austria. URL http://www.R-project.org/.

Rameez, S., Mostafa, S. S., Miller, C. & Shukla, A. A. (2014) High-throughput miniaturized bioreactors for cell culture process development: reproducibility, scalability, and control. *Biotechnology Progress*, 30(3), pp. 718-727.

Revelle, W. (2014) psych: Procedures for Personality and Psychological Research, Northwestern University, Evanston, Illinois, USA. URL http://CRAN.R-project.org/package=psych.

Richman, P. G., Orlowski, M. & Meister, A. (1973). Inhibition of γ-glutamylcysteine synthetase by L-methionine-S-sulfoximine. *Journal of Biological Chemistry*, 248(19), pp. 6684-6690.

Robe, P. A., Bentires-Alj, M., Bonif, M., Rogister, B., Deprez, M., Haddada, H., Khac, M. T., Jolois, O., Erkmen, K., Merville, M. P., Black, P. M. & Bours, V. (2004). In vitro and in vivo activity of the nuclear factor-kappaB inhibitor sulfasalazine in human glioblastomas. *Clinical Cancer Research*, 10(16), pp. 5595-5603.

Rotoli, B. M., Bussolati, O., Dall'Asta, V. & Gazzola, G. C. (1989) The transport of L-arginine in Chinese hamster ovary cells. *Biochemical and Biophysical Research Communications*, 164(3), pp. 1093-1098.

Sato, H., Tamba, M., Ishii, T. & Bannai, S. (1999) Cloning and expression of a plasma membrane cystine/glutamate exchange transporter composed of two distinct proteins. *The Journal of Biological Chemistry,* 274(17), pp. 11455-11458.

Schiöth, H. B., Roshanbin, S., Hägglund, M. G. & Fredriksson, R. (2013) Evolutionary origin of amino acid transporter families SLC32, SLC36 and SLC38 and physiological, pathological and therapeutic aspects. *Molecular Aspects of Medicine*, 34(2-3), pp. 571-585.

Schroeder, A., Mueller, O., Stocker, S., Salowsky, R., Leiber, M., Gassmann, M., Lightfoot, S., Menzel, W., Granzoe, M. & Ragg, T. (2006) The RIN: an RNA integrity number for assigning integrity values to RNA measurements. *BMC Molecular Biology*, 7:3.

Schroeder, H. W. Jr. & Cavacini, L. (2010) Structure and function of immunoglobulins. *Journal of Allergy and Clinical Immunology*, 125, S41-52.

Schummp, B. & Schlaeger, E. J. (1992) Growth study of lactate and ammonia double-resistant clones of HL-60 cells. *Cytotechnology*, 8(1), pp. 39-44.

Segawa, H., Fukasawa, Y., Miyamoto, K., Takeda, E., Endou, H. & Kanai, Y. (1999) Identification and functional characterization of a Na+-independent neutral amino acid transporter with broad substrate selectivity. *Journal of Biological Chemistry*, 274(28), pp. 19745-19751.

Sellick, C. A., Croxford, A. S., Maqsood, A. R., Stephens, G., Westerhoff, H. V., Goodacre, R. & Dickson, A. J. (2011) Metabolite profiling of recombinant CHO cells: designing tailored feeding regimes that enhance recombinant antibody production. *Biotechnology and Bioengineering,* 108(12), pp. 3025-3031.

Selvarasu, S., Ho, Y. S., Chong, W. P., Wong, N. S., Yusufi, F. N., Lee, Y. Y., Yap, M. G. & Lee, D. Y. (2012) Combined in silico modeling and metabolomics analysis to characterize fed-batch CHO cell culture. *Biotechnology and Bioengineering,* 109(6), pp. 1415-1429.

Sengupta, N., Rose, S. T. & Morgan, J. A. (2011) Metabolic flux analysis of CHO cell metabolism in the late non-growth phase. *Biotechnology and Bioengineering,* 108(1), pp. 82- 92.

Shen, D., Kiehl, T. R., Khattak, S. F., Li, Z. J., He, A., Kayne, P. S., Patel, V., Neuhaus, I. M. & Sharfstein, S. T. (2010) Transcriptomic responses to sodium chloride-induced osmotic stress: a study of industrial fed-batch CHO cell cultures. *Biotechnology Progress*, 26(4), pp. 1104-1115.

Shennan, D. B., Thomson, J., Gow, I. F., Travers, M. T. & Barber, M. C. (2004) L-leucine transport in human breast cancer cells (MCF-7 and MDA-MB-231): kinetics, regulation by estrogen and molecular identity of the transporter. *Biochimica et Biophysica Acta,* 1664(2), pp. 206-216.

Shih, A. Y., Erb, H., Sun, X., Toda, S., Kalivas, P. W. & Murphy, T. H. (2006) Cystine/glutamate exchange modulates glutathione supply for neuroprotection from oxidative stress and cell proliferation. *The Journal of Neuroscience,* 26(41), pp. 10514-10523.

Shotwell, M. A., Jayme, D. W., Kilberg, M. S. & Oxender, D. L. (1981) Neutral amino acid transport systems in Chinese hamster ovary cells. *The Journal of Biological Chemistry,* 256(11), 5422-5427.

Shukla, A. A. & Thommes, J. (2010) Recent advances in large-scale production of monoclonal antibodies and related proteins. *Trends in Biotechnology,* 28(5), pp. 253-261.

Singer, D., Camargo, S. M., Huggel, K., Romeo, E., Danilczyk, U., Kuba, K., Chesnov, S., Caron, M. G., Penninger, J. M. & Verrey, F. (2009) Orphan transporter SLC6A18 is renal neutral amino acid transporter B0AT3. *Journal of Biological Chemistry*, 284(30), pp. 19953-19960.

Smith, D. E., Clémençon, B. & Hediger, M. A. (2013). Proton-coupled oligopeptide transporter family SLC15: physiological, pharmacological and pathological implications. *Molecular Aspects of Medicine*, 34(2-3), pp. 323-336.

Sou, S. N., Sellick, C., Lee, K., Mason, A., Kyriakopoulos, S., Polizzi, K. M. & Kontoravdi, C. (2015) How does mild hypothermia affect monoclonal antibody glycosylation? *Biotechnology and Bioengineering*, 112(6), pp. 1165-1176.

Sugawara, M., Nakanishi, T., Fei, Y. J., Martindale, R. G., Ganapathy, M. E., Leibacj, F. H. & Ganapathy, V. (2000). Structure and function of ATA3, a new subtype of amino acid transport system A, primarily expressed in the liver and skeletal muscle. *Biochimica et Biophysica Acta*, 1509(1-2), pp. 7-13.

Tabuchi, H., Sugiyama, T., Tanaka, S. & Tainaka, S. (2010) Overexpression of taurine transporter in Chinese Hamster Ovary cells can enhance cell viability and product yield, while promoting glutamine consumption. *Biotechnology and Bioengineering*, 107(6), pp. 998-1003.

Taschwer, M., Hackl, M., Bort, J. A., Leitner, C., Kumar, N., Puc, U., Grass, J., Papst, M., Kunert, R., Altmann, F. & Borth, N. (2012) Growth, productivity and protein glycosylation in a CHO EpoFc producer cell line adapted to glutamine-free growth. *Journal of Biotechnology*, 157(2), pp. 295-303.

Torrents, D., Estevez, R., Pineda, M., Fernandez, E., Lioberas, J., Shi, Y. B., Zorzano, A. & Palacin, M. (1998) Identification and characterization of a membrane protein (y+L amino acid transporter-1) that associates with 4F2hc to encode the amino acid transport activity y+L. A candidate gene for lysinuric protein intolerance. *Journal of Biological Chemistry*, 273(49), pp. 32437-32445.

Templeton, N., Dean, J., Reddy, P. & Young, J. D. (2013) Peak antibody production is associated with increased oxidative metabolism in an industrially relevant fed-batch CHO cell culture. *Biotechnology and Bioengineering*, 110(7), pp. 2013-2024.

Timmerman, L. A., Holton, T., Yuneva, M., Louie, R. J., Padro, M., Daemen, A., Hu, M., Chan, D. A., Ethier, S. P., van' t Veer, L. J., Polyak, K., McCormick, F. & Gray J. W. (2013) Glutamine sensitivity analysis identifies the xCT antiporter as a common triple-negative breast tumor therapeutic target. *Cancer Cell*, 24(4), pp. 450-465.

Trapnell, C., Roberts, A., Goff, L., Pertea, G., Kim, D., Kelley, D. R., Pimentel, H., Salzberg, S. L., Rinn, J. L. & Pachter, L. (2012) Differential gene and transcript expression analysis of RNA-seq experiments with TopHat and Cufflinks. *Nature Protocols*, 7(3), pp. 562-578.

Toung, J. M., Morley, M., Li, M. & Cheung, V. G. (2011). RNA-sequence analysis of human B-cells. *Genome Research*, 21(6), pp. 991-998.

Ugawa, S., Sunouchi, Y., Ueda, T., Takahashi, E., Saishin, Y. & Shimada, S. (2001) Characterization of a mouse colonic system B(0+) amino acid transporter related to amino acid absorption in colon. *American Journal of Physiology*, 281(2), pp. G365-G370.

Utsunomiya-Tate, N., Endou, H. & Kanai, Y. (1996) Cloning and functional characterization of a system ASC-like Na^+-dependent neutral amino acid transporter. *The Journal of Biological Chemistry,* 271(25), pp. 14883-14890.

Vander Heiden, M. G., Cantley, L. C. & Thompson, C. B. (2009) Understanding the Warburg effect: the metabolic requirements of cell proliferation. *Science,* 324(5930), pp. 1029- 1033.

Varoqui, H., Zhu, H., Yao, D., Ming, H. & Erickson, J. D. (2000) Cloning and functional identification of a neuronal glutamine transporter. *Journal of Biological Chemistry*, 275(6), pp. 4049-4054.

Vekony, N., Wolf, S., Boissel, J. P., Gnauert, K. & Closs, E. I. (2001) Human cationic amino acid transporter hCAT-3 is preferentially expressed in peripheral tissues. *Biochemistry*, 40(41), pp. 12387-12394.

Wahl, C., Liptay, S. Adler, G. & Schmid, R. M. (1998) Sulfasalazine: a potent and specific inhibitor of nuclear factor kappa B. *Journal of Clinical Investigation*, 101(5), pp. 1163-1174.

Walsh, G. & Jefferis, R. (2006) Post-translational modifications in the context of therapeutic proteins. *Nature Biotechnology,* 24(10), pp. 1241-1252.

Walsh, G. Biopharmaceutical benchmarks (2014) *Nature Biotechnology*, 32(10), pp. 992-1000.

Wang, Q., Beaumont, K. A., Otte, N. J., Font, J., Bailey, C. G., van Geldermalsen, M., Sharp, D. M., Tiffen, J. C., Ryan, R. M., Jormakka, M., Haass, N. K., Rasko, J. E. & Holst, J. (2014) Targeting glutamine transport to suppress melanoma cell growth. *International Journal of Cancer*, 135(5), pp. 1060-1071.

Warburg, O. (1956). On the origin of cancer cells. *Science*, 123(3191), pp. 309-314.

Wei, T. (2013) corrplot: Visualization of a correlation matrix. R package version 0.73. URL http://CRAN.R-project.org/package=corrplot.

Whitford, W. G. (2006) Fed-batch mammalian cell culture in bioproduction. *BioProcess International*, pp. 30-40.

Wise, D. R., DeBerardinis, R. J., Mancuso, A., Sayed, N., Zhang, X. Y., Pfeiffer, H. K., Nissim, I., Daikhin, E., Yudkoff, M., Mcmahon, S. B. & Thompson, C. B. (2008) Myc regulates a transcriptional program that stimulates mitochondrial glutaminolysis and leads to glutamine addiction. *PNAS,* 105(48), pp. 18782-18787.

Wise, D. R. & Thompson, C. B. (2010) Glutamine addiction: a new therapeutic target in cancer. *Trends in Biochemical Sciences,* 35(8), pp. 427-433.

Wlaschin, K. F., Nissom, P. M., Gatti, Mde. L., Ong, P. F., Arleen, S., Tan, K. S., Rink, A., Cham, B., Wong, K., Yap, M. & Hu, W. S. (2005) EST sequencing for gene discovery in Chinese hamster ovary cells. *Biotechnology and Bioengineering*, 91(5), pp. 592-606.

Wlaschin, K. F. & Hu, W. S. (2007) Engineering cell metabolism for high-density cell culture via manipulation of sugar transport. *Journal of Biotechnology*, 131(2), pp. 168-176.

Wong, D. C., Wong, K. T., Lee, Y. Y., Morin, P. N., Heng, C. K. & Yap, M. G. (2006a). Transcriptional Profiling of Apoptotic Pathways in Batch and Fed-Batch CHO Cell Cultures. *Biotechnology and Bioengineering*, 94(2), pp. 373-382.

Wong, D. C., Wong, K. T., Nissom, P. M., Heng, C. K. & Yap, M. G. (2006b). Targeting Early Apoptotic Genes in Batch and Fed-Batch CHO Cell Cultures. *Biotechnology and Bioengineering*, 95(3), pp. 350-361.

Wullschleger, S., Loewith, R. & Hall, M. N. (2006) TOR signaling in growth and metabolism. *Cell,* 124(3), pp. 471-484.

Wurm, F. M. & Hacker, D. (2011) First CHO genome. *Nature Biotechnology,* 29(8), pp. 718- 720.

Xing, Z., Kenty, B., Koyrakh, I., Borys, M., Pan, S. & Li, Z. J. (2011) Optimizing amino acid composition of CHO cell culture media for a fusion protein production. *Process Biochemistry*, 46(7), pp. 1423-1429.

Xu X., Nagarajan, H., Lewis N. E. et al. (2011) The genomic sequence of the Chinese hamster ovary (CHO)-K1 cell line. *Nature Biotechnology*, 29(8), pp. 735-741.

Yang, H., Ierapetritou, M. G. & Roth, C. M. (2010) Effects of amino acid transport limitations on cultured hepatocytes. *Biophysical Chemistry*, 152(1-3), pp. 89-98.

Yang, Y., Mariati, Chusainow, J. & Yap, M. G. (2010b) DNA methylation contributes to loss in productivity of monoclonal antibody-producing CHO cell lines. *Journal of Biotechnology*, 147(3-4), pp. 180-185.

Yanagida, O., Kanai, Y., Chairoungdua, A. et al. (2001) Human L-type amino acid transporter 1 (LAT1): characterization of function and expression in tumor cell lines. *Biochimica et Biophysica Acta,* 1514(2), pp. 291-302.

Yao, D., Mackenzie, B., Ming, H., Varogui, H., Zhu, H., Hediger, M. A. & Erickson, J. D. (2000) A novel system A isoform mediating Na+/neutral amino acid cotransport. *Journal of Biological Chemistry*, 275(30), pp. 22790-22797.

Yee, J. C., de Leon Gatti, M., Philp, R. J., Yap, M. & Hu, W. S. (2008) Genomic and Proteomic Exploration of CHO and Hybridoma Cells Under Sodium Butyrate Treatment. *Biotechnology and Bioengineering*, 99(5), pp. 1186-1204.

Yu, M., Hu, Z., Pacis, E., Vijayasankaran, N., Shen, A. & Li, F. (2011) Understanding the intracellular effect of enhanced nutrient feeding toward high titer antibody production process. *Biotechnology and Bioengineering*, 108(5), pp. 1078-1088.

Yuk, I. H., Zhang, J. D., Ebeling, M., Berrera, M., Gomez, N., Werz, S., Meiringer, C., Shao, Z., Swanberg, J. C., Lee, K. H., Luo, J. & Szperalski, B. (2014) Effects of Copper on CHO Cells: Insights from Gene Expression Analyses. *Biotechnology Progress*, 30(2), pp. 429-442.

Zagari, F., Jordan, M., Stettler, M., Broly, H. & Wurm, F. M. (2013) Lactate metabolism shift in CHO cell culture: the role of mitochondrial oxidative activity. *New Biotechnology,* 30(2), pp. 238-245.

Zaia, K. A. & Reimer, R. J. (2009) Synaptic Vesicle Protein NTT4/XT1 (SLC6A17) Catalyzes Na+-coupled Neutral Amino Acid Transport. *Journal of Biological Chemistry*, 284(13), pp. 8439-8448.

Zeng, W. & Mortazavi, A. (2012) Technical considerations for functional sequencing assays. *Nature Immunology*, 13(9), pp. 802-807.

Zhang, F., Sun, X., Yi, X. & Zhang, Y. (2006) Metabolic characteristics of recombinant Chinese hamster ovary cells expressing glutamine synthetase in presence and absence of glutamine. *Cytotechnology,* 51(1), pp. 21-28.

Zhang, H., Wang, H., Liu, M., Zhang, T., Zhang, J., Wang, X. & Xiang, W. (2013) Rational development of a serum-free medium and fed-batch process for a GS-CHO cell line expressing recombinant antibody. *Cytotechnology,* 65(3), pp. 363-378.

Zhou, M., Crawford, Y., Ng, D., Tung, J., Pynn, A. F., Meier, A., Yuk, I. H., Vijayasankaran, N., Leach, K., Joly, J., Snedecor, B. & Shen, A. (2011) Decreasing lactate level and increasing antibody production in Chinese Hamster Ovary cells (CHO) by reducing the expression of lactate dehydrogenase and pyruvate dehydrogenase kinases. *Journal of Biotechnology*, 153(1-2), pp. 27-34.